Nitric oxide tolerance and antimicrobial susceptibility in Escherichia coli clinical isolates

PhD Thesis for the degree of PhD in Microbiology

Faculty of Sciences
School of Biosciences
University of Kent

Cláudia A. Ribeiro

2018

Declaration

I confirm that no part of this thesis has been submitted in support of an application for any degree or qualification at either the University of Kent, any other university or higher education learning institution.

Cláudia Ribeiro

18th September 2018

Abstract

The emergence of antibiotic resistance has been a serious concern for the last few decades. It hinders the treatment of infectious diseases, raising mortality and morbidity rates, as well as increasing the cost of healthcare. To investigate the problem of antibiotic resistant E. coli, 50 E. coli bacteraemia clinical isolates (Kent collection) were collected from East Kent Hospitals University NHS Foundation and phenotypically/genotypically characterized for antibiotic resistance, virulence factors, and the presence of putative plasmids. High levels of resistance were detected for amoxicillin and trimethoprim, and 14% of the isolates showed a multidrug-resistant phenotype. ST73 isolates exhibited the highest virulence potential while ST131 exhibited the highest levels of antibiotic resistance, although no correlation was detected between the two variables. In accordance with previous observations, co-carriage of CTX-M-15 and aac(3)-IIa, aac(6')Ib-cr, and blaOXA was observed in the collection, providing a possible explanation on why ESBL-producing isolates are often multidrug resistant.

The production of nitric oxide (NO) by the mammalian immune system and its well-known anti-bacterial properties has prompted the investigation exogenously administered NO as an alternative to antibiotics. While combinatorial treatments of NO and antibiotics have proved to be successful against bacterial biofilms, this strategy has not been investigated in planktonic bacterial cells. Moreover, recent studies have shown that the generation of reactive oxygen species (ROS) resulting from hyperactivation of the aerobic respiratory chain of E. coli occurs in response to treatment with bactericidal antibiotics. This secondary effect of antibiotics is an important part of the as part of the lethality of bactericidal antibiotics under aerobic conditions. Given that NO is a well-known respiratory inhibitor, it was hypothesised this would diminish the toxic effects of antibiotics. To test this hypothesis, the effect of NO upon the lethality of a bactericidal antibiotic (gentamicin) was tested on a multidrug resistant E. coli. Pre-exposure to the NO-donor GSNO or NOC-12 prior to gentamicin treatment was found to increase bacterial tolerance to the antibiotic in planktonic cells: the presence of NO elicits a 10-fold increase in IC_{50} for gentamicin lethality against an E. coli clinical isolate. Further investigation showed that cytochrome bd-I, a NO-tolerant respiratory oxidase expressed maximally under microaerobic conditions in E. coli, is largely responsible for the sensitization of E. coli to gentamicin during NO exposure.

The work herein reports that NO elicits a dramatic increase in the tolerance of E. coli to antibiotics. Hence, this work has revealed a huge void in knowledge related to

antibiotic potency during conditions relevant to infection (i.e. in the presence of NO). Furthermore, this work reveals that the cytochrome bd-I respiratory oxidase sensitises E. coli to antibiotics in the presence of NO. These findings shed light on how NO encountered during infection could impair the function of antibiotics and will prompt future research into how controlling levels of respiratory inhibition during infection may be used to improve antibiotic efficacy.

Acknowledgements

First and foremost, I would like to thank my supervisor Mark Shepherd for giving me the opportunity to do this PhD and for his encouragement and ideas. His unwavering positivity throughout the entirety of this project was motivating and kept me pushing forward, even during the tough times.

During my time at the University of Kent I was greeted by a community of people willing to help each other. A big thank you to Ian Blomfield and Gary Robinson for all the helpful discussions and ideas. Thank you to past and present members of the Shepherd, Blomfield, and Robinson Lab, fondly nicknamed “Sheblomson Lab” - Louise, Ami, Sara, Charlie, James Yorke, Taylor, Sarah, Büke, Joy, and Louis: thank you for the encouragement, advice, and the light-hearted and funny office conversations. I am indebted to our taught MSc student Luke Rahman and our undergraduate final year project student James Newton for performing the bacterial survival assays in EC958 (wild-type, cydAB, and cyoA), and engineering the Hmp-overexpressing EC958 strain, respectively, both of which are included in this thesis. I would also like to thank Jeremy Rossman and the members of his lab, as well as Campbell Gourley and Lucian Duvenage for kindly providing me with the equipment and training necessary for my macrophage work.

This work would not have been possible without the kindness of our collaborators. Thank you to Robert Poole (University of Sheffield) and Mark Schembri (University of Queensland) for kindly providing me with some of the strains and plasmids used in this work. I am grateful to Fahad Alhashash and Allan McNally for carrying out the typing (MLST) of the 50 E. coli clinical isolates. To Ian Goodhead, a very big thank you for allowing me to visit his lab at the University of Salford (Manchester) and use his Illumina sequencing platform, as well as for his patience, help, and advise throughout the analysis of the sequencing data.

I am thankful to the University of Kent, to KentHealth for funding my PhD, as well as to the Biochemical Society for funding my trip to Hamburg for the XIXth Oxygen Binding and Sending Proteins Meeting (2016).

Finally, I would like to thank my family. My parents, for all their love and support in my journey, for supporting my decision to study for a BSc degree in Biology, for supporting my decision to move to a different country to pursue my PhD, and for always being there for me with love, hugs, and good food. To my little two nieces for inspiring me to be better. To my sister, for being her supportive annoying self. To my grandparents, for all the love,

enthusiasm, and for encouraging me to follow my dream and keep an open mind. This would not have been possible without all of you. Thank you.

Table of Contents

List of Figures

List of Tables

Supplementary Data

Presentations and Publications

Publications:

Shepherd, M., Achard, M. E. S., Idris, A., Totsika, M., Phan, M. -D., Peters, K. M., Sarkar, S., **Ribeiro, C. A.**, Holyoake, L. V., Ladakis, D., Ulett, G. C., Sweet, M. J., Poole, R. K., McEwan, A. G., and Schembri, M. A. (2016) The cytochrome bd-I respiratory oxidase augments survival of multidrug-resistant Escherichia coli during infection. Scientific Reports **6**, 35285.

Poster presentation:

Ribeiro, Cláudia A.; Shepherd, Mark. Cytochrome bd-I and flavohaemoglobin Hmp confer tolerance to nitric oxide in multidrug-resistant E. coli. XIXth Oxygen Binding and Sensing Proteins Meeting (O2BiP), Hamburg, Germany, 2016.

Chapter 1

Introduction

1.1. The Antibiotic Paradox

1.1.1. A brief history of antibiotics

Ever since the discovery of penicillin by Sir Alexander Fleming (Fleming, 1929) in 1928, antibiotics have undoubtedly become one of medicines greatest achievements. Their use drastically improved the treatment of infectious diseases, patient outcome, and transformed the face of medicine: invasive surgeries became common practice, immune-compromising therapies were introduced to fight cancer, organ transplant procedures helped save the lives of millions of people. The combined result was the improvement in quality of life and increase in life expectancy. Fleming's discovery might have revolutionized medicine, but antibiotics have been around for much longer. In 1980, tetracycline-stained human Nubian bones from a civilization that pre-dates the modern antibiotic era were discovered (Bassett et al., 1980); the medical properties of mould have been known since ancient times (Aminov, 2010), and most antibiotics are natural products or derived from natural products (Harvey, 2000).

In the four decades following the discovery of penicillin, also known as the 'golden era of antibiotic discovery', ten new classes of antibiotics were discovered (Figure 1.1), but in the 1960s the discovery of new antibiotic classes halted. Alternatively, the chemical modification of the natural scaffolds of existing antibiotics was successfully implemented during this period, but the limited number of effective iterations soon also placed this strategy in hiatus. Only two synthetic classes of antibiotics (fluoroquinolones – e.g. ciprofloxacin; and oxazolidinones - e.g. linezolid) were discovered during the golden era. Despite the technological advances and efforts, mainly driven by the pharmaceutical industry, no new synthetic drug has emerged in the last 20 years (Aminov, 2010; Lewis, 2013) with similar efficacy to conventional antibiotics (Brown and Wright, 2016). One of the biggest obstacles of synthetic compounds is the bacterial membrane, as fully synthetic compounds do not have the benefit of evolution to facilitate membrane transit (Lewis, 2013; Brown and Wright, 2016). The difficulty of producing compounds with a broad spectrum of activity combined with avoiding toxic and possible life-threatening side effects, and the low profit margins compared to other drugs has resulted in many pharmaceutical companies ceasing research and development on antibiotics.

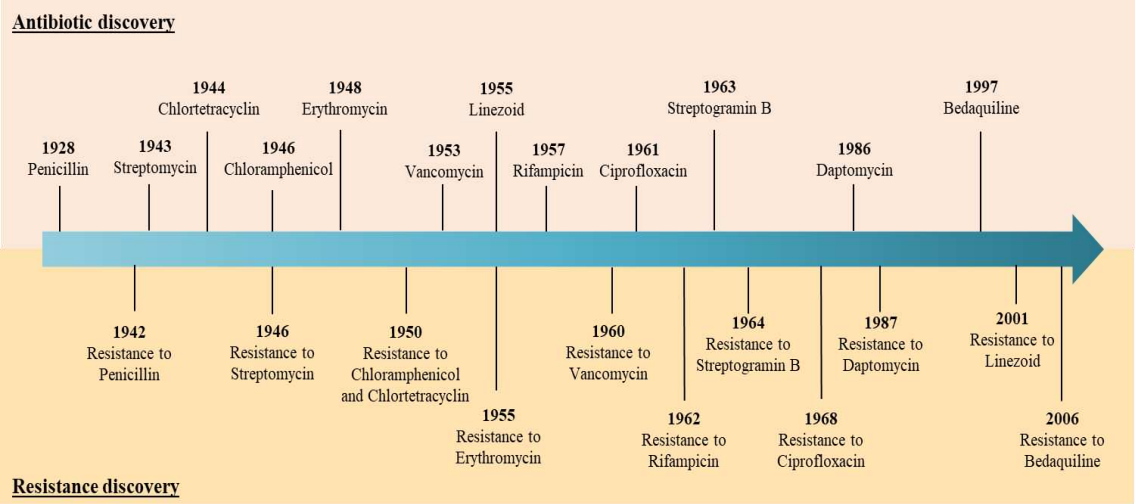

Figure 1.1 – Timeline of antibiotic discovery and appearance of resistance. The golden era of antibiotic discovery started in the 1930s. After four decades, antibiotic discovery decreased significantly, aggravating the problem posed by the emergence of antibiotic resistant bacteria.

1.1.2. Antibiotic Resistance

1.1.2.1. Causes, consequences, and prevention

Antibiotics were a turning point in human history and have saved many lives. Nevertheless, public health is now compromised due to the emergence of antibiotic-resistant bacteria. Shortly after the discovery of penicillin, strains of staphylococci resistant to this antibiotic were found (Barber, 1947), a trend that has now been observed over several decades for many other bacterial species and antibiotics (Figure 1.1), with some bacteria developing resistance to two or more classes of antibiotics making the treatment of infections very problematic, sometimes even impossible.

The Centre for Disease Control (CDC) has estimated that over two million people every year are afflicted with an antibiotic-resistant infection in the United States, with 23,000 dying as a result (CDC, 2013). In Europe, the number of deaths per year resulting from antibiotic-resistant infections is 25,000 (ECDC/EMEA Joint Working Group, 2009). If no measures and policies are put in place in an effort to counteract this problem, these numbers will only get worse: a recent British study claimed that by the year 2050, 10 million people could die every year due to infections cause by antibiotic-resistant microorganisms (Review on Antimicrobial Resistance, 2016).

To successfully tackle the problem of antibiotic resistance, it is important to understand the causes. Paradoxically, the main driver of antibiotic resistance is the use of antibiotics. Ever since their discovery, millions of tons of antibiotics have been produced, used, and discarded into the environment creating a selective pressure that facilitates the

survival of bacteria carrying the resistance determinant. Antibiotics are often incorrectly prescribed to treat viral infections, against which antibiotics are ineffective. Increases in human-life expectancy and the advance of medicine has led to the survival of severely ill patients and elderly patients, both of which are at higher risk for infection. One prime example are cystic fibrosis patients which are known to be at higher risk for pulmonary infections and thus frequently require administration of antibiotics. In fact, Pseudomonas aeruginosa, an opportunistic Gram-negative bacterium, is known to cause chronic infections in cystic fibrosis patients and is currently listed as a "Serious Threats" by the CDC (CDC, 2013). Antibiotics are also used in agriculture to promote the growth of livestock, and although this practice has been banned in the European Union, it continues in other countries, such as the United States, providing an excellent reservoir for antibiotic-resistant bacterial populations and a means to later colonize humans. It was estimated that antibiotic consumption in livestock increased by 30% in the last decade and it is projected to increase by another 37% by 2030 (Van Boeckel et al., 2015).

The consequences of antibiotic resistance are two-fold: increase in the cost of healthcare and increase in mortality. Infections caused by antibiotic-resistant bacteria, and especially multidrug-resistant bacteria, are difficult to treat and lead to an increase in the duration of hospital stay, thus increasing healthcare expenses. Moreover, the therapy may be unsuccessful, thus increasing the mortality rate associate with infectious diseases. The CDC estimated a loss of $20 billion US dollars per year in healthcare expenditures due to antibiotic resistant infections, with indirect costs due to loss of members of the work force estimated to be $35 billion US dollars (CDC, 2013). In Europe, the total cost was estimated to be €1.5 billion per year (ECDC/EMEA Joint Working Group, 2009). Additionally, antibiotic resistance has an impact on the world economy. Low-income countries could experience an increase of up to 25% per year in healthcare costs by 2050, compared to the 15% and 6% estimated for middle and high-income countries, respectively, increasing the economic rift between high- and low-income countries and sending millions of people into extreme poverty (Adeyi et al., 2017).

Irresponsible use of antibiotics combined with the adaptability of bacteria has led to the emergence and alarming dissemination of antibiotic resistance, and has left us on the brink of a post-antibiotic era (World Health Organization (WHO), 2014). Thus, it is of the utmost importance to combat antibiotic resistance. Local, national and global surveillance systems need to be put in place to monitor antibiotic resistance and facilitate the choice of treatment and implementation of policies to help control resistance. Moreover, in the face of decrease in antibiotic efficacy, it is imperative to use them wisely

and decrease their usage in general. This could be accomplished by decreasing the usage of antibiotics in agriculture, development of fast and reliable tests to identify the causative agent and its resistance pattern which would allow for a more targeted treatment, and public awareness and education on the dangers of antibiotic misuse and overuse (Aminov, 2010; Davies and Davies, 2010; Michael et al., 2014). More importantly, there is a dire need for the development of new safe and efficient drugs and alternative therapies, a problem that will require more private and public investment in research (Alanis, 2005).

1.1.2.2. Mechanisms of Antibiotic Resistance

Antibiotic resistance is a natural phenomenon. In fact, even before the widespread use of penicillin, observations made by Abraham and Chain suggested that bacteria could destroy penicillin (Abraham and Chain, 1940). Over the years, the continued selective pressure led to the emergence of bacteria exhibiting different resistance mechanisms than that initially identified for penicillin but, overall, resistance mechanisms can be divided into three categories: 1) Inactivation or modification of the antibiotic molecule; 2) Mutation or substitution of the target; and 3) Decreased uptake or efflux of antibiotic (Table 1.1).

The best-known example of antibiotic inactivation are beta-lactamases. This group of enzymes is very diverse, varying in physical/chemical properties and spectrum of activity (Bush et al., 1995). They are responsible for the inactivation of beta-lactam antibiotic classes, which includes penicillins, cephalosporins, monobactams, and carbapenems. Bacteria expressing these enzymes export it into the periplasmic space where the antibiotic is inactivated through the hydrolysis of the beta-lactam ring. Presently, one of the biggest concerns is the emergence of extended-spectrum beta-lactamases (ESBLs). Initially detected in Klebsiella pneumoniae (K. pneumoniae) (Bradford, 2001), these enzymes have since spread to other members of the Enterobacteriaceae family, such as Escherichia coli (E. coli), and are currently widely disseminated and responsible for many 'difficult-to-treat' infections (Lau et al., 2008; Croxall et al., 2011). Alternatively, antibiotic modifications can be achieved by addition of an adenylyl, phosphoryl, or acetyl groups to the molecule through the action of nucleotidyltransferases, phosphotransferases, and acetyltransferases, respectively (Alekshun and Levy, 2007). Many aminoglycosides, such as streptomycin and gentamicin, are inactivated through this mechanism. Another example is chloramphenicol, which is inactivated by the action of a chloramphenicol acetyltransferase that is usually encoded by the cat gene.

Owing to the specificity of the antibiotic:target interaction, subtle structural changes in the cellular target can prevent said interaction while still allowing the target to maintain normal function. For example, high-level resistance to fluoroquinolones in E. coli is mainly attributed to mutations in genes encoding subunit A of DNA gyrase (gyrA) (McDermott et al., 2003; Alekshun and Levy, 2007). Structural alterations in bacterial lipopolysaccharide (LPS) have also enabled K. pneumoniae to evade the action of polymyxins: mutations in mgrB result in increased synthesis of sugar 4-amino-4-deoxy-L-arabinose (L-ara4N), and its insertion in the lipid A moiety of LPS results in an altered target (Cannatelli et al., 2013; Cannatelli et al., 2014; Poirel et al., 2015). Bacteria can also evade antibiotic toxicity through expression of alternative forms of the targeted enzyme. The prototypical example is a penicillin-binding–protein (PBP) variant in methicillin-resistant Staphylococcus aureus (MRSA). This variant is encoded by mecA and exhibits low affinity for derivatives of penicillin, and cell wall biosynthesis therefore remains unaffected by exposure to these beta-lactam antibiotics (Alekshun and Levy, 2007).

With the exception of polymyxins, all antibiotics currently available target intracellular bacterial proteins. As such, efficacy is dependent on whether the antibiotic reaches the target in sufficient quantity. Bacteria can prevent intracellular accumulation of the antibiotic by changing membrane permeability or through the export of the antibiotic by efflux pumps. The latter can be specific to an antibiotic or antibiotic class, or can be promiscuous and capable of exporting a wide array of antibiotics resulting in a multidrug-resistant phenotype (McDermott et al., 2003; Džidić et al., 2008). Interestingly, recent studies have shown a synergy between efflux pumps and mutations in intracellular drug targets (Fange et al., 2009; Lovmar et al., 2009). Lovmar and colleagues (Lovmar et al., 2009) showed that mutations in the L22 protein of the 50S subunit of the E. coli ribosome, conferring erythromycin resistance, was only effective in a drug efflux pump proficient E. coli strain, whilst in an E. coli strain unable to effectively export antibiotic, susceptibility to erythromycin was similar to that observed in the E. coli strain without the ribosomal mutation, i.e. sensitive to erythromycin. This shows that drug efflux deficiency can “mask” antibiotic resistance arising from drug target mutations. Furthermore, it also shows that inhibition of efflux pumps of pathogenic bacteria with altered cytoplasmic drug targets, arising due to mutation, could provide an alternative therapy to fight antibiotic resistant bacterial infections.

Table 1.1 – Targets and common resistance mechanism for different antibiotic classes.

Antibiotic class	Target	Resistance mechanism
Aminoglycosides (Streptomycin, Gentamycin)	Protein synthesis	Antibiotic modification
Beta-lactams (Penicillins, Monobactams, Cephalosporins, Carbapenems)	Cell wall synthesis	Hydrolysis; Target modification/substitution
Phenicols (Chloramphenicol)	Protein synthesis	Antibiotic modification
Fluoroquinolones (Ciprofloxacin)	DNA Replication	Target modification
Glycopeptides (Vancomycin)	Cell wall synthesis	Target modification/substitution
Polypeptides (Polymyxins)	Cell membrane	Target modification/substitution; Efflux
Pyrimidines (Trimethroprim)	Folic acid metabolism	Target modification/substitution; Efflux
Rifamycins (Rifampin)	Transcription	Target modification/substitution; Efflux
Sulphonamides	Folic acid metabolism	Target modification/substitution; Efflux
Tetracyclines	Protein synthesis	Target modification/substitution; Efflux

1.1.2.3. Genetics of Antibiotic Resistance

Resistance to antibiotics can be intrinsic (natural) or acquired. In intrinsic resistance, the bacterium exhibits the innate ability to resist the activity of specific antibiotics mediated by, for example, the bacterial outer membrane or by efflux pumps (Henriques Normark and Normark, 2002). However, studies have shown that there are many other naturally-occurring genes in different bacterial species that also contribute to an antibiotic-resistant phenotype. One such example is the chromosomal-encoded AmpC beta-lactamase of E. coli, which confers resistance to many beta-lactam antibiotics (Alekshun and Levy, 2007). Interestingly, work by Adam et al. (2008) suggests that epigenetic effects occurring during exposure to low concentrations of ampicillin are responsible for further activation AmpC expression, usually poorly expressed in E. coli and thus unable provide substantial protection to ampicillin, thus resulting in a more potent antibiotic resistance. This study by Adam and colleagues further shows the complexity of antibiotic resistance.

Acquired resistance arises through mutations in chromosomal genes, or horizontal gene transfer (HGT), via transduction (transfer of genetic material using a bacteriophage as a vector), conjugation (direct transfer between bacterial cells through the pilus produced by the donor cell), or transformation (direct uptake of exogenous DNA) (McDermott et al., 2003; Alekshun and Levy, 2007; Džidić et al., 2008), During HGT resistance genes are carried on mobile genetic elements (plasmids, transposons, and integrons) and acquired by the host bacterium from other bacterial species. Plasmid-mediated transmission of resistance genes is, by far, the most common form of HGT and main contributor to antibiotic resistance among clinical isolates (Davies and Davies, 2010). Plasmids are extra-chromosomal DNA segments that replicate independently of the hosts chromosome, can be transferred to other bacteria and often carry genes that provide the host with a selective advantage, such as resistance to an antibiotic (McDermott et al., 2003) Moreover, plasmids can also provide a vehicle for other mobile genetic elements, such as transposons and integrons. Transposons are mobile genetic elements which can be incorporated into a plasmid or the hosts chromosome via the action of the site-specific transposases encoded within the transposon (Henriques Normark and Normark, 2002; McDermott et al., 2003; Alekshun and Levy, 2007). Integrons represent an interesting situation and provide a unique, albeit problematic, role to the antibiotic resistance problem. Integrons are DNA elements that promote the capture of one or more resistance genes to form a cluster that is under the control of a single strong promoter. Hence, due to this co-expression, exerting a selective pressure with one antibiotic will also select the remaining adjacent genes, resulting in a multidrug resistant phenotype (Henriques Normark and Normark, 2002; McDermott et al., 2003; Džidić et al., 2008; Davies and Davies, 2010). Taken together, the existence of different mobile genetic elements and modes of transmission, combined with the increasing selective pressure caused by the growing use of antibiotics, resulted in the perfect set of conditions that gave rise to the alarming emergence and dissemination of antibiotic resistance currently observed.

It is important to note that acquisition and expression of resistance determinants genetically encoded is not the only method of antibiotic resistance. Bacteria can also develop a tolerant phenotype, i.e. alter their physiology and metabolism in response to environmental conditions which result in an antibiotic resistant phenotype (adaptive resistance). Persister cells are a prime example of this. Persister cells are a phenotypic variant that forms within a bacterial population (Lechner et al., 2012; Lewis, 2013). Whilst the mechanism by which they form is still not well understood, their metabolically

inactive phenotype allows for persister cells to survive treatment with antibiotics (e.g. Fluoroquinolones target DNA synthesis and, thus, are only effective against actively dividing cells) (Lewis, 2013). Another mechanism of adaptive resistance is epigenetic inheritance (Adam et al., 2008): DNA methylation, resulting in different gene expression patterns, and methylation of bacterial ribosomal RNA (rRNA) have both been shown to lead to the development of drug resistance (Motta et al., 2015; Manderwad, 2017).

1.2. Nitric Oxide

1.2.1. Physical and chemical properties of nitric oxide

Nitric oxide (NO), discovered by Joseph Priestly in 1772, is in gaseous form under atmospheric conditions and for a long time it was thought that it was merely a product of pollution. It wasn't until the 1980s that the role of NO in biological systems started to unravel.

In mammals, NO is synthesized by nitric oxide synthase (NOS), which converts the amino acid L-arginine into NO and citrulline, and is involved in critical roles, such as vasoregulation, smooth muscle relaxation, platelet aggregation, and neurotransmission (Snyder and Bredt, 1992; Vallance, 2003).

The reactivity of NO is highly dependent on its physical and chemical properties. NO is a small diatomic molecule of lipophilic nature and high diffusivity (Hughes, 2008). However, its unpaired electron is the most significant property of NO conferring it its radical natural and determining its high reactivity (Hughes, 2008; Lancaster Jr, 2015) and, consequently, its short half-life (5-15 seconds) (Kröncke et al., 1997; Lancaster Jr, 1997; Hughes, 2008). Due to the presence of the unpaired electron NO displays high chemical reactivity towards other free radicals, such as superoxide, giving rise to higher reactive species with different biological consequences (Mateo and de Artiñano, 2000; Hughes, 2008). NO can also react with transition metals, such as iron, copper, and zinc, an interaction which results in the formation of a metal-nitrosyl complex which may lead to changes in the function of the targeted protein. A prime example is the interaction with soluble guanylyl cyclase (sGC), a well-known intracellular receptor of NO in mammals. The binding of NO to the haem prosthetic group of sGC results in an increase of cGMP levels, which in turn regulates downstream processes involved in smooth muscle relaxation, vasodilatation, and neurotransmission (Nisbett and Boon, 2016). NO can also react with thiol groups of molecules, forming S-nitrosothiols, compounds which can either be an inert form of NO storage but also a S-nitrosating agent, thus capable of

altering or inhibiting the function of other target proteins (MacMicking et al., 1997; Schindler and Bogdan, 2001).

Whilst its reactivity, high rate of diffusion, and lipophilic nature provide NO with the necessary properties to carry out its important role as a messenger molecule, it is important to note that in high concentrations NO is highly toxic. Indeed, NO has been implicated in many pathophysiological states including septic shock, hypertension, and neurodegenerative diseases (Vallance, 2003; Pacher et al., 2007). As such, its synthesis must be tightly regulated to prevent cytotoxicity. However, high levels of NO are known to be produced by iNOS, the inducible NOS expressed by cells of the mammalian immune system (macrophages and neutrophils) (Schairer et al., 2012; Nisbett and Boon, 2016), in response to infection (see section 1.2.2.).

1.2.2. Nitric oxide and immunity

An important feature of NO, and of particular interest in this antibiotic resistance era, is its antimicrobial activity. Immune cells such as macrophages and neutrophils express the inducible form of NOS (iNOS) upon activation with proinflammatory cytokines (Figure 1.2), which in turn produces NO from L-arginine. The highly reactive nature of NO makes the biochemistry and antimicrobial activity of NO very complex. On its own, NO can strongly bind to the iron of haem groups and iron-sulphur ([Fe-S]) clusters, both important cofactors in a plethora of bacterial proteins (Wink et al., 2011). The destruction of [Fe-S] clusters by NO prompts the release of ferrous iron (Fe^{2+}), which in combination with hydrogen peroxide (H_2O_2) leads to formation of the highly toxic hydroxyl radical (Kröncke et al., 1997). However, it is the ability to react with other free radicals and create other nitrogen oxides that makes NO so toxic. Peroxynitrite ($ONOO^-$) is a reactive nitrogen species (RNS) formed through the fast reaction of NO with superoxide (O_2^-). It rapidly reacts with lipids and proteins, limiting its ability to diffuse into target cells but nonetheless has a much greater cytotoxicity than NO and superoxide alone. Peroxynitrite can also lead to the formation of other toxic RNS, including dinitrogen trioxide (N_2O_3) and nitrogen dioxide (NO_2) (Bogdan, 2001; Pacher et al., 2007). Additionally, peroxynitrite is more effective at producing highly-toxic hydroxyl radicals than the Fenton reaction, which forms hydroxyl radicals through the reaction of hydrogen peroxide (H_2O_2) with ferrous iron (Fe^{2+}) (Pacher et al., 2007). NO can also react with glutathione (GSH) to form S-nitrosoglutathione (GSNO), a S-nitrosating agent involved in signalling and NO storage in mammalian cells, but also toxic to bacteria due to its ability to nitrosylate cysteines. Hence, NO is capable of directly and indirectly

damaging or inhibiting important cellular functions, such as damaging DNA, inhibiting protein synthesis, inhibiting protein function through S-nitrosylation or disruption of [Fe-S] clusters and haem groups, and disruption of cellular membrane through lipid peroxidation. Although the toxic effects of NO contribute to the host defence against invading pathogens, they are also toxic to mammalian cells in high concentrations. Protection from the toxic effects of NO and related RNS in mammalian cells occurs through formation of inert NO-storage/transport compounds, which also allow for a more efficient and far-reaching NO signalling, since the reactivity of NO towards a plethora of cellular components and radicals limits its diffusion (Kröncke et al., 1997; MacMicking et al., 1997; Mateo and de Artiñano, 2000; Villanueva and Giulivi, 2011), and through compartmentalization (e.g. acidic compartments such as lysosomes), which restricts the toxic effects of NO and its RNS derivatives to a small sub-cellular location (Villanueva and Giulivi, 2011).

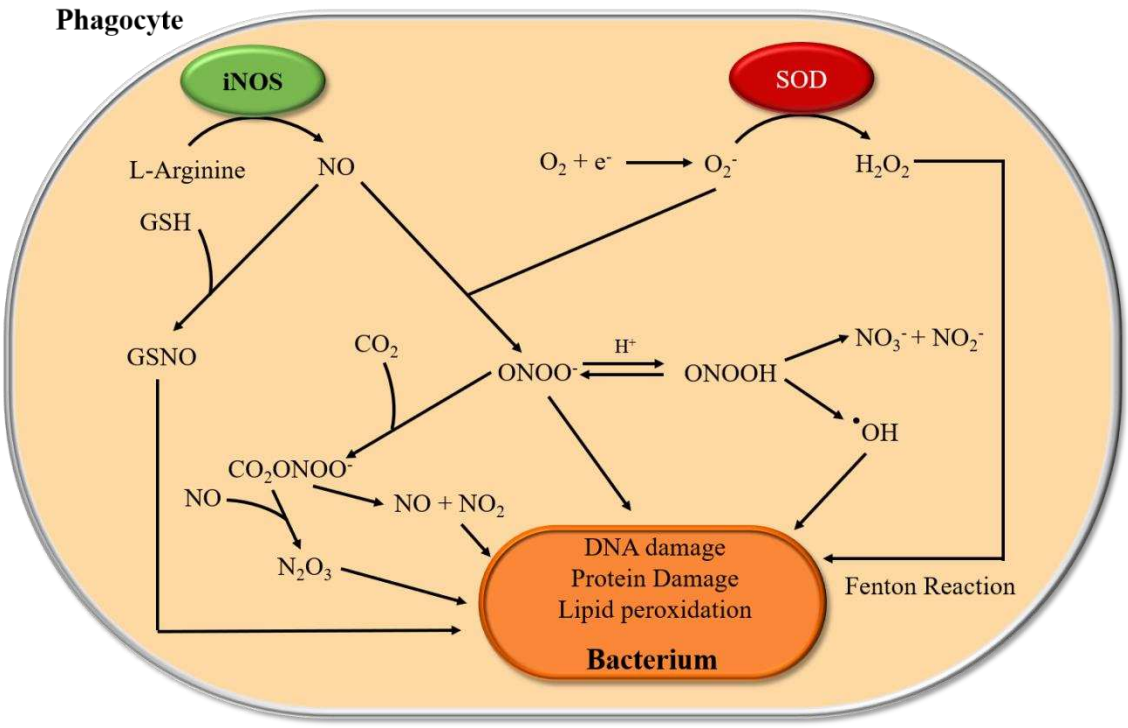

Figure 1.2 – Chemistry of nitric oxide. In the mammalian immune system, NO is produced by iNOS and rapidly reacts with superoxide (O_2^-) to form peroxynitrite. ($ONOO^-$), a highly toxic RNS capable of forming other RNS through reaction with carbon dioxide (CO_2) and hydroxyl radicals ($^{\cdot}OH$). NO also reacts with glutathione (GSH) to form S-nitrosoglutathione (GSNO), a S-nitrosating agent. All these species combined can lead to DNA damage, protein damage and peroxidation of membrane lipids, and are an effective means of combating bacterial infections.

It is important to note that the role of NO in immunity extends beyond its antimicrobial properties: NO synthesized by iNOS also exerts a regulatory function, most notably a role in the maturation and regulation of the activity of Natural Killer (NK) cells (Coleman, 2001; Wink et al., 2011), required for a robust immune response.

1.2.3. Nitrosative stress in E. coli

Bacteria encounter NO in a wide range of environments: during infection, neutrophils and activated macrophages are a source of NO which is used to combat invading pathogens; NO can also be produced at low concentrations as a by-product of bacterial anaerobic respiration (Bender and Conrad, 1994) or by bacterial homologues of the mammalian NOS (Crane, 2008; Sudhamsu and Crane, 2009; Crane et al., 2010).

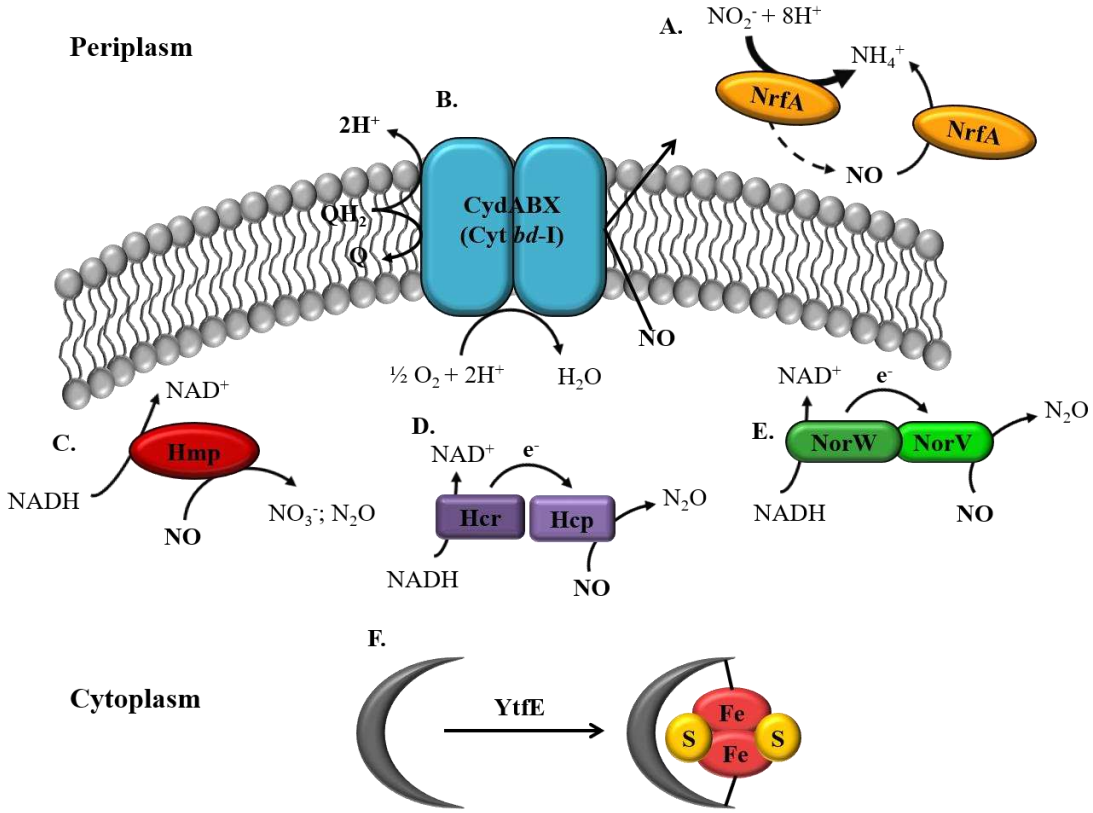

Figure 1.3 – NO resistance mechanisms of E. coli. A) Periplasmic cytochrome c nitrite reductase (NrfA, the catalytic subunit of the Nrf complex) reduces nitrite to ammonium, releasing NO in the process, which in turn can be also converted to ammonium by NrfA; B) Cytochrome bd-I is a NO-tolerant respiratory oxidase that facilitates aerobic respiration; C) Flavohaemoglobin Hmp converts NO to nitrate or to nitrous oxide in the presence or absence of oxygen respectively; D) The hybrid cluster protein, Hcp, and its partner reductase, Hcr, convert NO to nitrous oxide under anoxic conditions; E) Flavorubredoxin, NorV, and its partner reductase, Flavorubredoxin reductase NorW, converts NO to nitrous oxide under anaerobic conditions; F) YtfE, a di-iron protein, repairs iron-sulphur clusters damaged by nitrosative stress.

Like many other bacteria, E. coli has a remarkable capacity to respond to environmental stresses through a series of well-coordinated mechanisms. Thus, the existence of mechanisms in E. coli that helps to circumvent the toxic effects of NO and its derivatives is unsurprising (Figure 1.3). Studies have shown that bacterial NO detoxification increases in response to NO or NO-releasing molecules such as GSNO (Hausladen et al., 1998; Flatley et al., 2005; Jarboe et al., 2008). E. coli possesses various NO-detoxifying enzymes, including the periplasmic cytochrome c nitrite reductase (NrfA), the cytoplasmic flavohaemoglobin (Hmp), flavorubredoxin (NorV), and hybrid-cluster protein (Hcp). Alongside them there are mechanisms that repair the damage caused by NO, such as via the action of YtfE which repairs [Fe-S] clusters. Furthermore, the NO-tolerannt cytochrome bd-I respiratory oxidase facilitates aerobic respiration in the presence of NO. These mechanisms are discussed in more detail below.

1.2.3.1. Flavohaemoglobin Hmp

Flavohaemoglobins are widely distributed microbial proteins comprising two domains: a N-terminal globin-like domain containing haem b, and a C-terminal ferredoxin-$NADP^+$ reductase (FNR)-like domain with binding sites for FAD and NAD(P)H. As the best studied microbial flavohaemoglobin, the role of E. coli Hmp during nitrosative stress has been intensely studied. Encoded by the hmp gene in E. coli, microarray studies have shown that Hmp expression is up-regulated after cells are exposed to NO (Justino et al., 2005), GSNO (Mukhopadhyay et al., 2004; Flatley et al., 2005), and NO-releasing compounds (NOC) (Pullan et al., 2007), both aerobically and anaerobically. In the presence of oxygen this cytoplasmic protein catalyses a NO dioxygenation reaction by binding O_2 at the ferrous haem giving rise to a ferrous (Fe^{2+}) haem:superoxide intermediate that rapidly reacts with NO and produces nitrate. The FAD cofactor at the C-terminal catalyses the reduction of the now ferric (Fe^{3+}) haem to its original ferrous form through a sequential electron transfer from NADH to the bound haem in the globin-like domain (Figure 1.4). A hmp mutant was shown to be unable to catalyse NO consumption (Hausladen et al., 1998) and exhibited a more pronounced growth inhibition compared to wild-type cells when in presence NO or S-nitrosothiols (Gardner et al., 1998; Hausladen et al., 1998). NO consumption by Hmp was inhibited by cyanide, indicating that the NO reaction occurs at the oxyhaem, and possibly arises due to interference of cyanide in the reduction of ferric haem to ferrous haem (Hausladen et al., 1998). Additionally, Hmp was found to have higher affinity for NADH rather than NADPH, with K_m for NADPH being 10-fold higher than that of NADH (Anjum et al.,

1998). In addition, Wu et al. (2004) and Membrillo-Hernández et al. (1996) demonstrated formation of superoxide by Hmp during aerobic NO turnover in vitro and in vivo, the latter accomplished by monitoring the transcription of sodA (superoxide dismutase), which is up-regulated in the presence of superoxide. Under anoxic conditions, Hmp catalyses the NADH-dependent reduction of NO to nitrous oxide (N_2O) with formation of a nitrosyl intermediate complex (Hausladen et al., 1998; Kim et al., 1999). Taken together these findings support the proposed reaction described and presented in figure 1.4.

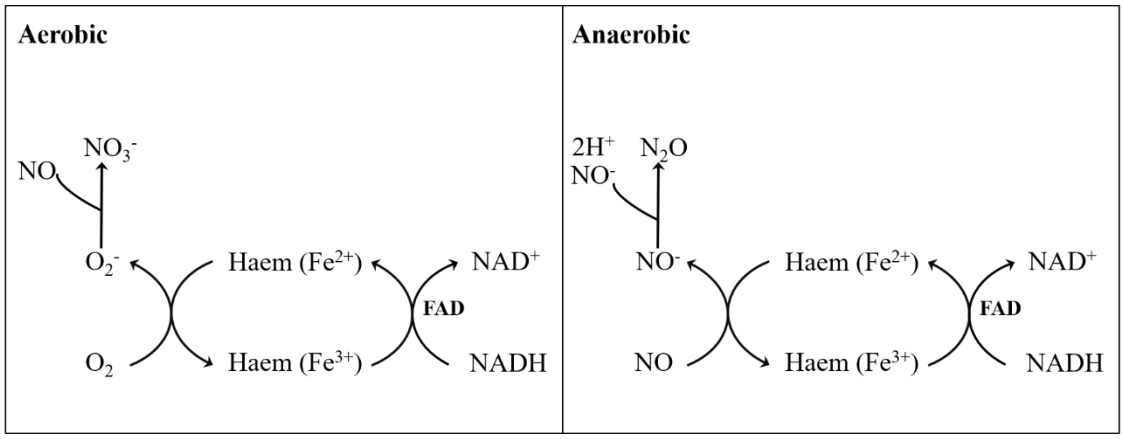

Figure 1.4 – NO detoxification by Hmp. Electrons are transferred from NADH to FAD and then to the haem group where under aerobic conditions (left) O_2 is reduced to form superoxide, which in turn reacts with NO (oxygenation reaction) yielding nitrate. Under anaerobic conditions (right), ferrous heam reacts with NO giving rise to a nitrosyl species. Further reaction yields nitrous oxide as the final product.

NO inhibits the function of many bacterial proteins by binding to their cofactors, such as haem and [Fe-S] clusters. This includes the haem-binding respiratory oxidase complexes involved in aerobic respiration, which have been shown to be inhibited in E. coli by NO in an O_2-dependent manner, i.e. respiratory inhibition is more profound at lower oxygen tensions (Yu et al., 1997). Hmp is able to protect aerobic respiration catalysed by cytochrome bo' or cytochrome bd from NO-mediated inhibition (Stevanin et al., 2000). Respiration rates in cells lacking either cytochrome bd or cytochrome bo' was measured following the addition of NO gas and it was shown that inhibition of respiration catalysed by either cytochrome was more profound in a hmp mutant, thus establishing the importance of a functional Hmp in alleviating NO-mediated respiratory inhibition (Stevanin et al., 2000). Hmp has also been shown to protect the activity of aconitase, an important enzyme of the citric acid cycle with a [4Fe-4S] cofactor, from NO-mediated inhibition (Gardner and Gardner, 2002).

The protection against NO that is conferred by Hmp make it a valuable virulence factor during infection. In Salmonella, the virulence of different mutant strains was investigated in a mouse infection model, which showed that compared to the parental strain, the hmp mutant exhibited an almost complete loss of virulence, which was restored after addition of an iNOS inhibitor, hence suggesting that loss of virulence was due to inability of mutant to cope with RNS produced by the host during infection (Bang et al., 2006). In E. coli, survival of a hmp mutant is significantly reduced in both murine macrophages and human neutrophils (Shepherd et al., 2016). In addition to NO tolerance, the generation of reactive ROS by Hmp (Membrillo-Hernández et al., 1996; Mills et al., 2001; Wu et al., 2004) leads to intracellular oxidative stress and, as such, some systems involved in the response to oxidative stress are activated (Membrillo-Hernandez et al., 1999). This shows that not only is the presence of a functional Hmp important during infection for protection of bacterial cells against host-derived RNS, but it is also important for the expression of other important virulence factors and induction of a more robust SOS response.

Overexpression of Hmp has been shown to exacerbate oxidative stress in both Salmonella (Bang et al., 2006; McLean et al., 2010) and E. coli (Membrillo-Hernández et al., 1996; Mills et al., 2001; Wu et al., 2004). Thus, Hmp expression needs to be tightly regulated to prevent intracellular oxidative stress (Figure 1.5). Fumarate nitrate reduction (FNR) regulator is a member of the cyclic-AMP receptor family of transcriptional regulators and a repressor of Hmp expression (Poole et al., 1996). The [4Fe-4S] cluster of FNR is sensitive to both O_2 and NO, with both inhibiting DNA-binding activity of FNR and allowing de-repression of genes involved in anaerobic metabolism and respiration, including hmp (Green et al., 2014). FNR is able to detect NO levels as low as 5 µM, making it a relevant NO-sensor in vivo (Cruz-Ramos et al., 2002). MetR is a transcriptional regulator involved in the control of genes encoding proteins that participate in methionine biosynthesis, and has also been implicated in the induction of the hmp gene by GSNO and sodium nitroprusside (SNP) (Membrillo-Hernández et al., 1998). Interestingly, microarray studies by Pullan et al. (2007) using NOC compounds to induce nitrosative stress revealed no upregulation of the met genes, which was attributed to GSNO and NOC compounds behaving differently with respect to homocycteine (Hcy), the cofactor of MetR: GSNO reacts with Hcy forming S-nitroso-Hcy and depleting the Hcy intracellular pool; in the absence of Hcy, MetR binds to the promoter of hmp and activates transcription (Membrillo-Hernández et al., 1998; Pullan et al., 2007). However, NO released by NOC compounds did not nitrosylate the homocysteine pool.

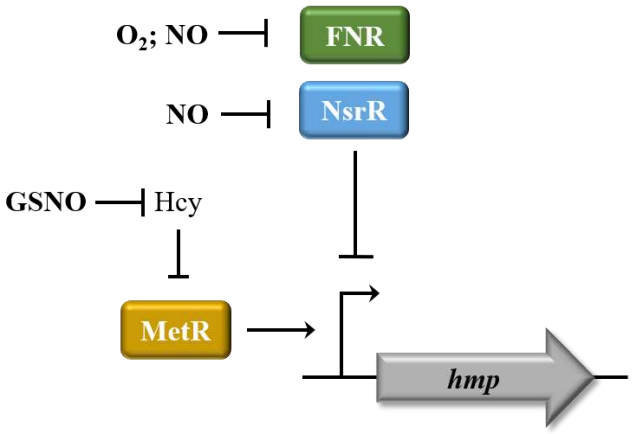

Figure 1.5 – Regulation of Hmp expression. FNR and NsrR are both negative regulators of hmp transcription. NO interacts with the [Fe-S] clusters of these transcriptional factors and prevents DNA-binding, leading to de-repression of hmp. MetR-dependent transcriptional activation of hmp was shown to occur only in the presence of nitrosating compounds, such as GSNO, which depletes the intracellular homocysteine pool resulting in MetR activation.

NsrR (Nitrite-sensitive repressor) is a NO-sensor with a [2Fe-2S] cluster that is nitrosylated by NO, which results in the formation of a cysteine-bound dinitrosyl iron complex that abolishes the DNA-binding activity of NsrR, resulting in de-repression of hmp transcription (Figure 1.5) (Filenko et al., 2007; Tucker et al., 2008).

1.2.3.2. Flavorubredoxin NorV and partner reductase NorW

Flavorubredoxin (FIRd) is encoded by the norV gene in E. coli and the NorV protein possesses three distinct domains: a N-terminal metallo-beta-lactamase domain containing a non-haem di-iron centre, a flavodoxin-like domain containing one FMN element, and a C-terminal rubredoxin (Rd)-like domain (Gomes et al., 2000; Gomes et al., 2002; Vicente et al., 2007). FIRd is associated with FIRd-reductase, a member of the NAD(P)H:rubredoxin oxireductase family of proteins encoded by the norW gene in E. coli. FIRd-reductase catalyses the transport of electrons from NADH to the Rd domain of FIRd, which then proceed to the FMN moiety followed by transfer to the di-iron site where they become available to efficiently reduce NO to nitrous oxide (Gomes et al., 2000; Gomes et al., 2002; Vicente et al., 2007) (Figure 1.6).

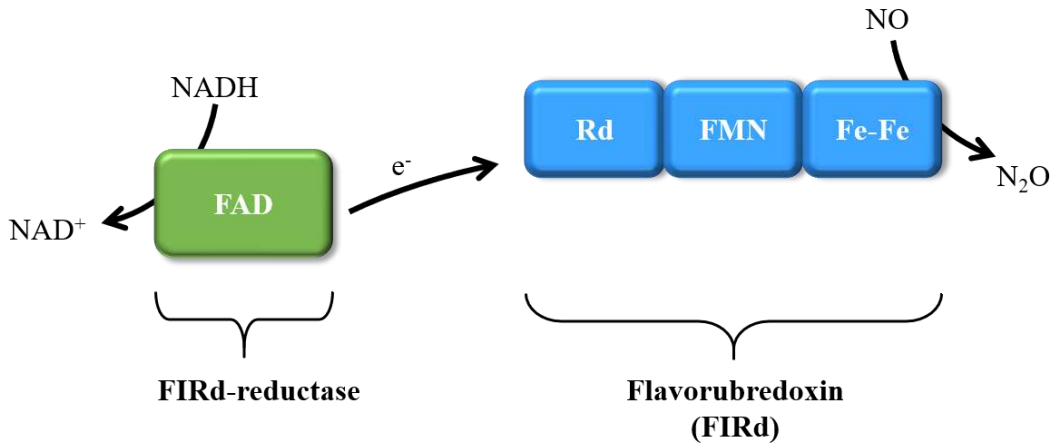

Figure 1.6 – NO reduction by NorVW. FIRd-reductase catalyses the electron transfer from NADH to FIRd, which in turn reduce NO to nitrous oxide. Sourced from Vicente et al. (2007).

Total RNA transcriptomics showed an increase in mRNA levels for norV and norW in response to GSNO (Mukhopadhyay et al., 2004; Flatley et al., 2005), NO (Justino et al., 2005), and NOC compounds (Pullan et al., 2007), in both aerobic and anaerobic conditions. Interestingly, studies using norV-lacZ and norW-lacZ fusions have shown that induction of norV and norW was significantly inhibited in fully aerated conditions (200- and 20-fold less for norV and norW, respectively, compared to anoxic conditions), and other studies have also revealed NorVW has higher NO-metabolizing activity under anaerobic conditions (Gardner et al., 2002). Combined with the observation by Gardner and Gardner (2002) that NO consumption in cells expressing high levels of Hmp is higher in the presence of oxygen, and only in the presence of oxygen was Hmp capable of protecting aconitase activity from NO-dependent inactivation, it was hypothesized that under anaerobic conditions NorVW plays a more predominant role in NO detoxification than Hmp. Conversely, Hmp was proposed to be more important in the presence of oxygen. This hypothesis was supported by studies that monitored Hmp and NorVW protein levels following exposure to NO in an anoxic environment: expression of NorV occurred immediately after NO-exposure and remained constant throughout the experiment, while Hmp expression reached maximal expression much later (Justino et al., 2005). Interestingly, deletion of both norV and hmp results in a severe impairment of growth in the presence of nitrosative stress under anoxic conditions, more so than in hmp or norV single mutants suggesting that despite the predominant role of NorVW in NO-detoxification in anaerobic conditions, Hmp still plays an important, albeit minor, role (Justino et al., 2005).

The NO-sensing transcription factor NorR, encoded by the norR gene in E. coli that is divergently transcribed from norVW, is responsible for NO-mediated regulation of the norVW operon (Figure 1.7). NorR has three domains: a N-terminal GAF domain containing a mononuclear non-haem iron which reversibly binds NO and is responsible for signal sensing (Gardner et al., 2003; D'Autréaux et al., 2005); a central AAA domain with ATPase activity; and a C-terminal DNA-binding domain (D'Autréaux et al., 2005; Spiro, 2007). Binding of NO stimulates the ATPase activity of the central AAA domain and initiates transcription of the norVW operon (D'Autréaux et al., 2005; Spiro, 2007).

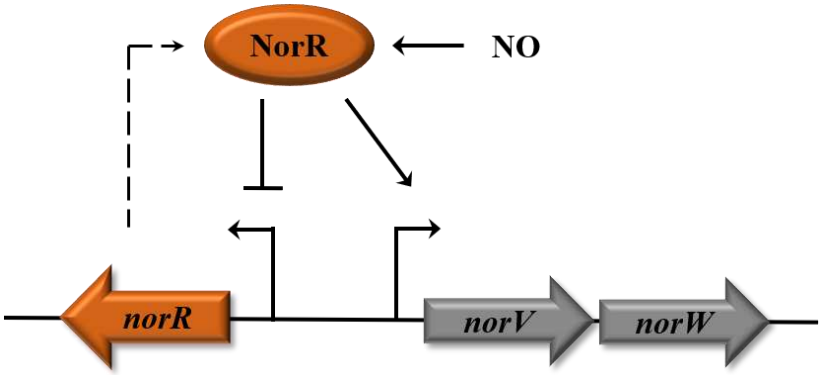

Figure 1.7 – NorRVW transcriptional unit. In the presence of NO, NorR is activated and initiates transcription of the norVW operon. Activated NorR is capable of self-regulation.

1.2.3.3. Hybrid-cluster protein system: Hcp-Hcr

The hybrid cluster protein (Hcp), encoded by hcp in E. coli, is a cytoplasmic protein of approximately 60 kDa with unique [Fe-S] cluster properties: it contains one conventional [2Fe-2S] cluster and a hybrid [4Fe-2S-2O] cluster (van den Berg et al., 2000; Aragão et al., 2008). Downstream the hcp gene, the gene hcr encodes a NAD(P)H oxidoreductase of approximately 34.6 kDa that binds a FAD cofactor and a [2Fe-2S] cluster (van den Berg et al., 2000). Hcr catalyses the reduction of Hcp in vitro in the presence of the electron donor NADH, to which Hcr demonstrates relatively high affinity (K_m=10 µM for NADH while K_m for NADPH is approximately 0.3 mM). Electrons are transferred from NADH to the hybrid [4Fe-2S-2O] cluster of Hcp via the [2Fe-2S] clusters of Hcr and Hcp, which are used in the subsequent reduction of NO to nitrous oxide (van den Berg et al., 2000).

Induction of Hcp-Hcr was shown to occur in both aerobic and anaerobic cultures exposed to either GSNO (Flatley et al., 2005) or NOC compounds (Pullan et al., 2007), however the rate of NO reduction by Hcp in cells grown aerobically was low, suggesting oxygen inactivates Hcp activity in vivo (Wang et al., 2016). In anoxic conditions, deletion

of hcp resulted in a NO-mediated growth impairment and loss of activity of aconitase and fumarase, two enzymes involved in central carbon metabolism that are dependent on functional [Fe-S] clusters (Wang et al., 2016). Despite the role in NO detoxification, Hcp inactivation is triggered by NO concentrations above 200 nM. Thus, it was suggested that Hcp-Hcr provides protection against nitrosative stress under anaerobic conditions only when NO concentrations are low and unable to cause substrate-mediated inactivation of Hcp (Karlinsey et al., 2012; Wang et al., 2016).

The hcp-hcr genes are regulated by FNR and NsrR. In an E. coli fnr mutant, exposure to NO-donor spermine NONOate is unable to induce transcription of hcp to wild-type levels, suggesting that FNR is responsible for the activation of hcp-hcr operon transcription under anaerobic conditions (Filenko et al., 2007; Wang et al., 2016). Furthermore, gel-shift assays showed binding of FNR to hcp promoter in vitro, further supporting the role of FNR in transcriptional regulation of hcp-hcr regulon (Filenko et al., 2007). In Salmonella, the putative consensus binding site of NsrR is present in the predicted promoter region of hcp-hcr operon, and microarray and qRT-PCR data showed it was a part of the NsrR regulon in this Gram-negative bacterium (Karlinsey et al., 2012). Moreover, a Salmonella nsrR mutant displayed a 678.1-fold induction of the hcp-hcr operon compared to wild-type (Karlinsey et al., 2012), with similar results obtained for a E. coli nsrR mutant (Filenko et al., 2007). In an assay involving a multi-copy plasmid containing the promoter of a known NsrR target, thus relieving NsrR-mediated repression of the target genes through titration of NsrR, a strong induction of hcp-hcr was observed (Filenko et al., 2007). Taken together this data shows that NsrR is a repressor of hcp-hcr operon.

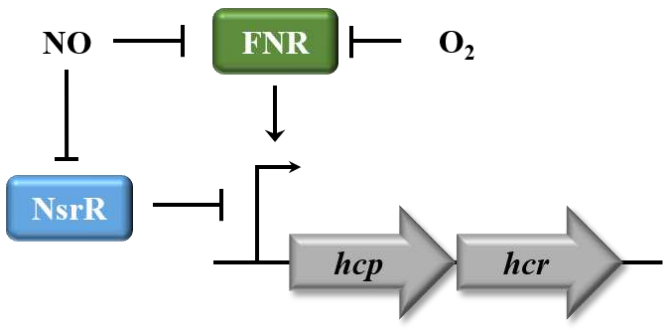

Figure 1.8 – Transcriptional regulation of the hcp-hcr operon. In the presence of NO, NsrR-mediated repression is lifted; FNR acts as a transcriptional activator under anaerobic conditions.

1.2.3.4. Detoxification of NO by NrfA

The periplasmic cytochrome c nitrite reductase of E. coli, NrfA, is a homodimeric protein containing five c-type haems per monomer. Expressed under microaerobic and anaerobic conditions in the presence of nitrate or nitrite (Wang and Gunsalus, 2000), NrfA catalyses the reduction of nitrite to ammonium (Darwin et al., 1993) via a NO intermediate (Figure 1.3). NO consumption by NrfA was observed by Poock et al. (2002) using an E. coli strain with a $nirA^-$ background to better assess the contribution of NrfA towards NO consumption. NirA is a cytoplasmic nitrite reductase expressed under microaerobic or anoxic conditions, and thus could mask the effect of NrfA on NO metabolism. Under aerobic conditions, the $nirA^-$ $nrfA^+$ strain reduced NO at a maximal rate 300 nmol of NO (mg of $protein^{-1}$ min^{-1}), whilst NO consumption was abolished in a $nirA^-$ $nrfA^-$ strain under aerobic condition, consistent with the absence of NrfA expression in these conditions (Poock et al., 2002). Furthermore, anaerobic growth of $nrfA^-$ strains has been shown to be more sensitive to NO than the parental strain, further suggesting a role for NrfA in NO tolerance (Poock et al., 2002; Pittman et al., 2007; van Wonderen et al., 2008). The periplasmic location of NrfA is well-suited for NO detoxification in vivo, metabolizing NO before it enters the cell. Interestingly, NrfA has also been implicated in NO production as a consequence of its anaerobic nitrite reductase activity (Corker and Poole, 2003). Nevertheless, the low NO levels produced by NrfA during anaerobic respiration of nitrite can be easily dealt with by Hmp and NorVW, preventing inactivation of FNR, an important transcriptional regulator of various important genes, including NrfA (Corker and Poole, 2003).

The gene encoding NrfA is positively regulated by FNR (Spiro, 2006). However, due to sensitivity of its [Fe-S] cluster, FNR is prone to NO-mediated inactivation resulting in NrfA down-regulation (Pullan et al., 2007), a result that is not consistent with its proposed protective role during nitrosative stress. A possible explanation for this phenomenon arose from studying the role of NrfA in Salmonella. Mills et al. (2008) showed that under NrfA-inducing conditions (i.e. anaerobic growth in minimal medium with glycerol as a carbon source and nitrate and fumarate as respiratory electron acceptors), NrfA is unable to protect Salmonella from NO in the absence of NorV and Hmp, suggesting that NrfA is not a vital component of the immediate response to NO under these conditions. Hence, whereas the NO-reductase activity of NrfA provides an advantage under conditions in which NrfA is already being expressed, its absence due to inactivation of FNR by NO does not affect cellular viability in response to nitrosative

stress. A microarray study has shown that nrfA transcription increases 2.2-fold in a nsrR mutant, suggesting that nrfA is a member of the NsrR regulon (Filenko et al., 2007).

1.2.3.5. Iron-sulphur cluster repair: YtfE

[Fe-S] clusters are prosthetic groups that are present in a variety of important bacterial proteins. Since NO is well-known to nitrosylate [Fe-S] clusters, it is unsurprising that bacteria possess systems capable of repairing the damage inflicted to these cofactors during nitrosative stress. In E. coli, YtfE is a member of the Repair of Iron Centres (RIC) family of proteins with a di-iron centre and aids in the tolerance of E. coli to nitrosative stress by repairing [Fe-S] clusters (Justino et al., 2006; Justino et al., 2007). Several microarray studies of total RNA have shown an increase in ytfE transcription in response to NO (Justino et al., 2005), GSNO (Mukhopadhyay et al., 2004; Flatley et al., 2005), and NOC compounds (Pullan et al., 2007), suggesting a protective role for YtfE during nitrosative stress. This hypothesis was further corroborated by Justino et al. (2005) when a ytfE E. coli mutant showed higher sensitivity than parental strain to 50 µM NO. Furthermore, activity of the [Fe-S] cluster containing enzymes aconitase and fumarase was diminished following exposure to NO in cells lacking ytfE (Justino et al., 2007). Importantly, activity of aconitase and fumarase was restored in the parental strain after a period of time, but cells lacking ytfE were unable to do so, suggesting that NO caused damage that was irreversible due to lack of a functional repair system (Justino et al., 2006; Justino et al., 2007). Deletion of ytfE in E. coli has also been shown to exhibit increased sensitivity to killing by human neutrophils and decreased survival in murine macrophages (Shepherd et al., 2016).

In E. coli, the ytfE gene has been shown to be a part of both the FNR and NsrR regulons (Figure 1.9). Filenko et al. (2007) showed ytfE to be one of the most up-regulated genes in response to NsrR titration, strongly implicating NsrR as a transcriptional repressor of ytfE. This was also inferred for Salmonella, as ytfE exhibits a 314.5-fold induction in the absence of nsrR (Karlinsey et al., 2012). In a fnr strain of E. coli, ytfE mRNA levels are elevated (Justino et al., 2006), although no FNR binding site motif was found in the putative promoter of ytfE, suggesting the possibility of an indirect mechanism for FNR-mediated regulation (Justino et al., 2006).

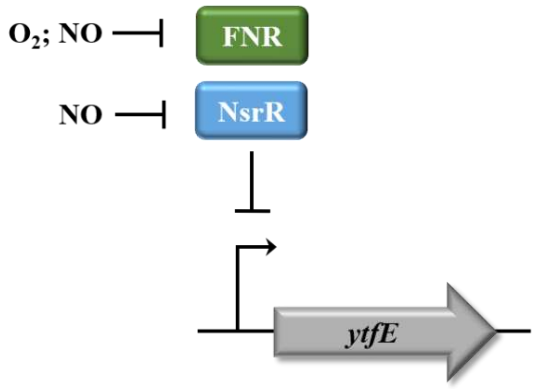

Figure 1.9 – FNR- and NsrR-dependent transcription of ytfE. Both transcription factors FNR and NsrR have been implicated in regulation of ytfE expression, with the effects of FNR possibly being indirect.

1.2.3.6. Cytochrome bd-I and NO tolerance

One key target of NO are respiratory oxidases such as cytochrome bo' and cytochrome bd-I, the latter containing three haem cofactors: b_{558}, b_{595}, and d. (Goldman et al., 1996). Both cytochromes are expressed in the presence of oxygen, with cytochrome bo' exhibiting maximal expression under aerobic conditions and cytochrome bd-I achieving maximal expression in microaerobic environments (Cotter et al., 1990; Fu et al., 1991; Cotter et al., 1997). This differential expression allows for the best suited cytochrome to be expressed in different conditions, with cytochrome bd-I being more suitable under microaerobic conditions due to its high affinity for oxygen, with a K_m of 3-8 nM (D'mello et al., 1996) compared to a K_m of 0.016-0.085 µM for cytochrome *bo'* (D'Mello et al., 1995). This fine-tuned expression of cytochrome bd-I, encoded by the genes cydABX in E. coli, is achieved through the combined effects of FNR and the oxidative-sensing two-component system ArcAB (aerobic respiration control proteins) (Figure 1.10). In oxygen rich environments, neither FNR nor ArcAB are active. However, when oxygen levels drop, ArcB phosphorylates ArcA which binds to the promoter of the cydABX operon, initiating transcription. When oxygen is absent, FNR is activated and mediates cydABX repression. The antagonistic effects of ArcA and FNR on cydABX were demonstrated by Tseng et al. (1996) by determining expression of a cyd-lacZ fusion in a range of different oxygen concentrations in both fnr and arcA single mutants. To date, induction of cydABX expression in response to nitrosative stress has only been shown to occur under anoxic conditions (Pullan et al., 2007) and it is in agreement with the current model for cydABX regulation: FNR inactivation by NO will impede repression of the operon under anaerobic conditions.

The correct assembly of cytochrome bd-I is dependent on the cydDC operon (Georgiou et al., 1987; Poole et al., 1994; Goldman et al., 1996), which encodes a heterodimeric ABC transporter (Cook et al., 2002) important for the maintenance of the periplasmic redox balance through export of the low molecular weight thiols glutathione and cysteine (Pittman et al., 2002; Pittman et al., 2005). Deletion of the cydC gene in E. coli results in a non-functional cytochrome bd-I due to absence of haem incorporation (Georgiou et al., 1987). Predictably, a cydDC mutant strain exhibits many of the same phenotypic traits as a cydAB mutant, namely temperature sensitivity, hypersensitivity to hydrogen peroxide, and loss of viability in stationary phase under aerobic conditions (Poole et al., 1994; Goldman et al., 1996; Siegele et al., 1996). All of these phenotypes were shown to be corrected by overexpression of cydAB from a plasmid (Goldman et al., 1996), suggesting the phenotypes can be solely attributed to loss of a functional cytochrome bd-I in a cydDC mutant.

Cytochrome bd-I was first thought to be involved in NO tolerance after a transcriptomic study revealed cydA and cydB to be upregulated after exposure to a NOC compound under anoxic conditions (Pullan et al., 2007). Growth and respiratory rates of E. coli strains lacking either cytochrome *bo'* (cyo^- cyd^+) or cytochrome bd-I (cyo^+ cyd^-) in response to NO were assessed, with data revealing a significant growth inhibition of cyo^+ cyd^- compared to wild-type (Mason et al., 2009; Shepherd et al., 2016). IC_{50} values for NO were greater in cyo^- cyd^+ cells, meaning cytochrome bd-I has higher tolerance for NO than cytochrome *bo'* (Mason et al., 2009). Moreover, a faster respiratory recovery was observed in cytochrome bd-I, with NO dissociating faster from cytochrome bd-I resulting in weaker binding of NO to cytochrome bd-I (NO off rate (k_{off}) = 0.163 s^{-1}) compared to cytochrome *bo'* (NO off rate (k_{off}) = 0.03 s^{-1}) (Mason et al., 2009). In E. coli, a cydAB mutant exhibited increased susceptibility to killing by human neutrophils and murine macrophages and showed impaired virulence in a mouse urinary tract infection model (Shepherd et al., 2016), revealing its importance during infection. The contribution of CydDC towards cytochrome bd-I-mediated NO tolerance has also been investigated. Interestingly, deletion of cydDC resulted in a more profound NO-sensitive phenotype than the one exhibited by the cytochrome bd-I mutant, and it was suggested the low molecular weight thiols exported by CydDC to the periplasm interact with NO in the periplasm and restrict the flow of NO into the cytoplasm (Holyoake et al., 2016). Taken together, these results show that cytochrome bd-I and the ABC transporter CydDC both provides a physiological advantage in the presence of nitrosative stress.

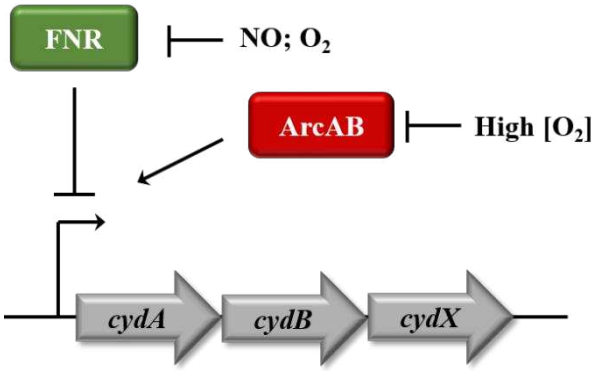

Figure 1.10 – Transcriptional regulation of cydABX. Under aerobic conditions, neither FNR nor ArcAB are active and expression of cydABX is kept at very low basal levels. As the oxygen in the environment decreases, ArcB phosphorylates ArcA which binds to the promoter and induces transcription of the cydABX operon. In an anaerobic environment, FNR is activated and represses expression of cydABX. In the presence of NO, FNR is inactivated, resulting in an abolishment of FNR-mediated repression of cydABX transcription under anaerobic conditions.

1.2.3.7. Secondary NO sensors: Fur, OxyR, and SoxR

Transcriptomic analysis of the bacterial response to nitrosative stress (Mukhopadhyay et al., 2004; Justino et al., 2005; Pullan et al., 2007) revealed up-regulation of genes from specific regulons controlled by transcriptional regulators with primary functions unrelated to nitrosative stress: these were therefore described as secondary NO sensors. A prototypal example of such a sensor is FNR, which primarily senses oxygen. However, due to its involvement in the regulation of many of the NO-tolerant mechanisms described so far, FNR will not be described in this section.

The ferric uptake regulator (Fur) is an iron-dependent transcriptional repressor responsible for sensing iron limitation: in an iron-limited environment Fur is inactivated due to lack of a ferrous iron cofactor (Fe^{2+}), allowing de-repression of genes involved in iron acquisition (Andrews et al., 2003). A possible role in responding to nitrosative stress was suggested for Fur after transcriptomic studies revealed de-repression of Fur-targeted genes in response to GSNO (Mukhopadhyay et al., 2004) and NO (Justino et al., 2005): notable examples include genes of the suf operon, which encode the machinery necessary for assembly of [Fe-S] clusters. This contrasts with the data obtained for defined media transcriptomic studies, which indicated that Fur was not involved in the response to GSNO (Flatley et al., 2005) or NOC compounds (Pullan et al., 2007). It was suggested the results observed in the work of Justino et al. (2005) and Mukhopadhyay et al. (2004) are an artefact due to poor bioavailability of iron (Flatley et al., 2005). In vitro studies revealed inactivation of Fur by NO (D'Autreaux et al., 2002; D'Autréaux et al., 2004)

providing further insight into the possible role of Fur during nitrosative stress. However, whether Fur has a more prominent role in NO tolerance or if the Fur-mediated effects during nitrosative stress are a consequence of Fur being a target of NO are still to be determined.

OxyR (oxidative stress regulator) is a thiol-containing transcriptional regulator responsible for primarily coordinating bacterial response to hydrogen peroxide. However studies have shown OxyR can be activated by S-nitrosylation (Hausladen et al., 1996). Furthermore, S-nitrosylated but not S-oxidized OxyR stimulated in vitro transcription at the hcp promoter (Seth et al., 2012). Hence it was proposed that S-oxidised and S-nitrosylated OxyR control different regulons, with exposure to nitrosative stress resulting in a different regulatory output than the one caused by oxidative stress (Seth et al., 2012; Green et al., 2014) (Figure 1.11). This hypothesis could explain why transcriptomic studies so far have not shown significant induction of members of the OxyR oxidative stress regulon.

The superoxide response protein (SoxR) controls the expression of many genes in response to superoxide (Green et al., 2014). Expression of soxS-lacZ, controlled by SoxR, was found to be up-regulated in response to NO gas with an even greater induction observed under anoxic conditions, suggesting that NO itself and not a downstream product is responsible for this increase in SoxS expression (Nunoshiba et al., 1993). Both in vivo and in vitro data reveal that both oxidation or nitrosylation of the two [2Fe-2S] clusters of SoxR are equally capable of activating this protein (Ding and Demple, 2000; Vasil'eva et al., 2001). Interestingly, while expression of soxS was observed in three different transcriptomic studies (Mukhopadhyay et al., 2004; Justino et al., 2005; Pullan et al., 2007), little to no change was observed in the remaining members of the SoxRS regulon, possibly because the levels of SoxS are insufficient to trigger induction of the remaining genes (Pullan et al., 2007).

It is important to note that in spite of the different mechanisms of NO-detoxification present in E. coli, these are not redundant systems but in fact provide E. coli with the necessary versatility to withstand the different environments it encounters.

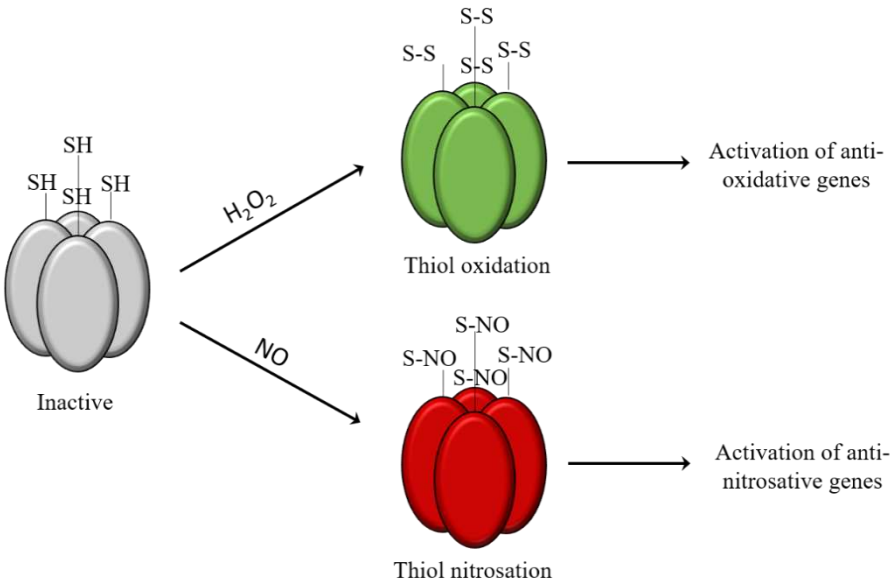

Figure 1.11 – Activation of OxyR. OxyR contains thiols which are oxidised in the presence of hydrogen peroxide, activating the expression of genes involved in the SOS response to oxidative stress. During nitrosative stress, the thiols are nitrosylated and a different set of genes is activated.

1.2.4. Nitric oxide role in bacterial pathogenicity

Nitric oxide is involved in many important biological processes in mammals. In bacteria, NO was initially thought to be only an intermediate product of anaerobic respiration, but the intrinsic role of NO as a bacterial signalling molecule capable of affecting bacterial metabolism and gene expression soon became obvious. This is exemplified by the NO sensors NsrR and NorR regulating the expression of different genes involved in the protection against nitrosative stress (discussed at length in section 1.2.1.). However, in this section the roles of NO in bacterial pathogenesis, beyond the nitrosative stress response, will be discussed.

1.2.4.1. Bacterial biofilms

Bacterial biofilms are complex multicellular structures that allow bacterial communities to withstand adverse environmental conditions such as osmotic pressure, extreme pH and temperature changes, and oxidative stress (Laverty et al., 2014). The formation of biofilms is initiated by environmental stresses sensed by planktonic bacterial cells that then attach to a surface, a process dependent on the expression of adhesion structures such as type I fimbriae encoded by the fim operon in E. coli, type IV pili encoded by the bfp operon in E. coli and necessary for attachment and twitching and swarming motility, and P pili encoded by the pap operon in E. coli (Laverty et al., 2014).

This is followed by a maturation stage where the bacteria grow and attach more firmly to the surface, increasing the production of an extracellular polymeric substance which acts as a protective layer and stabilizer of the biofilm structure (Kostakioti et al., 2013; Laverty et al., 2014). The life cycle is complete with the dispersal stage, wherein some cells detach from the three-dimensional structure returning to their planktonic form and thus allowing colonization of new surfaces (Kostakioti et al., 2013). The primary reason for biofilm formation is to facilitate bacterial survival in harsh environments, which interestingly includes resistance to most antibiotics: bacterial cells can exhibit extreme sensitivity to an antibiotic when in planktonic form yet biofilms of the same organism can be up to 1000 times more resistant to that same antibiotic (Mah and O'Toole, 2001). Increased resistance to antibiotics in a biofilm has been attributed to low permeability of the biofilm, decreased metabolic rate of the biofilm-contained cells, and heterogeneity of the structure (i.e. biofilms can often contain different bacterial species or cells in different metabolic states (Mah and O'Toole, 2001; Stewart and William Costerton, 2001; de la Fuente-Núñez, Reffuveille, Fernández, et al., 2013)).

Bacterial biofilms have had a serious impact upon the treatment of infections and are implicated in 65% of infections (de la Fuente-Núñez, Reffuveille, Fernández, et al., 2013), most occurring in cases where a medical device (e.g.: catheter or surgical implant) has been used. Biofilm-related infections are very difficult to treat and very often lead to relapse or chronic infection, as it is the case of cystic fibrosis patients. This contributes to the spread of antibiotic resistance, especially since biofilms can also facilitate transfer of plasmids and other genetic material (Ong et al., 2009) that encode antibiotic resistance determinants. Strategies have been designed to combat biofilm-mediated infection, ranging from hindering initial adhesion to the development of drugs capable of penetrating the biofilm. Another possible therapeutic approach is the dispersal of the biofilm followed by antibiotic treatment, since planktonic cells are more susceptible to antimicrobials.

Detection of nitrosative stress inside P. aeruginosa and S. aureus biofilms (Barraud et al., 2006; Miranda et al., 2011) prompted the investigation of the role of NO in biofilm formation. Exposure of P. aeruginosa biofilms to 500 nM of the NO-donor SNP led to a 80% decrease in biofilm biomass, with similar results observed when 1 µM GSNO was used instead of SNP (Barraud et al., 2006). In contrast, high concentrations of SNP resulted in an increase of biofilm biomass (Barraud et al., 2006). Furthermore, a nitrite reductase-deficient strain of P. aeruginosa (i.e. unable to endogenously produce NO) exhibited impaired swarming motility, a feature important for biofilm formation (de

la Fuente-Núñez, Reffuveille, Fairfull-Smith, et al., 2013), and low levels of SNP are shown to increase swimming and swarming motility in P. aeruginosa planktonic cells by 25% and 77%, respectively (Barraud et al., 2006). This data suggests that NO plays an important role in biofilm biogenesis and dispersal. Importantly, pre-exposure to SNP potentiated the effect of various antimicrobial agents (Barraud et al., 2006), and similar results were obtained when P. aeruginosa and E. coli biofilms were treated with the nitroxide Carboxy-TEMPO (a compound with NO mimetic properties) in combination with the antibiotic ciprofloxacin (Reffuveille et al., 2015).

1.2.4.2. Bacterial nitric oxide synthases

In mammals, NO can be synthesized by nitric oxide synthase (NOS) enzymes that concomitantly convert L-arginine to citrulline. Mammalian NOS enzymes are homodimers with a haem oxygenase domain and a reductase domain (Figure 1.12) (Crane, 2008; Crane et al., 2010). Analysis of various bacterial genomes led to the discovery that some Gram-positive bacteria, such as B. subtilis, B. anthracis, and S. aureus encode proteins similar to the oxidase domain of mammalian NOS. Bacterial NOS (bNOS) proteins are also homodimer, bind haem cofactors and catalyse the same conversion of arginine to produce NO (Crane, 2008). However, one striking difference is the lack of a reductase domain in bNOS (Figure 1.12) (Crane, 2008; Gusarov et al., 2008; Crane et al., 2010). In B. subtillis, bNOS was shown to be a somewhat promiscuous enzyme with different bacterial flavodoxins shown to be capable of supporting the bNOS-catalysed reaction in vitro (Wang et al., 2007).

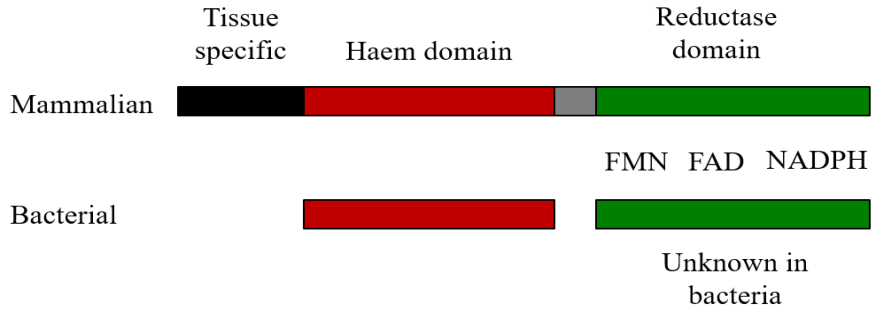

Figure 1.12 – Domain arrangement of mammalian and bacterial nitric oxide synthases. The haem-binding oxygenase domain is present in both NOS enzymes. However, bNOS does not have a reductase domain.

In B. subtillis and B. anthracis, bNOS-derived NO production has been implicated in the protection against oxidative stress (Gusarov and Nudler, 2005; Shatalin et al.,

2008). Endogenously-produced NO prevents the reduction of cysteine, an abundant thiol in Bacillus species that is responsible for maintaining redox balance. This in turn consequently interferes with the recycling of ferrous iron in the cell and ROS production via Fenton chemistry (Figure 1.13). Furthermore, NO stimulates the activity of KatA, a catalase enzyme that detoxifies hydrogen peroxide (Park and Imlay, 2003; Gusarov and Nudler, 2005; Shatalin et al., 2008). S. aureus also exhibited increased oxidative stress sensitivity when the nos gene was deleted (Van Sorge et al., 2013), further demonstrating the importance of bNOS in cytoprotection. The ability of bNOS-derived NO to rapidly activate antioxidant protective systems provides an advantage during the oxidative stress burst that often occurs during host infection (Shatalin et al., 2008). Furthermore, endogenously-produced NO also provides protection against antibiotics that mediate their toxic effects via the production of ROS (Gusarov et al., 2009; Van Sorge et al., 2013; Dwyer et al., 2014).

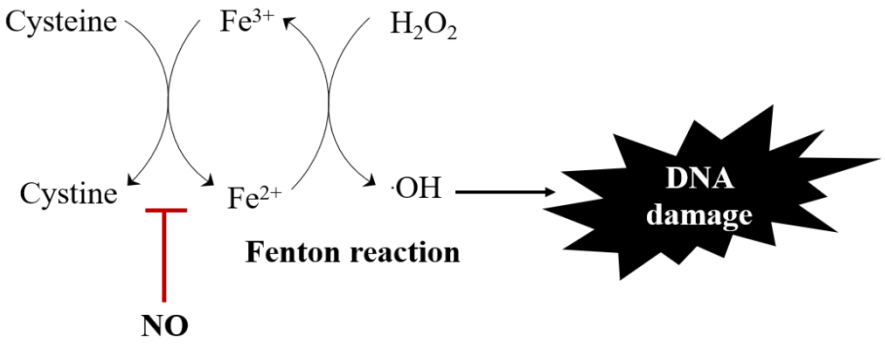

Figure 1.13 – Cysteine oxidation drives Fenton chemistry in Bacillus species. In species of Bacillus, cysteine reduces ferric iron to ferrous iron. The reaction between hydrogen peroxide and ferrous iron results in the formation of hydroxyl radicals, which causes DNA damage. The NO synthesized by bNOS transiently inhibits the reduction of cysteine to cystine, stopping the Fenton reaction from proceeding.

1.3. Project Aims

As antibiotic resistance becomes more and more common, the treatment of infections becomes more problematic, often relying on drugs that cause severe side-effects. Hence, the development of new strategies is of the utmost importance. The natural occurrence of nitric oxide in the mammalian immune system and its documented antimicrobial activity against bacterial pathogens make it a tempting candidate to use as an alternative therapy or even in combination with conventional antibiotics as a means to potentiate their action.

The overarching goal of this project was to determine the antimicrobial effects of NO in pathogenic E. coli and determine its suitability as a stand-alone therapy or in combination with conventional antibiotics. A collection of 50 E. coli clinical isolates (herein referred to as the Kent collection) was characterized for their antibiotic resistance, virulence gene carriage, plasmid content, and GSNO-susceptibility. Moreover, the effect of GSNO and NOC-compound in the survival of a pathogenic E. coli strain when combined with an antibiotic was tested, in both planktonic and biofilm-growing cells.

Another important aim of this project was to engineer an E. coli NO-producing E. coli strain that was also resistant to NO, and ultimately to determine if this strain could out-compete pathogenic strains of E. coli.

Chapter 2

Materials and Methods

2.1. Bacteriological Methods

2.1.1. Bacterial strains and plasmids

All bacterial strains and plasmids are listed in Table 2.1 and Table 2.2, respectively. All bacterial strains are E. coli, unless otherwise stated. The 50 E. coli blood culture isolates were collected from East Kent Hospitals University NHS Foundation Trust with approval from the Research Ethics Council in (ref: 12/SC/0673).

Table 2.1 – List of bacterial strains

Strain	Characteristics	Reference
MS1	CFT073; Uropathogenic strain (UPEC) belonging to clonal group ST73	Welch et al., 2002
MS2	MG1655; E. coli K-12 strain	Bachmann, 1996
MS3	MG1655 harbouring pKD46	Prof. Mark Schembri
MS10	EC958; UPEC strain belonging to clonal group ST131	Totsika et al., 2011
MS11	EC958 harbouring pKOBEG	Prof. Mark Schembri
MS16	EC958 cydAB::Cm	Prof. Mark Schembri; Shepherd et al., 2016
MS52	BW25113 F^-, Δ(araD-araB)597, ΔlacZ4787(del)::rrnB-3, LAM^-, rph-1, Δ(rhaD-rhaB)568, hdR514	Baba et al., 2006
MS92	EC958 hmp::Cm harbouring pSU2718-G-hmp	Prof. Mark Schembri; Shepherd et al., 2016
MS188 to MS237	Collection of 50 E. coli blood isolates from Kent belonging to different sequence types (Appendix A-1)	This work
MS343	83972; Asymptomatic bacteriuria strain	Prof. Mark Schembri; Klemm et al., 2006
MS344	83972 harbouring pKD46	Prof. Mark Schembri
MS345	BW25141 harbouring pKD3	Datsenko and Wanner, 2000
MS388	EC958 cydDC::Cm	Prof. Mark Schembri; Shepherd et al., 2016
MS389	EC958 ytfE::Cm	
MS390	EC958 hmp::Cm	
MS391	EC958 norVW::Cm	
MS392	EC958 nrfA::Cm	
MS403	EC958 cydAB::Cm pSU2718-G-cydABX	
MS436	MG1655 Phmp::Pbla-Cm	This work
MS472	BW25113 pSU2718-bNOS	This work
MS486	RKP2176 Phmp-lacZ	Same as RKP2178 from Membrillo-Hernández et al., 1996
MS491	RKP2176 Phmp-lacZ harbouring pSU2718-bNOS	This work
MS505	EC958 harbouring pSU2718-bNOS	This work
MS506	EC958 cyoA::Cm (Appendix G.1)	This work
MS546	RKP2176 Phmp-lacZ harbouring pSU2718	This work
MS547	EC958 harbouring pSU2718	This work

Table 2.2 – List of plasmids

Plasmid	Characteristics	Antibiotic	Reference
pKD46	λ-red recombinase, Temperature sensitive (Ts) replicon	Amp^R	Datsenko and Wanner, 2000
pKD3	Chloramphenicol resistance cassette flanked by FRT sites	Cm^R	
pKOBEG	λ-red recombinase; Temperature sensitive (Ts) replicon	$Gent^R$	Chaveroche et al., 2000
pSU2718-G-hmp	Complementation plasmid for hmp knockout	$Gent^R$	Prof. Mark Schembri
pSU2718-G-cydABX	Complementation plasmid for cydAB knockout	$Gent^R$	
pSU2718	Empty plasmid control for bacterial nitric oxide synthase (bNOS) expression	Cm^R	This work
pSU2718-bNOS	Plasmid for IPTG-inducible expression of bacterial nitric oxide synthase (bNOS)	Cm^R	This work

2.1.2. Oligonucleotides

All oligonucleotides used during this work are listed in Table 2.3. Oligonucleotides were designed using Vector NTI Advance 10. Each pair of primers were designed with less than 5°C difference in melting temperature (Tm) and less than a 5% difference in their GC content. Oligonucleotides were synthesized by Eurofins MWG.

2.1.3. Chemicals and water

All chemicals were purchased from Sigma unless otherwise stated. Nutrient agar, tryptone, and yeast extract were purchased from Oxoid. Distilled-deionized water was used throughout this work. Mili-Q water was used whenever a high degree of purity was required. Solutions were sterilised by autoclaving at 121°C, 15 psi (pound force per square inch) for 15 min, or by filtering using Millipore filters with a pore size of 0.22 µm.

2.1.4. Media and buffer solutions

2.1.4.1. Luria-Bertani medium

Luria-Bertani (LB) medium contained 10 g tryptone, 5 g yeast extract, and 5 g NaCl per litre. pH was adjusted to 7.0.

2.1.4.2. Iso-Sensitest Broth and Iso-Sensitest Agar

Both media were purchased from Oxoid and prepared according to manufacturer instructions.

Table 2.3 – List of oligonucleotides

Name	5'-3' Sequence	Use	Direction
pSU2718nssR_seqF	AAAAGCACCGCCGGACATCA	For screening of bNOS insert into pSU2718 vector	Forward
pSU2718nssR_seqR	CGAATTCGAGCTCGGTACCC		Reverse
hmp_Pbla_F	TAAGATGCATTTGAGATACATCAATTAAGATGCAAAAAAAGGAAGAC CATCATATGAATATCCTCCTTAG	Amplification of CmR cassette and Pbla promoter from pKD3 for substitution of native promoter of hmp	Forward
hmp_Pbla_R	AGTAAAGGGATGGTGGCTTTTACTGTAGCGATGGTTTGAGCGTCAAGC ATACTCTTCCTTTTTCAATATT		Reverse
Hmp_Sc_fw	GGCTACGCAAGGCTTTGGAG	For screening of Pbla promoter insertion upstream hmp gene	Forward
Hmp_Sc_rev	CTGGCGTAGGCGGCAATAGC		Reverse
SaUSA300_bNOS_Fw	CCCTGCGCATATAATTGCATATGCTACAC	Amplification of bNOS from S. aureus USA300 for pSU2718-hmp cloning	Forward
SabNOS_Rev2	CCCGGATCCTTAACAGGAAACAGCTATGTTATTTAAAGAGGCTCA		Reverse
cyoA_Cm_fw	CCGAACATCTTTATTCTTCCTCAACCCCTTTAATGGGCGGATTCCGCGT GGTGTAGGCTGGAGCTGCTTC	For cyoA KO in EC958 background	Forward
cyoA_Cm_rev2	CCACACACTTTAAACGCCACCAGATCCCGTGGAATTGAGGTCGTTAAA TGCATATGAATATCCTCCTTAG		Reverse
cyoA_Sc_fw	GTCAACGGAGGTCAGCCACT	To screen cyoA KO mutants	Forward
cyoA_Sc_rev2	CGCCCTTTTGCAACAGCTTC		Reverse
pSU2718seq_200_F	GTCGGGTGATGCTGCCAACT	For sequencing of pSU2718-bNOS	Forward
pSU2718seq_200_R	GCAGCTGGCACGACAGGTTT		Reverse
bNOS_sq150_rev	GGTGCTAAAATGGCTTGGCG		Reverse
pSU2718_Fw	GGATCCCCGGGTACCGAGCTC	For amplification of pSU2718 backbone	Forward
pSU2718_Rev	TGCGCAGCCTGAATGGCGAA		Reverse

2.1.4.3. M9 minimal medium

5x M9 salts were prepared [80.24 g $Na_2HPO_4.2H_2O$, 15 g KH_2PO_4, 2.5 g NaCl, and 5 g NH_4Cl per litre], autoclaved, and left to cool before use. To prepare 1L of 1X M9 medium, the following solutions were mixed: 200 mL of 5x M9 salts, 2 mL of a 1 M $MgSO_4$ filter sterilized solution, 100 µL of a 1 M $CaCl_2$ filter sterilized solution, 20 mL of 20% (w/v) glucose (filter-sterilized), 778 mL of autoclaved water.

2.1.4.4. SOB medium

SOB medium contained 20 g tryptone, 5 g yeast extract, 0.584 g NaCl, and 0.186 g KCl per litre.

2.1.4.5. SOC medium

One litre of SOC medium was prepared by addition of 10 mL of 2 M Mg^{2+} solution [20.33 g $MgCl_2$ and 24.65 g $MgSO_4$ per 100 mL. The solution was autoclaved and allowed to cool down before use] and 20 mL of a 1 M glucose sterile solution to 970 mL of sterile SOB medium.

2.1.4.6. Dulbecco's Modified Eagle Medium (DMEM)

DMEM medium was purchased from Thermo Fisher Scientific. The purchased medium is a complex medium containing high levels of glucose, L-glutamine, phenol red, sodium pyruvate, whereas the buffer HEPES is absent.

2.1.4.7. Sodium Phosphate Buffer

A 50 mM sodium phosphate buffer pH 8.0 was prepared with 94.7 mL 50 mM Na_2HPO_4 and 5.3 mL 50 mM NaH_2PO_4. The pH was checked prior to filter sterilization. The sterile buffer was then aliquoted and stored at 4°C.

2.1.4.8. Tris-Acetate-EDTA (TAE) Buffer

A 50x solution of Tris-Acetate-EDTA (TAE) buffer was prepared by adding 242 g of Tris base, 57.1 mL of acetic acid, and 100 mL of 0.5M EDTA to 900 mL of dH_2O. The pH was adjusted to 8.5 prior to adjusting the volume to one litre. For a working concentration of 1x, 20 mL of the 50x TAE buffer stock was diluted in 980 mL of water.

2.1.4.9. Z- Buffer

Z-buffer contained 60 mM $Na_2HPO_4.7H_2O$, 40 mM $NaH_2PO_4.H_2O$, 10 mM KCl, 1 mM $MgSO_4.7H_2O$. Prior to the addition of 50 mM beta-mercaptoethanol, the pH was adjusted to 7.0. The buffer was protected from light and stored at 4°C.

2.1.4.10. Phosphate-Buffered Saline (PBS)

A 10x concentrated solution of Phosphate-Buffered Saline (PBS) buffer contained 80 g NaCl, 2 g KCl, 15.4 g $Na_2HPO_4.2H_2O$, and 2.4 g KH_2PO_4 per litre. The pH was adjusted to 7.4 prior to volume being adjusted to one litre. The buffer solution was autoclaved and diluted to a working concentration of 1x by mixing 100 mL of the 10x stock solution with 900 mL of sterile milli-Q water.

2.1.5. Media Supplements

2.1.5.1. Antibiotics

Where appropriate, growth media was supplemented with 125 µg/mL of ampicillin, 25 µg/mL chloramphenicol, or 20 µg/mL gentamicin.

2.1.5.2. Casamino acids solution

A 2% (w/v) casamino acids solution was prepared by adding 2 g of dried casamino acids per 100 mL dH_2O, after which the solution was autoclaved and allowed to cool down before use.

2.1.5.3. Fumarate Solution

For anaerobic growth, it was necessary to supplement media with a respiratory electron acceptor as an alternative to oxygen. To that end, a 1 M stock solution of fumarate was prepared. Briefly, 116.07 g of fumaric acid was added to 500 mL of water. The pH was adjusted to 7.0 using NaOH prior to the volume being adjusted to 1L. The solution was filter sterilized, aliquoted, and stored at -20°C.

2.1.5.4. Nutrient agar

15 g of nutrient agar was used per litre of growth medium. Agar plates, unless otherwise stated, were inverted and incubated at 37°C.

2.1.6. Culture conditions

10 mL starter cultures were inoculated from single colonies and grown overnight in LB (37°C and 180 rpm). A 1% inoculum of overnight starter culture was used to

inoculate fresh media. Liquid cultures were grown in a New Brunswick™ Innova® 3100 water bath at 37°C and 180 rpm in 50 mL conical flasks containing 10 mL of LB medium, unless otherwise stated.

2.1.6.1. Culture optical density

The optical density of cultures was measured at 600 nm (OD_{600nm}) using a Shimadzu UV-1800 spectrophotometer in cuvettes with a 1 cm path length.

2.1.6.2. Preparation of E. coli glycerol stocks

Glycerol stocks of E. coli were prepared by mixing 750 µL of sterile 50% (v/v) glycerol with 750 µL of an overnight culture in a cryotube. The stocks were stored at -80°C.

2.1.7. Antibiotic susceptibility assays

Breakpoint values were obtained from the British Society for Antimicrobial Chemotherapy (BSAC) (version 13.0 from June 2014).

2.1.7.1. Antibiotic preparation

Antibiotics used to determine antibiotic susceptibility were prepared as shown in Table 2.4.

Table 2.4 – List of antibiotics tested

Antibiotic	Solvent	Stock concentration (mg/mL)	Disc content (µg)
Amoxicillin	DMSO	2	10
Cefotaxime	Water	6	30
Chloramphenicol	Ethanol	6	30
Ciprofloxacin	Water	0.2	1
Gentamicin	Water	2	10
Meropenem	Water	2	10
Nitrofurantoin	DMSO	50	200
Trimethoprim	DMSO	0.7	2.5
Polymixin E (Colistin)	Water	10	-

2.1.7.2. 0.5 McFarland Standard

A stock of 0.5 McFarland solution, corresponding to a cell density of 10^7-10^8 CFU/mL, was prepared by mixing 0.5 mL of 0.048 M $BaCl_2$ and 99.5 mL of 0.18 M H_2SO_4. The cell suspension was then mixed prior to absorbance reading at 625 nm

(A_{625nm}). If the absorbance was between 0.08 and 0.13, the solution was then aliquoted into glass vials, protected from light, and stored at room temperature.

2.1.7.3. Preparation of inoculum

Inocula were prepared according to the British Society for Antimicrobial Chemotherapy (BSAC) guidelines (Andrews, 2001b; Howe and Andrews, 2012). Briefly, colonies were used to inoculate 5 mL of Iso-Sensitest broth and incubated at 37°C and 180 rpm until visible turbidity was greater than that of the 0.5 McFarland standard. The density of the culture was adjusted to that of the 0.5 McFarland standard with sterile milli-Q water.

2.1.7.4. Disc diffusion assay

Iso-Sensitest agar plates were prepared and dried on the day of use. Each plate (90 mm) contained 20 mL of agar. Cell suspensions prepared as described in section 2.1.7.3 were diluted 1:100 in sterile milli-Q water. A sterile swab was dipped into the dilution and excess liquid was removed by pressing the swab against the side of the falcon tube. The inoculum was swabbed over the Iso-Sensitest agar in three different directions to obtain an even spread. A 5 mm sterile filter paper disc (Whatman™ No. 1) containing the appropriate antibiotic (see Table 2.4) was placed on the agar. Plates were incubated at 37°C for 16 ± 2 h prior to measuring zones of inhibition. BSAC testing v13.0 was used for the zone diameter breakpoint values.

2.1.7.5. Microdilution assay

Due to the poor agar diffusion of polymyxin E (colistin), susceptibility to this antibiotic was tested using the microdilution assay (Andrews, 2001a). A dilution range (two-fold from 0.0625 to 4 mg/L) of polymyxin E was prepared in Iso-Sensitest broth, and 75 µL of each dilution was dispensed to a sterile 96-well microtiter plate in duplicate. Cell suspensions prepared as described in section 2.1.7.3 were diluted 1:10 in sterile milli-Q water, and then further diluted 1:100 in Iso-Sensitest broth prior to 75 µL being added in duplicate to each antibiotic dilution. Incubation was carried out for 16 ± 2 hs at 37°C. BSAC testing v13.0 was used for the MIC breakpoint values.

2.1.8. Biofilm formation assay

An overnight starter culture was used to inoculate 5 mL of fresh M9 minimal medium supplemented with 0.1% casamino acids. This culture was then incubated at

37°C and 180 rpm for 1 h. 150 µL of the growing culture was dispensed into six wells of a 96-well microtiter plate, with a negative control consisting of 150 µL of fresh M9 medium included in each plate. A 24-h static incubation at 37°C was carried out, after which the media was completely discarded and 150 µL of a 0.1% (w/v) crystal violet solution was dispensed into each well, followed by a 30 min incubation at 4°C. The crystal violet solution was discarded and wells were washed until the negative control wells were clear. 150 µL of an ethanol/acetone (80:20 ratio) mix was added to each well and the microtiter plate was left on a rocker for 1 h at 60 rpm. Absorbance at 595 nm (A_{595nm}) was recorded using a SPECTROstar nano microplate reader (BMG Labtech).

2.1.9. Nitric oxide susceptibility

2.1.9.1. S-Nitrosoglutathione (GSNO) preparation

S-nitrosoglutathione (GSNO) was prepared as previously described by Hart (1985). Briefly, a solution containing 3.08 g of reduced glutathione, 0.69 g of $NaNO_2$, 0.83 mL of 12.1 M HCl, and 18 mL of distilled water was stirred for 40 min whilst in an ice bath. Following the addition of 20 mL of acetone, the solution was stirred for another 10 min. The red precipitate was collected by vacuum filtration and washed with five 2 mL volumes of cold distilled water, three 10 mL volumes of acetone, and three 10 mL volumes of ether. The precipitate was then dried overnight in a vacuum desiccator and kept at -80°C for no longer than one month. Immediately before use, GSNO was dissolved in distilled water, filter sterilized and quantified using a Cary 60 UV-vis spectrophotometer (Agilent Technologies) before use (Extinction coefficient (ε) at 545nm = 15.9 M^{-1} cm^{-1}).

2.1.9.2. Well-diffusion assay

Cultures were prepared in M9 minimal medium supplemented with 0.1% casamino acids and incubated at 37°C and 180 rpm until OD_{600nm} was approximately 0.4-0.5. Cultures were then plated in M9 minimal agar using the pour plate method, i.e. 1 mL of culture was mixed with 19 mL of agar and poured into a 90 mm petri dish. Agar was allowed to set, at which point six 6 mm wells were cut into the agar and filled with 80 µL of an 80 mM solution of GSNO. Plates were incubated in an upright position at 37°C under aerobic (for 16 ±2 h), microaerobic (2% oxygen in an Invivo$_2$ 300 Hypoxia Workstation) (for 32 ± 2 h), or anaerobic (32 ± 2 h) conditions. For the latter, 50 mM fumarate was added to the agar and the plates were secured in an anaerobic jar with an

oxygen indicator and an anaerobic gas pouch (both purchased from Oxoid). After incubation, zones of inhibition were measured.

2.1.9.3. GSNO growth curves under microaerobic conditions

An overnight starter culture of strains MS2 and MS436 in M9 minimal medium supplemented with 0.1% casamino acids was used to inoculate 10 mL of fresh M9 minimal medium supplemented with 0.1% casamino acids and 0, 1, or 5 mM of GSNO to an initial OD_{600nm} of 0.04. The culture was dispensed into five wells of a 96-well microtiter in 200 µL aliquots and incubated at 37°C and 100 rpm in a SPECTROstar nano microplate reader (BMG Labtech). OD_{600nm} was followed every 15 min for at least 8 h.

2.1.9.4. GSNO growth curves under anaerobic conditions

An overnight starter culture of strains MS2 and MS436 in M9 minimal medium supplemented with 0.1% casamino acids was used to inoculate 30 mL of fresh M9 minimal medium supplemented with 0.1% casamino acids, 50 mM fumarate, and 0, 1, or 5 mM of GSNO to an initial OD_{600nm} of 0.04. Cultures were grown statically in a sealed serum glass bottle at 37°C, and OD_{600nm} was followed every hour for 6 h.

2.1.9.5. NOC-12 preparation

Growth curves were carried out using NOC-12 (purchased from Calbiochem), a nitric oxide donor with a half-life of 100 min at 37°C, pH 7.4. A 0.1 M stock of NOC-12 was prepared in 50 mM sodium phosphate buffer (pH 8) (see section 2.1.4.6.) immediately before use. To ensure an effect on bacterial growth was observed, a range of concentrations between 0.1 mM and 0.75 mM ware tested.

2.1.9.6. NOC-12 growth curves

An overnight starter culture in M9 minimal medium supplemented with 0.1% casamino acids was used to inoculate 10 mL of fresh M9 minimal medium supplemented with 0.1% casamino acids to an initial OD_{600nm} of 0.01. The culture was dispensed into five wells of a 96-well microtiter in 200 µL aliquots and incubated at 37°C and 100 rpm in a SPECTROstar nano microplate reader (BMG Labtech) until OD_{600nm} was approximately 0.04, at which point the NOC-12 compound was added. In control wells, 50 mM sodium phosphate buffer was added instead of NOC-12 solution. Incubation was carried out as before NOC-12 addition, and OD_{600nm} was followed every 15 min for at least 8 h.

2.1.10. Gentamicin cell survival assay

2.1.10.1. Exogenous nitric oxide source

An overnight starter culture in LB of EC958 wild-type (MS10), EC958 cydAB::Cm (MS16), or EC958 cyoA::Cm (MS506) was used to inoculate 10 mL of fresh M9 media supplemented with 0.1% (v/v) casamino acids, and incubated at 37°C and 180 rpm until OD_{600nm}~0.3 or higher. The culture was diluted to an OD_{600nm} of approximately 0.125 ($1x10^8$ cells/mL) in fresh M9 supplemented with 0.1% casamino acids, and 0 or 15 mM of GSNO, or 0 or 1 mM of NOC-12, was added, and cultures were incubated at 37°C for 30 min. Cells were further incubated at 37°C with different concentrations of gentamicin for 90 min. Serial dilutions were performed and 5 µL drops were plated in triplicate on LB-agar plates. Plates were incubated at 37°C overnight, and colony counts performed to determine CFU/mL.

For in vitro biofilm assay, all steps were as described above with the following exceptions: 200 µL of the $1x10^8$ cell/mL suspension was dispensed onto a 96-microtitre and incubated at 37°C statically for 24 h to allow biofilm formation. After the incubation biofilms were washed 2x with 1x PBS followed by an incubation at 37°C for 90 min with different concentrations of gentamicin and with or without 15 mM GSNO. Subsequently, biofilms were washed 2x with 1x PBS and resuspended in 200 µL of 1x PBS with vigorous pipetting and vortexing. Serial dilutions were performed and 5 µL drops were plated, in triplicate, on LB-agar plates. Plates were incubated at 37°C overnight, and colony counts performed to determine CFU/mL.

2.1.10.2. Endogenous nitric oxide source

All steps were as described in section 2.1.10.1, with the following exceptions: strains EC958 pSU2718 and EC958 pSU2718-bNOS were used. After diluting cultures to an OD_{600nm} of approximately 0.125 ($1x10^8$ cells/mL) in fresh M9 supplemented with 0.1% casamino acids, 0.4 mM IPTG and 10 mM L-arginine were added followed by an incubation at 37°C for 30 min.

2.1.11. Intra-macrophage survival assays

2.1.11.1. Cell line maintenance

For this assay, the Raw-Blue™ macrophage cell line (InvivoGen) was used. This murine cell line was maintained in complete medium (DMEM medium supplemented with 10% (v/v) of foetal bovine serum (FBS; purchased from Gibco®)) supplemented

with 200 units of penicillin, and 200 µg/mL of streptomycin, and incubated at 37°C in 5% CO_2 until approximately 80% confluency was reached.

2.1.11.2. Preparation of bacterial cells for infection

Approximately 1.8 mL of an overnight culture of EC958 wild-type (MS10) was placed in a sterile eppendorf tube and cells were pelleted by centrifugation (1 min at 16 000 xg). The supernatant was carefully discarded, and the cell pellet washed twice with 1 mL of 1x PBS. The cell pellet was re-suspended in 1.5 mL of 1x PBS and further diluted 1:5 in 1x PBS. The bacterial suspension was further diluted in 1x PBS until and OD_{600nm} of approximately 0.5 was reached (approximately $4x10^8$ cells/mL), at which point the appropriate volume of the suspension to achieve $1.5x10^7$ cells/mL was diluted in complete medium with or without 2 mM of N_ω-Nitro-L-arginine methyl ester (L-NAME), an inhibitor iNOS.

2.1.11.3. Preparation of macrophage cells for infection

Macrophage cells were allowed to proliferate in a T-75 flask to approximately 80% confluency, at which point they were collected with gentle scraping. The cell suspension was transferred to a sterile 15 mL falcon tube and centrifuged in an Eppendorf centrifuge 5418 for 5 min at 500 xg. The cell pellet was re-suspended in 5 mL of complete medium and the number of cells/mL determined using an hemocytometer. Each well on a 96-well microtitre was seeded with $1.5x10^5$ cells. For macrophage activation 1 µg/mL of lipopolysaccharides (LPS) from Escherichia coli O127:B8 and 10 ng/mL of interferon gamma (IFN-γ; purchased from ThermoFisher) were added per well, with or without 2 mM of L-NAME. Cells were incubated for 18 ± 2 h at 37°C, 5% CO_2.

2.1.11.4. Macrophage infection

Media was carefully removed from each well, as to not disturb the macrophage cells, and replaced with 100 µL of the $1.5x10^7$ cells/mL bacterial cell suspension prepared in section 2.4.1.2., resulting in a multiplicity of infection (MOI) of approximately 10:1 (bacteria:macrophage). After a 20 min incubation at 37°C in 5% CO_2, the medium was removed and the cells washed 2x with complete media supplemented with 200 µg/mL gentamicin. After a 20 min incubation in complete medium supplemented with 200 µg/mL at 37°C in 5% CO_2, the media was removed and cells were washed 3x with complete media. 100 µL of complete media, with or without 2 mM L-NAME and different concentrations of gentamicin (20 or 200 µg/mL) was added to each well and a

90 min incubation was carried out at 37°C in 5% CO_2. Cells were washed 3x with 1x PBS and lysed with a 0.1% (v/v) solution of Triton-X in 1x PBS. The lysate was serial diluted in 1x PBS and 5 µL drops were plated on LB-agar in triplicate. Plates were incubated overnight at 37°C and colony counts performed to determine CFU/mL. An uptake plate to determine the average uptake of bacteria by macrophages per condition was also prepared for every assay and used to normalize CFU/well.

2.2. Genetic Methods

2.2.1. Isolation of plasmid DNA

Plasmid DNA was isolated using QIAprep Spin Miniprep Kit (QIAGEN) according to manufacturers' instructions. Overnight cultures were pelleted at 7155 xg for 10 min using a Sigma Laboratory Centrifuge 2k15. Following this step, all centrifugations were carried out at 16000 xg in an Eppendorf 5415R micro centrifuge.

2.2.2. Polymerase chain reaction (PCR)

For colony PCR, each bacterial colony was re-suspended in 50 µL of sterile water, and 2 µL were used as template in the PCR reaction. A typical colony PCR reaction would contain 400 nM of each primer (forward and reverse), 12.5 µL of 2x PCRBIO Taq Mix Red (PCRBiosystems), and sterile water to make up the end volume to 25 µL. PCR tubes were then placed in a T3000 thermocycler machine (Biometra®) programmed with the following: one cycle at 95°C for 4 min, 35 cycles at 95°C for 15 s, 55°C to 65°C (annealing temperature depending on the primers used) for 15 s and 72°C for 15 s per kilo base (extension time dependent on the length of the expected PCR product), and finally one cycle at 72°C for 2 min.

2.2.3. DNA electrophoresis on agarose gels

1% (w/v) agarose gels were prepared in 1x TAE buffer (see section 2.1.4.7) and electrophoresis was carried out using a gel apparatus at 150 V, 300 mA, for 45 min, in 1x TAE buffer. 5 µL samples were mixed with 1 µL of Blue/Orange 6x loading dye (Promega) before being loaded onto gel wells. A 1 kb DNA ladder (Promega) was also loaded onto the gel in order to determine the size of the DNA present in the sample. Gels were stained post-electrophoresis for 30 min at 60 rpm in 100 mL of water containing 0.5 mg/mL of ethidium bromide and visualised with a UV box.

2.2.4. Cloning bacterial nitric oxide synthase (bNOS) into pSU2718

2.2.4.1. Preparation of bNOS fragment for cloning

A PCR reaction to amplify a bacterial nitric oxide synthase (bNOS) gene contained the following: 25 µL Q5 2x Mastermix (NEB), 500 nM SaUSA300_bNOS_Fw primer, 500 nM SabNOS_Rev2 primer, 5 µL of a 1:10 dilution of Staphylococcus aureus USA300 genomic DNA, and 15 µL of sterile water for a total of 50 µL. The reaction was then transferred to a T3000 thermocycler machine (Biometra®) programmed with the following: 98°C for 30 s, 35 cycles of 98°C for 10 s, 60°C for 30 s, and 72°C for 1 min, and finally 72°C for 2 min. The PCR product was purified using a QIAquick PCR purification kit (QIAGEN) and digested with BamHI-HF (NEB) and FspI (NEB) restriction enzymes according to manufacturers' instructions. The digested product was again purified using a QIAquick PCR purification kit (QIAGEN), and the DNA concentration was quantified with a NanoPhotometer® N50 (Implen) prior to use in a ligation reaction with pSU2718 (see section 2.2.4.3).

2.2.4.2. Preparation of pSU2718 for cloning

pSU2718-hmp plasmid was isolated from MS18 (see section 2.2.1.) and digested with BamHI-HF (NEB) and FspI (NEB) restriction enzymes according to manufacturers' instructions. This restriction digest would result in two DNA fragments, one being the desired plasmid backbone (2167 bp) and the other corresponding to the hmp gene (1345 bp). The restriction digest reaction was loaded onto an agarose gel (see section 2.2.3.) and the desired fragment extracted and purified using QIAquick Gel Extraction kit (QIAGEN). DNA concentration in the sample was quantified with NanoPhotometer® N50 (Implen) prior to use in a ligation reaction with bNOS fragment (see section 2.2.4.3.). pSU2718 backbone for re-ligation was amplified by PCR using primers pSU2718_Fw and pSU2718_Rev.

2.2.4.3. Ligation reaction

Ligation reactions were carried out using T4 DNA ligase (Promega) according to manufacturers' instructions. Briefly, 50 ng of cut pSU2718 plasmid was incubated in 1x T4 DNA ligase Reaction Buffer with bNOS fragment in a 1:3 ratio (vector:insert), along with 1.5U T4 DNA ligase and sterile water to make up 10 µL. The reaction was incubated at 15°C for 16 ± 2 h and used to transform BW25113 competent cells (see sections 2.2.5. and 2.2.6.). To obtain the pSU2718 empty plasmid, the PCR-amplified backbone was used in a ligation reaction as described above, but bNOS was omitted from the reaction.

2.2.5. Preparation of E. coli competent cells

An overnight starter culture in LB was used for a 1% (v/v) inoculation of 10 mL of fresh LB medium. This culture was incubated at 37°C and 180 rpm until OD_{600nm} was approximately 0.5, at which point 1 mL of culture was pelleted at 2300 xg for 5 min. The supernatant was discarded and the cell pellet re-suspended in 750 µL of ice-cold 100 mM $CaCl_2$, followed by a 1 h incubation on ice. The cells were again pelleted as described above, supernatant carefully removed, and cell pellet re-suspended in 100 µL of ice-cold 100 mM $CaCl_2$. Following another incubation on ice for 1 h the cells were transformed with plasmid DNA.

2.2.6. Transformation of E. coli competent cells

Plasmid DNA (2-5 µL) or various volumes of ligation reaction were mixed with 100 µL of competent cells and incubated on ice for 30 min before being heat shocked for 45 s at 42°C. The transformation mixture was immediately incubated on ice for 2 min after the heat shock, and 900 µL of SOC medium was added to aid recovery. An incubation at 37°C and 180 rpm was carried out for 1 h, followed by a centrifugation step at 2300 xg for 5 min. 900 µL of supernatant was carefully removed, and cells were re-suspended in the remaining 100 µL prior to being plated onto the appropriate selective LB-agar plate.

2.2.7. λ-red mutagenesis

The λ-red mutagenesis (Datsenko and Wanner, 2000) approach was used to replace the cyoA gene in E. coli EC958 background with a chloramphenicol resistance cassette (Figure 2.1), and also to replace the hmp native promoter with a P_{bla} promoter in a E. coli MG1655 background. The phage λ-Red recombinase system is encoded in a temperature sensitive plasmid and under the control of an arabinose-induced promoter. The recombinase system allows homologous recombination between the PCR product and the genome, which results in a knockout mutation.

2.2.7.1. Amplification of PCR fragment for λ-Red mutagenesis

For the amplification of the PCR fragment containing the chloramphenicol resistance cassette alone (cyoA gene knockout) or the chloramphenicol resistance cassette and the P_{bla} promoter, PCR reactions was prepared as follows: 25 µL 2x PCRBIO Taq Mix Red (PCRBiosystems), 400 nM of appropriate forward primer, 400 nM of appropriate reverse primer, 0.5 µL pKD3 plasmid, and sterile water was used to top-up

the volume to 50 µL. PCR tubes were placed in a T3000 thermocycler machine (Biometra®) programmed with the following: 95°C for 1 min, 35 cycles at 95°C for 15 s, 50°C for 15 s and 72°C for 30 s, and finally one cycle at 72°C for 2 min. Reaction was purified using a QIAquick PCR purification kit (QIAGEN), eluted in sterile mili-Q water, and used to transform MG1655 pKD46-containing strain (MS3) or EC958 pKOBEG-containing strain (MS11) (see sections 2.2.7.3 and 2.2.7.4).

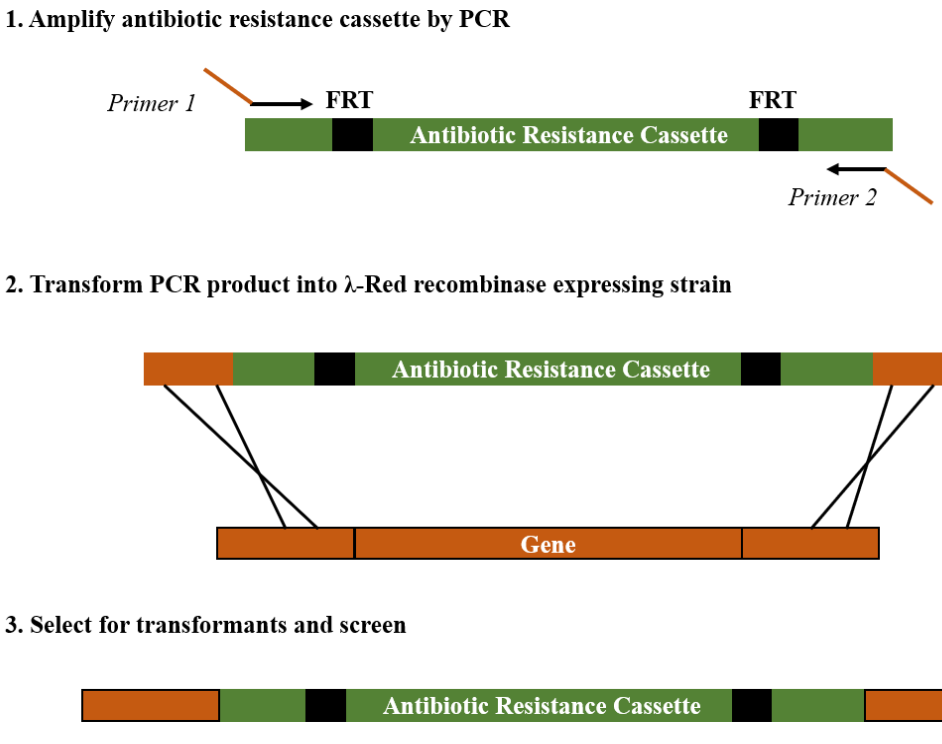

Figure 2.1 – λ-red mutagenesis. In the procedure described by Datsenko and Wanner (2000), an antibiotic resistance cassette is amplified by PCR with primers that will allow the synthesis of extremities homologous to the regions flanking the gene of interest in the genome (1). The PCR product is then used to transform cells expressing the λ-red recombinase system, which will allow homologous recombination between the PCR product and the genome (2), thus creating a knockout mutant (3).

2.2.7.2. Preparation of electro-competent cells

Electro-competent cells were prepared using strains MS3 and MS11, containing the temperature sensitive plasmid pKD46 (Ap^R) and pKOBEG (Gm^R) respectively. These plasmids encode the phage λ-derived Red recombination system and allows the homologous recombination between a PCR product and the genome. An overnight starter culture in LB grown at 28°C and 180 rpm was used for a 1% inoculation of 50 mL of fresh SOB medium (see section 2.1.4.4.) supplemented with the appropriate antibiotic and 20 mM L-arabinose, to induce expression of the λ-Red system from the P_{BAD}

promoter. Cells were incubated at 28°C and 180 rpm until OD_{600nm} was between 0.4-0.8, at which point the cells were transferred to a chilled 50 mL falcon tube and spun at 3000 xg, 4°C, for 10 min. Supernatant was discarded and the cell pellet was gently re-suspended in 5 mL of ice-cold 10% (v/v) glycerol. This step was repeated a total of three times prior to the cell pellet being re-suspended in a final volume of 200 µL of ice-cold 10% (v/v) glycerol. 40 µL of the now electro-competent cells were used per transformation by electroporation (see section 2.2.7.3.).

2.2.7.3. Transformation by electroporation

DNA was placed into a chilled 2-mm electroporation cuvette prior to 40 µL of electro-competent cells being added. Adequate mixing and placement of the sample at the bottom was achieved by tapping the cuvette. The cuvette was then placed into the chamber of the electroporator (Bio-Rad) and pulsed at 2.45 kV, 200 Ω resistance, and 25 µF capacitance. To aid cell recovery, 1 mL of SOC (see section 2.1.4.5.) was added to the cuvette and then transferred into a 1.5 mL Eppendorf for incubation at 37°C and 180 rpm for 1 h. To select for incorporation of resistance gene onto the chromosome, cells were plated onto LB-agar supplemented with the appropriate antibiotic, and colony PCR was carried out to identify mutant colonies.

2.2.8. Sequencing of DNA

To confirm successful knockout of the gene or successful cloning of fragment into plasmid, DNA samples were sequenced by GeneWiz and data was analysed using BioEdit v7.2.5 (Hall, 1999). For whole genome sequencing, library preparation was performed using Nextera® XT DNA Library Prep Kit from Illumina® following manufacturers' instructions. Library preps were then sequenced on an Illumina® MiSeq benchtop sequencer using a MiSeq reagent kit v3.

2.3. Biochemical Methods

2.3.1. Beta-galactosidase assay

For NO detection using a beta-galactosidase assay, RKP2176 was transformed with pSU2718 and pSU2718-bNOS. RKP2176 is an E. coli strain similar to RKP2178 used by Poole et al. (1996) in which the native lacZ gene was inactivated and a hmp-lacZ fusion (Φ hmp-lacZ) was engineered.

Overnight starter cultures of both RKP2176 harbouring pSU2718 (MS546) and pSU2718-bNOS (MS491) were used for a 1% inoculation of 10 mL of fresh M9 minimal medium supplemented with 0.1% casamino acids and 25 µg/mL chloramphenicol. Cultures were incubated at 37°C and 180 rpm until OD_{600nm} was approximately 0.15, at which point 0.4 mM of IPTG and 10 mM of L-arginine were added. Beta-galactosidase activity was measured every 30 min as follows: OD_{600nm} of each culture was recorded at every time point, and 50 µL of cell culture directly removed from the cuvette was mixed with 450 µL of Z-buffer (see section 2.1.4.8.) in a glass test tube. 5 µL of a 0.1% (w/v) sodium dodecyl sulphate (SDS) solution and 10 µL of chloroform were added to each tube, and samples were vortexed for at least 10 s, to ensure disruption of the cell membrane, and placed in a water bath at 28°C for 5 min. The assay was started by adding 100 µL of a 4 mg/mL ortho-Nitrophenyl-β-galactoside (ONPG; dissolved in Z-buffer) solution, and the reaction was stopped when a yellow colour developed by adding 250 µL of a 1 M Na_2CO_3 solution. Both start and end times were recorded. Absorbance at 420 nm (A_{4420nm}) and at 550 nm (A_{550nm}) were measured for each sample in quartz cuvettes and using a "no cell" control sample (50 µL of fresh M9 minimal medium supplemented with 0.1% casamino acid was used instead of cell culture) to blank the Shimadzu UV-1800 spectrophotometer. Miller units were calculated as follows:

$$Miller\ Units\ = 1000\ \times \frac{(A420 - (1.75\ \times A550))}{(t\ \times\ (2\ \times\ V)\ \times\ OD600)}$$

in which 'A420' is absorbance at 420 nm, 'A550' is absorbance at 550 nm, 't' is time of assay (in min), 'V' is volume of cell culture used (in mL), and 'OD600' is the optical density of culture at 600 nm.

2.3.2. Griess assay

Activation of macrophages was assessed by indirectly assessing NO production through quantification of one of the oxidation products, nitrite. This was achieved using the Griess assay (Griess, 1879). Briefly, nitrite standard solutions with concentrations ranging from 0 to 25 µM were prepared in DMEM complete medium and dispensed into a 96-well microtiter in triplicate (50 µL per well). 50 µL samples of culture supernatants (from activated macrophages) were also dispensed in triplicate. 50 µL of a sulphanilamide solution (1% sulphanilamide in 5% phosphoric acid) was added to both sample and nitrite standard wells. After a 10 min incubation at room temperature in the dark, 50 µL of a

0.1% (w/v) solution of N-(1-naphtyl) ethylenediamine dihydrochloride (NED) was added to each well, followed by a 10 min incubation at room temperature in the dark. Absorbance at 540nm (A_{540nm}) was read using a SPECTROstar nano microplate reader (BMG Labtech). The data was averaged, and the average of the 0 µM standard was subtracted from all other averages obtained for the standards, as well as the samples, prior to plotting, and a line was fitted using linear regression. The concentration of nitrite from experimental samples was obtained using the equation of the line fitted for the standard samples.

2.4. Bioinformatics Methods

2.4.1. Whole genome sequencing data

2.4.1.1. Assembly and annotation

Prior to assembling the reads obtained with Illumina® MiSeq, their quality was assessed with FastQC (http://www.bioinformatics.babraham.ac.uk/projects/fastqc) and trimmed using Trimmomatic (Bolger et al., 2014), which improves the quality of the reads by removing sequencing adapters, trimming bases at beginning and end of reads if they fall below the stipulated quality threshold and eliminates reads that do not possess the necessary minimum read length (36 bp by default). A de novo assembly of the reads was carried out using SPAdes Genome Assembler (Bankevich et al., 2012), and Mauve (Darling et al., 2004) was used to order the resulting contigs to a reference genome. For this purpose, the genome sequence of E. coli MG1655 (NC_000913.3) was used followed by an automated annotation using Prokka (Seemann, 2014). With the exception of FastQC, trimmommatic, and Mauve, all other tools were accessed and used through the MRC CLIMB microbial informatics infrastructure funded under grant reference MR/L015080/1.

2.4.1.2. Screening for antibiotic resistance genes, virulence genes, and replicons

Genome sequences were mined for acquired antibiotic resistance genes, virulence genes, and replicon presence using ABRicate (https://github.com/tseemann/abricate) to search the ResFinder v2.1 database (Zankari et al., 2012) for hits above 98% identity and above 90% coverage, the VFDB database (Chen et al., 2005) also for hits above 98% identity and above 90% coverage, and the PlasmidFinder v1.3 database (Carattoli et al., 2014) for hits above 80% identity and above 90% coverage, respectively. For detection of fluoroquinolone resistance, the protein sequence of gyrase subunit A was extracted

from all the genomes, and aligned with T-Coffee (Notredame et al., 2000). Shading was accomplished using BoxShade 3.21 server (https://embnet.vital-it.ch/software/BOX_form.html). ABRicate was accessed and used through MRC CLIMB microbial informatics infrastructure funded under grant reference MR/L015080/1.

2.4.1.3. Protein and DNA alignments

Protein sequences were aligned with T-Coffee (Notredame et al., 2000), and BioEdit v.7.2.5 (Hall, 1999) was used to calculate protein identity and similarity of each pairwise alignment. Where required, alignments were carried out with references MG1655 (NC_000913.3), EC958 wild-type (NZ_HG941718.1), and CFT073 (NC_004431.1). Structural analyses were performed using RaptorX (Källberg et al., 2012) and CCP4MG software (McNicholas et al., 2011). Whole-genome sequence alignments were achieved using the online tool GVIEW server (https://server.gview.ca/). In brief, the genbank file of E. coli MG1655 (NC_000913.3) genome was uploaded as the reference genome, and FASTA files of each of the isolates of the Kent collection were uploaded as query files and organized accordingly to their sequence-type. The default settings were applied for comparison (i.e. 100% sequence coverage; 80% sequence identity).

2.4.1.4. Phylogenetic analysis

The core genome of the isolates in the Kent collection was determined with Roary (Page et al., 2015) using MG1655 genome sequence as a reference (NC_000913.3) and default settings for percentage sequence identity (95%). The core genome gene alignment output by Roary was then used as input in FastTree v2.1.9 (Price et al., 2009; Price et al., 2010), and phylogenetic relationships between the isolates determined. The resulting file was upload into the online tool iTOL v3 (Letunic and Bork, 2016) for editing. For phylogenetic group determination, the Clermont method was used (Clermont et al., 2011; Clermont et al., 2013). In brief, the genomic sequence of each isolate was concatenated in FASTA format and used for in silico PCR using Unipro UGENE platform (Okonechnikov et al., 2012) with the primer sequences used by Clermont et al. (2013). Both Roary and FastTree were used through MRC CLIMB microbial informatics infrastructure funded under grant reference MR/L015080/1.

Chapter 3

Exploring the use of NO as an antimicrobial to combat pathogenic E. coli

3.1. Summary

Urinary tract infections (UTI) are amongst the most common infections in humans, with E. coli being the etiological agent responsible for many UTIs worldwide. As the antibiotic resistance problem worsens, treatment of UTIs becomes increasingly more problematic. Hence, the development of new drugs and alternative therapies is imperative. Nitric oxide is endogenously produced by the mammalian immune system in response to invading pathogens and, as such, the use of NO as a stand-alone alternative therapeutic or in combination with conventional antibiotics is an attractive option. This chapter explores the potential for engineering a NO-producing asymptomatic UTI strain of E. coli to out-compete disease-causing strains in the bladder.

An attempt to engineer NO-production into E. coli UTI strain 83972 was carried out by expression of the NO synthase enzyme (bNOS) from S. aureus, and the efficacy of this system (i.e. NO production) was assessed using a Φhmp-lacZ fusion E. coli strain. In addition, it was of interest to engineer NO tolerance in the same strain: various NO-tolerance mechanisms present in E. coli were tested for their importance in uropathogenic strains under different oxygen conditions, and it is shown that under microaerobic conditions (i.e. the conditions encountered by E. coli during urinary tract infection), flavohaemoglobin Hmp-mediated protection has a predominant role. Simultaneous overexpression of Hmp and bNOS in E. coli 83972 under microaerobic conditions and endogenous production of NO by E. coli, which naturally outcompetes other uropathogenic strains of E. coli, could provide an alternative to conventional antibiotics. Overexpression of flavohaemoglobin Hmp resulted in increased sensitivity to GSNO in both the presence (low aeration) and absence of oxygen, leading us to speculate that the overexpression of Hmp is toxic to bacterial cells beyond the formation of superoxide. While insertion of the bNOS gene into the chromosome of E. coli 83972 was unsuccessful despite the many attempts, it was possible to clone a functional bNOS gene from S. aureus USA300 into a plasmid.

3.2. Introduction

For the most part, E. coli is a harmless bacterium and part of the intestinal flora of many mammals. However, some strains have acquired virulence traits that allows them to colonize different niches and establish infection. Urinary tract infections (UTI) are the most common infections in humans, and E. coli (i.e. uropathogenic E. coli – UPEC) is responsible for more than 80% of UTIs (Totsika et al., 2012; Bien et al., 2012). Conventional antibiotics such as amoxicillin were used for the treatment of uncomplicated UTI for a long time, but emergence of antibiotic resistance has forced a switch to other antibiotics. Currently nitrofurantoin is the antibiotic of choice, however it shows decreased efficacy in the treatment of acute kidney infection (pyelonephritis) due to its poor tissue penetration (Totsika et al., 2012).

3.2.1. Asymptomatic bacteriuria (ABU) 83972

Urinary tract infections can be symptomatic or asymptomatic. Symptomatic UTI are caused by uropathogenic strains of E. coli actively expressing a plethora of virulence factors, while asymptomatic UTIs are caused by asymptomatic bacteriuria (ABU) E. coli strains. The reasons why patients infected with ABU strains do not develop symptoms are still poorly understood, although transcriptomic and comparative genomic studies of ABU prototype strain 83972 revealed that this may not be due to a lack of virulence potential (i.e. potential to cause disease due to presence of virulence genes). 96% of the genes expressed by 83972 are also found in CFT073 (Welch et al., 2002), a well-known UPEC strain that is highly virulent (Hancock and Klemm, 2007). Interestingly, microarray studies from the urine of infected patients have revealed that most of the virulence genes of E. coli 83972 were down-regulated (Roos et al., 2006; Roos and Klemm, 2006), leading to the hypothesis that the down-regulation of virulence genes was necessary for long-term colonization, since some virulence genes, such as fimbriae, are responsible for activation of the immune system (Roos et al., 2006). Interestingly, E. coli 83972 does not express functional type I fimbriae due to a truncation in the fim operon, and also possesses a non-functional pap operon, both of which have previously been shown to be important for ascending UTI (Klemm et al., 2006). Nevertheless, the growth rate of E. coli 83972 in urine is higher than other more virulent UPEC strains, and it has been shown by Roos et al. (2006) that E. coli 83972 is capable of outcompeting other UPEC strains. These characteristics of E. coli 83972 make this strain useful as a

prophylactic treatment in spinal injury patients that are susceptible to recurring UTI (Hull et al., 2000).

In this work, it was hypothesized that engineering of an E. coli 83972 NO tolerant/NO producing strain by overexpression of its flavohaemoglobin Hmp and insertion of a functional bNOS gene onto its chromosome, combined with its natural ability to outcompete other UPEC strains, would result in an alternative and more aggressive form of treatment for UTIs (Figure 3.1).

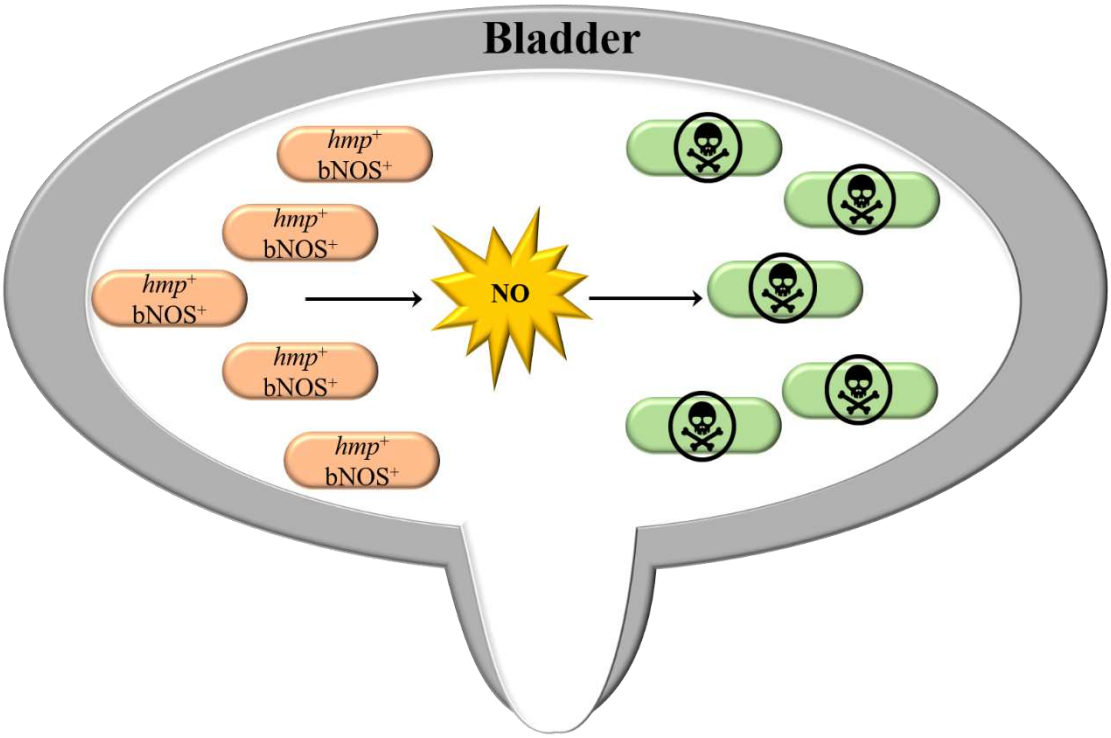

Figure 3.1 – NO-tolerant/NO-producing E. coli 83972 as an alternative treatment for UTIs. It was hypothesized that overexpression of flavohaemoglobin Hmp and insertion and expression of bNOS in E. coli 83972, an asymptomatic strain of E. coli capable of long-term colonization of the bladder and of naturally outcompeting UPEC strains, would result in an aggressive alternative treatment for hard-to-treat UTIs. Colour scheme: light-orange - NO-tolerant/NO-producing E. coli 83972; green – invading UPEC strains.

3.3. Results

3.3.1. Assessment of the role of bacterial NO protective mechanisms in pathogenic E. coli

E. coli possesses several mechanisms that allow it to cope with the toxic effects of NO and other RNS (Figure 1.3). These mechanisms have been intensely studied in E. coli K-12 strains, although studies of their importance in pathogenic strains are scarce. To investigate the importance of each known mechanism that participates in NO-tolerance, several single knockouts mutations were engineered into E. coli EC958, a well-characterized ST131 multidrug resistant UPEC (Totsika et al., 2011; Forde et al., 2014). The role of the hybrid cluster Hcp-Hcr system in NO tolerance was exhibited and published by Wang et al. (2016) at a later date, and as such this system was not tested in the present studies.

3.3.1.1. Well-diffusion assays

In several previous studies, a disc-diffusion assay has been used to test the sensitivity of E. coli to different NO-donors. In Flatley et al. (2005), discs were saturated with a 100 mM solution of the NO-donor (and nitrosating agent) GSNO and placed on bacterial lawns to assess tolerance to GSNO. In this work, a similar protocol was followed to assess sensitivity to GSNO of the different EC958 knockout mutants. However, the protocol proved ineffective as no zones of inhibition were observed for any of the mutants in either M9 minimal agar or LB agar. It was hypothesized that the reactive nature of GSNO combined with poor agar diffusion could be limiting its potency. Hence, a well-diffusion assay was combined with a 'pour plate' technique for generating bacterial lawns. In this assay, mid-exponential growing cultures were mixed with M9 minimal agar before pouring into petri plates; 6-mm wells were cut into the agar and a freshly prepared 80 mM solution of GSNO was used to fill each well. This method allowed us to not only use more GSNO solution (80 µL per well) but also to improve the exposure of bacteria to GSNO (Figure 3.2), thus increasing the overall efficacy.

Under aerobic conditions, both cydAB and cydDC mutants show higher sensitivity for GSNO compared to the isogenic wild-type strain (Figure 3.3), with the cydAB strain also exhibiting sensitivity under microaerobic conditions (Student's unpaired t-test; p-value < 0.05). Loss of hmp also impairs growth in the presence of GSNO under both aerobic and microaerobic conditions (Student's unpaired t-test; p-value < 0.05). In anoxic

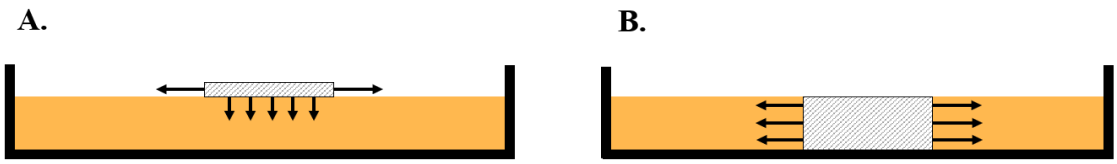

Figure 3.2 – Diagram of GSNO diffusion. A) In a disc diffusion assay, a filter paper disc saturated with GSNO solution is placed on top of a growing lawn of bacteria. The diffusion of GSNO occurs in two directions (arrows). However, downward diffusion will have minimal impact on the lawn of bacteria at the surface of the agar. B) In a well diffusion assay, bacteria are imbedded in the agar and GSNO diffusion from the well occurs only sideways, enhancing exposure of bacteria to GSNO.

conditions, only the loss of flavorubredoxin NorV and the partner reductase NorW induces GSNO sensitivity (Student's unpaired t-test; p-value < 0.05) (Figure 3.3).

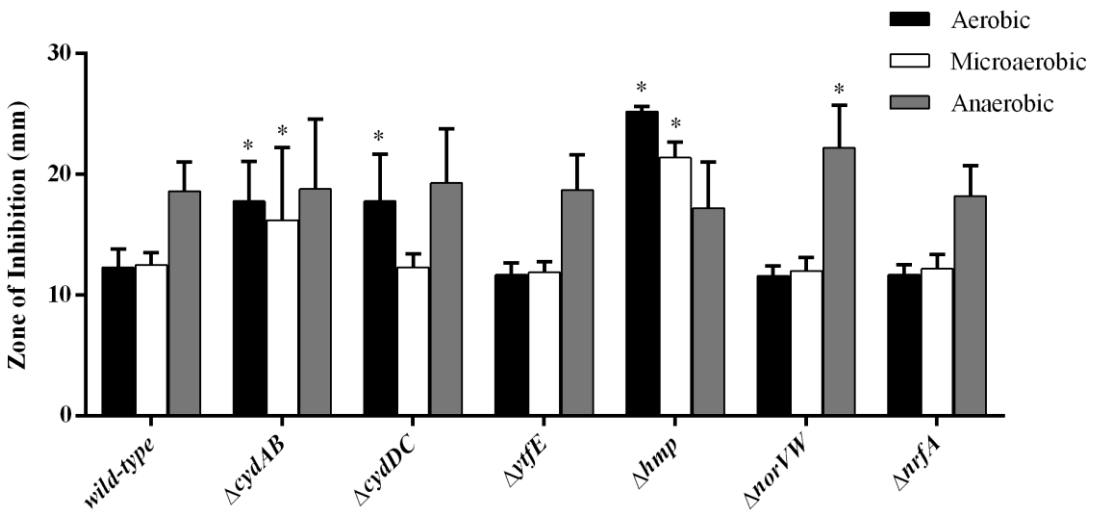

Figure 3.3 – GSNO sensitivity of EC958 knockout mutants. GSNO sensitivity of each mutant was tested in different oxygen conditions and compared to wild-type isogenic strain. Each data point reflects the mean of six replicates from three independent cultures. Error bars represent standard deviation. (*: Student's unpaired t-test p-value < 0.05).

3.3.1.2. NOC-12 growth curves and complementation

To determine if the growth inhibition observed in the well diffusion assay is NO specific and not merely due to other by-products of GSNO decomposition, the wild-type, hmp and cydAB strains (hmp^- and $cydAB^-$ respectively) were grown in M9 minimal medium supplemented with 0.1 % casamino acids in the presence and absence of an alternative NO-donor, NOC-12. In addition, to determine if the growth impairment was solely due to the loss of hmp or cydAB, and not a result of polar effects caused by

insertional mutagenesis, the knockout strains were transformed with a plasmid encoding hmp or cydAB (hmp^+ and $cydAB^+$ respectively) cloned downstream of the inducible lac promoter. In the presence of 0.1 mM NOC-12 both hmp^- and $cydAB^-$ exhibited growth impairment (Figure 3.4C and 3.4E), with doubling times (Figure 3.4A) being significantly

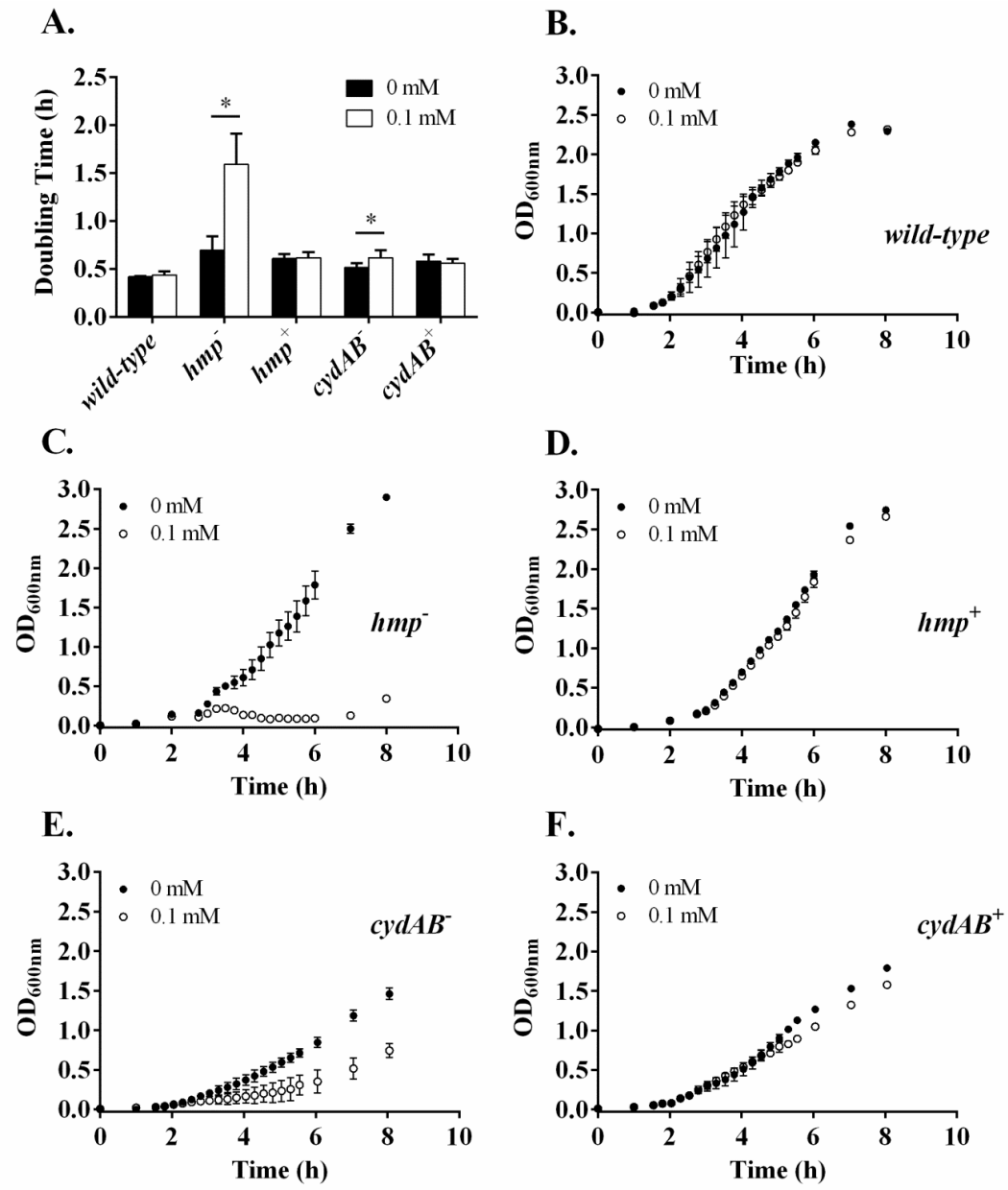

Figure 3.4 – Complementation of the NOC-12-sensitive growth phenotype of hmp and cydAB mutants. EC958 knockout hmp and cydAB mutants were transformed with pSU2718-G-hmp and pSU2718-G-cydABX expression plasmids, respectively. Cultures were grown in M9 minimal media supplemented with 0.1% casamino acids and with glucose as the carbon source. 96-well plates were incubated at 37°C and 100 rpm, the latter providing low aeration and better mimicking the microaerobic conditions encountered in the human urinary tract (B to F). Doubling times (A) were measured for 1.5h following addition of NOC-12 (0 or 0.1 mM) for all strains. Each data point reflects the mean of five replicates. Error bars represent standard deviation. (*: Student's unpaired t-test p-value < 0.05).

different (Student's unpaired t-test p-value < 0.05) than the no treatment control (0 mM NOC-12); complemented strains show no significant difference to the 'no treatment' control (Student's unpaired t-test p-value > 0.05). No NOC-12 growth sensitive phenotype was observed for the EC958 wild-type isogenic strains (Figure 3.4A-B).

GSNO sensitivity for the complemented mutant strains was also assessed using the well-diffusion assay (Figure 3.5). While the diffuse nature of zones of inhibition for the cydAB$^-$ strain precluded a quantitative measure of sensitivity, restoration of growth was confirmed qualitatively for both hmp$^+$ (Figure 3.5A-B) and cydAB$^+$ strains (Figure 3.5C-D).

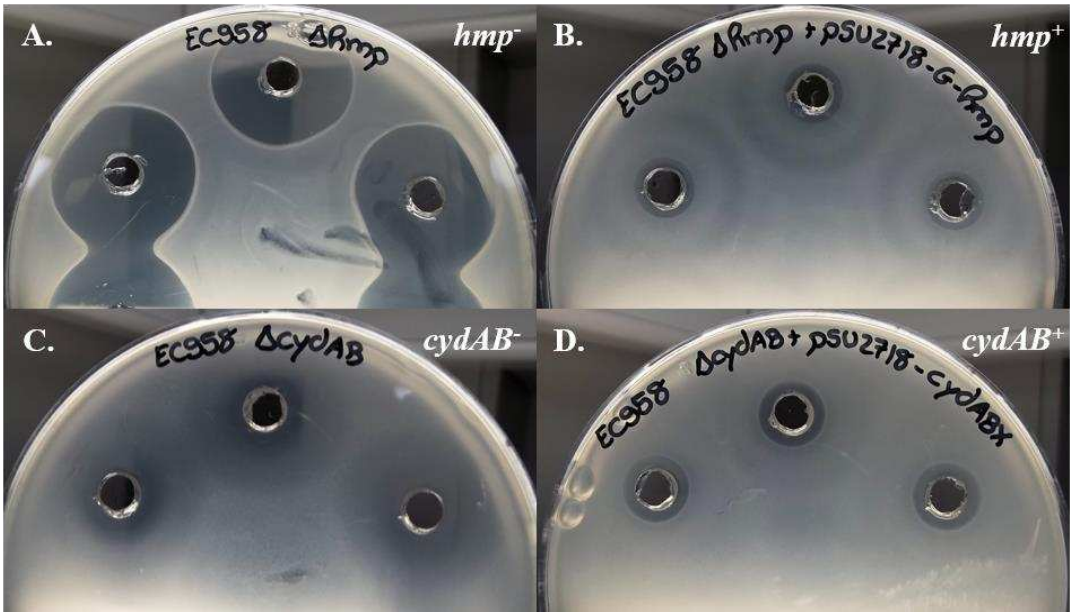

Figure 3.5 – Complementation of GSNO-sensitive growth phenotype of hmp and cydAB mutants. Well-diffusion assay was used for a qualitative observation of the complementation of the GSNO-sensitive growth phenotype. EC958 cydAB and hmp mutants (hmp$^-$ and cydAB$^-$, panels A and C respectively) and their respective complemented strains (hmp$^+$ and cydAB$^+$, panels B and D respectively) were grown in M9 minimal media to OD_{600nm}~0.5, at which point 1 mL of culture was mixed with 19 mL of M9 minimal agar and plated. Wells were cut into the agar and filled with 80 µL of 80 mM GSNO.

3.3.2. Engineering NO-tolerance in E. coli

3.3.2.1. Overexpression of hmp

The loss of hmp and cydAB resulted in a significant increase in GSNO susceptibility under microaerobic conditions (Figure 3.3). Thus, we hypothesized that overexpression of hmp could increase tolerance to NO. To test this hypothesis, a strategy

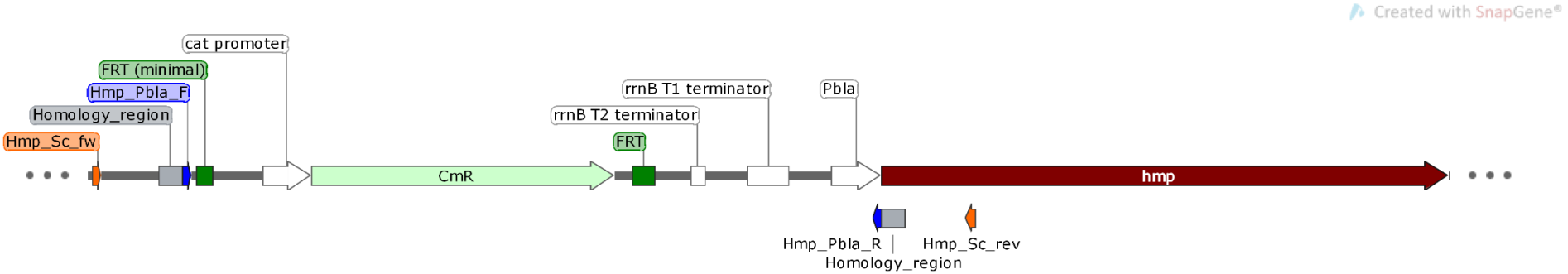

Figure 3.6 – Desired locus of the hmp gene following replacement of the native promoter with P_{bla}. Substitution of the native hmp promoter with the constitutive ampicillin resistance gene promoter (P_{bla}). A chloramphenicol cassette and P_{bla} were amplified from pKD3 – with primers Hmp_Pbla_F and Hmp_Pbla_R – and introduced onto the E. coli chromosome via lambda-red insertional mutagenesis. To achieve this, the primers contained 50 bp regions that were homologous to regions of the hmp locus (as indicated on the diagram by the grey areas identified as "Homology_region"). Primers Hmp_Sc_fw and Hmp_Sc_rev were the screening primers used for the colony PCR.

was devised to constitutively express the chromosomal copy of hmp in E. coli 83972, which involved substitution of the native hmp promoter with the constitutive promoter of the ampicillin resistance gene (P_{bla}). Primers were designed to amplify the P_{bla} promoter from the pKD3 plasmid (Datsenko and Wanner, 2000) to generate a fragment that also included the chloramphenicol resistance cassette to be used as a selective marker (Figure 3.6). The primers also included a 50 bp overhang each, homologous to the desired recombination sites on the E. coli chromosome. The resulting PCR fragment was inserted into 83972 and MG1655 strains of E. coli (via electroporation), both harbouring pKD46 that encodes the lambda-red recombinase (Datsenko and Wanner, 2000). Several attempts to produce a Hmp-overexpressing (P_{bla}-hmp) E. coli 83972 strain proved unsuccessful. However, insertion of the ampicillin resistance gene promoter upstream of hmp was achieved for E. coli MG1655: colony PCR revealed two colonies with a band between 1500-2000 bp (expected molecular size for positive colonies: 1859 bp). E. coli MG1655 wild-type strain was used as a positive control (expected molecular size: 387 bp) (Figure 3.7).

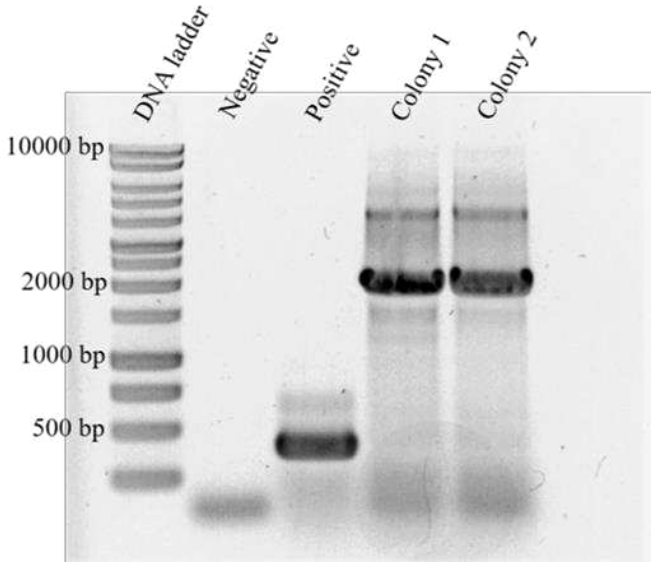

Figure 3.7 – Colony PCR confirming insertion of fragment. Insertion of P_{bla} promoter-containing fragment into chromosome of E. coli MG1655 was confirmed in two transformants ('Colony 1' and 'Colony 2' lanes) by colony PCR using screening primers Hmp_Sc_fw and Hmp_Sc_rev. For the negative control ('Negative' lane), DNA template was omitted from the reaction. For the positive control ('Positive' lane), one colony from E. coli MG1655 wild-type strain was used for DNA template (expected molecular size: 387 bp).

3.3.2.2. Assessment of hmp-overexpressing E. coli MG1655 sensitivity to GSNO

To determine whether constitutive expression of hmp afforded additional protection to GSNO, wild type and P_{bla}-hmp MG1655 strains were grown under low aeration/microaerobic conditions (Figure 3.8A-B) in M9 minimal medium in the presence of different concentrations of GSNO (0 mM, 1 mM, or 5 mM). Under low aeration/microaerobic conditions the P_{bla}-hmp strain exhibited a longer lag phase both in the presence and absence of GSNO. Despite reaching similar final cell densities, in the presence of 5 mM GSNO the lag phase is much longer in P_{bla}-hmp, suggesting a higher sensitivity to this compound. For growth under anoxic conditions, cells were growth statically at 37°C in sealed serum bottles filled to the top with M9 minimal media. As expected, the overall growth for both strains is lower under anaerobic conditions compared to microaerobic conditions. Moreover, P_{bla}-hmp (Figure 3.8D) exhibits higher sensitivity to GSNO than the wild-type strain (Figure 3.8C) under these conditions, with growth in the presence of 5 mM GSNO being almost abolished.

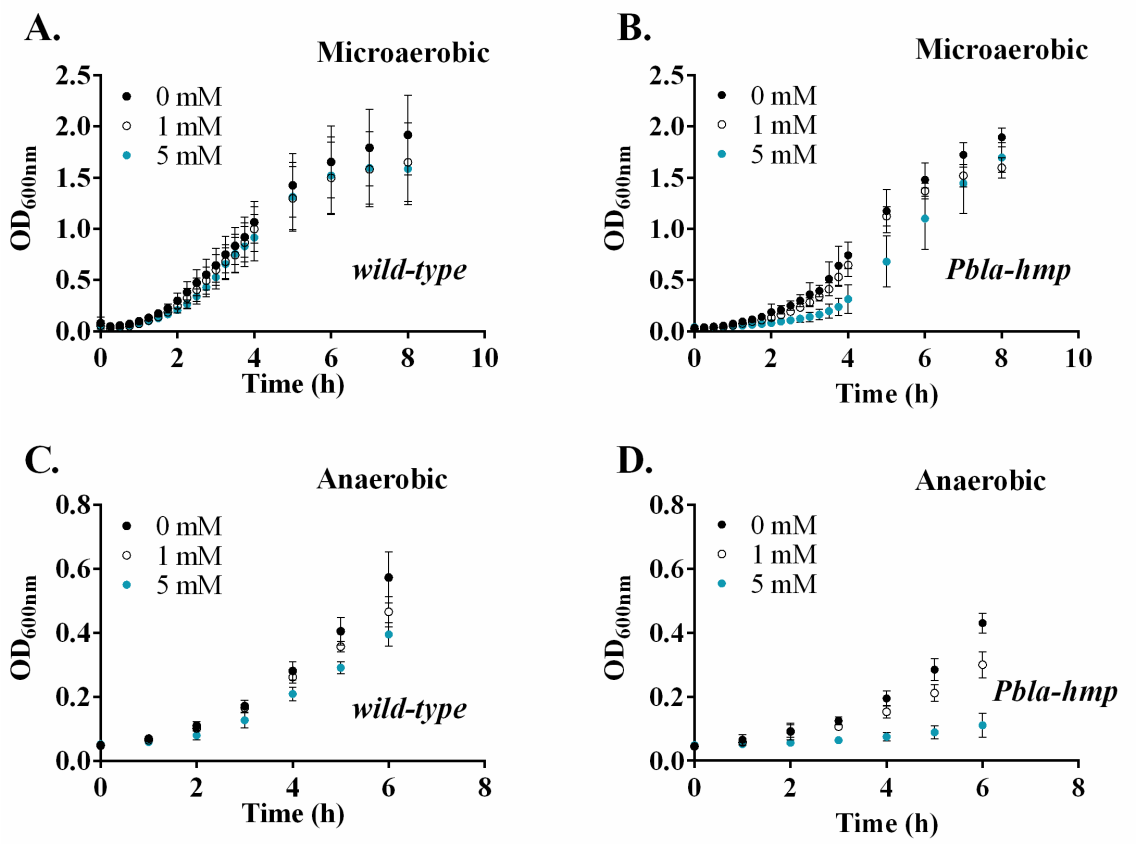

Figure 3.8 – Sensitivity of hmp-overexpressing strain to GSNO. Cells were grown in M9 minimal media at 37°C in 96-well plates at 100 rpm (for low aeration/microaerobic growth; panels A and B) or at 37°C, statically in filled serum bottles (for anaerobic growth; panels C and D). A fresh solution of GSNO was added for a final concentration of 0, 1, or 5 mM. Each data point reflects the mean of at least three different replicates from three independent cultures. Error bars represent standard deviation.

3.3.3. Engineering a NO-producing E. coli strain

An initial aim was to insert the bNOS-encoding gene from S. aureus into the non-functional fim locus of E. coli 83972. This, along with overexpression of the chromosomal copy of hmp, would then be used to generate a NO-tolerant/NO-producing strain which could potentially be used as an alternative to conventional antibiotics to combat UTIs. Despite the unsuccessful attempts to generate a NO-tolerant strain, engineering of an E. coli NO-producing strain was carried out by cloning of bNOS into a plasmid expression vector.

3.3.3.1. Cloning of bNOS

bNOS was amplified from the genomic DNA of S. aureus MRSA USA300, a Gram-positive bacteria known to possess a chromosomal copy of bNOS (Van Sorge et al., 2013). The gene was amplified by PCR, cloned onto pSU2718 downstream of the IPTG-inducible P_{lac} promoter (Figure 3.9A) and introduced into chemically competent E. coli BW25113 via transformation. Transformants were screened by colony PCR (expected molecular size for plasmid containing bNOS: 1197 bp) (Figure 3.9B), and E. coli BW25113 cells containing the pSU2718-hmp plasmid were used as a positive control for the PCR reaction (expected size: 1415 bp) (Figure 3.9B). Further confirmation of recombinant colonies (Figure 3.9B; Colony 5) was obtained by extraction of the plasmid and preparation of single (BamHI) and double (BamHI and FspI) restriction reactions, and subsequent DNA sequencing.

3.3.3.2 Detection of NO production in bNOS-expressing E. coli cells

After confirming the correct pSU2718-bNOS construct had been constructed, this plasmid was introduced into E. coli RKP2176 Φhmp-lacZ (MS486), an identical strain to RKP2178 described in Membrillo-Hernández et al., (1996). This strain was also transformed with the empty pSU2718 vector as a control. Since it is well-known that the hmp promotor repression by NsrR is alleviated in response to NO (Filenko et al., 2007; Tucker et al., 2008), this hmp-lacZ fusion strain would allow for detection of NO by measuring beta-galactosidase activity. Beta-galactosidase assays were conducted in M9 minimal media under aerobic conditions. Cells were grown to early exponential phase, at which point IPTG was added to induce bNOS expression, followed by addition of L-arginine to ensure substrate availability (for the bNOS enzyme). Beta-galactosidase activity was measured every 30 min for a total of 2.5 h. After addition of IPTG and L-arginine (time 0h), beta-galactosidase activity exhibits a rapid 2.6-fold increase over the

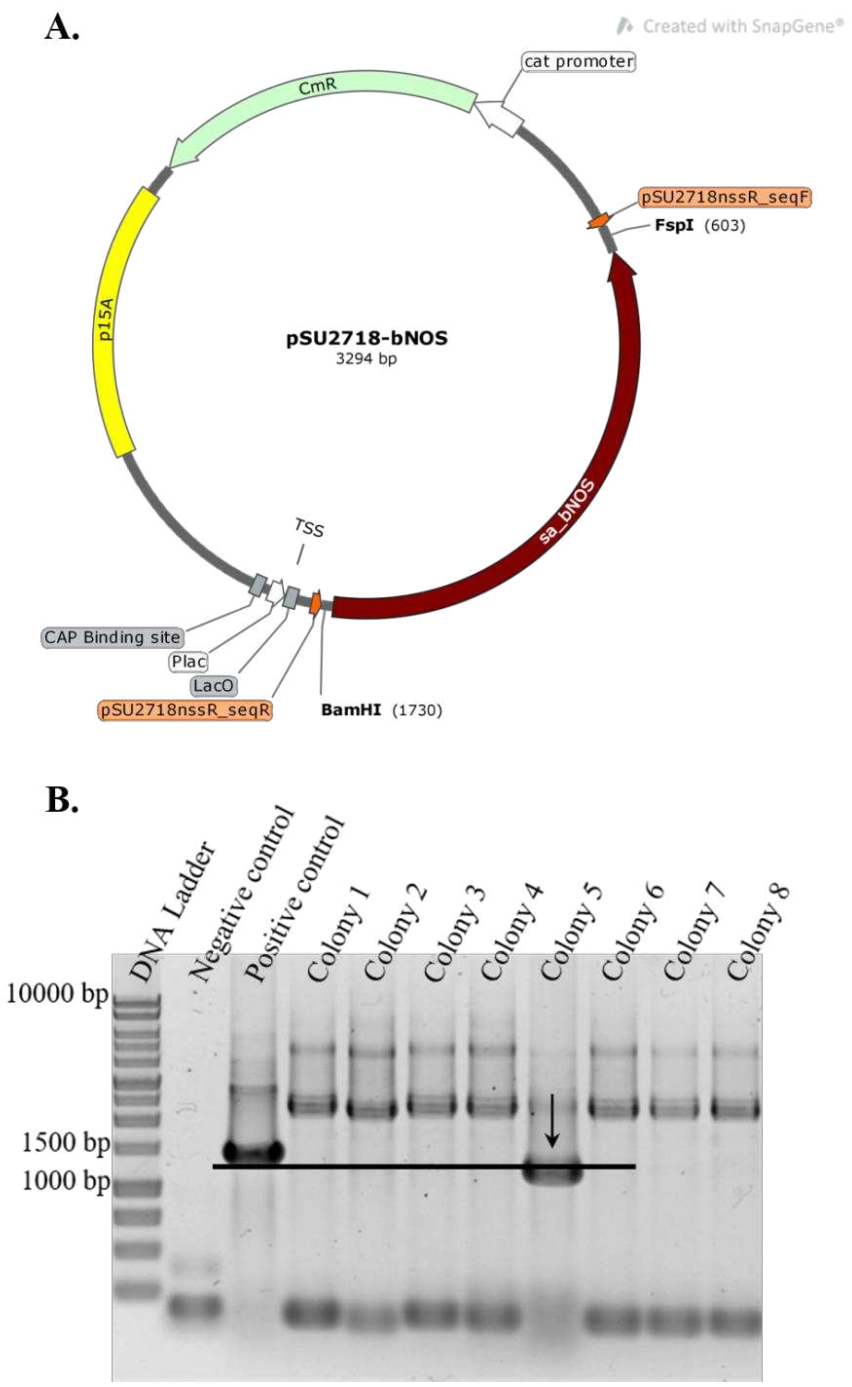

Figure 3.9 – Cloning of bNOS. A) Genetic map of the plasmid containing cloned bNOS gene from S. aureus USA300. B) Colony PCR of eight transformants ('Colony 1-8' lanes) was performed using the primers pSU2718nssR_seqF and pSU2718nssR_seqR to identify colonies with the correct recombinant plasmid (i.e. Colony 5; expected molecular size: 1197 bp). For the 'Negative control', DNA template was omitted from the PCR reaction. For the 'Positive control', E. coli BW25113 harbouring pSU2718-hmp plasmid was used for DNA template (expected molecular size: 1415 bp).

control (pSU2718) (Figure 3.10). Furthermore, beta-galactosidase activity remained higher than that observed for the control throughout the course of the assay (Figure 3.10), which is consistent with the production of NO by a functional bNOS enzyme.

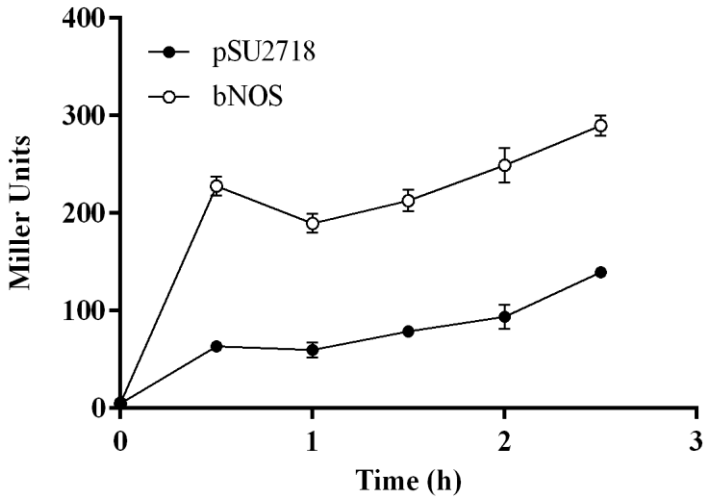

Figure 3.10 – Assessment of NO production by bNOS. A beta-galactosidase assay was used to determine NO production by monitoring the expression of hmp in an E. coli *Φhmp*-lacZ strain harbouring pSU2718-bNOS or the empty pSU2718 vector (control). Assay was performed in M9 minimal medium under aerobic conditions. Each data point reflects the mean of three different replicates from three independent cultures. Error bars represent standard deviation.

3.4. Discussion

3.4.1. Flavohaemoglobin Hmp, cytochrome bd-I, and flavorubredoxin NorVW confer tolerance to nitric oxide in a multidrug resistant E. coli strain

Nitric oxide tolerance mechanisms have been identified and studied in E. coli K-12 strains. However, studies of the importance of these systems in pathogenic E. coli are limited. To determine the importance of these systems in the multidrug resistant E. coli EC958 strain, a well diffusion assay was developed and found to be a more useful tool to measure GSNO sensitivity compared to disc diffusion assays. In the well-diffusion assays, two halos were often observed (Figure 3.5): one closer to the well in which no bacterial growth was observed, and a second in which bacterial growth is observed but slightly distinct from the growth observed in the rest of the plate. It was hypothesized this second halo could be due to lower GSNO concentrations further from the well causing intermediate bacteriostatic effects. Hence, for this reason only the inner zones of inhibition were evaluated where possible. The well-diffusion data confirmed that the flavohaemoglobin Hmp and cytochrome bd-I respiratory oxidase as the two main systems that confer protection against GSNO under both aerobic and microaerobic conditions (Figure 3.3). This was confirmed with complementation studies by expressing hmp or cydABX from a plasmid in the presence and absence of NOC-12 (Figure 3.4) or GSNO (Figure 3.5). Interestingly, the final cell density achieved by the complemented cydAB$^+$ was lower than that achieved by the wild-type or complemented hmp$^+$ strains in the absence of NOC-12. It is important to note that complementation of cydAB relied solely on the basal expression provided by leaky P_{lac} promoter, as it was observed that induction with IPTG concentrations as low as 0.1 mM caused severe growth impairment in both absence and presence of NOC-12. Aerobic bacterial respiration generates ROS (Kohanski et al., 2007; Dwyer et al., 2014; Lobritz et al., 2015) thus a tight regulation of respiratory oxidases is necessary to maintain bacterial viability. Hence, we suggest that even basal expression of cydABX from pSU2718-G-cydABX is enough for an increase in endogenous ROS production to levels that can still be slightly toxic to cells, and in the presence of the NO-donor NOC-12 this effect is more pronounced due to formation of toxic radicals such as peroxynitrite. This growth impairment also made it impossible to accurately measure the zones of inhibition of cydAB$^-$ when the well-diffusion assay was performed, hence only a qualitative approach was carried out using this assay to determine if the complementation was successful (Figure 3.5).

The loss of cydDC causes a significant increase in GSNO susceptibility under aerobic conditions compared to wild-type. This glutathione/L-cysteine ABC exporter is necessary for the assembly of cytochrome bd-I (Georgiou et al., 1987; Poole et al., 1994; Goldman et al., 1996), a role which explains the phenotype observed. However, contrary to expected, no significant susceptibility to GSNO was observed for the cydDC mutant under microaerobic conditions, conditions in which cytochrome bd-I expression is known to be maximal (Fu et al., 1991). Flavorubredoxin NorV and its partner reductase, NorW, were shown to have a prominent protective role against GSNO in the absence of oxygen. Because the main aim was to engineer a NO-tolerant/NO-producing strain that could be used to combat infections in the urinary tract, which is a microaerobic environment (Hagan et al., 2010), a complementation experiment was not attempted for this system. Moreover, the growth impairment exhibited by cydAB$^+$, along with the well-documented NO-detoxifying capability of Hmp, are the reasons why overexpression of hmp was chosen as a strategy to engineer a NO-tolerant strain.

3.4.2. Constitutive expression of Hmp does not confer additional protection to NO

Substitution of the native P_{hmp} promoter for the constitutive P_{bla} promoter was unsuccessful in E. coli 83972 but successful in an E. coli MG1655 background. Under low aeration/microaerobic conditions, the MG1655 P_{bla}-hmp strain exhibited a longer lag phase than its isogenic counterpart. While Anjum et al. (1998) and Wu et al. (2004) have previously shown that overexpression of Hmp under aerobic conditions exacerbates intracellular oxidative stress through the generation of superoxide radicals, it was hypothesised that lowering the oxygen would diminish this effect and permit the generation of an NO tolerant strain without a severe growth phenotype. However, the P_{bla}-hmp strain exhibited a longer lag phase compared to the wild type, and also displayed higher sensitivity to GSNO. This could be explained by the levels of oxygen still being too high, and the resultant superoxide generated by Hmp reacting with NO released by GSNO to form highly toxic peroxynitrite. In McLean et al. (2010), anaerobic growth of a nsrR mutant strain of Salmonella Typhimurium, which overexpresses Hmp due to loss of its negative regulator, exhibited higher tolerance to peroxynitrite than when grown under aerobic conditions. Due to the unwanted toxicity problems, even under low aeration conditions, the sensitivity to GSNO of the P_{bla}-hmp strain was tested in the absence of oxygen. Interestingly, in the presence of 5 mM GSNO, anaerobic growth of the Hmp-overexpressing strain was severely impaired. Constitutive expression of Hmp will result in very high levels of this flavohaemoglobin regardless of oxygen concentration, whereas

under anaerobic conditions the Salmonella nsrR mutant did not overexpress Hmp, presumably due to activity of FNR. One might postulate that these very high levels of Hmp might place additional demands upon the cell that could render the cell sensitive to GSNO, although it is premature to speculate what the underpinning mechanism may be.

3.4.3. NO-production by bNOS in E. coli

Despite the unsuccessful attempt at engineering a NO-tolerant E. coli 83972 strain, the cloning of bNOS was carried out. S. aureus bNOS was cloned into pSU2718 vector, and assessment of bNOS functionality was undertaken by measuring beta-galactosidase activity in a Φhmp-lacZ strain (Figure 3.10). A higher beta-galactosidase activity, i.e. higher hmp expression, was observed for the strain harbouring pSU2718-bNOS, thus suggesting that the bNOS construct is producing active bNOS. Quantification of both nitrate and nitrite, products of NO oxidation, from supernatants of bacterial cells expressing bNOS was attempted with a modified Griess assay. This proved to be an unreliable approach to study NO production in these engineered strains, perhaps due to slow NO production by bNOS resulting from poor cofactor insertion or availability of arginine in the cytoplas or resulting from a rapid turnover of nitrate and nitrite by E. coli cells. Alternatively, since the bNOS enzyme only comprises the haem-containing oxidase domain and therefore requires a redox partner (or endogenous reductants such as GSH) to supply reducing power for the reaction to take place, perhaps the availability of reductants is the limiting factor for the modest NO production observed herein.

3.4.4. NO-producing/NO-tolerant E. coli as an alternative therapy: is it possible?

Due to the involvement of NO in critical biological functions, its use in the treatment of diseases is not a new concept. In fact, inhalation of nitric oxide is used to treat neonatal pulmonary hypertension (Wessel et al., 1997; Hunt et al., 2016). Due to its antimicrobial properties, a strategy was devised to engineer a NO-producing/NO-tolerant strain that could potentially be used to fight multidrug resistant UTIs.

In this project a NO-producing E. coli strain was engineered by expressing bNOS (from S. aureus) from a plasmid. However, NO production was only achieved using an indirect method, i.e. a beta-galactosidase assay that quantified hmp promoter activity, and thus NO levels cannot be accurately inferred in this instance. Ideally, a more direct method of NO quantification, such as using a NO electrode, should have been used. The levels of NO being produced by bNOS are not the only limitation arising in this project. The very reactive nature of NO, combined with the cytoplasmic localization of bNOS in

our engineered E. coli strain, will limit the diffusion of NO to the point of very little to no NO diffusing to the outside of the cell and reach the intended target. Targeting bNOS to the periplasmic space could potentially circumvent this issue: NO would have less cellular targets to react with (compared to cytoplasm) which would result in a better diffusion and, potentially, higher levels of NO reaching the invading pathogen. Furthermore, the main NO detoxification mechanism of E. coli in the presence of oxygen (i.e. flavohaemoglobin Hmp) is localized in the cytoplasm, thus the periplasmic location of bNOS, and hence periplasmic production of NO, reduces the chance of flavohaemoglobin Hmp to completely interfere with NO levels.

Despite the absence of bacteria in urine in healthy individuals, it is becoming increasingly accepted that the bladder itself is not a sterile environment and, in fact, possesses a microbiome with a protective role (Brubaker and Wolfe, 2016; Thomas-White et al., 2016). In view of this information, one must consider the effects that NO will have on the natural microbiome; affecting the microbiome of the bladder in any way may, in fact, be more harmful to the host.

To engineer a NO-tolerant strain of E. coli, the wild-type hmp promoter was replaced by the constitutive P_{bla} promoter, and NO susceptibility was determined. Whilst increased sensitivity to GSNO in the presence of oxygen (Figure 3.8, panel A and B) could be explained by formation of superoxide (Membrillo-Hernández et al., 1996; Mills et al., 2001; Wu et al., 2004), the sensitivity exhibited under anaerobic conditions was surprising. It is possible that this sensitivity could be due to toxicity caused by high levels of flavohaemoglobin protein expression. However, this hypothesis would have to be tested by assessing the levels of flavohaemoglobin Hmp with a western blot, using the wild-type strain as a control.

Chapter 4

Phenotypic and genotypic characterisation of E. coli bacteraemia isolates

4.1. Summary

The emergence of antibiotic resistance has become a cause for concern as it is leading to an increase in mortality and morbidity associated with bacterial infections. Hence, not only is it necessary to find alternative therapies to combat resistant and multi-drug-resistant bacteria but to also monitor the appearance and dissemination of antibiotic resistance and antibiotic-resistant clones to better understand the problem and also to administer the most suitable treatment to patients and prevent patient relapse.

In this chapter, 50 bacteraemia E. coli isolates (i.e. collected from the blood of patients), were characterized phenotypically and genotypically for clonal lineage, antibiotic resistance, virulence, and presence of plasmids. Whilst most of the collection remained sensitive to all antibiotics experimentally tested, resistance to commonly used antibiotics such as amoxicillin and trimethoprim was highly prevalent. 14% of the clinical isolates showed a multidrug-resistant phenotype, with this number increasing to 30% when antibiotic resistance was detected by mining the genome sequences of the isolates for acquired resistance genes. However, in silico detection of antibiotic resistance resulted in many false negatives, mainly for ciprofloxacin resistance. In addition, in silico detection produced false positives for antibiotic resistance, mainly for chloramphenicol. Thus, whilst a convenient tool to detect antibiotic resistance, caution needs to be taken when interpreting in silico results and the data should always be complemented with a phenotypic assay.

Despite observing that ST73 isolates were, on average, more virulent and less resistant, and ST131 isolates were, on average, less virulent and more resistant, no correlation between both variables was detected in the isolate collection as a whole. However, an association between resistance and specific virulence factors cannot be discounted.

Evidence of an association between CTX-M-15 and aac(3)-IIa, aac(6')Ib-cr, and blaOXA-1 is shown, and could explain why ESBL-producing isolates often exhibit a multidrug-resistant phenotype. Moreover, an association between certain virulence genes and phylogenetic group B2, which comprises sequence-types known to be associated with UTIs, was also found.

4.2. Introduction

E. coli is usually a commensal bacterium and part of the normal human intestinal flora, where it promotes normal intestinal function and rarely causes disease. Some strains of E. coli, however, acquired certain genes (e.g. virulence genes) and took on a more pathogenic nature towards the host, and are thus capable of causing a broad spectrum of diseases. Pathogenic E. coli can be further subdivided according to their site of infection: enteropathogenic E. coli (EPEC) are responsible for many intestinal infections, particularly in infants, and extraintestinal pathogenic E. coli (ExPEC) are responsible for extraintestinal infections such as neonatal meningitis and UTIs. ExPEC are the most common cause of infection in humans and E. coli is the etiological agent responsible for 80% of UTIs (Totsika et al., 2012; Bien et al., 2012).

The ability of pathogenic E. coli to adapt and colonize new niches, combined with the emergence of antibiotic resistance, has led to a serious worldwide threat. One particular clonal type of E. coli, ST131, is the predominant lineage among ExPEC isolates. ST131-type strains, often associated with UTIs, are widespread and commonly reported to have an ESBL phenotype and exhibit fluoroquinolone resistance. Furthermore, it has been suggested that ST131 are responsible, at least in part, for the current increase of antibiotic-resistant E. coli, particularly ESBL-producing and fluoroquinolone-resistant E. coli (Johnson et al., 2010). This clonal group also contains a large virulence repertoire, and it was proposed that the combination of high antibiotic resistance levels and virulence genes confers an advantage to ST131 over other E. coli clonal groups, facilitating its dissemination (Johnson et al., 2010; Peirano et al., 2013). This combination contradicts the belief that increased levels of antibiotic resistance has a negative impact on fitness, thus resulting in less pathogenic strains (Johnson, Gajewski, et al., 2003; Houdouin et al., 2006; Moreno et al., 2006; Johnson et al., 2010).

The emergence of E. coli ST131 highlights the need to better understand the molecular mechanisms behind pathogenicity and how this might affect antibiotic resistance. Furthermore, a deeper understanding of the magnitude of the problem is also of the utmost importance. Whole genome sequencing is a powerful tool which could be used for these purposes. It would allow collection of important information, such as antibiotic resistance and virulence genes, in one single step, as well as the identification of novel targets for antibiotics or vaccines. In fact, whole genome sequencing was successfully used to screen the genome of serogroup B meningococcus and identify several conserved, surface-exposed antigens, which were then experimentally tested and used to develop a vaccine

against Neisseria meningitidis (Pizza et al., 2000; Savino et al., 2006). The use of whole genome sequencing for molecular diagnostics is not currently well established in clinical settings, but its application is predicted to assist with epidemiological typing, support clinicians during outbreaks, and improve patient treatment (Ellington et al., 2012; Köser et al., 2012; Fricke and Rasko, 2014).

4.3. Results

4.3.1. General genome features

In this work, the 50 E. coli bacteraemia isolates, collected from East Kent Hospitals University NHS Foundation, that comprise the designated Kent collection, were phenotypically and genotypically characterized. For the latter, whole genome sequencing was performed by preparing a library containing the genomic DNA of the clinical isolates using the Nextera® XT DNA Library Prep Kit, which is optimized for small genomes. This kit uses a transposome complex to simultaneously fragment genomic DNA and insert adapter sequences. The following PCR step uses the adapter to amplify the DNA fragments and add specific index sequences to each genomic DNA sample, thus allowing sequencing of pooled libraries. Following library preparation, samples were sequenced using an Illumina MiSeq benchtop sequencer. Key advantages of this sequencer include a fast run time and low-cost per run and per base pair, making it the ideal sequencer for small sequencing projects such as the one carried out in this work. The resulting short paired-end reads were assessed for quality with FastQC before and after trimming of the reads using Trimmomatic (Bolger et al., 2014), which removes the adapter sequences inserted during genomic DNA library preparation, as well as low quality bases and reads from the data. The trimmed reads were used as input in SPAdes Genome Assembler (Bankevich et al., 2012) for a de novo assembly of the bacterial genome. The resulting contigs were subsequently re-ordered using the genome of E. coli MG1655 as reference (NC_000913.3) with Mauve (Darling et al., 2004) and annotated with Prokka (Seemann, 2014).

The general features of all 50 E. coli genomes following assembly and annotation are shown in table 4.1. The smallest genome belonged to KC20 (4.66 Mb) and the largest to KC27 (5.52 Mb), and there is a clear linear relationship between the size of a genome and the number of CDS present (Figure 4.1) despite a relatively constant CDS density (0.93 ± 0.01 genes per kb) in all isolates of the collection.

Table 4.1 – General features of the assembled genomes

MS number	KC number	Genome size (Mb)	No. contigs	No. CDS	CDS density (CDS per kb)
188	KC1	5.18	134	4812	0.93
189	KC2	5.18	120	4861	0.94
190	KC3	4.85	90	4476	0.92

191	KC4	5.13	117	4716	0.92
192	KC5	5.08	109	4691	0.92
193	KC6	5.01	137	4697	0.94
194	KC7	5.14	134	4780	0.93
195	KC8	5.33	166	4959	0.93
196	KC9	5.27	195	4953	0.94
197	KC10	5.00	127	4687	0.94
198	KC11	5.21	229	4945	0.95
199	KC12	4.73	83	4402	0.93
200	KC13	5.41	187	5124	0.95
201	KC14	4.88	408	4611	0.94
202	KC15	5.18	106	4813	0.93
203	KC16	5.16	149	4767	0.92
204	KC17	4.79	104	4440	0.93
205	KC18	5.31	181	5059	0.95
206	KC19	4.96	135	4588	0.92
207	KC20	4.66	183	4278	0.92
208*	KC21	5.27	81	4965	0.94
209	KC22	4.91	118	4577	0.93
210	KC23	5.30	218	4922	0.93
211	KC24	4.90	403	4553	0.93
212	KC25	4.94	351	4554	0.92
213	KC26	4.78	1016	4434	0.93
214*	KC27	5.52	385	5145	0.93
215	KC28	4.88	408	4613	0.94
216	KC29	5.21	184	4826	0.93
217	KC30	5.26	154	4857	0.92
218	KC31	5.22	851	4997	0.96
219	KC32	5.04	233	4692	0.93
220	KC33	5.33	270	5052	0.95
221	KC51	5.10	216	4703	0.92
222	KC35	5.03	250	4677	0.93
223	KC36	4.66	721	4380	0.94
224	KC37	4.95	339	4556	0.92
225	KC38	4.93	56	4584	0.93
226	KC39	5.23	236	4871	0.93
227	KC40	5.23	265	4842	0.93
228	KC41	5.10	146	4802	0.94
229	KC42	5.28	148	4956	0.94
230	KC43	5.10	73	4765	0.94
231	KC44	5.08	144	4674	0.92
232	KC45	5.31	188	4899	0.92
233	KC46	5.28	246	4929	0.93
234	KC47	5.34	162	4979	0.93
235	KC48	5.22	207	4818	0.92

236	KC49	5.03	174	4676	0.93
237	KC50	5.13	135	4762	0.93

* Sequencing of these isolates was initially unsuccessful. As such, whole genome sequencing of these isolates was performed by MicrobesNG (Birmingham).

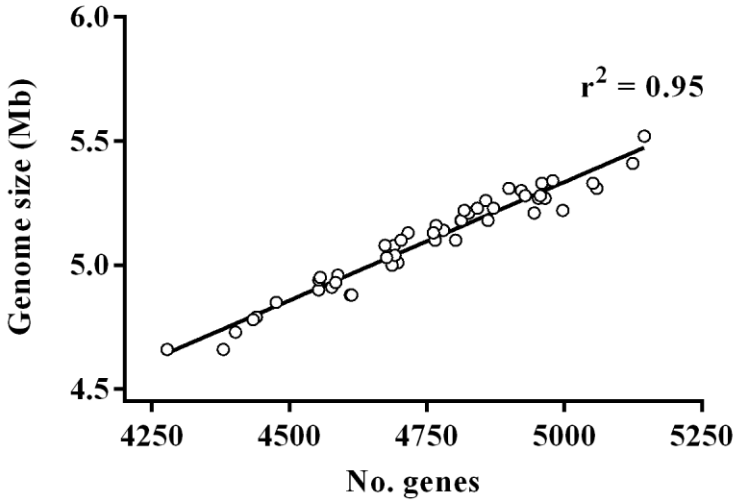

Figure 4.1 – Relationship between genome size and number of genes in the KC collection.

4.3.2. Clonal and phylogenetic analyses

4.3.2.1. Multi-locus sequence typing

Multi-locus sequence typing (MLST) was performed according to the Achtman typing scheme (Wirth et al., 2006), which uses the internal sequence of seven housekeeping genes (adk, fumC, gyrB, icd, mdh, purA, and recA) to assign each E. coli strain to a specific sequence type (ST). Each sequence is searched against a database and assigned an allelic profile number, and each ST is determined based on the combination of the seven alleles.

In total, 23 different STs were identified in the collection. The most prevalent STs in the Kent collection was ST73 (n=9; 18%), followed by ST69 (n=7; 14%) and ST131 (n=6; 12%). Sixteen isolates (32%) represented their own ST, with four of the isolates in the collection not assigned to any known ST, and thus represent four novel STs. A minimum spanning tree (Figure 4.2) was constructed based on the MLST profile (Appendix A-1) to illustrate the clonal relationship based solely on the allelic profile of the seven housekeeping genes. Two of the four novel STs (?2 – KC33; ?3 – KC51) differ from ST131 and ST73, respectively, by one single allele, and singletons ST685, ST421, ST1618 also share six identical alleles (out of seven) with ST10, ST95, and ST73, respectively. All other STs identified differ from other STs by three or more alleles.

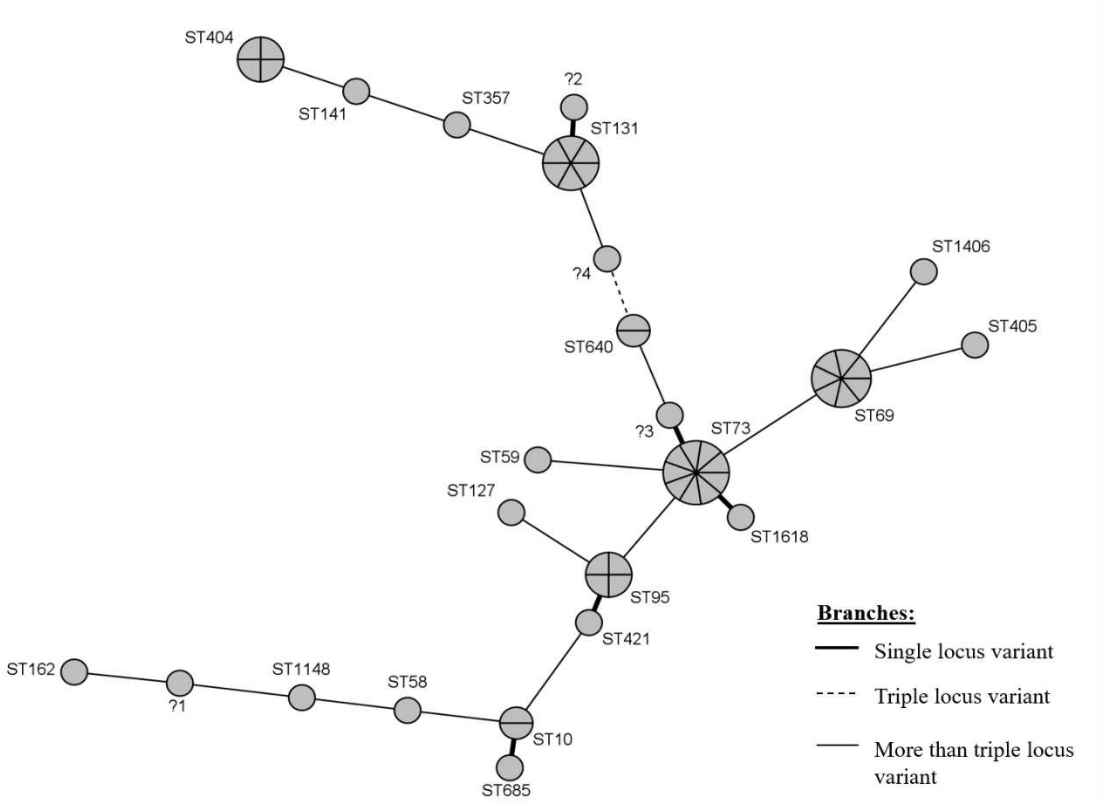

Figure 4.2 – Minimum spanning tree of E. coli STs from the Kent collection. Partitions indicate the proportion of isolates in the collection belonging to the indicated ST. Strains within the same ST possess seven identical alleles; a single locus variant possesses one different allele to the other ST; a triple locus variant differs by three alleles; and a more than triple locus variant differs by more than three alleles. The four unassigned STs are identified as '?1' (KC17), '?2' (KC33), '?3' (KC51), and '?4' (KC38).

4.3.2.2. Whole genome alignment

A whole genome sequence comparison circular map was generated using the BLAST atlas setting of the GView server (https://server.gview.ca/) (Figure 4.3). While there is some degree of genetic variation between STs, within the isolates of a particular ST very little variation is observed. The backbone of ST404 and ST640 genomes exhibit less variability among themselves, in comparison with the higher variability observed in isolates within ST73, ST131, ST69, ST10, and ST95. In ST69, most of the genetic variability appears to originate from KC28 (represented by the fourth lane, from the inside, of the ST69 set in figure 4.3).

4.3.2.3. Pan- and core-genome

Described for the first time by Medini et al. (2005), the term pan-genome refers to the complete collection of genes present in a bacterial species (Figure 4.4) and

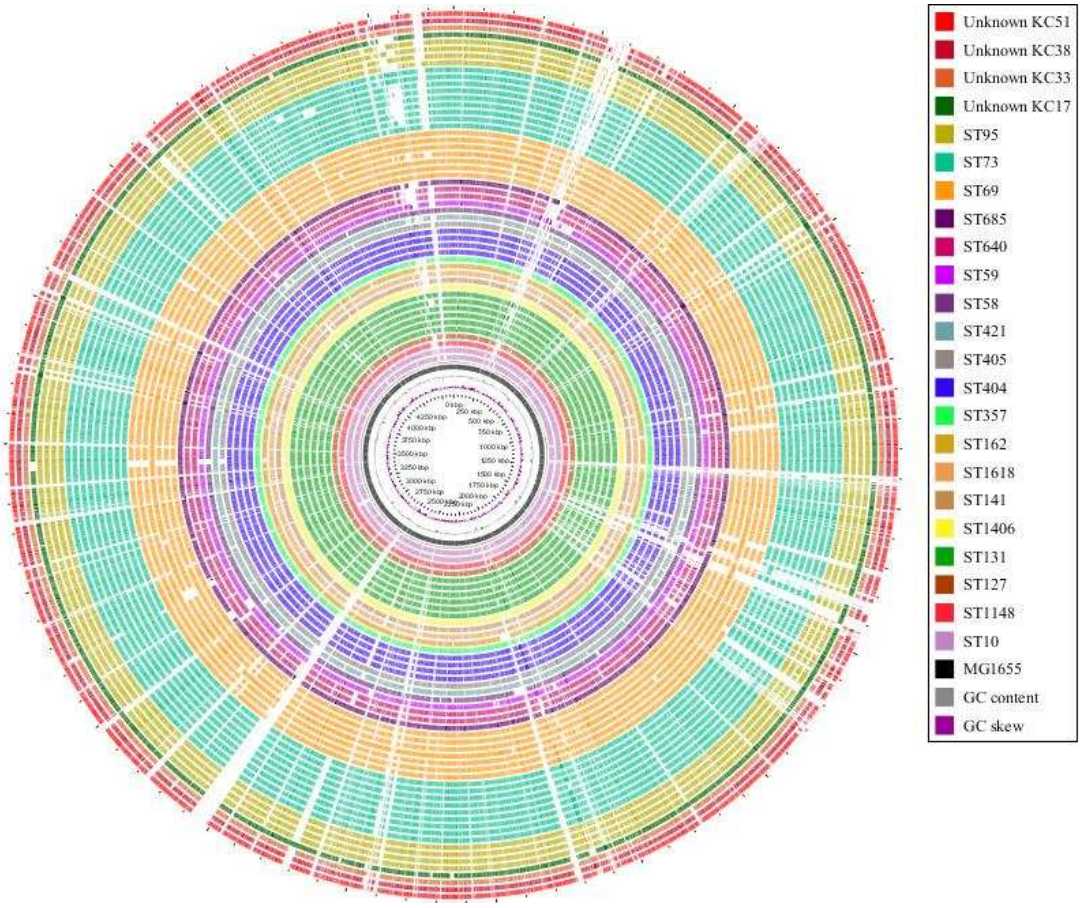

Figure 4.3 – Whole genome comparison of E. coli MG1655 with the 50 clinical isolates of the Kent collection. The inner black ring corresponds to E. coli MG1655 and with each lane thereafter corresponding to a genome. Isolates were coloured according to their ST (colour-key legend is on the right). The four outermost lanes correspond to the isolates of unknown ST. Blank spaces indicate that the gene at that position in the reference genome is not found in the genome of that lane.

comprises the core genome (i.e. the set of genes shared by all strains of a bacterial species and involved in fundamental physiological functions and phenotypic traits of the bacterial species), the dispensable genome (i.e. the set of genes present in only a small subset of strains), and unique genome (i.e. a set of genes present in only one strain) (Figure 4.4). Both the 'dispensable' and 'unique' genome encode proteins not essential for bacterial growth and instead possess genes that confer a selective advantage (e.g. antimicrobial resistance genes or virulence genes) (Medini et al., 2005).

The tool Roary (Page et al., 2015) was used to determine the distribution of core and dispensable genes in the Kent collection and in E. coli MG1655. Briefly, the general feature format (GFF) file of each genome generated by Prokka (Seemann, 2014) was used in Roary as input, which converted complete CDS nucleotide sequences to protein sequences, followed by a protein BLAST comparison of all sets of protein sequences (one

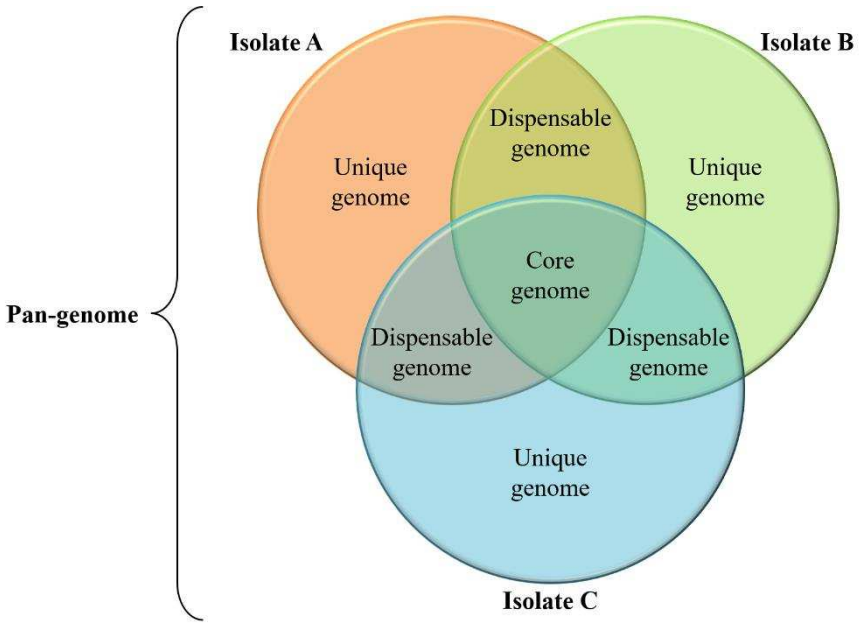

Figure 4.4 – Venn diagram of the pan-genome. The pan-genome is described as the pool of genes of a bacterial species (core genome + dispensable genome + unique genome).

per genome). The pan-genome of the Kent collection, including E. coli MG1655, is made up of 13,172 genes in total (Figure 4.5A). Only approximately 19.6% of the genes (n=2,580) are a part of the core genome (i.e. present in all isolates), while accessory genes make up the remaining 80.4% (n=10,592) of the entire pan-genome (Figure 4.5A). The pan-genome of E. coli is an open pan-genome (Figure 4.5B) meaning the number of total genes increases with every new genome added.

The multi-FASTA alignment file of the core genes created by Roary was used as input in FastTree (Price et al., 2009; Price et al., 2010) to deduce the approximately-maximum-likelihood phylogenetic relationship of the isolates of the Kent collection based on single nucleotide polymorphisms (SNPs) present in the core genome (Figure 4.6), and in silico PCR was used to determine the phylogenetic group of each E. coli isolate according to the Clermont quadruplex method (Clermont et al., 2013). Phylogenetic group B2 forms the basal group, with all other phylogenetic groups diverging later, and phylogenetic group A diverging last (Figure 4.6). Interestingly, KC20, also assigned to phylogenetic group B2, is shown to diverge much later than the remaining members of phylogenetic group B2, and is more closely related to members of phylogenetic group A. Over half of the entire collection (n=33; 65%) was assigned to phylogenetic group B2, including the isolates of sequence-type ST131, ST73, ST95, ST404, and three of the four isolates with novel STs. Interestingly, KC28, also belonging to ST69, was assigned to phylogenetic group A, along with KC14 and KC36 (both ST10),

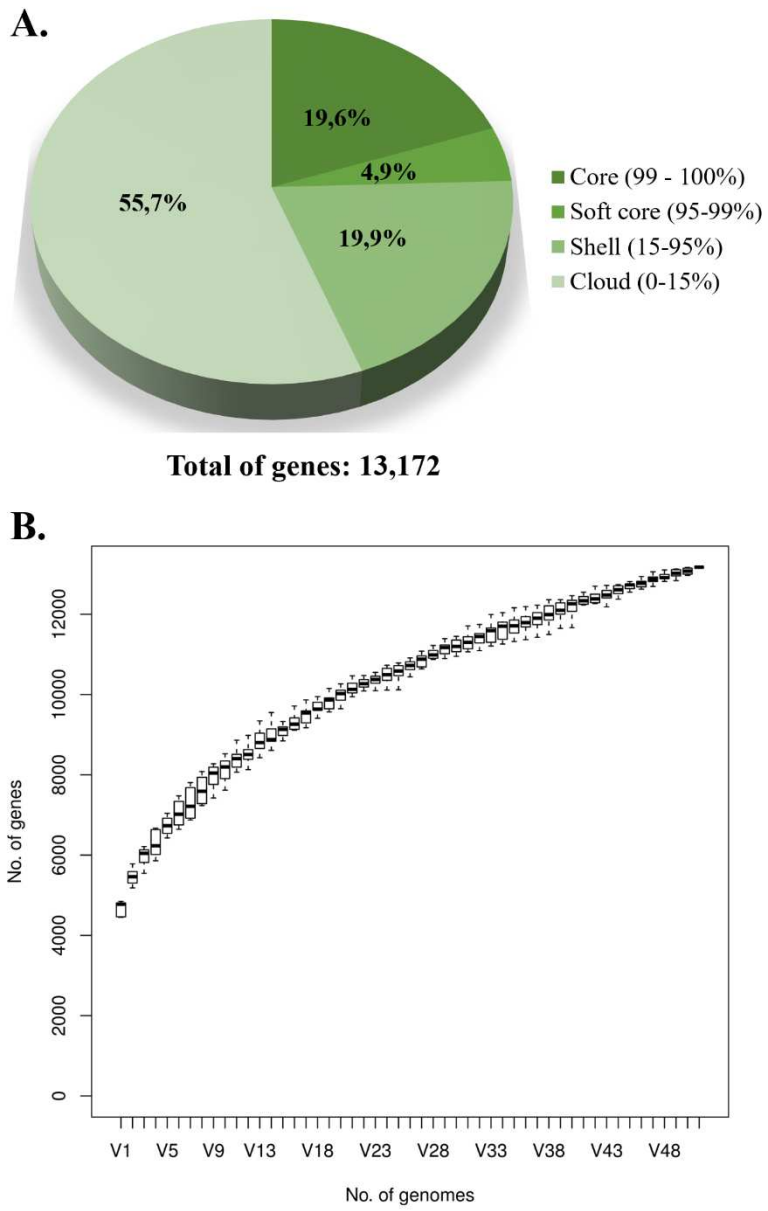

Figure 4.5 – The pan-genome of the Kent collection. A) The pan-genome of the Kent collection, including E. coli MG1655, comprises a total of 13,172 genes, with only 19% of these genes forming the core genome. B) The Kent collection exhibits an open pan-genome, with the number of genes increasing as more genomes are analysed.

and commensal E. coli MG1655. Apart from KC28 (ST69) and KC10 (ST131) that are assigned to phylogenetic group A and unknown phylogenetic group, respectively, STs with more than one isolate were assigned to the same phylogenetic group (Figure 4.6). Isolates from the same ST often cluster together, sharing a recent common ancestor.

4.3.3. Antibiotic resistance analysis

The phenotypic antibiotic resistance profile of the Kent collection was determined

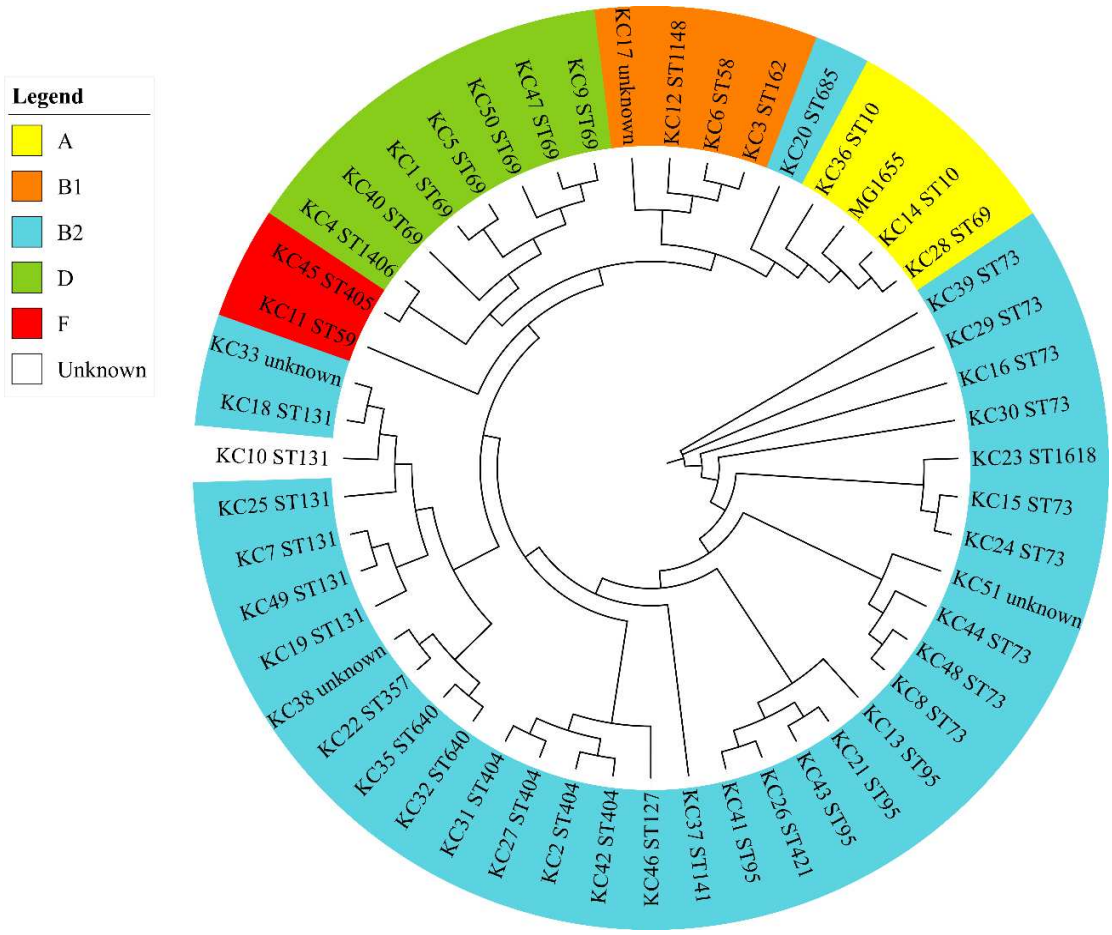

Figure 4.6 – Dendrogram for the genetic relationships of E. coli isolates in the Kent collection. Phylogenetic relationship of the E. coli isolates of the Kent collection was inferred based on SNPs present in the core genome. For all isolates, the ST is indicated besides their KC number. Apart from KC10 (highlighted in white), all isolates were assigned to a phylogenetic group: phylogenetic group A in yellow; phylogenetic group B1 in orange; phylogenetic group B2 in blue; phylogenetic group D in green; and phylogenetic group F in red.

using disc diffusion assays (see Appendix B-1 and Appendix C-1 for full characterization of the Kent collection). Resistance to nine antibiotics was experimentally tested: penicillins (amoxicillin – AMX), cephalosporins (cefotaxime – CTX), phenicols (chloramphenicol – CAP), fluoroquinolones (ciprofloxacin – CIP), aminoglycosides (gentamicin – GEN), carbapenems (meropenem – MEM), nitrofurans (nitrofurantoin – NIT), trimethoprim (TMP), and polypeptides (polymyxin E/colistin – PME). More than half of the collection – 56% (n=28) of the isolates remained sensitive to all antibiotics tested, while the remaining isolates (n=22) exhibited resistance to at least one of the antibiotics tested, with seven of these isolates (14%) exhibiting a multidrug-resistant phenotype (i.e. resistant to three or more antibiotic classes) (Magiorakos et al., 2012) (Figure 4.7A). Three of the isolates (6%) exhibited resistance to cefotaxime (Figure

4.7A), and further analysis of their genome revealed the presence of the highly disseminated ESBL CTX-M-15 (Nicolas-Chanoine et al., 2008; Lau et al., 2008). The highest level of resistance was observed for amoxicillin (n=21; 42%), followed by trimethoprim (n=14: 28%) and ciprofloxacin (n=9; 18%) (Figure 4.7B). No isolate in the collection exhibited resistance to either meropenem or colistin (Figure 4.7B).

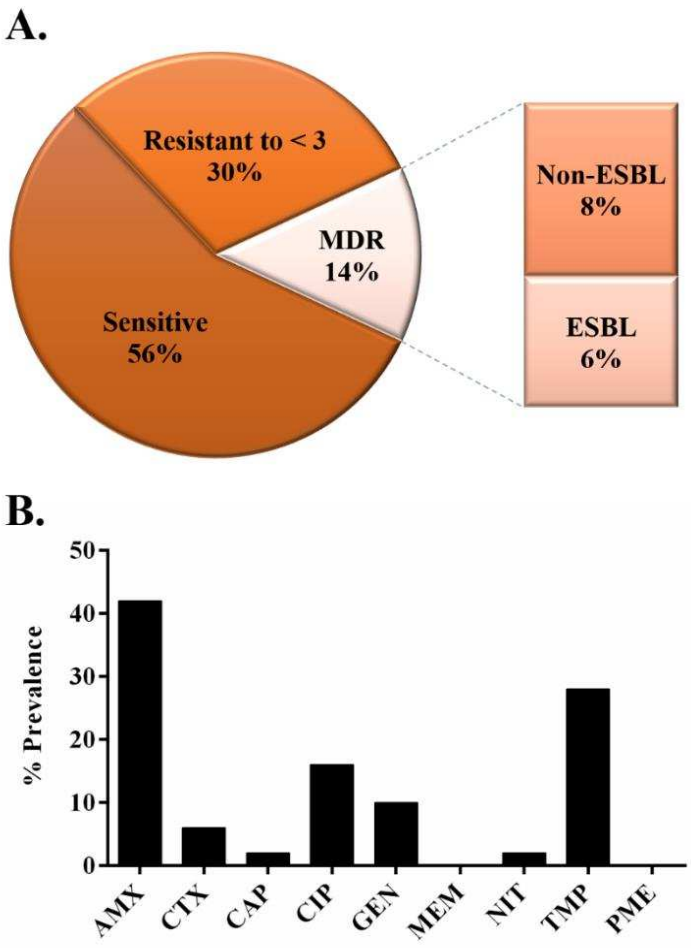

Figure 4.7 – Antibiotic susceptibility of the Kent collection. A) 14% of the isolates in the collection (n=7) exhibited a multidrug-resistant (MDR) phenotype, with 6% (n=3) displaying resistance to cephalosporins (cefotaxime) and shown to possess the ESBL CTX-M-15. B) The highest level of resistance is observed for amoxicillin (AMX), with 42% of the isolates (n=21) exhibiting resistance; no resistance was observed towards meropenem (MEM) and colistin (PME). Antibiotics tested are as follows: amoxicillin (AMX), cefotaxime (CTX), chloramphenicol (CAP), ciprofloxacin (CIP), gentamicin (GEN), meropenem (MEM), nitrofurantoin (NIT), trimethoprim (TMP), and colistin (PME).

The experimental phenotypic data obtained for antibiotic susceptibility was compared with the in silico data obtained by mining the genome sequences of all isolates for antibiotic resistance genes (Figure 4.8). For this purpose, the tool ABRicate was used to search the ResFinder 2.1 database (Zankari et al., 2012) and detect known acquired

resistance genes displaying ≥ 98% sequence identity over a minimum of 90% coverage of the gene. In silico detection of antibiotic resistance genes allowed for the detection of resistance to three extra classes of antibiotics that were not experimentally tested: macrolide-lincosamide-streptograminB (MLS), sulphonamides (SUL), and tetracycline (TET) (Figure 4.8). This revealed a total of 15 isolates (30%) with multidrug resistance, approximately twice as many as the ones revealed with the phenotypic assay.

Analysis of both in silico and experimental data revealed that ST131 strains exhibit higher levels of antibiotic resistance than the other sequence-types, and ST73 strain exhibit lower levels of antibiotic resistance. In silico analysis also confirmed a higher prevalence of resistance to amoxicillin (beta-lactams) and trimethoprim (sulphonamides) in the collection. However, it is important to note that the distribution of antibiotic resistance is not in complete agreement between both sets of data (in silico vs. experimental data).

Fisher's exact test (two-tailed) was used to test the significance of the association between resistance/sensitivity and phylogenetic group (B2 vs. non-B2), although no significant relationship was found between both variables (p-value > 0.05).

% Antibiotic Resistance (*in silico* data)

ST	AMX	CTX	CAP	CIP	GEN	MEM	NIT	TMP	PME	MLS	TET	SUL
ST131	83	17	0	83	33	0	0	50	0	33	17	67
ST69	43	0	14	14	0	0	0	43	0	14	29	43
ST73	67	0	0	0	0	0	0	33	0	0	22	67
Others	25	7	6	13	7	0	0	21	0	7	19	25

% Antibiotic Resistance (Experimental data)

ST	AMX	CTX	CAP	CIP	GEN	MEM	NIT	TMP	PME
ST131	83	17	0	67	50	0	0	50	0
ST69	67	0	0	17	0	0	0	50	0
ST73	67	0	0	0	0	0	0	33	0
Others	21	7	7	11	7	0	4	18	0

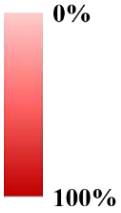

Figure 4.8 – Antibiotic resistance prevalence for the most common sequence types of the Kent collection. In silico analysis of genomic sequences identified resistance to two more classes of antibiotics (MLS and TET). In both data sets, ST131 isolates exhibit higher levels of antibiotic resistance, while ST73 exhibit the lowest levels of resistance.

4.3.4. Virulence repertoire

Virulence factors (VFs) were detected by mining the genome of each isolate with ABRicate. A total of 151 different genes encoding known VFs were detected among all the 50 isolates and used to predict the virulence potential of each isolate. Isolates with the

highest number of virulence genes theoretically possess a higher potential for virulence. The virulence potential (i.e. the % of the 151 VFs identified in a given isolate) of the collection ranged from a minimum of 21.9% (n=33) for KC20 (ST685), to a maximum of 69.5% (n=105) for KC16 (ST73), and an average of 49.1% observed for the entire collection. On average, ST73 strains exhibited a higher virulence potential (62%) than the other two main sequence-types identified in this study, ST69 (50%) and ST131 (43.9%) (Figure 4.9). Virulence genes entA, fepA, fyuA, fimH, and ompA show a high prevalence (> 80%) in all sequence-types (Figure 4.9).

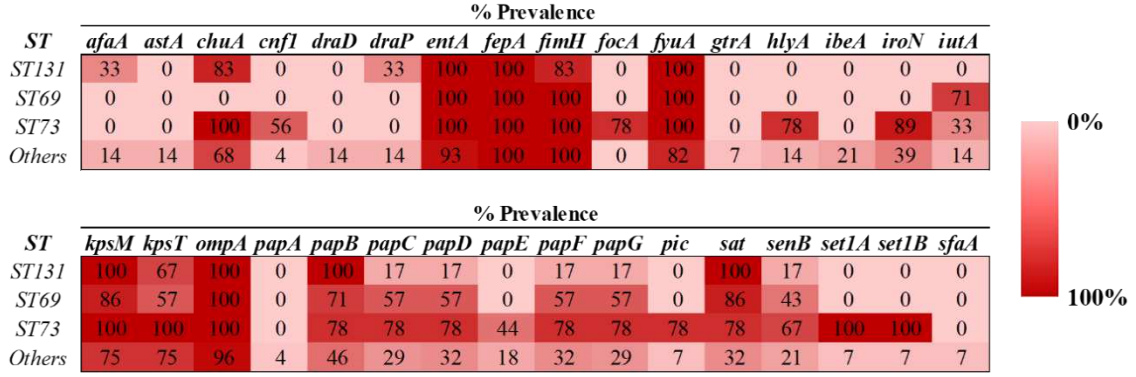

Figure 4.9 – Prevalence of selected virulence genes in predominant STs. The prevalence of a small selection of virulence genes in the three main STs identified in the collection was assessed. ST73 exhibits a higher virulence potential than other the STs identified in the collection.

The statistical significance of the association of virulence genes and phylogenetic groups (B2 vs. non-B2) was tested with Fisher's exact test (two-tailed) (Table 4.2). The genes set1A, set1B, hlyA, pic, papB, papE, chuA, and kpsM were significantly more prevalent (p-value < 0.05) in phylogenetic group B2 (Table 4.2), with an overall higher prevalence in ST73 isolates (Figure 4.9). Furthermore, no significant correlation was found between antibiotic resistance and virulence potential (Pearson r = - 0.0097, p-value = 0.95) (Appendix D-1).

4.3.5. Plasmid typing

The use of whole genome sequencing allows for the capture of sequencing data derived from both the bacterial chromosome and from any plasmids that might be present. While the assembly of plasmids from WGS short-read sequencing data is extremely difficult, some bioinformatic predictive tools have been developed to allow for plasmid

Table 4.2 – Presence of virulence genes in each phylogenetic group

Trait	Gene[1]	No. of isolates (%)							
		Total	Phylogenetic group						
			A (n = 3)	B1 (n = 4)	B2 (n = 33)	D (n = 7)	F (n = 2)	Unknown (n = 1)	p-value[2]
Adherence	afaA	6 (12)	0 (0)	0 (0)	6 (18.2)	0 (0)	0 (0)	0 (0)	-
	draD	4 (8)	0 (0)	0 (0)	4 (12.1)	0 (0)	0 (0)	0 (0)	-
	draP	6 (12)	0 (0)	0 (0)	6 (18.2)	0 (0)	0 (0)	0 (0)	-
	fimH	49 (98)	3 (100)	4 (100)	32 (97.0)	7 (100)	2 (100)	1 (100)	-
	focA	7 (14)	0 (0)	0 (0)	7 (21.2)	0 (0)	0 (0)	0 (0)	-
	papA	1 (2)	0 (0)	0 (0)	1 (3.0)	0 (0)	0 (0)	0 (0)	-
	papB	31 (62)	0 (0)	0 (0)	24 (72.7)	5 (71.4)	1 (50)	1 (100)	0.0254
	papC	20 (40)	0 (0)	0 (0)	16 (48.5)	4 (57.1)	0 (0)	0 (0)	-
	papD	21 (42)	0 (0)	0 (0)	16 (48.5)	4 (57.1)	1 (50)	0 (0)	-
	papE	9 (18)	0 (0)	0 (0)	9 (27.3)	0 (0)	0 (0)	0 (0)	0.0198
	papF	21 (42)	0 (0)	0 (0)	16 (48.5)	4 (57.1)	1 (50)	0 (0)	-
	papG	20 (40)	0 (0)	0 (0)	15 (45.5)	4 (57.1)	1 (50)	0 (0)	-
	sfaS	3 (6)	0 (0)	0 (0)	3 (9.1)	0 (0)	0 (0)	0 (0)	-
Iron uptake	chuA	33 (66)	0 (0)	0 (0)	32 (97.0)	0 (0)	1 (50)	0 (0)	< 0.0001
	entA	48 (96)	2 (66.7)	4 (100)	32 (97.0)	7 (100)	2 (100)	1 (100)	-
	fepA	50 (100)	3 (100)	4 (100)	33 (100)	7 (100)	2 (100)	1 (100)	-
	fyuA	45 (90)	3 (100)	2 (50)	31 (93.9)	6 (85.7)	2 (100)	1 (100)	-
	iroN	19 (38)	1 (33.3)	2 (50)	16 (48.5)	0 (0)	0 (0)	0 (0)	-
	iutA	12 (24)	2 (66.7)	0 (0)	5 (15.2)	4 (57.1)	1 (50)	0 (0)	-
Invasion	ompA	49 (98)	3 (100)	4 (100)	32 (97.0)	7 (100)	2 (100)	1 (100)	-

	ibeA	6 (12)	0 (0)	0 (0)	6 (18.2)	0 (0)	0 (0)	0 (0)	-
	kpsM	38 (76)	0 (0)	0 (0)	31 (93.9)	5 (71.4)	2 (100)	0 (0)	< 0.0001
	kpsT	9 (18)	0 (0)	0 (0)	8 (24.2)	0 (0)	1 (50)	0 (0)	-
Toxin	astA	4 (8)	0 (0)	0 (0)	3 (9.1)	1 (14.3)	0 (0)	0 (0)	-
	cnf1	6 (12.5)	0 (0)	0 (0)	6 (18.2)	0 (0)	0 (0)	0 (0)	-
	gtrA	2 (4)	0 (0)	0 (0)	2 (6.1)	0 (0)	0 (0)	0 (0)	-
	hlyA	11 (22)	0 (0)	0 (0)	11 (33.3)	0 (0)	0 (0)	0 (0)	0.0091
	pic	9 (18)	0 (0)	0 (0)	9 (27.3)	0 (0)	0 (0)	0 (0)	0.0198
	sat	28 (56)	2 (66.7)	0 (0)	19 (57.6)	5 (71.4)	1 (50)	1 (100)	-
	senB	16 (32)	0 (0)	0 (0)	13 (39.4)	3 (42.9)	0 (0)	0 (0)	-
	set1A	11 (22)	0 (0)	0 (0)	11 (33.3)	0 (0)	0 (0)	0 (0)	0.0091
	set1B	11 (22)	0 (0)	0 (0)	11 (33.3)	0 (0)	0 (0)	0 (0)	0.0091

1) Not all VF detected are present in this table

2) p-values (B2 vs. non-B2), by Fisher's exact test (2-tailed), are shown where $p < 0.05$.

prediction and typing from WGS data sets. In this work, the ABRicate tool was used to mine the assembled and re-ordered genome of the isolates of the Kent collection against the PlasmidFinder database (Carattoli et al., 2014), to identify replicon sequences (i.e. plasmid origins of replication). Each replicon is assigned to an incompatibility group, with the premise that plasmids within the same incompatibility group cannot co-exist within the same bacterial cell.

IncFIB replicons were highly prevalent in the collection (74%), followed by Col(156) (66%), and IncFII (54%) replicons. In contrast, IncI2, IncN, IncX1, IncX4, IncY, and p0111 replicons were the least prevalent (2%). Except for five isolates (KC5, KC17, KC25, KC26, and KC44), at least one replicon was identified in all remaining isolates of the collection, including in isolates which exhibited a pan-susceptible phenotype (Table 4.3). Interestingly, the four main IncF incompatibility groups identified in the collection (IncFIA, IncFIB, Inc FIC, and IncFII) are all present in the three isolates (KC18, KC33, and KC45) that exhibit multidrug resistance, ciprofloxacin resistance arising from the presence of aac(6')Ib-cr, and identified as CTX-M-15 ESBL (Table 4.3).

Table 4.3 – Distribution of replicons in the Kent collection

MS number	KC number	Replicons	Notes
MS188	KC1	Col(156); IncFII	Pan-susceptible
MS189	KC2	Col(MG828); Col(RNAI)	Pan-susceptible
MS190	KC3	IncFIB; IncFIC; IncFII; IncQ1	MDR; Ciprofloxacin resistance
MS191	KC4	Col(MG828); Col(RNAI); IncFIA; IncFIB; IncFII	
MS192	KC5	-	Pan-susceptible
MS193	KC6	Col(156); Col(pVC); IncFIB; IncFII; IncI2	
MS194	KC7	IncFIB; IncFII; IncI1; IncN	Ciprofloxacin resistant
MS195	KC8	Col(MG828); Col(156); IncB/O/K/Z; IncFIB; IncFIC; IncFII	
MS196	KC9	Col(156); Col(8282); IncFIB; IncFII; IncQ1	
MS197	KC10	Col(156); Col(8282); Col(RNAI); IncFIA; IncFII; IncX4	Ciprofloxacin resistant
MS198	KC11	Col(BS512); Col(MP18); Col(156); Col(RNAI); IncB/O/K/Z	Pan-susceptible
MS199	KC12	Col(RNAI)	Pan-susceptible
MS200	KC13	IncB/O/K/Z; IncFIB; IncFII; IncY	

MS201	KC14	Col(MG828); Col(MP18); Col(156); Col(RNAI); IncFIB; IncFIC; IncFII	Pan-susceptible
MS202	KC15	Col(156); IncFIB; IncFIC; IncFII	
MS203	KC16	IncFIB; IncFIC; IncFII	Pan-susceptible
MS204	KC17	-	Pan-susceptible
MS205	KC18	IncFIA; IncFIB; IncFIC; IncFII	MDR; Posesses CTX-M-15; Ciprofloxacin resistant
MS206	KC19	IncFIA; IncFIB; IncFII	MDR; Ciprofloxacin resistant
MS207	KC20	Col(RNAI)	Pan-susceptible
MS208	KC21	Col(BS512); Col(MG828); IncB/O/K/Z; IncFIB; IncFII	Pan-susceptible
MS209	KC22	Col(RNAI); IncI1	Pan-susceptible
MS210	KC23	Col(MG828); Col(156); Col(8282); IncFIB; IncFIC; IncFII	Pan-susceptible
MS211	KC24	Col(MG828); Col1(56); Col(8282); IncFIB; IncFII	Pan-susceptible
MS212	KC25	-	Pan-susceptible
MS213	KC26	-	Pan-susceptible
MS214	KC27	Col(156); IncFIB; IncFII	Pan-susceptible
MS215	KC28	Col(MG828); Col(MP18); Col(156); Col(RNAI); IncFIB; IncFIC; IncFII	
MS216	KC29	Col(156); IncFIB; IncFIC; IncFII	
MS217	KC30	Col(MG828); IncFIA; IncFIB; IncFII; IncQ1	
MS218	KC31	Col(MG828); Col(156); IncFIB; IncFII	Pan-susceptible
MS219	KC32	Col(RNAI); IncFIB; IncFIC; IncFII	Pan-susceptible
MS220	KC33	IncFIA; IncFIB; IncFIC; IncFII	MDR; Posesses CTX-M-15; Ciprofloxacin resistant
MS221	KC51	Col(MG828); Col(156); Col(RNAI); IncFIB; IncFII	Pan-susceptible
MS222	KC35	Col(RNAI); IncFIB; IncFIC; IncFII	Pan-susceptible
MS223	KC36	Col(MG828); Col(pVC); Col(RNAI); IncFIB; IncFII	Pan-susceptible
MS224	KC37	Col(MG828); IncFIB; IncFIC; IncFII	Pan-susceptible
MS225	KC38	Col(MG828); Col(8282); Col(RNAI); IncFIB; IncFIC; IncFII	Pan-susceptible
MS226	KC39	Col(156); IncFIB; IncFIC; IncFII	
MS227	KC40	Col(156); IncFIB; IncFII	Pan-susceptible
MS228	KC41	Col(MG828); Col(156); Col(RNAI); IncFIB; IncFII	Pan-susceptible

MS229	KC42	Col(156); Col(RNAI); IncFIB; IncFII	Pan-susceptible
MS230	KC43	Col(156); Col(RNAI); IncFIB; IncFII	Pan-susceptible
MS231	KC44	-	Pan-susceptible
MS232	KC45	Col(156); IncFIA; IncFIB; IncFIC; IncFII; p0111	MDR; Posesses CTX-M-15; Ciprofloxacin resistant
MS233	KC46	Col(156); IncFIB; IncFII; IncI1	
MS234	KC47	Col(156); Col(8282); IncFIB; IncFII; IncQ1	MDR; Ciprofloxacin resistant
MS235	KC48	IncB/O/K/Z	
MS236	KC49	Col(156); IncFIA; IncFIB; IncX1	MDR; Ciprofloxacin resistant
MS237	KC50	Col(156); Col(8282); Col(RNAI); IncFIB; IncFII; IncQ1	

4.4. Discussion

4.4.1. The E. coli genome

Following genome assembly and annotation, general genome information for each isolate was gathered, including total genome size and number of genes in each genome. Unsurprisingly, comparison of genome size and number of genes showed a linear relationship between the two (Figure 4.1). Acquisition of mobile genetic elements, such as plasmids and pathogenicity islands, contribute to the genetic variability of E. coli. In fact, out of 13,172 unique genes present in the Kent collection, only 19% belong to the core genome, while the remaining 91% of genes vary among isolates, a testament to the variability encountered among E. coli clinical isolates.

Interestingly, isolates belonging to phylogenetic groups F, D and B2 had, on average, larger genomes (5.26, 5.19, and 5.13 Mb respectively) than isolates belonging to phylogenetic groups A and B1 (4.81 and 4.84 Mb respectively). Assigning a phylogenetic group to an isolate can provide further information on the nature of the isolate, including phenotypic and genotypic traits, ecological niche, and pathogenicity (Clermont et al., 2013). Commensal strains of E. coli are routinely assigned to phylogenetic group A, while pathogenic strains are assigned to the remaining phylogenetic groups (Johnson and Stell, 2000). As such, phylogenetic group A, as well as phylogenetic group B1, a sister group of A (Gordon et al., 2008), contain isolates of low pathogenic potential. In contrast, phylogenetic groups B2, D, and F, with the latter comprising strains that are closely related to strains of group B2 (Clermont et al., 2011), contain more pathogenic strains. The results obtained above suggest the presence of extra genes that confer a greater ability to cause disease in strains belonging to phylogenetic groups B2, D, and F.

4.4.2. E. coli isolates from the Kent collection are an epidemiologically heterogeneous population

The Kent collection consisted of 23 different STs, including four novel ones. ST73 was the most prevalent ST in the collection (Figure 4.2), contrasting with previous reports by Croxall et al. (2011) and Johnson et al. (2010) that reported a higher prevalence of ST131 in the UK and USA, respectively. However, the presence of E. coli ST131 in the collection further emphasises the widespread dissemination of this clonal group (Nicolas-Chanoine et al., 2008).

Predictably, whole genome sequence alignment (Figure 4.3) revealed greater similarity between genomes of the same ST than between genomes of different STs. In ST69 isolates, the KC28 genome seems to differ greatly from the other six ST69 genomes. Further analysis revealed that KC28 was assigned to phylogenetic group A, while all other isolates belonging to ST69 were assigned to phylogenetic group D (Figure 4.6), and revealed a closer phylogenetic relationship with both ST10 in the collection (KC14 and KC36) and E. coli MG1655, all of which were assigned to phylogenetic group A. A similar scenario was observed for KC20 (ST685): while assigned to phylogenetic group B2, this strain exhibited a closer phylogentic relationship with isolates belonging to phylogroup A than the remaining members of phylogenetic group B2 (Figure 4.6). Overall, E. coli isolates cluster together according to phylogenetic group and also by ST, with phylogenetic group B2, which is associated with ExPEC virulence, forming the ancestral group from which all others diverged until the most recent phylogenetic group A, which comprises commensal strains. This is in accord with a study conducted by Le Gall and colleagues (Le Gall et al., 2007) which suggests that the E. coli ancestor was likely to be a facultative or opportunistic pathogen. Furthermore, the virulence potential observed between phylogenetic groups of the Kent collection was, on average, highest for phylogenetic group B2 (52.4%), of which ST73 isolates had the highest virulence potential, followed closely by phylogenetic groups D and F (52.1% and 47.7%, respectively), and finally sister phylogenetic groups B1 and A (36.4% and 28.9% respectively). Also, phylogenetic group B2 is known to comprise many asymptomatic strains of E. coli (Nicolas-Chanoine et al., 2014), of which E. coli 83972 is the archetypal strain. It was previously suggested that the ability of E. coli 83972 to colonize the urinary tract for long periods of time without evoking a host response is not due to the absence of virulence genes in its genome, but rather due to its ability to down-regulate the expression of the virulence genes that will activate host responses (Wullt et al., 2000; Roos et al., 2006). These observations lead us to speculate on the advantage of virulence genes for the maintenance and dissemination of E. coli and propose that instead of acquisition of virulence genes, the opposite could have occurred during the evolutionary process of E. coli, giving rise to well-adapted commensal strains with smaller genomes and fewer genes, and thus avoiding the evolutionary pitfalls often found by pathogens that cause host death or easily trigger the host immune system.

4.4.3. Relationships between CTX-M-15 and aac(3)-IIa, aac(6')Ib-cr, and blaOXA-1

Despite over 50% of the Kent collection remaining sensitive to all nine antibiotics experimentally tested, a very high level of resistance was still observed, especially for amoxicillin, trimethoprim, and ciprofloxacin. This was unsurprising as these are three of the most commonly used antibiotics, hence there is a significant selective pressure driving the emergence of resistance to these antibiotics. Overall, 14% of the isolates exhibited multidrug resistance to antibiotics experimentally tested (Figure 4.7A). This number increased to 30% when analysing in silico data. It is important to note that the tool used to detect resistance genes in the genomic data of each isolate detected resistance genes belonging to three classes of antibiotics not tested experimentally, and it is very likely that the discrepancy between experimental and in silico datasets arises due to this phenomenon. Furthermore, in silico data obtained from ABRicate only contains known acquired resistance genes, while resistance to some antibiotics such as ciprofloxacin arises from mutations in the cellular target (e.g. DNA gyrase). As such, while three of the isolates carried the aac(6')Ib-cr (Appendix C-1) resistance gene which confers resistance to some aminoglycosides but also resistance to low-levels of ciprofloxacin, the remaining isolates exhibiting a ciprofloxacin-resistant phenotype were not detected with ABRicate. Hence, a multiple sequence alignment of gyrase subunit A (GyrA) was performed (Appendix E-1), which is the main target for ciprofloxacin in E. coli. This was carried out to identify mutations known to confer ciprofloxacin resistance (Weigel et al., 1998), and enabled in silico confirmation for all experimentally-tested ciprofloxacin-resistant isolates. The inability of ABRicate (and the ResFinder v2.1 database) to identify resistance arising from mutations in the target protein could also explain why the nitrofurantoin resistance experimentally detected in KC3 was not identified in silico. Thus, while genome sequencing is a good tool to detect antibiotic resistance genes in genome sequences, phenotypic assays to detect resistance are preferable as they can detect resistance arising from both acquision of resistance genes and mutation on the antibiotic target, as well as detecting resistance which arises from currently unknown mechanisms.

Interestingly, the three isolates carrying the aac(6')Ib-cr resistance gene also possessed codon changes that would result in amino acid substitutions in the GyrA protein (Appendix E-1). Analysis of the acquired resistance genes identified in silico (Appendix C-1) further showed that these three isolates (KC18, KC33, and KC45) were also the only isolates carrying ESBL CTX-M-15, aac(6')Ib-cr, aac(3)-IIa, and blaOXA-1, all of which confer resistance to antibiotics of different classes (Alekshun and Levy, 2007). CTX-M-15 with blaOXA-1 and aac(6')Ib-cr are known to be located on IncF-type plasmids

(Carattoli, 2009), and four IncF-type replicon sequences were identified in the three isolates (Table 4.3). However, it was observed that the presence of an IncF-type plasmid, or the presence of any putative plasmid or number of plasmids, does not necessarily coincide with antibiotic resistance. In fact, many replicon sequences were identified in isolates that exhibited a pan-susceptible phenotype to all antibiotics tested (Table 4.3). Furthermore, carriage of CTX-M-15 and both of aac(3)-IIa and *aac(6')Ib*-cr has been previously observed in K. pneumoniae isolates (Peerayeh et al., 2014). An association between these different resistance genes could explain the high levels of multidrug resistance often observed in CTX-M-15 ESBL-producing isolates (Nicolas-Chanoine et al., 2008; Hoban et al., 2010).

4.4.4. No evidence for a correlation between antibiotic resistance and virulence

For a long time, it was thought that antibiotic resistance and virulence were mutually exclusive in E. coli, with the former having a negative impact on fitness which would result in less pathogenic strains. However, the emergence and dissemination of ST131 isolates exhibiting significantly higher levels of antibiotic resistance and virulence (Johnson et al., 2010; Peirano et al., 2013) is not consistent with this model. Furthermore, it has been suggested that this correlation is the reason for the success of ST131 isolates (Nicolas-Chanoine et al., 2008; Johnson et al., 2010; Peirano et al., 2013). In this study, however, while ST131 was more resistant, on average, than the other two most prevalent STs (ST69 and ST73), ST131 did not exhibit higher levels of virulence. In fact, ST73 isolates, which exhibit the lowest antibiotic resistance levels, exhibited, on average, the highest virulence potential. To determine whether a correlation exists between levels of antibiotic resistance (reflected by the number of antibiotics to which phenotypic resistance was detected) and virulence potential, the Pearson correlation coefficient was calculated (Appendix D-1) but no significant correlation was found between the two variables.

A high prevalence of iron uptake genes (entA, fepA, and fyuA) was found in the collection. While colonizing the host, pathogenic strains encounter environments with low concentrations of free iron. Since iron is essential for bacterial growth and is sequestered in the body by the process of nutritional immunity, it is unsurprising that many pathogenic strains encode siderophores such as enterobactin (entA), ferrienterobactin (fepA), and yersiniabactin (fyuA). The high prevalence of fimH (type I fimbriae adhesin) and ompA (outer membrane protein A) was also found in a high number of both pathogenic and commensal E. coli strains (Salmon et al., 2003; Dhakal et al.,

2008; Hagan et al., 2010). Overall, these results suggest that these genes might be broadly conserved among different sequence-types.

Virulence genes set1A, set1B, hlyA, pic, papB, papE, chuA, and kpsM were significantly more prevalent in phylogenetic group B2, potentially a reflection of the high prevalence of UPEC strains (e.g. ST131, ST73, and ST95) in this phylogenetic group, where the virulence genes above are frequently encountered (Mobley et al., 1990; Wullt et al., 2000; Hagan and Mobley, 2007; Wiles et al., 2008; Bien et al., 2012; Nicolas-Chanoine et al., 2014; Karami et al., 2016).

Chapter 5

Nitric oxide may abrogate the toxic effects of antibiotics

5.1. Summary

Nitric oxide is a small molecule with important biological roles. In mammals, NO is produced by a specialized family of enzymes (mNOS family) and is involved in vasoregulation, platelet aggregation, and neurotransmission (Snyder and Bredt, 1992; Vallance, 2003). One member of the NOS family of enzymes (iNOS) is expressed in cells of the immune system, such as macrophages, and is involved in the response against invading pathogens during infection. In bacteria, the role of NO is not fully understood beyond its toxic effects, however it is known to be important for the life cycle of bacterial biofilms (Barraud et al., 2006; Barraud et al., 2015). Some Gram-positive bacteria possess mNOS homologues (bNOS), which provide an endogenous source of NO that has been shown to have an important role in the protection of these bacteria against oxidative stress associated with exposure to antimicrobials (Gusarov and Nudler, 2005; Shatalin et al., 2008; Gusarov et al., 2009).

The antimicrobial capabilities of NO and its natural occurrence in mammals, have made it a good candidate to be used as an alternative to antibiotics or co-administered with antibiotics to increase their efficacy (Reffuveille et al., 2015). However, several studies have demonstrated that ROS generation by the aerobic respiratory chain is inextricably linked to the lethality of various classes of antibiotics. Hence, herein we hypothesised inhibition of aerobic respiration by nitric oxide might abrogate the toxic effects of antibiotics. As such, experiments were designed to test the effects of nitric oxide on the lethality of gentamicin, a bactericidal antibiotic, against a well-characterized multidrug-resistant UPEC strain. Bacterial survival to gentamicin in the presence or absence of exogenously administered NO-donors (NOC-12 or GSNO) was determined for both planktonic cells and biofilms of E. coli EC958 wild-type, with both showing an increase in bacterial tolerance to gentamicin when NO is present. Furthermore, the effects of macrophage-derived NO combined with gentamicin treatment on bacterial intra-macrophage survival was assessed, and although no significant differences in survival was observed for gentamicin, we cannot discard an effect for other bactericidal antibiotics.

Recent work showed that exposure to bactericidal antibiotics increases bacterial respiration and leads to the accumulation of toxic ROS (Kohanski et al., 2007; Dwyer et al., 2014; Lobritz et al., 2015). Aerobic bacterial respiration is carried out by cytochrome oxidases, one of the main bacterial targets of NO. As such, we tested the susceptibility of E. coli EC958 strains lacking cytochrome *bo'* (cyoA$^-$) and cytochrome bd-I (cydAB$^-$) to

gentamicin in the presence and absence of a NO-donor. The presence of GSNO increased bacterial survival in all the three strains tested. However, higher gentamicin tolerance was achieved in the strain of E. coli EC958 lacking cytochrome bd-I (cydAB$^-$), suggesting that this respiratory oxidase is involved in antibiotic-mediated ROS generation, even in the presence of NO. This work has important implications for our understanding of antibiotic susceptibility during infection (i.e. where NO is produced by the innate immune system).

5.2. Introduction

5.2.1. Overview of bacterial energy generation

E. coli is a facultative anaerobic bacterium which can obtain energy in two ways: i) via substrate-level phosphorylation (e.g. glycolysis), or ii) via oxidative phosphorylation, where an electron transport chain is responsible for generating a proton motive force (PMF) that is then used to drive ATP synthesis by the ATP synthase. Alternative routes for ATP production in E. coli confer a certain degree of metabolic flexibility that can respond to environmental changes and energetic needs. For example, under anoxic conditions, E. coli can either perform substrate-level phosphorylation if a fermentable carbon source is present (e.g. glucose) or perform oxidative phosphorylation in the presence of alternative electron acceptors (e.g. nitrate). There is, however, a hierarchy, with aerobic respiration, i.e. oxygen as the final electron acceptor, taking precedence over anaerobic respiration, which in turn takes precedence over fermentation. Fermentation is an anaerobic process that does not result in the formation of a PMF to drive the ATP synthase, and thus exhibits the lowest energy yield out of the three processes. Aerobic and anaerobic respiration both generate a PMF, which is an efficient route for the conservation of energy that is used in the generation of ATP.

Inhibition of the electron transport chain can severely impair antibiotic lethality by decreasing metabolism, thus reducing toxic by-products generated by the bacterial cell during antibiotic exposure (Dwyer et al., 2014), or due to decreased expression of the antibiotic cellular target expression; or by disruption of PMF, in which case antibiotics whose uptake is PMF-dependent are unable to reach their cellular target (e.g. aminoglycosides) (Hancock, 1981; Allison et al., 2011).

The main E. coli pathogen used in the current work is the urosepsis-causing EC958 strain (Totsika et al., 2011; Forde et al., 2014), and during infection of the urinary tract E. coli encounters a predominantly microaerobic environment (Hagan et al., 2010). Hence, the aerobic respiratory chain of E. coli will be discussed in detail below.

5.2.2. Aerobic respiration in E. coli

E. coli possesses a branched aerobic respiratory chain and can express different respiratory complexes depending upon the environmental conditions. The aerobic respiratory chain in E. coli is comprised of two main classes of respiratory complexes: NADH dehydrogenases (NDH-1 or NDH-2) and cytochromes oxidases (cytochrome *bo'* or cytochrome bd-I). E. coli also contains a third respiratory oxidase, Cytochrome bd-II,

that is expressed under phosphate and carbon limitation (Atlung and Brondsted, 1994; Vitaliy B. Borisov et al., 2011; Vitality B. Borisov et al., 2011): this complex is not a major focus of the current study. Both NADH dehydrogenases feed electrons into the system by transferring them from NADH onto the quinone pool on the cytoplasmic membrane (Figure 5.1). However, while NDH-1 has a stoichiometry of four protons translocated for every NADH oxidised (i.e. two electrons), NDH-2 does not translocate protons to the periplasmic space (Matsushita et al., 1987) and, as such, does not contribute to generation of the PMF. The cytochrome oxidases perform the terminal step in the electron transport chain, the reduction of oxygen to water, a reaction linked to the re-oxidation of the quinone pool and re-setting of the system (Figure 5.1).

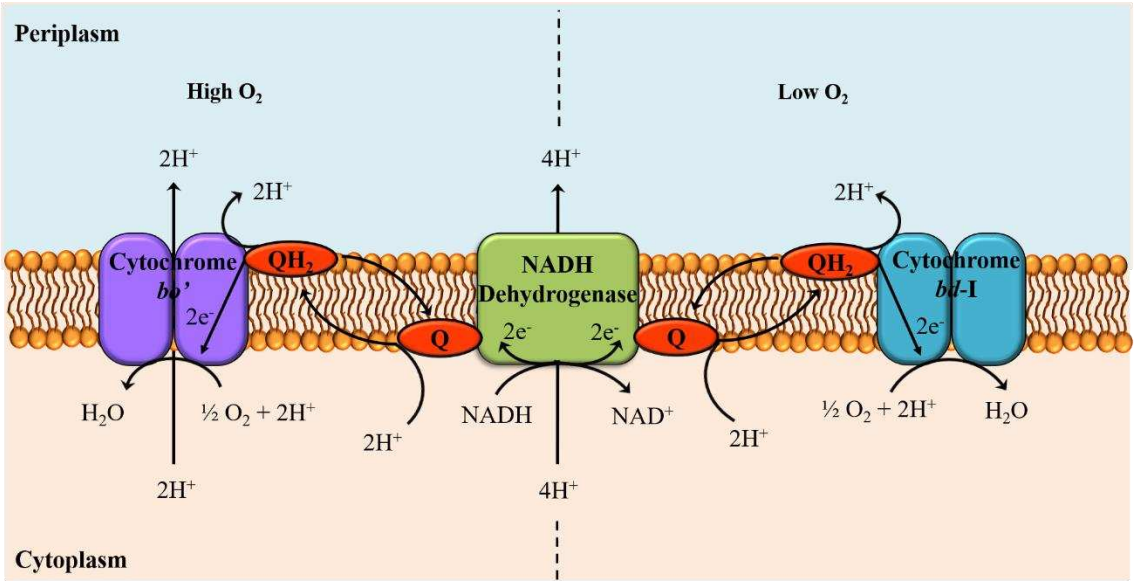

Figure 5.1 – Aerobic respiratory chain of E. coli. NADH dehydrogenase I catalyses the oxidation of NADH and transfers two electrons (e^-) into the quinone pool. In a well-aerated environment, cytochrome bo' oxidase is expressed and catalyses the reduction of oxygen to water, coupled with the translocation 4 protons (H^+) per $2e^-$ via both scalar and vectorial proton translocation. In a microaerobic environment, E. coli maximally expresses cytochrome bd-I. This cytochrome oxidase reduces oxygen to water and has a ratio of $1H^+$ per e^- that is supported solely by vectorial proton translocation. Unlike NDH-1, NDH-2 does not translocate protons.

5.2.2.1. Cytochrome bo'

Cytochrome *bo'* is a transmembrane enzyme that catalyses the reduction of oxygen to water, during which it also functions as a proton pump and translocates protons from the cytoplasm into the periplasmic space, contributing to the generation of a PMF (Puustinen et al., 1989) (Figure 5.1). The reduction of molecular oxygen occurs in the binuclear haem-copper site, making it a member of the haem-copper superfamily of terminal oxidases (Abramson et al., 2000; Stenberg et al., 2007).

In E. coli, cytochrome *bo'* is encoded by the cyoABCDE operon, with cyoABCD encoding subunits II, I, III and IV of the cytochrome respectively, and cyoE encoding a proto-haem farnesyltransferase (haem o synthase) (Chepuri et al., 1990; Saiki et al., 1993). Tseng and colleagues used a cyo-lacZ fusion to show that expression of cytochrome *bo'* is maximal in highly aerated conditions (air saturation above 15%) (Tseng et al., 1996), with expression of cyoA-lacZ decreasing by 140-fold in anaerobically cultured cells (Cotter et al., 1990). Moreover, under low oxygen concentration, the expression of cytochrome *bo'* was found to be higher in a fnr or arcA mutant, when compared to the wild-type isogenic strain, suggesting both FNR and ArcA act as transcriptional repressors of the cyo operon.

5.2.2.2. Cytochrome bd-type oxidases

Despite the functional equivalence of cytochrome *bo'* and cytochrome bd-I in E. coli, cytochrome *bo'* is maximally expressed under aerobic conditions while cytochrome bd-I exhibits maximal expression under microaerobic conditions (Fu et al., 1991; Tseng et al., 1996). This differential expression of cytochrome oxidases confers a distinct advantage: cytochrome bd-I has higher affinity for oxygen (K_m of 3-8 nM (D'mello et al., 1996)) than cytochrome *bo'* (K_m of 0.016-0.085 µM (D'Mello et al., 1995)), and it is able to perform aerobic cellular respiration under microaerobic conditions. Moreover, cytochrome bd-I is less susceptible to NO-mediated inhibition compared to cytochrome bo' (Mason et al., 2009), an advantage for pathogenic E. coli during infection (Shepherd et al., 2016). However, unlike cytochrome *bo'*, cytochrome bd-I does not directly translocate protons onto the periplasm (Figure 5.1) (D'Mello et al., 1995), and instead liberates protons into the periplasm via the oxidation of ubiquinol (Miller and Gennis, 1985), also known as vectorial proton translocation.

A third cytochrome oxidase, cytochrome bd-II, was identified by Dassa et al. (1991): the proteins encoded by appC and appB show 60% and 57% homology with subunit I and subunit II of E. coli cytochrome bd-I, respectively. The enhanced sensitivity to oxygen of the mutant lacking all respiratory oxidases (cyo^- cyd^- $appB^-$) compared to the cyo^- cyd^- double mutant (Dassa et al., 1991), and in vitro quinol oxidase activity of AppCB (Jünemann, 1997) confirmed Dassa's initial observations. While initially considered non-electrogenic, i.e. no contribution to the PMF (Bekker et al., 2009), it was later shown that cytochrome bd-II generates a PMF in a manner identical to that of cytochrome bd-I (Vitality B. Borisov et al., 2011). In E. coli, expression of cytochrome bd-II is induced in response to phosphate starvation, entry into stationary phase, and microaerobic and

anaerobic conditions (Atlung and Brondsted, 1994), and controlled by transcriptional activators AppY and ArcA, the latter also controlling expression of cytochrome bd-I and cytochrome *bo'* as a transcriptional activator and transcriptional repressor, respectively. In contrast to both cydABX and cyoABCDE operons, induction of appCB is independent of FNR (Vitaliy B. Borisov et al., 2011).

5.2.3. Cellular respiration and antibiotic efficacy

Despite the wide array of targets, antibiotics are generally classified as bactericidal, i.e. cause bacterial cell death, or bacteriostatic, i.e. inhibit bacterial cell growth. Until recently, the lethal effects of bactericidal antibiotics were largely attributed to their primary mode of action. However, independent studies have led to the model that bactericidal antibiotics cause a metabolic shift which leads to the generation of toxic ROS that contributes to lethality (Kohanski et al., 2007; Wang and Zhao, 2009; Dwyer et al., 2014) (Figure 5.2). Kohanski et al. (2007) observed that three different bactericidal antibiotics - ampicillin, norfloxacin, and kanamycin – belonging to three separate classes – beta-lactams, quinolones, and aminoglycosides, respectively -, thus different primary targets, all induced hydroxyl radical formation, while formation of this radical was not detected in E. coli cells treated with different bacteriostatic antibiotics. Furthermore, addition of an iron chelator or thiourea, a hydroxyl radical scavenger, to drug-treated E. coli resulted in an increase in bacterial survival, further implicating the formation of hydroxyl radicals in bactericidal antibiotic lethality, and suggesting a critical role for the Fenton reaction (Kohanski et al., 2007; Wang and Zhao, 2009). This hypothesis was further supporter by Wang and Zhao (2009). In their work, a mutant strain lacking superoxide dismutase exhibited increased survival to different bactericidal antibiotics when compared to the wild-type strain. This phenotype was attributed to decreased hydroxyl radical production via the Fenton reaction due to low levels of its substrate, hydrogen peroxide, which is produced by superoxide dismutase (Wang and Zhao, 2009). Furthermore, testing bactericidal antibiotic efficacy in tonB, a protein required for iron transport, and iscS, involved in [Fe-S] cluster synthesis, single mutants revealed that intracellular iron originating from [Fe-S] clusters is the main driver for Fenton-mediated hydroxyl radical formation during exposure to bactericidal antibiotics (Kohanski et al., 2007). Hence, the involvement of the bacterial respiratory chain in bactericidal antibiotic lethality was proposed due to the established fact that destruction of [Fe-S] clusters occurs mainly via superoxide, which in turn is generated mainly through the respiratory electron transport chain (Kohanski et al., 2007). This is supported by observations of upregulation

of NADH dehydrogenase I in cells treated with different bactericidal antibiotics, an increase in NADH consumption (Kohanski et al., 2007), and an increase in oxygen consumption rates of E. coli or S. aureus cultures treated with bactericidal antibiotics, which is the opposite of what was observed in cultures treated with bacteriostatic antibiotics (Lobritz et al., 2015). Furthermore, a triple respiratory E. coli mutant (cyoA$^-$ cydB$^-$ appB$^-$) has been shown to exhibit significant resistance to bactericidal antibiotics in comparison to wild-type (Lobritz et al., 2015). Together, these results suggest that presence of bactericidal antibiotics leads to superoxide generation via the bacterial respiratory chain and, consequently, the production of other ROS (Figure 5.2).

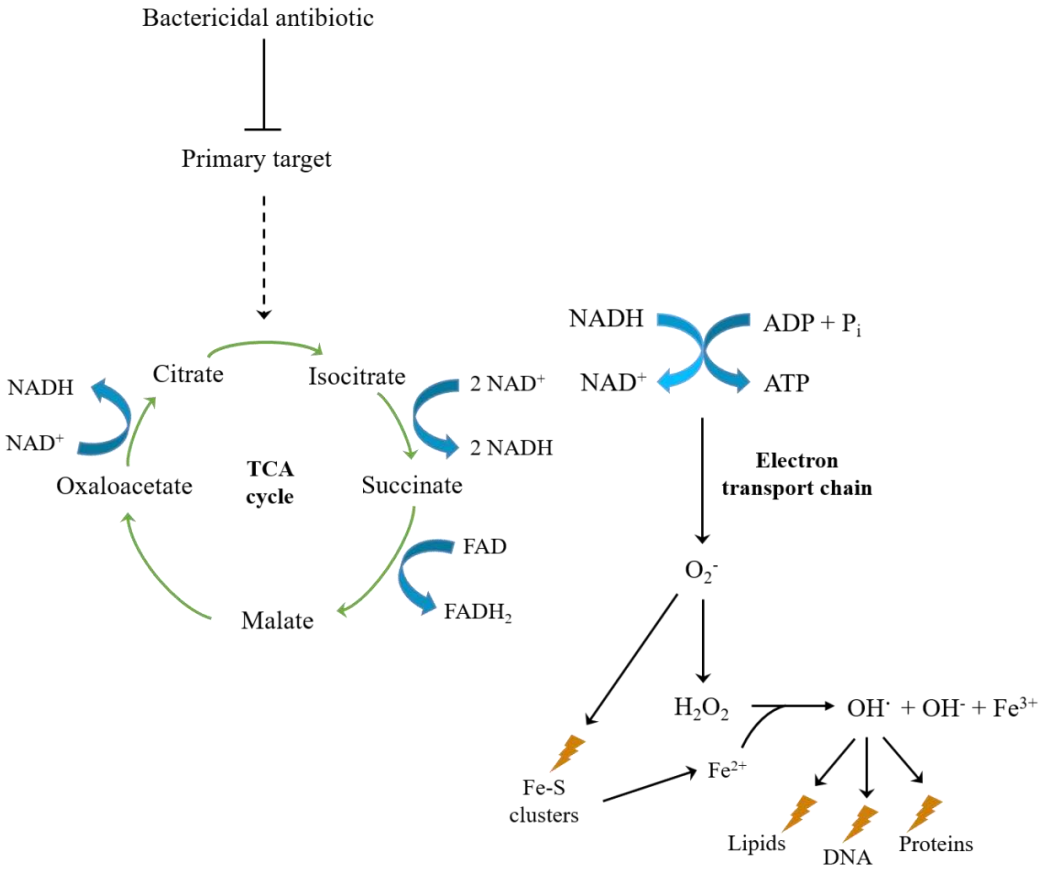

Figure 5.2 – ROS-mediated antibiotic killing. Bactericidal antibiotics have different but well-established primary targets, but they all appear to have a common ROS-mediated killing pathway. The current model involves both the tricarboxylic acid (TCA) cycle and the electron transport chain. The presence of bactericidal antibiotics leads to hyperactivation of the electron transport chain and thus rapid depletion of NADH, whose regeneration is dependent upon the TCA cycle. Hyperactivation of the respiratory chain leads to formation of superoxide which damages intracellular iron-sulphur clusters, releasing ferrous iron, which in turn exacerbates the Fenton reaction, leading to formation of the hydroxyl radical and damage of important cellular components.

5.2.3.1. The ROS-antibiotic controversy

Despite the growing evidence suggesting a role for ROS in antibiotic lethality, there is still some debate over this subject.

Part of the criticism against ROS involvement in bactericidal antibiotic-mediated killing lies with the use of hydroxyphenyl fluorescein (HPF) to detect ROS. This non-fluorescent probe reacts with hydroxyl radicals with high specificity, giving rise to the fluorescent product fluorescein. However, data has shown that E.coli cells treated with bactericidal antibiotics exhibit an increase in autofluorescence, possibly due to filamentation and, as such, the increase in fluorescence observed in cells treated with both antibiotic and HPF, attributed to an increase in the level of ROS, could be an artefact (Van Acker and Coenye, 2017). Another main point of discussion is the difficulty to separate the effects caused by the metabolic shift and the generation of ROS, since both are intrinsically connected: generation of ROS occurs due to hyperactivation of cellular metabolism. Hence, it is possible that the shift in metabolism observed after exposure to bactericidal antibiotics is itself the contributor to antibiotic lethality and ROS may play only a minor role, if at all (Van Acker and Coenye, 2017; Yang, Bhargava, et al., 2017). Previous studies have also shown that lethality of several bactericidal antibiotics is not affected under anaerobic conditions compared to aerobic conditions (Liu and Imlay, 2013), thus showing that the presence of oxygen, a requisite for ROS formation, is not required for antibiotic lethality. However, it is important to note that the data obtained by Liu and Imlay (2013) was not obtained under strict anaerobic conditions, i.e. exposure to antibiotics was performed in an anoxic chamber, but all subsequent experimental work (dilutions, plating, and incubation) was carried out under aerobic conditions. In contrast, experiments performed by Dwyer et al. (2014) under strict anaerobic conditions have shown that antibiotic lethality is significantly diminished in the absence of oxygen, but restored when nitrate, an alternative electron acceptor in bacterial respiration, is added, thus supporting the notion that bacterial cellular respiration plays a role in antibiotic lethality, but not necessarily involvement of ROS since no oxygen was present under the experimental conditions employed by Dwyer and colleagues (Dwyer et al., 2014).

In light of these studies, it is still premature to assume that ROS are involved in antibiotic lethality. However, the involvement of bacterial respiration in antibiotic lethality is well-established.

5.2.3.2. Implications for the treatment of bacterial infections

For many years, the lethality of antibiotics was attributed to its interaction with the bacterial target. However it has now become clear that downstream effects contribute to antibiotic lethality, and these effects are sensitive to environmental cues (Yang, Bening, et al., 2017). Reduced metabolic activity is linked to lower antibiotic efficacy (Rowan et al., 2016; Yang, Bening, et al., 2017), a state that is often observed in bacterial biofilms (Mah and O'Toole, 2001) or when in a nutrient-limited environment. In support of this is the work of Lobritz et al. (2015), in which they observed that treatment of E. coli cultures with a bacteriostatic antibiotic, which decreases bacterial metabolism usually by targeting protein synthesis, prior to or after exposure to a bactericidal antibiotic, which accelerates bacterial respiration and metabolism (Kohanski et al., 2007; Wang and Zhao, 2009; Dwyer et al., 2014), inhibited the bactericidal activity of the latter (Lobritz et al., 2015).

As presented in section 5.2.3., the lethality of bactericidal antibiotics is linked to a downstream cascade of events that result in hyperactivity of the bacterial respiratory chain which can lead to over-production of ROS. Bacteria possess a plethora of defence mechanisms against ROS (e.g. catalase and superoxide dismutase), enzymes that repair ROS-induced damage, and systems that help to maintain the redox poise of the cell. It is therefore possible that activation of ROS-defence mechanisms could attenuate the lethality of bactericidal antibiotics. This is supported by observation that loss of superoxide dismutase function results in elevated resistance to the bactericidal antibiotics norfloxacin, ampicillin, and kanamycin (Wang and Zhao, 2009). Additionally, expression of the transcriptional regulator OxyR, one of the main regulators of the oxidative stress response, was up-regulated in Burkholderia cenocepacia after exposure to a bactericidal antibiotic (Van Acker and Coenye, 2017).

Further studies on the lethality of antibiotics are crucial in other to maximise the potential of the few drugs currently available. Combinatorial antibiotic treatments are often used to treat bacterial infections, but as shown by the work of Lobritz et al. (2015) this may not always be the best approach as bacteriostatic antibiotics can decrease the efficacy of bactericidal antibiotics. The discovery that bactericidal antibiotics increase ROS production may potentially lead to new treatments: inhibition of specific components of the bacterial oxidative stress response may increase the efficacy of bactericidal antibiotics. In support of this is the increased susceptibility to quinolones observed for a catalase E. coli mutant (Wang and Zhao, 2009).

5.3. Results

5.3.1. Antibiotic resistance and nitric oxide susceptibility

The antimicrobial effects of NO are well-known, targeting many bacterial components such as haem cofactors, thiols, and [Fe-S] clusters (Fang, 1997; Keszler et al., 2010), as well as being effective in the dispersal of E. coli and P. aeruginosa biofilms (de la Fuente-Núñez, Reffuveille, Fairfull-Smith, et al., 2013). NO exposure has long been considered as a potential alternative to antibiotics or for use in combination with antibiotics as a way of potentiating their effect, which has been shown to be effective against bacterial biofilms (Reffuveille et al., 2015). Thus, it is important to understand the relationship between NO tolerance and antibiotic resistance. To investigate this, a subset of isolates from the Kent collection (KC3, KC4, KC6, KC13, KC30; KC33; KC45, KC46, and KC47) exhibiting different degrees of antibiotic resistance and of different sequence-types (Figure 5.3A) was tested for GSNO susceptibility using the well-diffusion assay. Pan-susceptible E. coli MG1655, multidrug-resistant ST131 E. coli strain EC958 (Totsika et al., 2011; Forde et al., 2014), pan-susceptible and highly invasive pyelonephritis-causing ST73 E. coli strain CFT073 (Kao et al., 1997), and pan-susceptible ABU E. coli strain 83972 (Klemm et al., 2006; Roos and Klemm, 2006) were also tested due to their clinical relevance and as control samples. Apart from isolate KC45, no significant difference was found in GSNO susceptibility for the remaining isolates compared to the controls (Student's unpaired t-test p-value > 0.05) (Figure 5.3B). Isolate KC45 exhibited significantly higher susceptibility to GSNO (Student's unpaired t-test p-value < 0.05) under both aerobic and microaerobic conditions (Figure 5.3B). Further investigation of this isolate using the alternative NO-donor NOC-12 revealed no sensitivity of KC45 to this compound (Appendix F-1). It is possible that the higher sensitivity observed to GSNO is due to the much broader nitrosative nature of GSNO or one of its breakdown products (possibly glutathione), rather than NO itself. As such, when assessing the correlation between antibiotic resistance and GSNO susceptibility for the different oxygen conditions, KC45 was omitted from the analysis (Figure 5.3C). Analysis of the data obtained for the remaining 12 strains revealed no correlation between antibiotic resistance and GSNO susceptibility (Pearson r = 0.08, 0.04 and 0.19 for aerobic, microaerobic, and anaerobic conditions respectively; p-values of 0.79, 0.91, and 0.56 were obtained for aerobic, microaerobic, and anaerobic conditions, respectively) (Figure 5.3C).

A.

Strain	ST	Notes	AMX	CTX	CAP	CIP	GEN	MEM	NIT	TMP	PME
MG1655	N/A	K-12	-	-	-	-	-	-	-	-	-
CFT073	ST73	UPEC	-	-	-	-	-	-	-	-	-
83972	N/A	ABU	-	-	-	-	-	-	-	-	-
EC958	ST131	UPEC	+	+	-	+	-	-	-	+	-
KC3	ST162		+	-	+	+	-	-	+	+	-
KC4	ST1406		+	-	-	-	-	-	-	-	-
KC6	ST58		+	-	-	-	-	-	-	+	-
KC13	ST95	UPEC	-	-	-	-	-	-	-	+	-
KC30	ST73	UPEC	+	-	-	-	-	-	-	+	-
KC33	Unknown		+	+	-	+	+	-	-	+	-
KC45	ST405	UPEC	+	+	-	+	+	-	-	+	-
KC46	ST127	UPEC	+	-	-	-	-	-	-	-	-
KC47	ST69	UPEC	+	-	-	+	-	-	-	+	-

B.

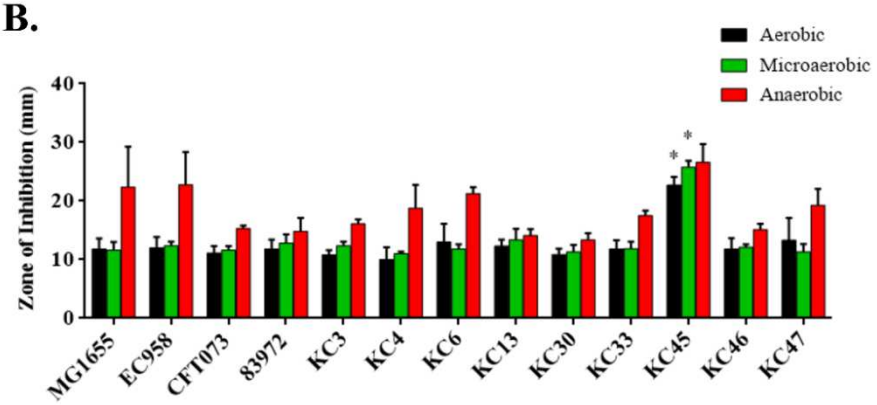

C.

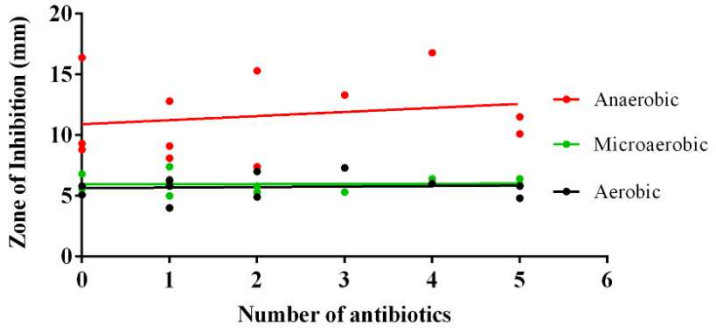

Figure 5.3 – Antibiotic resistance does not correlate with increase/decrease in GSNO susceptibility. (A) Antibiotic resistance profiles of the subset of strains used to determine the relationship between antibiotic resistance and GSNO susceptibility. (B) GSNO susceptibility of the isolates in the presence (aerobic and microaerobic) and absence (anaerobic) of oxygen. Values represent the mean ± SD from 6 replicates of two independent cultures. (*: Student's unpaired t-test; p-value < 0.05). (C) Linear regression (R^2 values of 0.007, 0.001, and 0.035 for aerobic, microaerobic, and anaerobic conditions, respectively) and correlation (Pearson r=0.08, 0.04 and 0.19 for aerobic, microaerobic, and anaerobic conditions respectively. p-values=0.79, 0.91, and 0.56 for aerobic, microaerobic, and anaerobic conditions, respectively) between GSNO susceptibility and antibiotic resistance (reflected by the number of antibiotics to which each isolate was experimentally resistant to) was calculated with all strains in panels A and B except KC45. Abbreviations: AMX, Amoxicillin; CTX, Cefotaxime; CAP, Chloramphenicol; CIP, Ciprofloxacin; MEM, Meropenem; NIT, Nitrofurantoin; TMP, Trimethoprim; PME, Polymyxin E/Colistin; (-), Sensitive; (+), Resistant. N/A – Not Applicable.

5.3.2. Nitric oxide affects gentamicin lethality

In light of recent evidence showing that deletion of respiratory oxidases increases bacterial tolerance to bactericidal antibiotics (Lobritz et al., 2015), an experiment was devised to determine the effects the respiratory inhibitor NO upon the lethality of a bactericidal antibiotic. Due to the clinical implications of such a study, a well-known multidrug-resistant E. coli strain (EC958) was chosen for the assay.

For this assay, an early exponential culture of E. coli EC958 grown in M9 minimal medium was exposed to 1 mM of NOC-12 for 30 min, prior to exposure to different concentrations of gentamicin. Serial dilutions and colony counts were carried out to determine CFU/mL and calculate % survival. In the absence of NOC-12 pre-treatment (i.e. 30 min exposure to sodium phosphate buffer, used to prepare the NOC-12 solution), the IC_{50} of gentamicin was measured as 12.3 µg/mL (Figure 5.4). In contrast, pre-exposure to 1 mM NOC-12 significantly diminished (Student's unpaired t-test p-value < 0.05) gentamicin-mediated cell killing, resulting in a 14-fold increase of the IC_{50} (Figure 5-4).

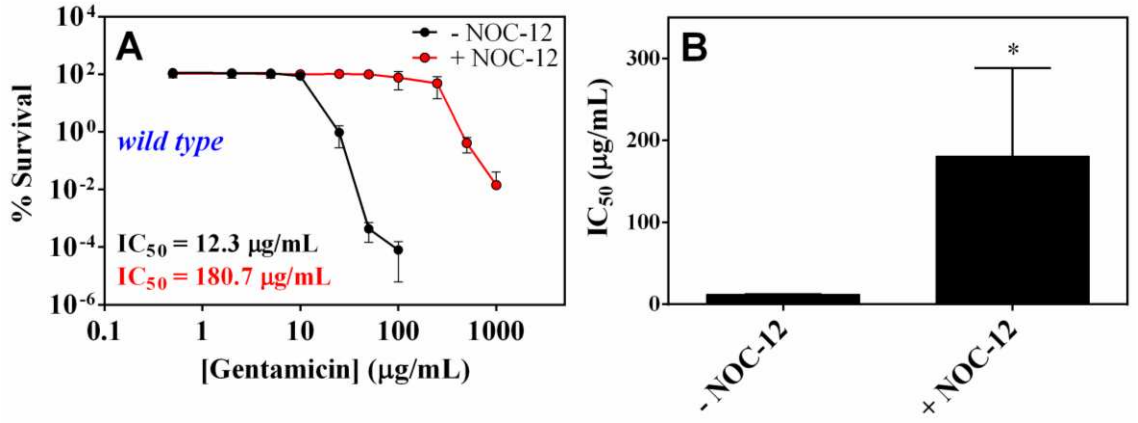

Figure 5.4 – NO decreases gentamicin lethality. A) Cell survival was determined for multidrug resistant E. coli EC958 following 90-min treatment with different concentrations of gentamicin. Pre-treatment with 1 mM NOC-12 was carried out for 30 min. B) IC_{50} of gentamicin in the absence or presence of NOC-12 pre-treatment. Each data point reflects the mean of three replicates from three independent cultures. Error bars represent standard deviation. (*: Student's unpaired t-test p-value < 0.05).

5.3.3. Endogenous NO production does not diminish gentamicin lethality

To complement the observations above with exogenously added NO, a NO-producing strain of E. coli EC958 (see chapter 3) was used to investigate the effects of endogenously-produced NO upon the sensitivity gentamicin. In Gram-positive bacteria, the endogenous production of NO by bNOS has been shown to provide protection against

bactericidal antibiotics (Gusarov et al., 2009; Van Sorge et al., 2013), and thus we hypothesized that endogenous NO-production through expression of a functional bNOS in E. coli would yield a similar result. Since the bNOS gene was cloned into the pSU2718 vector, which requires selection with chloramphenicol, the empty pSU2718 vector backbone was also transformed into E. coli EC958 to be used as a 'no nitric oxide' control (E. coli EC958 pSU2718), with the added advantage of accounting for the effects of chloramphenicol on gentamicin lethality. Early exponential cultures of E. coli EC958 pSU2718 and E. coli EC958 pSU2718-bNOS (henceforward designated by E. coli EC958 bNOS) grown in M9 minimal media supplemented with chloramphenicol were exposed to IPTG and L-Arginine for 30 min, to ensure expression of bNOS and synthesis of NO. The cultures were then subjected to a 90-min exposure to different concentrations of gentamicin. Serial dilutions and colony counts were carried out to determine CFU/mL. Surprisingly, no significant change was observed in the survival of E. coli EC958 bNOS compared to the control strain (Figure 5.5A). In fact, the IC_{50} of gentamicin for the NO-producing strain (9.5 µg/mL) is lower, albeit not statistically significant (Student's unpaired t-test p-value > 0.05), than the IC_{50} observed for the empty vector control (14.3 µg/mL) (Figure 5.5B).

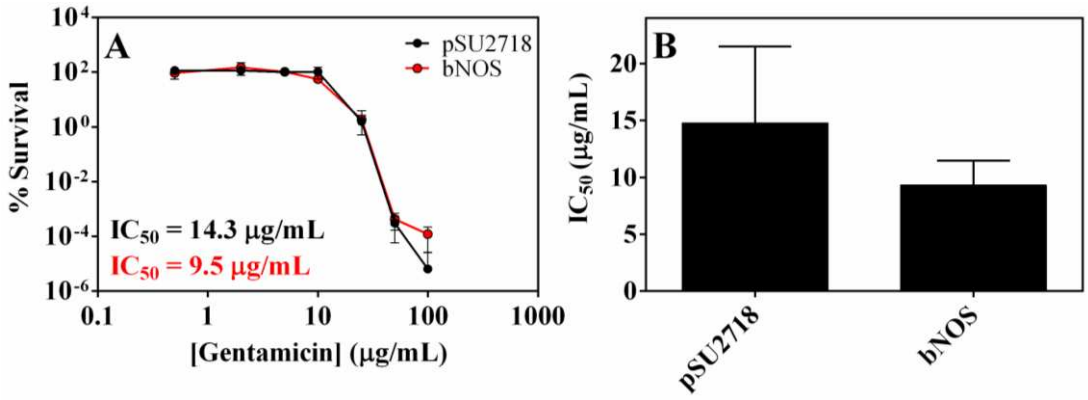

Figure 5.5 – Endogenously-produced NO does not affect gentamicin lethality. A) Bacterial survival to gentamicin is not affected by the endogenous production of NO (bNOS) compared to control (pSU2718). B) The IC_{50} of gentamicin does not significantly change in response to the endogenous production of NO (Student's unpaired t-test p-value > 0.05).

5.3.4. Macrophage-derived NO does not affect gentamicin lethality

Nitric oxide is produced by phagocytic cells, such as macrophages, of the mammalian immune system in response to infection. Following our observation that exogenous NO disrupts gentamicin lethality, we hypothesized that macrophage-derived

NO could affect the lethality of gentamicin in vivo (Figure 5.6). To test this hypothesis, the RAW-Blue™ macrophage cell line, derived from the RAW 264.7 cell line, was used

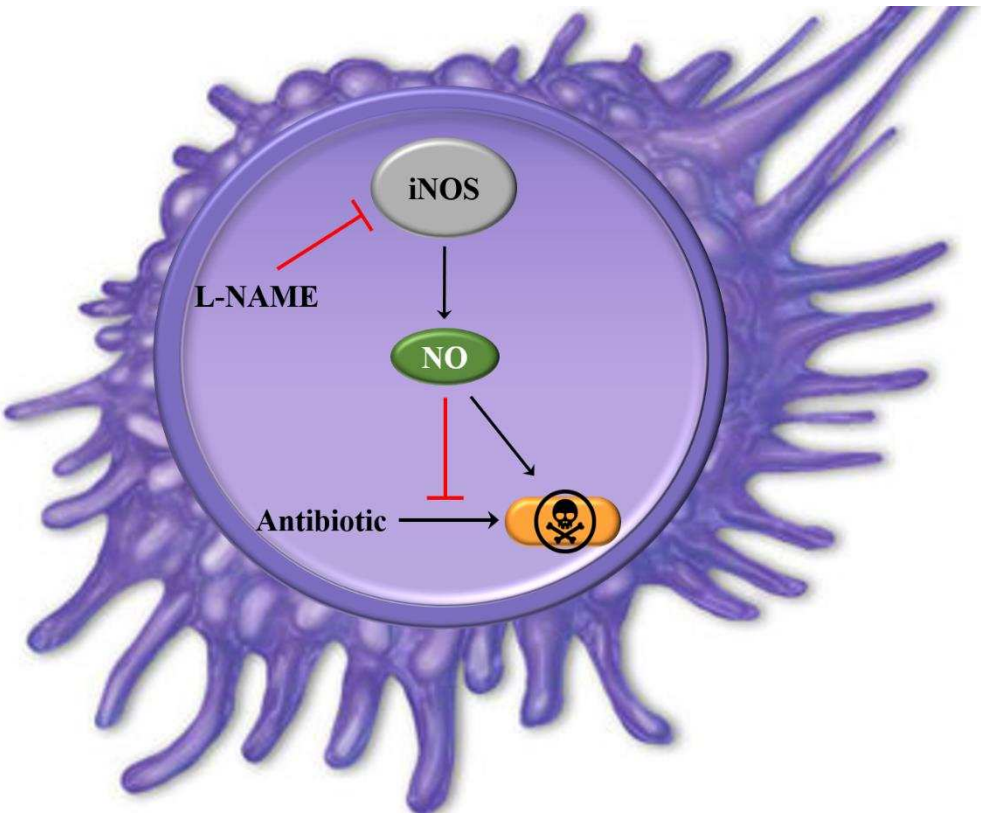

Figure 5.6 – Macrophage-derived NO could abrogate bactericidal antibiotic lethality. On their own, both macrophage-derived NO and bactericidal antibiotics are toxic to invading bacteria (in orange). However, NO and bactericidal antibiotics have antagonistic effects on bacterial respiration. We hypothesize that in the presence of a bactericidal antibiotic (gentamicin), macrophage-derived NO (produced by iNOS upon macrophage activation) will promote intra-macrophage bacterial survival. To test this hypothesis, NO-production with the iNOS inhibitor L-NAME is used to control NO production.

for intra-macrophage bacterial infection assays, along with the iNOS inhibitor L-NAME, an arginine analogue that inhibits production of NO.

In the first instance, macrophage activation conditions were assessed. To ensure expression of iNOS, and thus synthesis of NO, macrophages were activated with both LPS from E. coli and IFN-γ. Furthermore, a 2 mM concentration of L-NAME was chosen to inhibit iNOS-derived NO production. Production of NO by the macrophages under these conditions was evaluated using the Griess assay, a colourimetric assay that detects nitrite, a product of the oxidation of NO. The medium used to propagate the macrophages was shown to contain low levels of nitrite (2.14 µM) (Figure 5.7), and a similar amount of nitrite (2.64 µM) was detected in the medium containing non-activated macrophages

(i.e. no addition of LPS or IFN-γ) (Figure 5.7). In contrast, after an 18 h exposure of macrophages to LPS and IFN-γ, a statistically significant increase (Student's unpaired t-test p-value < 0.05) in the concentration of nitrite was measured in the growth medium (14.89 µM of nitrite) (Figure 5.7). Moreover, an 18 h exposure of macrophages to LPS, IFN-γ, and L-NAME resulted in low levels of nitrite present which exhibited a statistical significant difference to the levels observed for activated macrophage (Student's unpaired t-test p-value < 0.05), but not to the other two conditions tested (Figure 5.7), showing that a 2 mM concentration of L-NAME is sufficient to inhibit NO synthesis by activated macrophages.

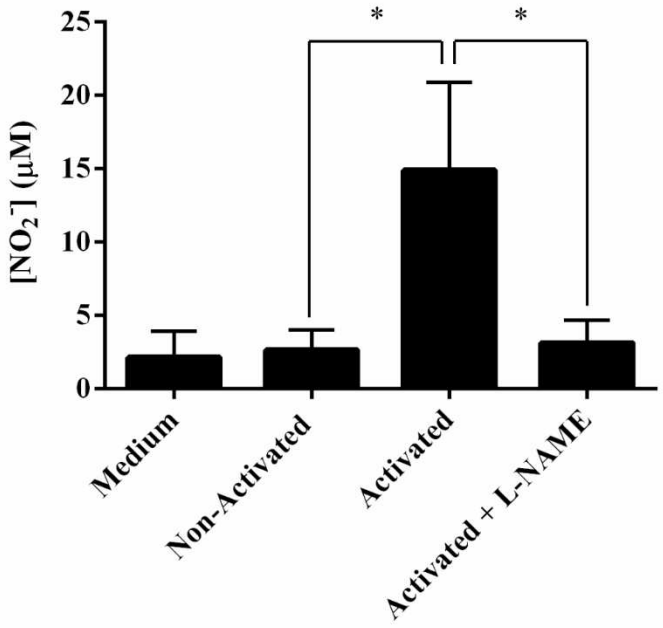

Figure 5.7 – Griess assay reveals NO production in activated macrophages. Activated macrophages exhibit high levels of nitrite. In the presence of 2 mM L-NAME, the levels of nitrite detected decreased, indicating that the inhibition of NO-production is successful under these conditions. Each data point reflects the mean of three replicates from three independent cultures. Error bars represent standard deviation. (*: Student's unpaired t-test p-value < 0.05).

For the intra-macrophage bacterial survival assay, activated and L-NAME-treated activated macrophages were exposed to E. coli EC958 with a multiplicity of infection (MOI) of 10. After sufficient time for bacterial uptake (20 min), extracellular bacteria were removed with a combination of washes and incubation with a high concentration of gentamicin for 20 min. Following this step, the different concentrations of gentamicin were applied to each well. After a 90 min exposure to gentamicin, infected macrophage cells were lysed and CFU/mL was determined. No significant difference was observed

for the bacterial load in the presence or absence of L-NAME at either 20 or 200 µg/mL of gentamicin (Figure 5.8). Interestingly, bacterial load increased after 90 min, with the '20 µg/mL without L-NAME' condition exhibiting the highest increase in CFU/mL ($4.4x10^4$ CFU/mL) compared to the bacterial load immediately following uptake (t = 0) ($2.3x10^4$ CFU/mL).

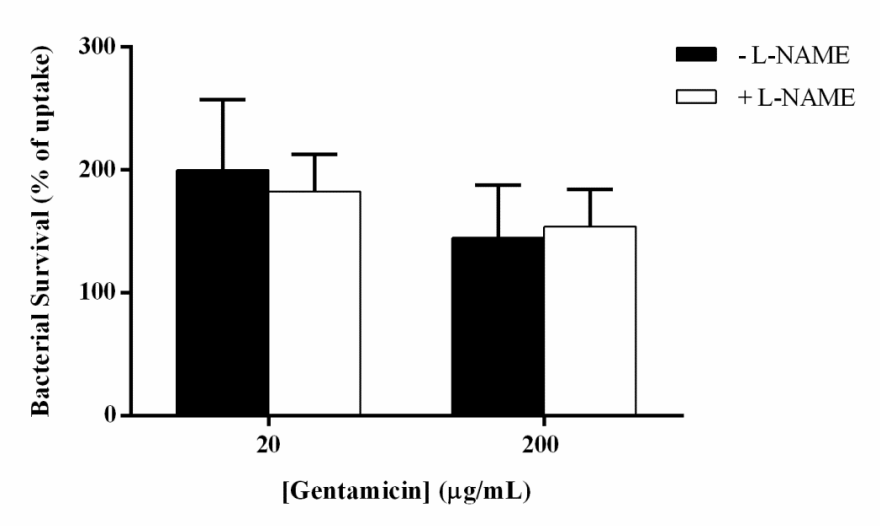

Figure 5.8 – Combination of macrophage-derived NO and gentamicin does not affect bacterial survival. After a 90-min exposure to 20 µg/mL or 200 µg/mL of gentamicin, in the presence or absence of iNOS inhibitor L-NAME, no significant difference was observed in bacterial survival. Each data point reflects the mean of three replicates from two independent cultures. Error bars represent standard deviation.

5.3.5. Cytochrome bd-I augments sensitivity to gentamicin

The cytochrome oxidases of the bacterial respiratory chain are well-known to be inhibited by the respiratory inhibitor NO. In light of recent observations that the respiratory chain plays an important role in the lethality of bactericidal antibiotics (Kohanski et al., 2007; Lobritz et al., 2015), we hypothesized that inhibition of bacterial respiration by NO could be, at least in part, responsible for the disruption of gentamicin lethality observed when bacterial cells were pre-exposed to NOC-12 (Figure 5.4). The sensitivity of respiratory mutants of E. coli to gentamicin was measured in the presence and absence of a NO donor. For this assay the compound NOC-12 was replaced by GSNO, an alternative NO-donor with similar effect on gentamicin lethality. Wild-type EC958 cells that were pre-treated with 15 mM of GSNO for 30 min exhibited an 11-fold increase in IC_{50} for gentamicin (Figure 5.9A). The cydAB (lacks cytochrome bd-I) and cyoA (lacks cytochrome bo') (Appendix G.1) deletion mutants of E. coli EC958 were also tested. In the absence of GSNO, both cydAB (Figure 5.9B) and cyoA (Figure 5.9C) exhibit

a similar survival pattern to the wild-type strain under the same conditions, with no significant difference to the IC_{50} of gentamycin (Student's unpaired t-test p-value > 0.05). When pre-exposed to GSNO, all strains exhibit an increase in the resistance to gentamicin (Figure 5.9A-C), with an 11-, 15-, and 2-fold increase in the IC_{50} for gentamicin for wild-type, cydAB mutant, and cyoA mutant strains, respectively (Figure 5.9). Interestingly, in the presence of pre-exposure to GSNO, no significant difference exists between the IC_{50} of the wild-type strain and the IC_{50} of the cyoA mutant. However, the IC_{50} of gentamicin for the cydAB mutant after pre-exposure to GSNO is higher and statistically different than the IC_{50} observed for the wild-type isogenic strain (Student's unpaired t-test p-value < 0.05) (Figure 5.9D).

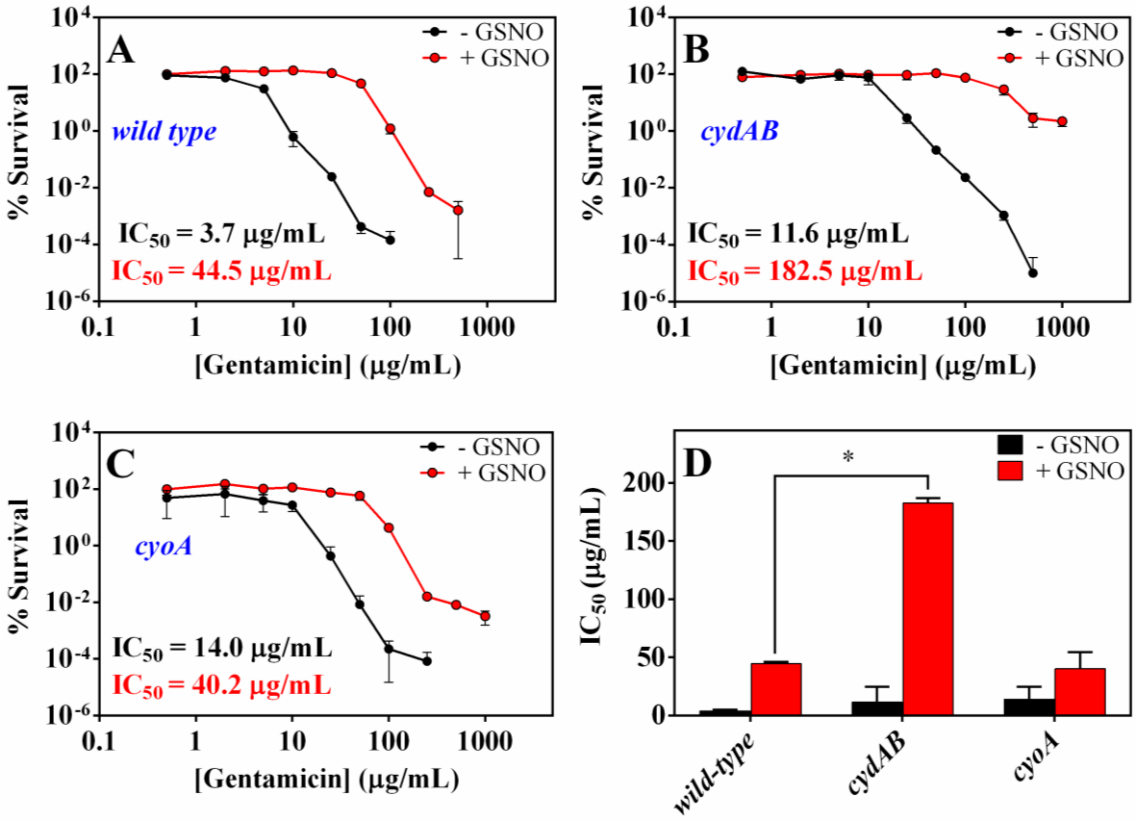

Figure 5.9 – Nitric oxide effect on gentamicin lethality is linked to bacterial respiration. Cell survival was measured in function of gentamicin concentration, in the presence or absence of pre-exposure to NO-donor GSNO, for A) wild-type EC958; B) EC958 cydAB mutant; and C) EC958 cyoA mutant. D) IC_{50} of gentamicin in the absence or presence of GSNO, for each of the strains tested. Each data point reflects the mean of three replicates from at least two independent cultures. Error bars represent standard deviation. (*: Student's unpaired t-test p-value < 0.05).

5.3.6. Nitric oxide inhibits the effect of gentamicin of E. coli biofilms

Bacterial biofilms are complex abiotic-associated structures that allow bacterial communities to withstand environmental stresses (Laverty et al., 2014), such as antibiotic

therapy, and are often responsible for many persistent and chronic infections (de la Fuente-Núñez, Reffuveille, Fernández, et al., 2013). Biofilms are heterogeneous cellular structures containing bacterial cells in different growth and metabolic states (de la Fuente-Núñez, Reffuveille, Fernández, et al., 2013). Nitric oxide has been shown to have an important role in the dispersal of biofilms of several bacterial species, including P. aeruginosa and E. coli (Miranda et al., 2011; Barraud et al., 2015; Reffuveille et al., 2015) and act synergistically with ciprofloxacin to eradicate biofilms (Reffuveille et al., 2015). Given the dramatic effects of NO upon gentamicin sensitivity in planktonic cells, it was also of interest to investigate the effects of combinatorial treatments of GSNO and gentamicin upon E. coli biofilms.

In the first instance, the biofilm-forming capability of E. coli EC958 wild-type strain in comparison to an E. coli K-12 strain, a well-known and pan-susceptible UPEC strain (E. coli CFT073), and a pan-susceptible ABU UTI strain (E. coli 83972) was determined. Biofilm formation was assessed by growing statically for 24 h in M9 medium, followed by staining of the adherent bacteria with a solution of crystal violet. Under these experimental conditions, E. coli EC958 exhibited the lowest biofilm-forming capability of all four strains tested, with significant differences observed when compared to E. coli MG1655 and E. coli CFT073 (Student's unpaired t-test p-value < 0.05) but not to E. coli 83972 (Student's unpaired t-test p-value > 0.05) (Figure 5.10). These observations can be attributed to an insertion in the fimB gene of E. coli EC958 (Totsika et al., 2011) and a non-functional fim operon in E. coli 83972 (Klemm et al., 2006). Interestingly, biofilm formation of the ABU E. coli strain 83972 is significantly lower than E. coli CFT073, contrasting results previously observed in human urine (Hancock et al., 2007).

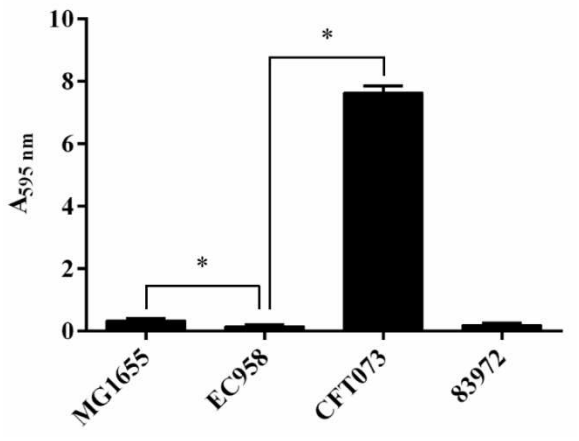

Figure 5.10 – Biofilm formation ability E. coli strains. E. coli EC958 exhibited the lowest biofilm-forming capability of all four strains tested. (*; Student's unpaired t-test p-value < 0.05).

GSNO has been previously shown to cause dispersal of P. aeruginosa biofilms (Barraud et al., 2006), and a combinatorial treatment of the nitroxide Carboxy-TEMPO and ciprofloxacin led to an almost complete eradication of E. coli mature biofilm (Reffuveille et al., 2015). Thus, we assayed the effects of 15 mM GSNO on the biomass of the bacterial biofilm of E. coli EC958, in the presence of different concentration of gentamicin with the crystal violet assay (Figure 5.11). No significant decrease in biofilm biomass was observed at different gentamicin concentrations compared to the "no gentamicin" control in the absence of GSNO. In the presence of GSNO, biofilm biomass decreased but not in a statistically significant manner (Student's unpaired t-test p-value > 0.05), with an average decrease of 20%, and no correlation was found between the decrease in biofilm biomass and gentamicin concentration (Pearson r = 0.1907, p-value > 0.05).

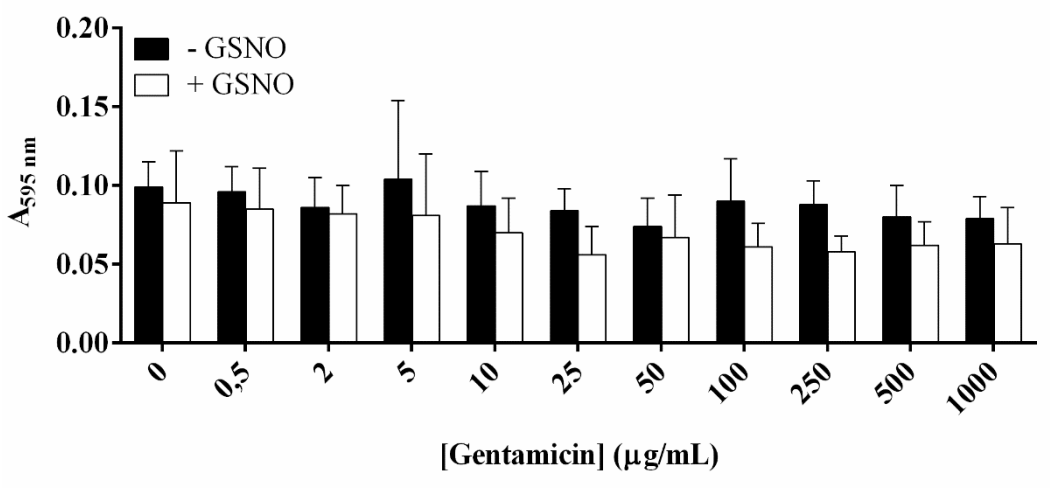

Figure 5.11 – GSNO does not significantly affect biofilm biomass. Biofilms of E. coli EC958 wild-type were allowed to form in M9 medium for 24 h prior to a 90 min exposure to different concentrations of gentamicin with or without 15 mM of GSNO. Exposure to GSNO did not significantly decrease biofilm biomass (Students's unpaired t-test p-value > 0.05).

To determine the effects of GSNO upon gentamicin lethality against E. coli EC958 wild-type biofilms, biofilms were allowed to form in M9 medium for 24 h. Medium was replaced by fresh M9 medium containing different concentrations of gentamicin with or without 15 mM of GSNO. After a 90 min incubation, biofilms were disrupted by vortex and vigorous pipetting for CFU enumeration. Unsurprisingly, the IC_{50} of gentamicin observed for E. coli EC958 wild-type biofilms (18.8 µg/mL) is higher than the one observed for planktonic cells (3.7 µg/mL). Similar to the results obtained for planktonic cells, the presence of GSNO also diminishes the susceptibility of bacterial

biofilms to gentamicin (Figure 5.12A), resulting in a significant 2.6-fold increase in the IC_{50} for this antibiotic (Student's unpaired t-test p-value < 0.05) (Figure 5.12B).

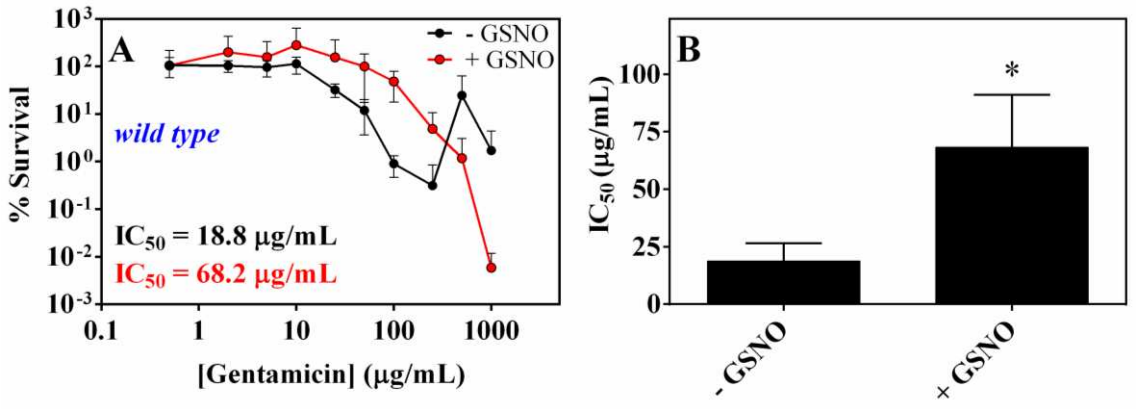

Figure 5.12 – GSNO diminishes susceptibility of bacterial biofilms to gentamicin. A) In the presence of NO-donor GSNO E. coli EC958 wild-type biofilms exhibit higher tolerance for the bactericidal antibiotic gentamicin. B) The IC_{50} of gentamicin for bacterial biofilms increases in the presence of GSNO. (*: Student's unpaired t-test p-value < 0.05).

5.3.7. Cytochrome bd-I protein sequences

In this work, it is shown that loss of NO-tolerant cytochrome bd-I leads to higher tolerance to gentamicin (see section 5.3.5). Given the prolonged use of antibiotics and the role of aerobic respiration in their mechanism of lethality, one might anticipate that loss-of-function mutations in cytochrome bd-I may have arisen to de-sensitise clinical isolates to antibiotics. Hence, the degree of conservation of this protein complex was analysed in the Kent collection. In the first instance, protein sequences of the subunits of cytochrome bd-I (CydA, CydB, and CydX) of E. coli EC958, CFT073, and ABU 83972 were aligned using T-Coffee (Notredame et al., 2000; Di Tommaso et al., 2011), and pairwise alignments were performed with BioEdit v7.2.5 (Hall, 1999). CydA, CydB, and CydX of E. coli EC958 exhibited 100% sequence identity with CydA, CydB, and CydX of the three reference strains, suggesting a high degree of conservation. The CydA, CydB, and CydX protein sequences for each isolate of the Kent collection were extracted and aligned to the respective proteins in E. coli MG1655. Only four isolates possessed mutations in at least one subunit (Table 5.1). A total of five mutations were identified in the entire collection: three in CydA, and the remaining two in CydB. No mutations were found in the CydX subunit. Only one of the mutations identified resulted in a non-conservative mutation (Table 5.1), i.e. resulted in a change in the property of the amino acid. In this case, it resulted in a change from a non-polar amino acid (alanine) at position 521 of CydA, to a polar amino acid (threonine).

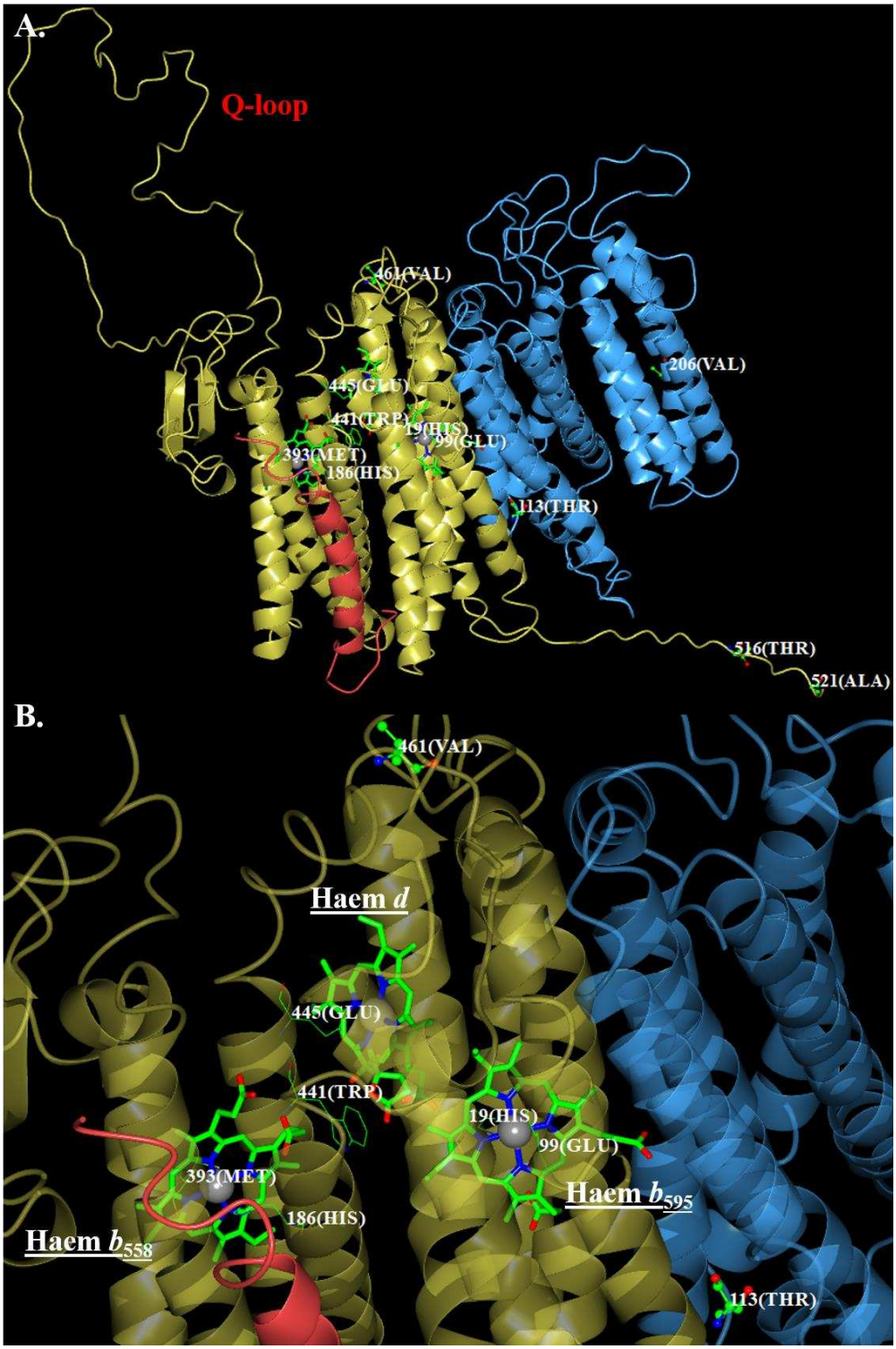

Figure 5.13 – Structural modelling of E. coli cytochrome bd-I. A) Cytochrome bd-I comprises three subunits: CydA (gold), CydB (blue), and CydX (red). The structure of E. coli CydABX was modelled upon the crystal structure of CydABX from Geobacillus thermodenitrificans (PDB ID: 5DOQ) using RaptorX (Källberg et al., 2012). The cofactors haem b_{558}, haem $b_{595,}$ and haem d, and their binding sites (M393, H186, W441, E445, H19 and E99) as well as the positions where amino acids substitutions were identified for the CydABX protein sequences of the Kent collection isolates (Table 5.1) were mapped onto the structure. B) Detailed zoom shows that none of the amino acid substitutions are located near the cofactors.

A structural model of E. coli cytochrome bd-I was generated using the RaptorX server (Källberg et al., 2012). Protein sequences of the three subunits of E. coli MG1655 cytochrome bd-I (CydA, CydB, and CydX) were submitted to RaptorX (Källberg et al., 2012) for structural prediction based on the recently characterized structure of the bd complex of Geobacillus thermodenitrificans (Safarian et al., 2016). To generate a model with haem cofactor, the E. coli modelled subunits were superposed onto the G. thermodenitrificans structure using CCP4MG software (McNicholas et al., 2011). The mutations identified by protein sequence alignment were mapped onto the structure and are displayed in figure 5.13. None of the amino acid substitutions identified in CydA (A521T, V461G, and T516S) are located near the haem cofactors in CydA. In the E. coli model, the haem b_{558}, can be ligated by H186 and M393, the haem b_{595} can be ligated by H19 and E99, and the d–type haem is adjacent to a glutamic acid (E445) and tryptophan (W441) that are thought to be involved in proton and electron delivery, respectively (Safarian et al., 2016).

Table 5.1 – Amino acid substitutions present cytochrome bd-I subunits

Protein	KC	Mutation	Classification
CydA	KC11	A521T	Non-conservative
	KC31	V461G	Conservative
	KC37	T516S	Conservative
CydB	KC11	V206L	Conservative
	KC20	T113N	Conservative

5.4. Discussion

5.4.1. Exogenously administered NO affects gentamicin lethality

The antimicrobial properties of NO and its use by the mammalian immune system in response to infection are well-known. With the emergence of antibiotic resistance, the use of exogenously supplied NO as an alternative treatment to antibiotics, or co-administered with antibiotics, has been the focus of recent studies (Bang et al., 2014; Reffuveille et al., 2015). However, the recent observation that the effects of bactericidal antibiotics are not solely due to its primary interaction with the bacterial target, and have complex downstream metabolic effects partially involving the aerobic respiratory chain (Kohanski et al., 2007; Dwyer et al., 2014; Lobritz et al., 2015), leading us to question the strategy of combinatorial treatments of nitric oxide (a potent respiratory inhibitor) with bactericidal antibiotics.

After ascertaining that the degree of antibiotic resistance does not correlate with a change in nitric oxide sensitivity (Figure 5.3), the effect of nitric oxide in antibiotic efficacy was tested on E. coli EC958, a well-characterized multidrug-resistant UPEC strain (Totsika et al., 2011; Forde et al., 2014). The multidrug-resistant phenotype of this strain posed an initial difficulty when choosing the bactericidal antibiotic to be tested, as this strain is only sensitive to a few of the antibiotics tested, not all of them bactericidal. Fortunately, E. coli EC958 exhibits sensitivity to gentamicin, a bactericidal antibiotic used in the treatment of several types of infection, including UTIs.

To better mimic infection, planktonic cells were exposed to the NO-donor NOC-12 prior to exposure to the antibiotic gentamicin. Pre-exposure to NOC-12 resulted in a 14-fold increase of the IC_{50} for gentamicin (Figure 5.4), thus showing potent inhibition of gentamicin lethality by NO. In contrast, and contrary to what was observed in Gram-positive bacteria, this was not observed for E. coli EC958 bNOS (Figure 5.5), a strain capable of producing NO endogenously. One possible explanation for these contrasting results is the rapid breakdown of NO in the bacterial cytoplasm by NO-detoxifying mechanisms, such as flavohaemoglobin Hmp. An effective NO-detoxification response would lead to low concentrations of NO, perhaps insufficient to elicit an effect. A way to test this hypothesis would be to transform pSU2718-bNOS into E. coli EC958 mutant for NO-detoxifying mechanisms, starting with flavohaemoglobin Hmp as it is an important NO detoxification mechanism under aerobic conditions, as determined in section 3.3.1.

5.4.2. Macrophage-derived NO does not abrogate gentamicin efficacy

Due to the synthesis of NO by cells of the mammalian immune system, it was of interest to measure the effects of macrophage-derived NO upon antibiotic sensitivity. Hence, infection of murine macrophage by E. coli EC958 was carried out. Activation of macrophages with LPS and IFN-γ is known to increase the expression of iNOS and thus synthesis of NO, and elevated nitrite levels under these conditions are consistent with this (Figure 5.7). Activation of macrophages in the presence of the iNOS inhibitor L-NAME was also shown to dramatically diminish nitrite accumulation (Figure 5.7), consistent with lower iNOS activity. For the infection assay, two different concentrations of gentamicin were chosen: 20 µg/mL gentamicin, equivalent to five times the minimum inhibitory concentration (MIC) for Enterobacteriaceae according to BSAC testing v13.0 and an approximate concentration to the peak concentration in human serum (C_{max} = 18 µg/mL); and 200 µg/mL, to maximise the likelihood of antibiotic entry to the macrophage. The permeability of macrophage to this drug is low but intra-macrophage accumulation has been observed for high extracellular concentrations of gentamicin (Barcia-Macay et al., 2006). After infection with E. coli EC958, no significant difference was observed in the bacterial load in the presence of L-NAME compared to its absence. The intracellular environment of macrophages is complex and bacterial clearance during infection is achieved by the collective action of ROS, RNS, and lysosomal enzymes (Figure 5.14), and it is perhaps possible that this complex environment can interfere with the function of gentamicin. In fact, gentamicin is known to concentrate in lysosomes, which have a naturally acidic environment that interferes with gentamicin activity (Barcia-Macay et al., 2006). Despite the results observed for gentamicin, it remains possible that macrophage-derived NO may impact upon the lethality of other bactericidal antibiotics.

5.4.3. Cytochrome bd-I confers sensitivity to gentamicin

In the recent work of Lobritz et al. (2015), a link between bacterial respiration and lethality of bactericidal antibiotics was shown, with treatment of bacterial cells with bactericidal antibiotics resulting in a significant increase in cellular respiration. Nitric oxide targets many bacterial proteins, including the haem-containing cytochrome oxidases involved in bacterial aerobic respiration (Wink et al., 2011).

The role of two cytochrome oxidases, cytochrome bo’ and the NO-tolerant cytochrome bd-I, was determined by assessing bacterial survival to gentamicin of E. coli EC958 cyoA and E. coli EC958 cydAB null single mutants in the presence and absence of

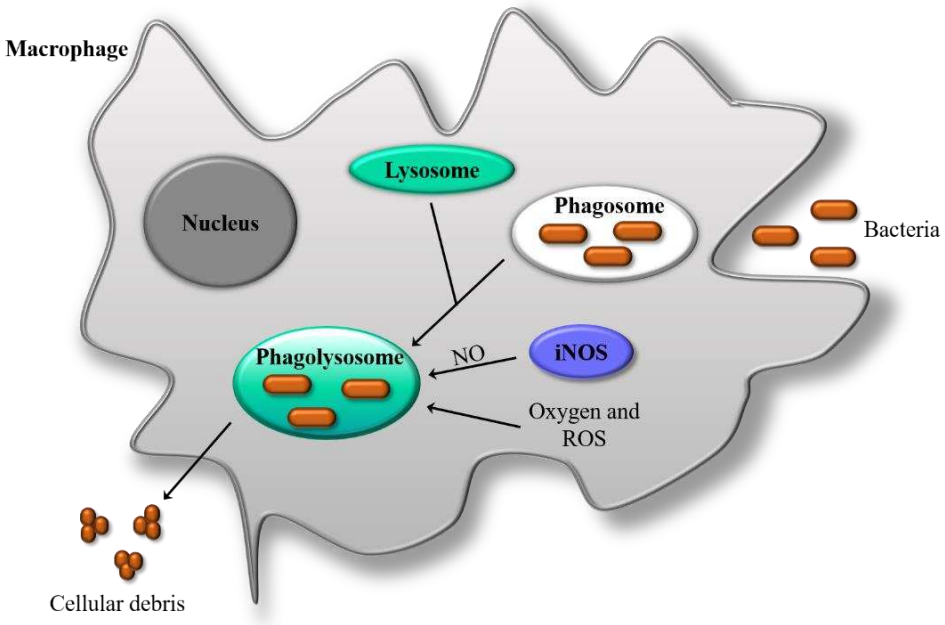

Figure 5.14 – Bacterial clearance by macrophages. Invading bacteria are phagocytised by macrophages, forming a phagosome which then fuses with a lysosome, a vacuole containing enzymes that hydrolyse a plethora of bacterial constituents. In the resulting phagolysosome, the hydrolytic enzymes, along with ROS and RNS kill and digest the invading bacteria.

the NO-releaser GSNO. While no significant differences were observed in the absence of GSNO, pre-exposure of both mutant and wild-type strains with GSNO resulted in an increase in gentamicin tolerance for all strains. However, the increase in the IC_{50} of gentamicin in the presence of GSNO was more pronounced for cydAB, with the IC_{50} of gentamicin increasing by 15-fold in the presence of GSNO compared to the 11-fold increase observed for the wild-type isogenic strain (Figure 5.9). In the cyoA null mutant, bacterial cells are still expressing the NO-tolerant cytochrome bd-I (Mason et al., 2009) allowing bacterial respiration to continue in the presence of nitric oxide and, possibly, the generation of ROS arising from the accelerated metabolism response that occurs in the presence of gentamicin. In contrast, in the cydAB mutant bacterial respiration is easily inhibited by NO due to the presence of NO-sensitive cytochrome *bo'* (Mason et al., 2009), hence it is possible that gentamicin-mediated ROS production is abolished resulting in a higher tolerance for gentamicin. Alternatively, the abolishment of bacterial respiration is likely to result in a disruption of the PMF, which is necessary for the uptake of aminoglycosides such as gentamicin (Hancock, 1981; Allison et al., 2011). However, to determine whether ROS or decreased uptake of gentamicin are responsible for the decreased sensitivity to gentamicin, further investigation would be required. Despite this,

based on the results presented here, we propose that cytochrome bd-I in the presence of NO increases bacterial sensitivity to bactericidal antibiotics and hypothesized that in the presence of NO bacterial species lacking the cytochrome bd-I complex, such as Campylobacter jejuni (Jackson et al., 2007), may be more tolerant to antibiotics.

Given the sensitization of bacterial cells expressing cytochrome bd-I to gentamicin, loss-of-function mutations in cytochrome bd-I complex was hypothesised. However, sequence analysis of cytochrome bd-I subunits in the pathogenic E. coli isolates of the Kent collection shows a high level of conservation, which is consistent with the lack of NO-susceptibility observed in the Kent Collection (Figure 5.3B). These results suggest that maintaining respiration in the presence of NO (by cytochrome bd-I) is a stronger evolutionary driver than reducing sensitivity to antibiotics in the presence of NO (through loss of cytochrome bd-I activity). E. coli frequently encounters NO in the absence of antibiotics, in which case cytochrome bd-I will facilitate growth and survival by allowing continued aerobic respiration. Furthermore, it has also been shown in previous studies that cytochrome bd-I is important for bacterial survival during infection of the mammalian host (Shepherd et al., 2016). Hence, it is perhaps not surprising that mutations in cytochrome bd-I are rare.

5.4.4. Exposure of biofilms to GSNO increases tolerance to gentamicin

Bacterial biofilms are often formed in response to environmental stresses, and the sessile cells found in bacterial biofilms are both phenotypically and physiologically different from planktonic cells. Furthermore, nitric oxide has been implicated in the dispersal events of P. aeruginosa and E. coli biofilms (Barraud et al., 2006; Barraud et al., 2015; Reffuveille et al., 2015). This led us to question whether exogenous nitric oxide would affect resistance to gentamicin in biofilms. Out of the four strains tested for biofilm-forming capabilities, E. coli EC958 and E. coli 83972 formed the lowest biofilm biomass (Figure 5.10), which can be explained by an insertion in the fimB gene of E. coli EC958 (Totsika et al., 2011), a gene which encodes a recombinase that switches on the expression of type I fimbriae. Also, there is no functional fim operon in E. coli 83972 (Klemm et al., 2006). In both cases, expression of type I fimbriae, important in the initial stages of biofilm development, is not possible. We also observed a difference between biofilm biomass of E. coli CFT073 and E. coli 83972, with the former forming significantly more biofilm. However, this contrasts with what was observed by Hancock et al. (2007) in human urine, where E. coli 83972 formed significantly more biofilm.

E. coli EC958 24 h biofilms showed a 4-fold increase in the IC_{50} for gentamicin (Figure 5.12) compared to planktonic cells (Figure 5.9). This result was expected as increased resistance to antibiotics is a well-known phenotype of bacterial biofilms (Mah and O'Toole, 2001). In the presence of GSNO, the resistance of biofilms to gentamicin further increases by 2.6-fold (Figure 5.12). Assessment of GSNO-induced biofilm dispersal (Figure 5.11) showed that GSNO does not elicit a significant change in biofilm biomass, so the increase in IC_{50} of gentamicin in the presence of GSNO cannot be explained by NO-induced alterations in biofilm dispersal. Biofilms are heterogenous structures, formed by cells in different metabolic states. For example, P. aeruginosa biofilms possess areas with low metabolic activity and areas with high metabolic activity (Pamp et al., 2008). Thus, one possible explanation is that this same heterogeneity is present in biofilms of E. coli EC958 and GSNO interference with its many targets, including respiratory cytochrome oxidases, slows down the metabolism of previously active cells and increases tolerance to gentamicin. However, further studies are required to test this hypothesis.

Chapter 6

Final Discussion

6.1. Background

The emergence of antibiotic-resistant bacteria is an increasing concern worldwide. Of particular importance is the emergence of bacteria exhibiting a multidrug-resistant phenotype, i.e. resistant to three or more classes of antibiotics. This makes the treatment of bacterial infections more difficult, in some cases even impossible, with negative impacts upon morbidity, mortality and the cost of healthcare. As such, surveillance of antibiotic resistance among bacterial pathogens and the development of alternative therapies are of the utmost importance to help tackle this problem.

Nitric oxide is a small molecule which can be toxic to both mammals and bacteria Nevertheless, NO is produced in mammals where it carries out important physiological roles, such as smooth muscle relaxation. Furthermore, NO is known for its antimicrobial properties and its produced by cells of the mammalian immune system as part of its response to invading pathogens. As such, the use of NO as a potential alternative therapy against resistant and multidrug resistant bacteria has been an appealing prospect for some time. Indeed, NO has been shown to be effective against bacterial biofilms (Barraud et al., 2006; de la Fuente-Núñez, Reffuveille, Fairfull-Smith, et al., 2013). However, bacteria often possess a plethora of mechanisms that allow detoxification of NO and other toxic RNS, as well as tolerance, thus allowing bacteria to survive and grow even in the presence of this toxic molecule. Herein, the antibiotic resistance of E. coli bacteraemia isolates was assessed with both phenotypic and genomic tools. Furthermore, the potential use of nitric oxide as a therapeutic was assessed on its own, but also in combination with conventional antibiotics, in both planktonic and biofilm structures of a multidrug-resistant pathogenic E. coli strain.

6.2. Conclusions

6.2.1. Insights into antibiotic resistance in E. coli

E. coli bacteria are a normal part of the human gut flora where its commensal nature promotes normal intestinal function. However, E. coli can take on a more pathogenic nature and cause diseases such as UTI, intestinal infections, and neonatal meningitis. The rise of antibiotic resistance, particularly amongst E. coli clinical isolates, is thus a global concern, and it is vital to track the patterns and rise of antibiotic resistance in order to implement the best treatment. As part of this work, a collection of 50 E. coli bacteraemia clinical isolates from Kent (UK) was characterised using phenotypic and genomic tools.

A resistant phenotype was observed in 44% of the isolates, with 14% exhibiting a multidrug resistant phenotype, with the highest level of resistance observed for amoxicillin, trimethroprim, and ciprofloxacin. This result was unsurprising and can easily be explained by the wide use of these antibiotics in the treatment of bacterial infections and in agricultural settings, which results in a higher selective pressure that drives the development of antibiotic resistance. Furthermore, these results are in agreement with the surveillance report carried out by the ECDC which shows high levels of resistance to fluoroquinolones (e.g. ciprofloxacin) and penicillins (e.g. amoxicillin) in E. coli in several European countries, including in the UK (ECDC, 2017). In silico detection of antibiotic resistance was also carried out in this work by performing whole genome sequencing of the 50 E. coli clinical isolates. This allowed not only the detection of acquired resistance genes, but also for a more comprehensive characterization of the entire collection (e.g. presence of virulence genes and phylogenetic analysis). In silico analysis identified 30% of the isolates as being multidrug-resistant (i.e. resistant to three or more classes of antibiotics (Magiorakos et al., 2012)), nearly twice as more isolates as those identified using the disc diffusion assay. However, this discrepancy can easily be explained by the identification of resistance to two extra classes of antibiotics using in silico analysis. Whilst in silico approaches can rapidly identify patterns of antibiotic resistance, these techniques require up-to-date and well curated databases with all known genes and/or mutations known to confer resistance to antibiotics (Ellington et al., 2012; Fricke and Rasko, 2014). Additionally, discrepancies between predicted resistance and experimentally verified resistance can occur: herein we encountered isolates that encode chloramphenicol resistance genes, but the phenotype was not observed during the disc diffusion assays. As such, it remains necessary to verify resistance phenotypes

experimentally, particularly as it would allow detection of antibiotic resistance arising through novel and unidentified mechanisms (Ellington et al., 2012). Furthermore, no isolate in the collection exhibited resistance to meropenem nor colistin. The existence of beta-lactamases capable of hydrolysing carbapenems (e.g. meropenem) have been known quite some time (reviewed in Poole, 2004) and their spread among bacterial pathogens are of particular concern due to their ability to inactivate virtually all beta-lactam antibiotics, and their association with other antibiotic resistance determinants, thus leading to a multidrug-resistant phenotype (Yong et al., 2009; Walsh et al., 2011). In agreement with the data presented here, the ECDC surveillance report (ECDC, 2017) reveals that levels of resistance to carbapenems among E. coli remain low (0.1%) amongst European countries. The absence of colistin-resistance in the Kent collection can be explained by the very recent emergence of plasmid-borne colistin resistance in China (Liu et al., 2016), thus it is likely that dissemination of the plasmid-associated mcr-1 gene, which confers resistance to colistin, is still in its early stages. However, the absence of meropenem and colistin resistance in the Kent collection highlights the importance of implementing strict rules and control for the usage of these antibiotics in order to diminish the dissemination of resistance towards these antibiotics.

The antibiotic resistance problem is aggravated with the development of multidrug resistance. E. coli ST131 is currently the most worrying clonal group of E. coli. E. coli ST131, an UPEC strain, is prevalent in most parts of the world and is frequently associated with fluoroquinolone resistance and the expression of CTX-M-15, an ESBL capable of inactivating penicillins (e.g. amoxicillin) and cephalosporins (e.g. cefotaxime) (Nicolas-Chanoine et al., 2014), and it has been hypothesized that the worldwide dissemination of E. coli ST131, success attributed to a combination of antibiotic resistance and high virulence (Johnson et al., 2010; Peirano et al., 2013; Nicolas-Chanoine et al., 2014), has contributed to the increase in antibiotic resistance observed in E. coli (Johnson and Stell, 2000; Peirano et al., 2013). Contrary to previous epidemiological studies reporting E. coli ST131 as the most prevalent clonal lineage in the UK and USA (Johnson et al., 2010; Croxall et al., 2011), E. coli ST131 represented 12% of the Kent collection, surpassed by both ST73 (18%) and ST69 (14%). Furthermore, despite exhibiting high levels of resistance, the ST131 isolates in this collection did not exhibit high virulence, contrasting the previous findings by Johnson et al., 2010 and Peirano et al., 2013, and further supporting the long standing hypothesis that high levels of virulence cannot co-exist with high levels of antibiotic resistance in E. coli, as the latter

would affect fitness thus leading to decreased virulence (Johnson, Kuskowski, et al., 2003).

6.2.2. Flavohaemoglobin Hmp, cytochrome bd-I and flavorubredoxin NorVW are the main nitric oxide tolerance mechanisms in E. coli

The emergence of multidrug resistance in poses a threat to public health. As such, alternative strategies to combat antibiotic resistance is urgently needed. Nitric oxide, a small radical molecule naturally produced by the mammalian immune system in response to infection, can potentially be used as an alternative antimicrobial. In fact, inhalation of nitric oxide is currently used to treat pulmonary hypertension (Wessel et al., 1997; Hunt et al., 2016), and studies have shown a potential use for nitric oxide in the eradication of bacterial biofilms (Barraud et al., 2006; Reffuveille et al., 2015; Ren et al., 2016). However, no strategies currently exist for the sustained delivery of NO at the site of infection. As such, one of the main aims of this project was to engineer a NO-producing/NO-tolerant strain of asymptomatic strain of E. coli that could potentially be used to help treat UTIs caused by multidrug-resistant E. coli. The strategy employed in this work involved the overexpression of the chromosomal copy of flavohaemoglobin Hmp combined with expression of bNOS.

Due to the toxicity of nitric oxide, it comes as no surprise that E. coli possesses several mechanisms that help the cell cope with the toxic effects of NO (see section 1.2.3). To engineer NO-tolerance in a strain of E. coli, it was important to determine the importance of these mechanisms under different oxygen conditions in order to choose the appropriate mechanism for overexpression. A well diffusion assay showed that in the presence of oxygen flavohaemoglobin Hmp and NO-tolerant cytochrome bd-I respiratory oxidase played an important role in protecting E. coli EC958 from GSNO, whilst flavorubredoxin/flavorubredoxin reductase NorVW is important under anaerobic conditions. Congruent with the data present here is the work of Gardner and colleagues (Gardner et al., 1998; Gardner and Gardner, 2002) in a non-pathogenic E. coli, showing that the protection afforded by flavohaemoglobin Hmp was much greater when oxygen was present. Furthermore, NO-metabolizing NorVW activity was shown to be higher under anaerobic conditions (Gardner et al., 2002). Cytochrome bd-I has been previously shown to be a NO-tolerant respiratory oxidase (Mason et al., 2009) and crucial for the survival of E. coli during infection (Shepherd et al., 2016). The presence of a functional cytochrome bd-I during nitrosative stress and in the presence of oxygen allows for bacteria to carry out aerobic respiration (Mason et al., 2009), the most effective form of

ATP generation, a characteristic that explains the sensitivity of the E. coli EC958 cydAB mutant observed in this work.

Based on the microaerobic conditions of the bladder (Hagan et al., 2010), and the sensitivity of the cytochrome bd-I complementation strain (see section 3.3.2), possibly due to the generation of high levels of toxic ROS (Kohanski et al., 2007; Dwyer et al., 2014; Lobritz et al., 2015) due to high expression levels of cytochrome bd-I, overexpression of flavohaemoglobin Hmp was chosen instead in an attempt to create a strain of E. coli highly tolerant to NO. Following the successful substitution of the native Hmp promoter with a constitutive promoter, GSNO susceptibility was assessed. Whilst the increased sensitivity of the Hmp-overexpressing strain in the presence of oxygen can be explained with formation of toxic superoxide (Membrillo-Hernández et al., 1996; Anjum et al., 1998; Wu et al., 2004) and, consequently, peroxynitrite in the presence of NO, the sensitivity to GSNO observed under anaerobic conditions is much more surprising. This could be due to 1) formation of superoxide from the remaining oxygen present in the media since the bacterial growth assay was not carried out under strict anaerobiosis or 2) the Hmp protein levels resulting from constitutive expression lead to toxicity.

NO-production was attempted with cloning of bNOS onto a plasmid. Induction of hmp promoter, whose activity increases in the presence of NO or nitrosative stress (Poole et al., 1996), in the strain of E. coli harbouring pSU2718-bNOS was observed. However, a more direct measurement of NO needs to be carried out to determine the levels of NO being produced with certainty (e.g. using a NO electrode for NO quantification).

6.2.3. Nitric oxide diminishes lethality of gentamicin

For many decades, the lethality of bactericidal antibiotics was thought to result directly from the primary mode of action of the antibiotic. However, studies have recently suggested that bacterial metabolic activity has an effect on the efficacy of the bactericidal antibiotic (Rowan et al., 2016; Yang, Bening, et al., 2017). Recent work by Lobritz and colleagues (Lobritz et al., 2015) show that deletion of the three main respiratory oxidases, cytochrome bd-I, cytochrome bd-II, and cytochrome *bo'*, in a non-pathogenic E. coli strain resulted in a higher tolerance for a wide array of bactericidal antibiotics and led us to hypothesize that a potent respiratory inhibitor such as NO could lead to a reduction in antibiotic efficacy (Figure 6.1).

In this work, the impact of the respiratory inhibitor NO upon the lethality of the bactericidal antibiotic gentamicin was investigated in a multidrug-resistant E. coli EC958

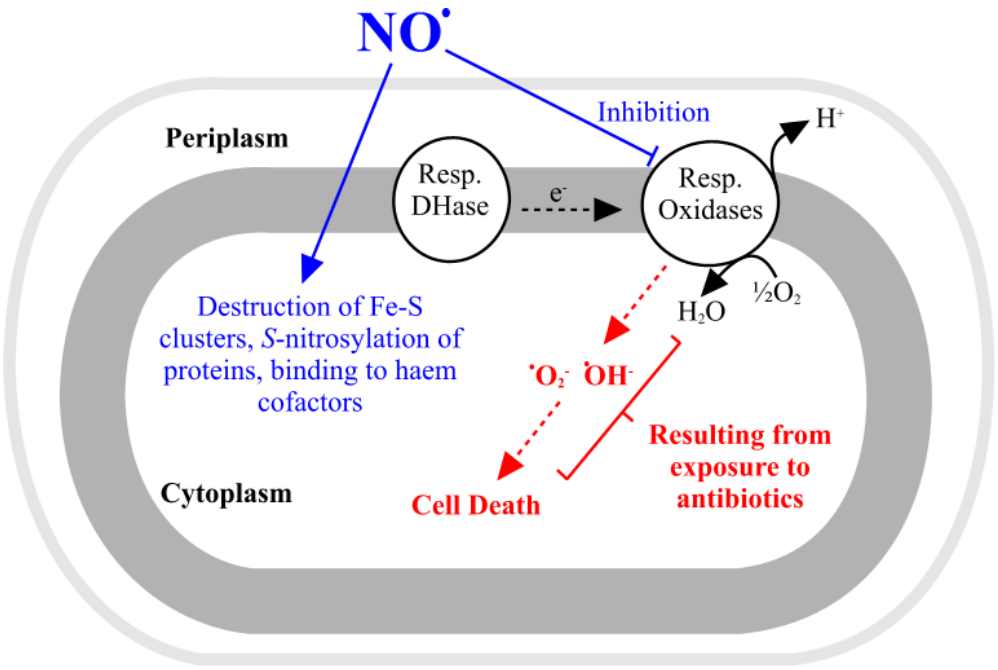

Figure 6.1 – Model for the roles of NO during bacterial exposure to antibiotics. Bactericidal antibiotics cause downstream effects on bacterial metabolism that lead to the accumulation of ROS (red). Nitric oxide exposure (blue) can have deleterious and protective effects where nitrosylation of multiple cellular targets is toxic and respiratory inhibition can diminish the generation of ROS that results from antibiotic treatment. Abbreviations: Resp DHase, Respiratory Dehydrogenase; Resp Oxidases, Respiratory Oxidases.

strain in planktonic cultures and biofilms. Pre-exposure to either NOC-12 or GSNO greatly increased the IC_{50} for gentamicin, suggesting that NO offers significant protection against the effects of gentamicin, for both bacterial planktonic cells and biofilms, presumably due to inhibition of aerobic bacterial respiration. Bacterial aerobic respiration is carried out by cytochrome oxidases bo' and cytochrome bd-I, both well-known NO targets. However, whilst cytochrome bo' is rapidly inhibited by NO, cytochrome bd-I is a NO-tolerant respiratory oxidase (Mason et al., 2006). The work carried herein shows that the IC_{50} of gentamicin is significantly higher for the cydAB knockout mutant of E. coli EC958, compared to the cyoA knockout or wild-type isogenic strains, both of which share similar IC_{50}, in the presence of GSNO. This suggests that the presence of cytochrome bd-I increases bacterial sensitivity to gentamicin when GSNO is present. The NO-tolerant nature of cytochrome bd-I (Mason et al., 2006) allows aerobic bacterial respiration to continue. As previously mentioned, it has been suggested that the lethality of bactericidal antibiotics is due, in part, to the synthesis of ROS (Kohanski et al., 2007; Wang and Zhao, 2009; Dwyer et al., 2014) generated by the bacterial respiratory chain. Thus, it is possible that the susceptibility to gentamicin observed in the presence of GSNO

in both the wild-type and cyoA knockout strain of E. coli EC958 is due to the hyperactivation of cytochrome bd-I, thus production of lethal ROS, which, in contrast, is completely abolished in the cydAB knockout mutant. However, it is also a well-established fact that uptake of aminoglycosides, such as gentamicin, into the bacterial cell requires a PMF threshold (Hancock, 1981; Humbert and Altendorf, 1989), which maintained by the bacterial respiratory chain. Hence, it is also possible that the sensitivity to gentamicin herein observed in the presence of GSNO occurs because cytochrome bd-I is capable of maintaining the PMF threshold required for gentamicin uptake through vectorial translocation of protons (Miller and Gennis, 1985). Further studies are required to determine the underpinning mechanism.

Despite increasing sensitivity of bacteria to antibiotics, the primary sequences of of cytochrome bd-I (CydA, CydB, and CydX) were found to be highly conserved in E. coli. Cytochrome bd-I has been shown to play an important role in bacterial survival during infection (Shepherd et al., 2016), and it is plausible that bacteria such as E. coli encounter NO in the absence of antibiotics more frequently than in the presence of antibiotics. Thus, it is possible that the importance of cytochrome bd-I in niches where antibiotics are not present potentially outweighs the evolutionary driver for antibiotic tolerance.

6.3. Further work

In chapter 3, attempts at quantifying nitrate and nitrite as a measure of NO production by the bNOS gene were unsuccessful during this work. It was proposed that the fast consumption of nitrite and nitrate by E. coli wild-type cells could be partially responsible for the negative result. The assay could be repeated following transformation of pSU2718-bNOS into a strain of E. coli lacking nitrite reductases and/or nitrate reductases, thus increasing the amount of nitrite and nitrate for detection by the Griess assay. Alternatively, and preferably, NO levels could be measured directly with a NO electrode.

Further in chapter 3, it was proposed that GSNO susceptibility exhibited by the Hmp-overexpressing strain under anaerobic conditions was a result of protein accumulation and consequent toxicity. Hence, Hmp protein levels need to be assessed with a western blot.

In chapter 4, phylogenetic analysis showed that commensal strains of E. coli have diverged more recently, and it was hypothesised that the evolutionary process of E. coli has resulted in loss of virulence genes, aiming for a commensal relationship with the host that allows long-term colonization and survival. However, it is possible that the rapid emergence of antibiotic resistance could disrupt this pattern and a more detailed comprehensive analysis, perhaps even including a larger number of genome sequences belonging to E. coli (or even other bacterial species) is necessary to determine how antibiotic resistance may influence the evolution of virulent strains.

In chapter 5, one of the isolates of the Kent collection (KC45) exhibited a significantly higher susceptibility to GSNO in the presence of oxygen. Further work could focus on investigating the cause of this phenotype (e.g. glutathione susceptibility), as this isolate did not show increased sensitivity to NOC-12, a more specific NO-donor than GSNO. Also in chapter 5, the effects of NO upon the efficacy of gentamicin, a bactericidal antibiotic, were tested. It was shown that the presence cytochrome bd-I results in elevated susceptibility to gentamicin during NO exposure. For a more complete analysis, a mutant of cytochrome bd-II could be engineered and tested for susceptibility to gentamicin, and other bactericidal antibiotics, in the absence and presence of pre-exposure to NO. Given the similarity between bd-II and bd-I, one might predict that the bd-II terminal oxidase could also support ROS generation in the presence of NO, especially if the cells were grown under conditions where bd-II is maximally expressed. Additionally, to avoid the problems associated with bacterial uptake and elimination of extracellular bacteria,

neutrophils could provide an extracellular nitrosative burst to the bacteria as previously described (Shepherd et al., 2016). Finally, to confirm the general model for NO protecting bacteria against antibiotic-mediated ROS generation during NO exposure, similar experiments with a range of other bactericidal antibiotics and other bacterial species would be useful. These experiments could provide important insights into how different bacteria respond to different antibiotics during infection and pave the way for future interventions that are required to combat the spread of multidrug-resistant strains.

References

Abraham, E.P., and Chain, E. (1940) An enzyme from bacteria able to destroy penicillin. Nature **146**: 837–837.

Abramson, J., Riistama, S., Larsson, G., Jasaitis, A., Svensson-Ek, M., Laakkonen, L., et al. (2000) The structure of the ubiquinol oxidase from Escherichia coli and its ubiquinone binding site. Nat Struct Mol Biol **7**: 910.

Acker, H. Van, and Coenye, T. (2017) The role of reactive oxygen species in antibiotic-mediated killing of bacteria. Trends Microbiol **25**: 456–466.

Adam, M., Murali, B., Glenn, N.O., and Potter, S.S. (2008) Epigenetic inheritance based evolution of antibiotic resistance in bacteria. BMC Evol Biol **8**: 52.

Adeyi, O.O.B., Baris, E., Jonas, O.B., Irwin, A., Berthe, F.C.J., Gall, F.G. Le, et al. (2017) Drug-resistant infections: A Threat to Our Economic Future. World Bank Doc Reports **3**.

Alanis, A.J. (2005) Resistance to antibiotics: are we in the post-antibiotic era? Arch Med Res **36**: 697–705.

Alekshun, M.N., and Levy, S.B. (2007) Molecular mechanisms of antibacterial multidrug resistance. Cell **128**: 1037–1050.

Allison, K.R., Brynildsen, M.P., and Collins, J.J. (2011) Metabolite-enabled eradication of bacterial persisters by aminoglycosides. Nature **473**: 216–220.

Aminov, R.I. (2010) A brief history of the antibiotic era: lessons learned and challenges for the future. Front Microbiol **1**: 134.

Andrews, J.M. (2001a) Determination of minimum inhibitory concentrations. J Antimicrob Chemother **48**: 5–16.

Andrews, J.M. (2001b) BSAC standardized disc susceptibility testing method. J Antimicrob Chemother **60**: 20–41.

Andrews, S.C., Robinson, A.K., and Rodríguez-Quiñones, F. (2003) Bacterial iron homeostasis. FEMS Microbiol Rev **27**: 215–237.

Anjum, M.F., Ioannidis, N., and Poole, R.K. (1998) Response of the NAD(P)H-oxidising flavohaemoglobin (Hmp) to prolonged oxidative stress and implications for its physiological role in Escherichia coli. FEMS Microbiol Lett **166**: 219–223.

Aragão, D., Mitchell, E.P., Frazão, C.F., Carrondo, M.A., and Lindley, P.F. (2008) Structural and functional relationships in the hybrid cluster protein family: structure of the anaerobically purified hybrid cluster protein from Desulfovibrio vulgaris at 1.35 Å resolution. Acta Crystallogr Sect D Biol Crystallogr **64**: 665–674.

Atlung, T., and Brondsted, L. (1994) Role of the transcriptional activator AppY in regulation of the cyx appA operon of Escherichia coli by anaerobiosis, phosphate

starvation, and growth phase. J Bacteriol **176**: 5414–5422.

Baba, T., Ara, T., Hasegawa, M., Takai, Y., Okumura, Y., Baba, M., et al. (2006) Construction of Escherichia coli K-12 in-frame, single-gene knockout mutants: the Keio collection. Mol Syst Biol **2**: 1–11.

Bachmann, B.J. (1996) Derivations and genotypes of some mutant derivatives of Escherichia coli K-12. In Escherichia coli and Salmonella: cellular and molecular biology. ASM Press, Washington, DC, pp. 2460–2488.

Bang, C.S., Kinnunen, A., Karlsson, M., Önnberg, A., Söderquist, B., and Persson, K. (2014) The antibacterial effect of nitric oxide against ESBL-producing uropathogenic E. coli is improved by combination with miconazole and polymyxin B nonapeptide. BMC Microbiol **14**: 65.

Bang, I.S., Liu, L., Vazquez-Torres, A., Crouch, M.L., Stamler, J.S., and Fang, F.C. (2006) Maintenance of nitric oxide and redox homeostasis by the Salmonella flavohemoglobin Hmp. J Biol Chem **281**: 28039–28047.

Bankevich, A., Nurk, S., Antipov, D., Gurevich, A.A., Dvorkin, M., Kulikov, A.S., et al. (2012) SPAdes: a new genome assembly algorithm and its applications to single-cell sequencing. J Comput Biol **19**: 455–477.

Barber, M. (1947) Staphylococcal infection due to penicillin-resistant strains. Br Med J **2**: 863.

Barcia-Macay, M., Seral, C., Mingeot-Leclercq, M.-P., Tulkens, P.M., and Bambeke, F. Van (2006) Pharmacodynamic evaluation of the intracellular activities of antibiotics against Staphylococcus aureus in a model of THP-1 macrophages. Antimicrob Agents Chemother **50**: 841–851.

Barraud, N., Hassett, D.J., Hwang, S.H., Rice, S. a., Kjelleberg, S., and Webb, J.S. (2006) Involvement of nitric oxide in biofilm dispersal of Pseudomonas aeruginosa. J Bacteriol **188**: 7344–7353.

Barraud, N., Kelso, M.J., and Rice, S.A. (2015) Nitric oxide: a key mediator of biofilm dispersal with applications in infectious diseases. Curr Pharm Des **21**: 31–42.

Bassett, E.J., Keith, M.S., Armelagos, G.J., Martin, D.L., and Villanueva, A.R. (1980) Tetracycline-labeled human bone from ancient Sudanese Nubia (AD 350). Science (80-) **209**: 1532–1534.

Bekker, M., Vries, S. de, Beek, A. Ter, Hellingwerf, K.J., and Teixeira De Mattos, M.J. (2009) Respiration of Escherichia coli can be fully uncoupled via the nonelectrogenic terminal cytochrome bd-II oxidase. J Bacteriol **191**: 5510–5517.

Bender, M., and Conrad, R. (1994) Microbial oxidation of methane, ammonium and

carbon monoxide, and turnover of nitrous oxide and nitric oxide in soils. Biogeochemistry **27**: 97–112.

Berg, W.A.M. van den, Hagen, W.R., and Dongen, W.M.A.M. Van (2000) The hybrid-cluster protein ('prismane protein') from Escherichia coli. FEBS J **267**: 666–676.

Bien, J., Sokolova, O., and Bozko, P. (2012) Role of uropathogenic Escherichia coli virulence factors in development of urinary tract infection and kidney damage. Int J Nephrol **2012**.

Boeckel, T.P. Van, Brower, C., Gilbert, M., Grenfell, B.T., Levin, S.A., Robinson, T.P., et al. (2015) Global trends in antimicrobial use in food animals. Proc Natl Acad Sci **112**: 5649–5654.

Bogdan, C. (2001) Nitric oxide and the immune response. Nat Immunol **2**: 907.

Bolger, A.M., Lohse, M., and Usadel, B. (2014) Trimmomatic: a flexible trimmer for Illumina sequence data. Bioinformatics **30**: 2114–2120.

Borisov, V.B., Gennis, R.B., Hemp, J., and Verkhovsky, M.I. (2011) The cytochrome bd respiratory oxygen reductases. Biochim Biophys Acta (BBA)- Bioenerg **1807**: 1398–1413.

Borisov, V.B., Murali, R., Verkhovskaya, M.L., Bloch, D.A., Han, H., Gennis, R.B., and Verkhovsky, M.I. (2011) Aerobic respiratory chain of Escherichia coli is not allowed to work in fully uncoupled mode. Proc Natl Acad Sci **108**: 17320–17324.

Bradford, P. (2001) Extended-spectrum β-lactamases in the 21st century: characterization, epidemiology, and detection of this important resistance threat. Clin Microbiol Rev **14**: 933–951.

Brown, E.D., and Wright, G.D. (2016) Antibacterial drug discovery in the resistance era. Nature **529**: 336.

Brubaker, L., and Wolfe, A. (2016) The urinary microbiota: A paradigm shift for bladder disorders? Curr Opin Obstet Gynecol **28**: 407–412.

Bush, K., Jacoby, G.A., and Medeiros, A.A. (1995) A functional classification scheme for beta-lactamases and its correlation with molecular structure. Antimicrob Agents Chemother **39**: 1211.

Cannatelli, A., D'Andrea, M.M., Giani, T., Pilato, V. Di, Arena, F., Ambretti, S., et al. (2013) In vivo emergence of colistin resistance in Klebsiella pneumoniae producing KPC-type carbapenemases mediated by insertional inactivation of the PhoQ/PhoP mgrB regulator. Antimicrob Agents Chemother **57**: 5521–5526.

Cannatelli, A., Giani, T., D'Andrea, M.M., Pilato, V. Di, Arena, F., Conte, V., et al. (2014) MgrB inactivation is a common mechanism of colistin resistance in KPC

carbapenemase-producing Klebsiella pneumoniae of clinical origin. Antimicrob Agents Chemother **58**: 5696.

Carattoli, A. (2009) Resistance plasmid families in Enterobacteriaceae. Antimicrob Agents Chemother **53**: 2227–2238.

Carattoli, A., Zankari, E., García-Fernández, A., Voldby Larsen, M., Lund, O., Villa, L., et al. (2014) In silico detection and typing of plasmids using PlasmidFinder and plasmid multilocus sequence typing. Antimicrob Agents Chemother **58**: 3895–3903.

CDC (2013) Antibiotic resistance threats in the United States, 2013. Centres Dis Control Prev US Dep Heal Hum Serv .

Chaveroche, M.-K., Ghigo, J.-M., and D'Enfert, C. (2000) A rapid method for efficient gene replacement in the filamentous fungus Aspergillus nidulans. Nucleic Acids Res **28**: e97–e97.

Chen, L., Yang, J., Yu, J., Yao, Z., Sun, L., Shen, Y., and Jin, Q. (2005) VFDB: a reference database for bacterial virulence factors. Nucleic Acids Res **33**: D325–D328.

Chepuri, V., Lemieux, L., Au, D.C.-T., and Gennis, R.B. (1990) The sequence of the cyo operon indicates substantial structural similarities between the cytochrome o ubiquinol oxidase of Escherichia coli and the aa3-type family of cytochrome c oxidases. J Biol Chem **265**: 11185–11192.

Clermont, O., Christenson, J.K., Denamur, E., and Gordon, D.M. (2013) The Clermont Escherichia coli phylo-typing method revisited: improvement of specificity and detection of new phylo-groups. Environ Microbiol Rep **5**: 58–65.

Clermont, O., Gordon, D.M., Brisse, S., Walk, S.T., and Denamur, E. (2011) Characterization of the cryptic Escherichia lineages: rapid identification and prevalence. Environ Microbiol **13**: 2468–2477.

Coleman, J.W. (2001) Nitric oxide in immunity and inflammation. Int Immunopharmacol **1**: 1397–1406.

Cook, G.M., Cruz-Ramos, H., Moir, A.J.G., and Poole, R.K. (2002) A novel haem compound accumulated in Escherichia coli overexpressing the cydDC operon, encoding an ABC-type transporter required for cytochrome assembly. Arch Microbiol **178**: 358–369.

Corker, H., and Poole, R.K. (2003) Nitric oxide formation by Escherichia coli dependence on nitrite reductase, the NO-sensing regulator Fnr, and flavohemoglobin Hmp. J Biol Chem **278**: 31584–31592.

Cotter, P.A., Chepuri, V., Gennis, R.B., and Gunsalus, R.P. (1990) Cytochrome o (cyoABCDE) and d (cydAB) oxidase gene expression in Escherichia coli is regulated

by oxygen, pH, and the fnr gene product. J Bacteriol **172**: 6333–6338.

Cotter, P.A., Melville, S.B., Albrecht, J.A., and Gunsalus, R.P. (1997) Aerobic regulation of cytochrome d oxidase (cydAB) operon expression in Escherichia coli: roles of Fnr and ArcA in repression and activation. Mol Microbiol **25**: 605–615.

Crane, B.R. (2008) The enzymology of nitric oxide in bacterial pathogenesis and resistance. Biochem Soc Trans **36**: 1149–1154.

Crane, B.R., Sudhamsu, J., and Patel, B.A. (2010) Bacterial nitric oxide synthases. Annu Rev Biochem **79**: 445–470.

Croxall, G., Hale, J., Weston, V., Manning, G., Cheetham, P., Achtman, M., and McNally, A. (2011) Molecular epidemiology of extraintestinal pathogenic Escherichia coli isolates from a regional cohort of elderly patients highlights the prevalence of ST131 strains with increased antimicrobial resistance in both community and hospital care setting. J Antimicrob Chemother **66**: 2501–2508.

Cruz-Ramos, H., Crack, J., Wu, G., Hughes, M.N., Scott, C., Thomson, A.J., et al. (2002) NO sensing by FNR: regulation of the Escherichia coli NO-detoxifying flavohaemoglobin, Hmp. EMBO J **21**: 3235–3244.

D'Autréaux, B., Horner, O., Oddou, J.-L., Jeandey, C., Gambarelli, S., Berthomieu, C., et al. (2004) Spectroscopic description of the two nitrosyl-iron complexes responsible for Fur inhibition by nitric oxide. J Am Chem Soc **126**: 6005–6016.

D'Autreaux, B., Touati, D., Bersch, B., Latour, J.-M., and Michaud-Soret, I. (2002) Direct inhibition by nitric oxide of the transcriptional ferric uptake regulation protein via nitrosylation of the iron. Proc Natl Acad Sci **99**: 16619–16624.

D'Autréaux, B., Tucker, N.P., Dixon, R., and Spiro, S. (2005) A non-haem iron centre in the transcription factor NorR senses nitric oxide. Nature **437**: 769.

D'mello, R., Hill, S., and Poole, R.K. (1996) The cytochrome bd quinol oxidase in Escherichia coli has an extremely high oxygen affinity and two oxygen-binding haems: implications for regulation of activity in vivo by oxygen inhibition. Microbiology **142**: 755–763.

D'Mello, R., Hill, S., and Poole, R.K. (1995) The oxygen affinity of cytochrome bo' in Escherichia coli determined by the deoxygenation of oxyleghemoglobin and oxymyoglobin: Km values for oxygen are in the submicromolar range. J Bacteriol **177**: 867–870.

Darling, A.C.E., Mau, B., Blattner, F.R., and Perna, N.T. (2004) Mauve: multiple alignment of conserved genomic sequence with rearrangements. Genome reasech **14**: 1394–1403.

Darwin, A., Hussain, H., Griffiths, L., Grove, J., Sambongi, Y., Busby, S., and Cole, J. (1993) Regulation and sequence of the structural gene for cytochrome c_{552} from Escherichia coli: not a hexahaem but a 50kDa tetrahaem nitrite reductase. Mol Microbiol **9**: 1255–1265.

Dassa, J., Fsihi, H., Marck, C., Dion, M., Kieffer-Bontemps, M., and Boquet, P.L. (1991) A new oxygen-regulated operon in Escherichia coli comprises the genes for a putative third cytochrome oxidase and for pH 2.5 acid phosphatase (appA). Mol Gen Genet **229**: 341–352.

Datsenko, K.A., and Wanner, B.L. (2000) One-step inactivation of chromosomal genes in Escherichia coli K-12 using PCR products. Proc Natl Acad Sci **97**: 6640–6645.

Davies, J., and Davies, D. (2010) Origins and evolution of antibiotic resistance. Microbiol Mol Biol Rev **74**: 417–433.

Dhakal, B.K., Kulesus, R.R., and Mulvey, M.A. (2008) Mechanisms and consequences of bladder cell invasion by uropathogenic Escherichia coli. Eur J Clin Invest **38**: 2–11.

Ding, H., and Demple, B. (2000) Direct nitric oxide signal transduction via nitrosylation of iron-sulfur centers in the SoxR transcription activator. Proc Natl Acad Sci **97**: 5146–5150.

Dwyer, D.J., Belenky, P.A., Yang, J.H., MacDonald, I.C., Martell, J.D., Takahashi, N., et al. (2014) Antibiotics induce redox-related physiological alterations as part of their lethality. Proc Natl Acad Sci **111**: E2100–E2109.

Džidić, S., Šušković, J., and Kos, B. (2008) Antibiotic resistance mechanisms in bacteria: biochemical and genetic aspects. Food Technol Biotechnol **46**: 11–21.

ECDC/EMEA Joint Working Group (2009) The bacterial challenge: time to react. .

ECDC (2017) Antimicrobial resistance surveillance in Europe 2015. .

Ellington, M.J., Cartwright, E.J.P., Gillespie, S.H., Ko, C.U., Brown, N.M., Farrington, M., et al. (2012) Routine use of microbial whole genome sequencing in diagnostic and public health microbiology. PLoS Pathog **8**: e1002824.

Fang, F.C. (1997) Perspectives series: host/pathogen interactions. Mechanisms of nitric oxide-related antimicrobial activity. J Clin Invest **99**: 2818–2825.

Fange, D., Nilsson, K., Tenson, T., and Ehrenberg, M. (2009) Drug efflux pump deficiency and drug target resistance masking in growing bacteria. Proc Natl Acad Sci **106**: 8215–8220.

Filenko, N., Spiro, S., Browning, D.F., Squire, D., Overton, T.W., Cole, J., and Constantinidou, C. (2007) The NsrR regulon of Escherichia coli K-12 includes genes

encoding the hybrid cluster protein and the periplasmic, respiratory nitrite reductase. J Bacteriol **189**: 4410–4417.

Flatley, J., Barrett, J., Pullan, S.T., Hughes, M.N., Green, J., and Poolet, R.K. (2005) Transcriptional responses of Escherichia coli to S-nitrosoglutathione under defined chemostat conditions reveal major changes in methionine biosynthesis. J Biol Chem **280**: 10065–10072.

Fleming, A. (1929) On the antibacterial action of cultures of a penicillium, with special reference to their use in the isolation of B. influenzae. Br J Exp Pathol **10**: 226.

Forde, B.M., Zakour, N.L. Ben, Stanton-Cook, M., Phan, M.-D., Totsika, M., Peters, K.M., et al. (2014) The complete genome sequence of Escherichia coli EC958: a high quality reference sequence for the globally disseminated multidrug resistant E. coli O25b: H4-ST131 clone O25b:H4-ST131 Clone. PLoS One **9**: e104400.

Fricke, W.F., and Rasko, D.A. (2014) Bacterial genome sequencing in the clinic: bioinformatic challenges and solutions. Nat Rev Genet **15**: 49.

Fu, H.-A., Iuchi, S., and Lin, E.C.C. (1991) The requirement of ArcA and Fnr for peak expression of the cyd operon in Escherichia coli under microaerobic conditions. Mol Gen Genet MGG **226**: 209–213.

Gall, T. Le, Clermont, O., Gouriou, S., Picard, B., Nassif, X., Denamur, E., and Tenaillon, O. (2007) Extraintestinal virulence is a coincidental by-product of commensalism in B2 phylogenetic group Escherichia coli strains. Mol Biol Evol **24**: 2373–2384.

Gardner, A.M., and Gardner, P.R. (2002) Flavohemoglobin detoxifies nitric oxide in aerobic, but not anaerobic, Escherichia coli: Evidence for a novel inducible anaerobic nitric oxide-scavenging activity. J Biol Chem **277**: 8166–8171.

Gardner, A.M., Gessner, C.R., and Gardner, P.R. (2003) Regulation of the nitric oxide reduction operon (norRVW) in Escherichia coli: role of NorR and σ^{54} in the nitric oxide stress response. J Biol Chem **278**: 10081–10086.

Gardner, A.M., Helmick, R.A., and Gardner, P.R. (2002) Flavorubredoxin, an inducible catalyst for nitric oxide reduction and detoxification in Escherichia coli. J Biol Chem **277**: 8172–8177.

Gardner, P.R., Gardner, A.M., Martin, L.A., and Salzman, A.L. (1998) Nitric oxide dioxygenase: An enzymic function for flavohemoglobin. Proc Natl Acad Sci **95**: 10378–10383.

Georgiou, C.D., Fang, H., and Gennis, R.B. (1987) Identification of the cydC locus required for expression of the functional form of the cytochrome d terminal oxidase complex in Escherichia coli. J Bacteriol **169**: 2107–2112.

Goldman, B.S., Gabbert, K.K., and Kranz, R.G. (1996) The temperature-sensitive growth and survival phenotypes of Escherichia coli cydDC and cydAB strains are due to deficiencies in cytochrome bd and are corrected by exogenous catalase and reducing agents. J Bacteriol **178**: 6348–6351.

Gomes, C.M., Giuffré, A., Forte, E., Vicente, J.B., Saraiva, L.M., Brunori, M., and Teixeira, M. (2002) A novel type of nitric-oxide reductase Escherichia coli flavorubredoxin. J Biol Chem **277**: 25273–25276.

Gomes, C.M., Vicente, J.B., Wasserfallen, A., and Teixeira, M. (2000) Spectroscopic studies and characterization of a novel electron-transfer chain from Escherichia coli involving a flavorubredoxin and its flavoprotein reductase partner. Biochemistry **39**: 16230–16237.

Gordon, D.M., Clermont, O., Tolley, H., and Denamur, E. (2008) Assigning Escherichia coli strains to phylogenetic groups: multi-locus sequence typing versus the PCR triplex method. Environ Microbiol **10**: 2484–2496.

Green, J., Rolfe, M.D., and Smith, L.J. (2014) Transcriptional regulation of bacterial virulence gene expression by molecular oxygen and nitric oxide. Virulence **5**: 794–809.

Griess, P. (1879) Bemerkungen zu der Abhandlung der HH. Weselsky und Benedikt "Ueber einige Azoverbindungen." Berichte der Dtsch Chem Gesellschaft **12**: 426–428.

Gusarov, I., and Nudler, E. (2005) NO-mediated cytoprotection: instant adaptation to oxidative stress in bacteria. Proc Natl Acad Sci **102**: 13855–13860.

Gusarov, I., Shatalin, K., Starodubtseva, M., and Nudler, E. (2009) Endogenous nitric oxide protects bacteria against a wide spectrum of antibiotics. Science (80-) **325**: 1380–1384.

Gusarov, I., Starodubtseva, M., Wang, Z.Q., McQuade, L., Lippard, S.J., Stuehr, D.J., and Nudler, E. (2008) Bacterial nitric-oxide synthases operate without a dedicated redox partner. J Biol Chem **283**: 13140–13147.

Hagan, E.C., Lloyd, A.L., Rasko, D.A., Faerber, G.J., and Mobley, H.L.T. (2010) Escherichia coli global gene expression in urine from women with urinary tract infection. PLoS Pathog **6**: e1001187.

Hagan, E.C., and Mobley, H.L.T. (2007) Uropathogenic Escherichia coli outer membrane antigens expressed during urinary tract infection. Infect Immun **75**: 3941–3949.

Hall, T.A. (1999) BioEdit: a user-friendly biological sequence alignment editor and analysis program for Windows 95/98/NT. Nucleic Acids Symp Ser **41**: 95–98.

Hancock, R.E.W. (1981) Aminoglycoside uptake and mode of action-with special reference to streptomycin and gentamicin: I. Antagonists and mutants. J Antimicrob Chemother **8**: 249–276.

Hancock, V., Ferrières, L., and Klemm, P. (2007) Biofilm formation by asymptomatic and virulent urinary tract infectious Escherichia coli strains. FEMS Microbiol Lett **267**: 30–37.

Hancock, V., and Klemm, P. (2007) Global gene expression profiling of asymptomatic bacteriuria Escherichia coli during biofilm growth in human urine. Infect Immun **75**: 966–976.

Hart, T.W. (1985) Some observations concerning the S-nitroso and S-phenylsulphonyl derivatives of L-cysteine and glutathione. Tetrahedron Lett **26**: 2013–2016.

Harvey, A. (2000) Strategies for discovering drugs from previously unexplored natural products. Drug Discov Today **5**: 294–300.

Hausladen, A., Gow, A.J., and Stamler, J.S. (1998) Nitrosative stress: metabolic pathway involving the flavohemoglobin. Proc Natl Acad Sci **95**: 14100–14105.

Hausladen, A., Privalle, C.T., Keng, T., DeAngelo, J., and Stamler, J.S. (1996) Nitrosative stress: activation of the transcription factor OxyR. Cell **86**: 719–729.

Henriques Normark, B., and Normark, S. (2002) Evolution and spread of antibiotic resistance. J Intern Med **252**: 91–106.

Hoban, D.J., Bouchillon, S.K., Hawser, S.P., and Badal, R.E. (2010) Trends in the frequency of multiple drug-resistant Enterobacteriaceae and their susceptibility to ertapenem, imipenem, and other antimicrobial agents: data from the Study for Monitoring Antimicrobial Resistance Trends 2002 to 2007. Diagn Microbiol Infect Dis **66**: 78–86.

Holyoake, L. V., Hunt, S., Sanguinetti, G., Cook, G.M., Howard, M.J., Rowe, M.L., et al. (2016) CydDC-mediated reductant export in Escherichia coli controls the transcriptional wiring of energy metabolism and combats nitrosative stress. Biochem J **473**: 693–701.

Houdouin, V., Bonacorsi, S., Bidet, P., Bingen-Bidois, M., Barraud, D., and Bingen, E. (2006) Phylogenetic background and carriage of pathogenicity island-like domains in relation to antibiotic resistance profiles among Escherichia coli urosepsis isolates. J Antimicrob Chemother **58**: 748–751.

Howe, R.A., and Andrews, J.M. (2012) BSAC standardized disc susceptibility testing method (version 11). J Antimicrob Chemother **67**: 2783–2784.

Hughes, M.N. (2008) Chemistry of nitric oxide and related species. In Methods in

enzymology. pp. 3–19.

Hull, R., Rudy, D., Donovan, W., Svanborg, C., Wieser, I., Stewart, C., and Darouiche, R. (2000) Urinary tract infection prophylaxis using Escherichia coli 83972 in spinal cord injured patients. J Urol **163**: 872–877.

Humbert, R., and Altendorf, K. (1989) Defective gamma subunit of ATP synthase (F1F0) from Escherichia coli leads to resistance to aminoglycoside antibiotics. J Bacteriol **171**: 1435–1444.

Hunt, J.L., Bronicki, R.A., and Anas, N. (2016) Role of inhaled nitric oxide in the management of severe acute respiratory distress syndrome. Front Pediatr **4**.

Jackson, R.J., Elvers, K.T., Lee, L.J., Gidley, M.D., Wainwright, L.M., Lightfoot, J., et al. (2007) Oxygen reactivity of both respiratory oxidases in Campylobacter jejuni: the cydAB genes encode a cyanide-resistant, low-affinity oxidase that is not of the cytochrome bd type. J Bacteriol **189**: 1604–1615.

Jarboe, L.R., Hyduke, D.R., Tran, L.M., Chou, K.J.Y., and Liao, J.C. (2008) Determination of the Escherichia coli S-nitrosoglutathione response network using integrated biochemical and systems analysis. J Biol Chem **283**: 5148–5157.

Johnson, J.R., Gajewski, A., Lesse, A.J., and Russo, T.A. (2003) Extraintestinal pathogenic Escherichia coli as a cause of invasive nonurinary infections. J Clin Microbiol **41**: 5798–5802.

Johnson, J.R., Johnston, B., Clabots, C., Kuskowski, M.A., and Castanheira, M. (2010) Escherichia coli sequence type ST131 as the major cause of serious multidrug-resistant E. coli infections in the United States. Clin Infect Dis **51**: 286–294.

Johnson, J.R., Kuskowski, M.A., Owens, K., Gajewski, A., and Winokur, P.L. (2003) Phylogenetic origin and virulence genotype in relation to resistance to fluoroquinolones and/or extended-spectrum cephalosporins and cephamycins among Escherichia coli isolates from animals and humans. J Infect Dis **188**: 759–768 https://academic.oup.com/jid/article-lookup/doi/10.1086/377455.

Johnson, J.R., and Stell, A.L. (2000) Extended virulence genotypes of Escherichia coli strains from patients with urosepsis in relation to phylogeny and host compromise. J Infect Dis **181**: 261–272.

Jünemann, S. (1997) Cytochrome bd terminal oxidase. Biochim Biophys Acta (BBA)-Bioenergetics **1321**: 107–127.

Justino, M.C., Almeida, C.C., Gonçalves, V.L., Teixeira, M., and Saraiva, L.M. (2006) Escherichia coli YtfE is a di-iron protein with an important function in assembly of iron–sulphur clusters. FEMS Microbiol Lett **257**: 278–284.

Justino, M.C., Almeida, C.C., Teixeira, M., and Saraiva, L.M. (2007) Escherichia coli di-iron YtfE protein is necessary for the repair of stress-damaged iron-sulfur clusters. J Biol Chem **282**: 10352–10359.

Justino, M.C., Vicente, J.B., Teixeira, M., and Saraiva, L.M. (2005) New genes implicated in the protection of anaerobically grown Escherichia coli against nitric oxide. J Biol Chem **280**: 2636–2643.

Källberg, M., Wang, H., Wang, S., Peng, J., Wang, Z., Lu, H., and Xu, J. (2012) Template-based protein structure modeling using the RaptorX web server. Nat Protoc **7**: 1511.

Kao, J.S., Stucker, D.M., Warren, J.W., and Mobley, H.L.T. (1997) Pathogenicity island sequences of pyelonephritogenic Escherichia coli CFT073 are associated with virulent uropathogenic strains. Infect Immun **65**: 2812–2820.

Karami, N., Wold, A.E., and Adlerberth, I. (2016) Antibiotic resistance is linked to carriage of papC and iutA virulence genes and phylogenetic group D background in commensal and uropathogenic Escherichia coli from infants and young children. Eur J Clin Microbiol Infect Dis **36**: 721–729.

Karlinsey, J.E., Bang, I.-S., Becker, L.A., Frawley, E.R., Porwollik, S., Robbins, H.F., et al. (2012) The NsrR regulon in nitrosative stress resistance of Salmonella enterica serovar Typhimurium. Mol Microbiol **85**: 1179–1193.

Keszler, A., Zhang, Y., and Hogg, N. (2010) Reaction between nitric oxide, glutathione, and oxygen in the presence and absence of protein: How are S-nitrosothiols formed? Free Radic Biol Med **48**: 55–64.

Kim, S.O., Orii, Y., Lloyd, D., Hughes, M.N., and Poole, R.K. (1999) Anoxic function for the Escherichia coli flavohaemoglobin (Hmp): reversible binding of nitric oxide and reduction to nitrous oxide. FEBS Lett **445**: 389–394.

Klemm, P., Roos, V., Ulett, G.C., Schembri, M.A., and Svanborg, C. (2006) Molecular characterization of the Escherichia coli asymptomatic bacteriuria strain 83972: the taming of a pathogen. Infect Immun **74**: 781–785.

Kohanski, M.A., Dwyer, D.J., Hayete, B., Lawrence, C.A., and Collins, J.J. (2007) A common mechanism of cellular death induced by bactericidal antibiotics. Cell **130**: 797–810.

Köser, C.U., Holden, M.T.G., Ellington, M.J., Cartwright, E.J.P., Brown, N.M., Ogilvy-Stuart, A.L., et al. (2012) Rapid whole-genome sequencing for investigation of a neonatal MRSA outbreak. N Engl J Med **366**: 2267–2275.

Kostakioti, M., Hadjifrangiskou, M., and Hultgren, S.J. (2013) Bacterial biofilms:

development, dispersal, and therapeutic strategies in the dawn of the postantibiotic era. Cold Spring Harb Perspect Med **3**: a010306.

Kröncke, K.D., Fehsel, K., and Kolb-Bachofen, V. (1997) Nitric oxide: cytotoxicity versus cytoprotection - how, why, when, and where? Nitric oxide **1**: 107–120.

la Fuente-Núñez, C. de, Reffuveille, F., Fairfull-Smith, K.E., and Hancock, R.E.W. (2013) Effect of nitroxides on swarming motility and biofilm formation, multicellular behaviors in Pseudomonas aeruginosa. Antimicrob Agents Chemother **57**: 4877–4881.

la Fuente-Núñez, C. de, Reffuveille, F., Fernández, L., and Hancock, R.E. (2013) Bacterial biofilm development as a multicellular adaptation: antibiotic resistance and new therapeutic strategies. Curr Opin Microbiol **16**: 580–589.

Lancaster Jr, J.R. (1997) A Tutorial on the Diffusibility and Reactivity of Free Nitric Oxide. Nitric oxide **1**: 18–30.

Lancaster Jr, J.R. (2015) Nitric oxide: a brief overview of chemical and physical properties relevant to therapeutic applications. Futur Sci OA **1**: FSO59.

Lau, S.H., Kaufmann, M.E., Livermore, D.M., Woodford, N., Willshaw, G.A., Cheasty, T., et al. (2008) UK epidemic Escherichia coli strains A–E, with CTX-M-15 β-lactamase, all belong to the international O25: H4-ST131 clone. J Antimicrob Chemother **62**: 1241–1244.

Laverty, G., Gorman, S., and Gilmore, B. (2014) Biomolecular mechanisms of Pseudomonas aeruginosa and Escherichia coli biofilm formation. Pathogens **3**: 596–632.

Lechner, S., Lewis, K., and Bertram, R. (2012) Staphylococcus aureus persisters tolerant to bactericidal antibiotics. J Mol Microbiol Biotechnol **22**: 235–244.

Letunic, I., and Bork, P. (2016) Interactive tree of life (iTOL) v3: an online tool for the display and annotation of phylogenetic and other trees. Nucleic Acids Res **44**: W242–W245.

Lewis, K. (2013) Platforms for antibiotic discovery. Nat Rev Drug Discov **12**: 371.

Liu, Y., and Imlay, J.A. (2013) Cell death from antibiotics without the involvement of reactive oxygen species. Science (80-) **339**: 1210–1213.

Liu, Y.Y., Wang, Y., Walsh, T.R., Yi, L.-X., Zhang, R., Spencer, J., et al. (2016) Emergence of plasmid-mediated colistin resistance mechanism MCR-1 in animals and human beings in China: a microbiological and molecular biological study. Lancet Infect Dis **16**: 161–168.

Lobritz, M.A., Belenky, P., Porter, C.B.M., Gutierrez, A., Yang, J.H., Schwarz, E.G., et

al. (2015) Antibiotic efficacy is linked to bacterial cellular respiration. Proc Natl Acad Sci U S A **112**: 8173–8180.

Lovmar, M., Nilsson, K., Lukk, E., Vimberg, V., Tenson, T., and Ehrenberg, M. (2009) Erythromycin resistance by L4/L22 mutations and resistance masking by drug efflux pump deficiency. EMBO J **28**: 736–744.

MacMicking, J., Xie, Q., and Nathan, C. (1997) Nitric oxide and macrophage function. Annu Rev Immunol **15**: 323–350.

Magiorakos, A.-P., Srinivasan, A., Carey, R.B., Carmeli, Y., Falagas, M.E., Giske, C.G., et al. (2012) Multidrug-resistant, extensively drug-resistant and pandrug-resistant bacteria: an international expert proposal for interim standard definitions for acquired resistance. Clin Microbiol Infect **18**: 268–281.

Mah, T.F.C., and O'Toole, G.A. (2001) Mechanisms of biofilm resistance to antimicrobial agents. Trends Microbiol **9**: 34–39.

Manderwad, G.P. (2017) Epigenetic mode of bacterial drug resistance. Br Biomed Bull **5**.

Mason, M.G., Nicholls, P., Wilson, M.T., and Cooper, C.E. (2006) Nitric oxide inhibition of respiration involves both competitive (heme) and noncompetitive (copper) binding to cytochrome c oxidase. Proc Natl Acad Sci U S A **103**: 708–713.

Mason, M.G., Shepherd, M., Nicholls, P., Dobbin, P.S., Dodsworth, K.S., Poole, R.K., and Cooper, C.E. (2009) Cytochrome bd confers nitric oxide resistance to Escherichia coli. Nat Chem Biol **5**: 94.

Mateo, A.O., and Artiñano, M.A.A. de (2000) Nitric oxide reactivity and mechanisms involved in its biological effects. Pharmacol Res **42**: 421–427.

Matsushita, K., Ohnishi, T., and Kaback, H.R. (1987) NADH-ubiquinone oxidoreductases of the Escherichia coli aerobic respiratory chain. Biochemistry **26**: 7732–7737.

McDermott, P.F., Walker, R.D., and White, D.G. (2003) Antimicrobials: modes of action and mechanisms of resistance. Int J Toxicol **22**: 135–143.

McLean, S., Bowman, L.A.H., and Poole, R.K. (2010) Peroxynitrite stress is exacerbated by flavohaemoglobin-derived oxidative stress in Salmonella Typhimurium and is relieved by nitric oxide. Microbiology **156**: 3556–3565.

McNicholas, S., Potterton, E., Wilson, K.S., and Noble, M.E.M. (2011) Presenting your structures: the CCP4mg molecular-graphics software. Acta Crystallogr Sect D Biol Crystallogr **67**: 386–394.

Medini, D., Donati, C., Tettelin, H., Masignani, V., and Rappuoli, R. (2005) The microbial pan-genome. Curr Opin Genet Dev **15**: 589–594.

Membrillo-Hernandez, J., Coopamah, M.D., Anjum, M.F., Stevanin, T.M., Kelly, A., Hughes, M.N., and Poole, R.K. (1999) The flavohemoglobin of Escherichia coli confers resistance to a nitrosating agent, a "nitric oxide releaser", and paraquat and is essential for transcriptional responses to oxidative stress. J Biol Chem **274**: 748–754.

Membrillo-Hernández, J., Coopamah, M.D., Channa, A., Hughes, M.N., and Poole, R.K. (1998) A novel mechanism for upregulation of the Escherichia coli K-12 hmp (flavohaemoglobin) gene by the 'NO releaser', S-nitrosoglutathione: nitrosation of homocysteine and modulation of MetR binding to the *glyA-hmp* intergenic regio. Mol Microbiol **29**: 1101–1112.

Membrillo-Hernández, J., Ioannidis, N., and Poole, R.K. (1996) The flavohaemoglobin (HMP) of Escherichia coli generates superoxide in vitro and causes oxidative stress in vivo. FEBS Lett **382**: 141–144.

Michael, C.A., Dominey-Howes, D., and Labbate, M. (2014) The antimicrobial resistance crisis: causes, consequences, and management. Front Public Heal **2**: 145.

Miller, M.J., and Gennis, R.B. (1985) The cytochrome d complex is a coupling site in the aerobic respiratory chain of Escherichia coli. J Biol Chem **260**: 14003–14008.

Mills, C.E., Sedelnikova, S., Søballe, B., Hughes, M.N., and Poole, R.K. (2001) Escherichia coli flavohaemoglobin (Hmp) with equistoichiometric FAD and haem contents has a low affinity for dioxygen in the absence or presence of nitric oxide. Biochem J **353**: 207.

Mills, P.C., Rowley, G., Spiro, S., Hinton, J.C., and Richardson, D.J. (2008) A combination of cytochrome c nitrite reductase (NrfA) and flavorubredoxin (NorV) protects Salmonella enterica serovar Typhimurium against killing by NO in anoxic environments. Microbiology **154**: 1218–1228.

Miranda, J.E.A., Sotomayor, C.E., Albesa, I., and Paraje, M.G. (2011) Oxidative and nitrosative stress in Staphylococcus aureus biofilm. FEMS Microbiol Lett **315**: 23–29.

Mobley, H.L.T., Green, D.M., Trifillis, A.L., Johnson, D.E., Chippendale, G.R., Lockatell, C.V., et al. (1990) Pyelonephritogenic Escherichia coli and killing of cultured human renal proximal tubular epithelial cells: role of hemolysin in some strains. Infect Immun **58**: 1281–1289.

Moreno, E., Prats, G., Sabaté, M., Pérez, T., Johnson, J.R., and Andreu, A. (2006) Quinolone, fluoroquinolone and trimethoprim/sulfamethoxazole resistance in relation to virulence determinants and phylogenetic background among

uropathogenic Escherichia coli. J Antimicrob Chemother **57**: 204–211.

Motta, S.S., Cluzel, P., and Aldana, M. (2015) Adaptive resistance in bacteria requires epigenetic inheritance, genetic noise, and cost of efflux pumps. PLoS One **10**.

Mukhopadhyay, P., Zheng, M., Bedzyk, L.A., LaRossa, R.A., and Storz, G. (2004) Prominent roles of the NorR and Fur regulators in the Escherichia coli transcriptional response to reactive nitrogen species. Proc Natl Acad Sci U S A **101**: 745–750.

Nicolas-Chanoine, M.H., Bertrand, X., and Madec, J.-Y. (2014) Escherichia coli ST131, an intriguing clonal group. Clin Microbiol Rev **27**: 543–574.

Nicolas-Chanoine, M.H., Blanco, J., Leflon-Guibout, V., Demarty, R., Alonso, M.P., Caniça, M.M., et al. (2008) Intercontinental emergence of Escherichia coli clone O25: H4-ST131 producing CTX-M-15. J Antimicrob Chemother **61**: 273–281.

Nisbett, L.-M., and Boon, E.M. (2016) Nitric oxide regulation of H-NOX signaling pathways in bacteria. Biochemistry **55**: 4873–4884.

Notredame, C., Higgins, D.G., and Heringa, J. (2000) T-coffee: a novel method for fast and accurate multiple sequence alignment. J Mol Biol **302**: 205–217.

Nunoshiba, T., DeRojas-Walker, T., Wishnok, J.S., Tannenbaum, S.R., and Demple, B. (1993) Activation by nitric oxide of an oxidative-stress response that defends Escherichia coli against activated macrophages. Proc Natl Acad Sci **90**: 9993–9997.

Okonechnikov, K., Golosova, O., and Fursov, M. (2012) Unipro UGENE: a unified bioinformatics toolkit. Bioinformatics **28**: 1166–1167.

Ong, C.-L.Y., Beatson, S.A., McEwan, A.G., and Schembri, M.A. (2009) Conjugative plasmid transfer and adhesion dynamics in an Escherichia coli biofilm. Appl Environ Microbiol **75**: 6783–6791.

Pacher, P., Beckman, J.S., and Liaudet, L. (2007) Nitric oxide and peroxynitrite in health and disease. Physiol Rev **87**: 315–424.

Page, A.J., Cummins, C.A., Hunt, M., Wong, V.K., Reuter, S., Holden, M.T.G., et al. (2015) Roary: rapid large-scale prokaryote pan genome analysis. Bioinformatics **31**: 3691–3693.

Pamp, S.J., Gjermansen, M., Johansen, H.K., and Tolker-Nielsen, T. (2008) Tolerance to the antimicrobial peptide colistin in Pseudomonas aeruginosa biofilms is linked to metabolically active cells, and depends on the pmr and *mexAB-oprM* genes. Mol Microbiol **68**: 223–240.

Park, S., and Imlay, J.A. (2003) High levels of intracellular cysteine promote oxidative DNA damage by driving the fenton reaction. J Bacteriol **185**: 1942–1950.

Peerayeh, S.N., Rostami, E., Siadat, S.D., and Derakhshan, S. (2014) High rate of

aminoglycoside resistance in CTX-M-15 producing Klebsiella pneumoniae isolates in Tehran, Iran. Lab Med **45**: 231–237.

Peirano, G., Mulvey, G.L., Armstrong, G.D., and Pitout, J.D.D. (2013) Virulence potential and adherence properties of Escherichia coli that produce CTX-M and NDM β-lactamases. J Med Microbiol **62**: 525–530.

Pittman, M.S., Corker, H., Wu, G., Binet, M.B., Moir, A.J.G., and Poole, R.K. (2002) Cysteine Is Exported from the Escherichia coli Cytoplasm by CydDC, an ATP-binding Cassette-type Transporter Required for Cytochrome Assembly. J Biol Chem **277**: 49841–49849.

Pittman, M.S., Elvers, K.T., Lee, L., Jones, M.A., Poole, R.K., Park, S.F., and Kelly, D.J. (2007) Growth of Campylobacter jejuni on nitrate and nitrite: electron transport to NapA and NrfA via NrfH and distinct roles for NrfA and the globin Cgb in protection against nitrosative stress nitrosative stress. Mol Microbiol **63**: 575–590.

Pittman, M.S., Robinson, H.C., and Poole, R.K. (2005) A bacterial glutathione transporter (Escherichia coli CydDC) exports reductant to the periplasm. J Biol Chem **280**: 32254–32261.

Pizza, M., Scarlato, V., Masignani, V., Giuliani, M.M., Arico, B., Comanducci, M., et al. (2000) Identification of vaccine candidates against serogroup B meningococcus by whole-genome sequencing. Science (80-) **287**: 1816–1821.

Poirel, L., Jayol, A., Bontron, S., Villegas, M.-V., Ozdamar, M., Türkoglu, S., and Nordmann, P. (2015) The mgrB gene as a key target for acquired resistance to colistin in Klebsiella pneumoniae. J Antimicrob Chemother **70**: 75–80.

Poock, S.R., Leach, E.R., Moir, J.W.B., Cole, J.A., and Richardson, D.J. (2002) Respiratory detoxification of nitric oxide by the cytochrome c nitrite reductase of Escherichia coli. J Biol Chem **277**: 23664–23669.

Poole, K. (2004) Resistance to β-lactam antibiotics. Cell Mol Life Sci C **61**: 2200–2223.

Poole, R.K., Anjum, M.F., Membrillo-Hernandez, J., Kim, S.O., Hughes, M.N., and Stewart, V. (1996) Nitric oxide, nitrite, and Fnr regulation of hmp (flavohemoglobin) gene expression in Escherichia coli K-12. J Bacteriol **178**: 5487–5492.

Poole, R.K., Gibson, F., and Wu, G. (1994) The cydD gene product, component of a heterodimeric ABC transporter, is required for assembly of periplasmic cytochrome c and of cytochrome bd in Escherichia coli. FEMS Microbiol Lett **117**: 217–223.

Price, M.N., Dehal, P.S., and Arkin, A.P. (2009) FastTree: computing large minimum evolution trees with profiles instead of a distance matrix. Mol Biol Evol **26**: 1641–1650.

Price, M.N., Dehal, P.S., and Arkin, A.P. (2010) FastTree 2–approximately maximum-likelihood trees for large alignments. PLoS One **5**: e9490.

Pullan, S.T., Gidley, M.D., Jones, R.A., Barrett, J., Stevanin, T.M., Read, R.C., et al. (2007) Nitric oxide in chemostat-cultured Escherichia coli is sensed by Fnr and other global regulators: unaltered methionine biosynthesis indicates lack of S nitrosation. J Bacteriol **189**: 1845–1855.

Puustinen, A., Finel, M., Virkki, M., and Wikstrom, M. (1989) Cytochrome o (bo) is a proton pump in Paracoccus denitrificans and Escherichia coli. FEBS Lett **249**: 163–167.

Reffuveille, F., Fairfull-Smith, K.E., Robert, E., and Hancock, W. (2015) Potentiation of ciprofloxacin action against Gram-negative bacterial biofilms by a nitroxide. Pathog Dis **73**.

Ren, H., Wu, J., Colletta, A., Meyerhoff, M.E., and Xi, C. (2016) Efficient eradication of mature Pseudomonas aeruginosa biofilm via controlled delivery of nitric oxide combined with antimicrobial peptide and antibiotics. Front Microbiol **7**: 1260.

Review on Antimicrobial Resistance (2016) Tackling drug-resistant infections globally: final report and recommendations. .

Roos, V., and Klemm, P. (2006) Global gene expression profiling of the asymptomatic bacteriuria Escherichia coli strain 83972 in the human urinary tract. Infect Immun **74**: 3565–3575.

Roos, V., Ulett, G.C., Schembri, M.A., and Klemm, P. (2006) The asymptomatic bacteriuria Escherichia coli strain 83972 outcompetes uropathogenic E. coli strains in human urine. Infect Immun **74**: 615–624.

Rowan, A.D., Cabral, D.J., and Belenky, P. (2016) Bactericidal antibiotics induce programmed metabolic toxicity. Microb Cell **3**: 178.

Safarian, S., Rajendran, C., Müller, H., Preu, J., Langer, J.D., Ovchinnikov, S., et al. (2016) Structure of a bd oxidase indicates similar mechanisms for membrane-integrated oxygen reductases. Science (80-) **352**: 583–586.

Saiki, K., Mogi, T., Ogura, K., and Anraku, Y. (1993) In vitro heme O synthesis by the cyoE gene product from Escherichia coli. J Biol Chem **268**: 26041–26045.

Salmon, K., Hung, S., Mekjian, K., Baldi, P., Hatfield, G.W., and Gunsalus, R.P. (2003) Global gene expression profiling in Escherichia coli K12 the effects of oxygen availability and FNR. J Biol Chem **278**: 29837–29855.

Savino, S., Santini, L., Giuliani, M.M., Adu-bobie, J., Comanducci, M., Arico, B., et al. (2006) A universal vaccine for serogroup B meningococcus. Proc Natl Acad Sci **103**:

10834–10839.

Schairer, D.O., Chouake, J.S., Nosanchuk, J.D., and Friedman, A.J. (2012) The potential of nitric oxide releasing therapies as antimicrobial agents. Virulence **3**: 271–279.

Schindler, H., and Bogdan, C. (2001) NO as a signaling molecule: effects on kinases. Int Immunopharmacol **1**: 1443–1455.

Seemann, T. (2014) Prokka: rapid prokaryotic genome annotation. Bioinformatics **30**: 2068–2069.

Seth, D., Hausladen, A., Wang, Y.-J., and Stamler, J.S. (2012) Endogenous protein S-Nitrosylation in E. coli: regulation by OxyR. Science (80-) **336**: 470–473.

Shatalin, K., Gusarov, I., Avetissova, E., Shatalina, Y., Mcquade, L.E., Lippard, S.J., and Nudler, E. (2008) Bacillus anthracis-derived nitric oxide is essential for pathogen virulence and survival in macrophages. Proc Natl Acad Sci **105**: 1009–1013.

Shepherd, M., Achard, M.E.S., Idris, A., Totsika, M., Phan, M.-D., Peters, K.M., et al. (2016) The cytochrome bd-I respiratory oxidase augments survival of multidrug-resistant Escherichia coli during infection. Sci Rep **6**: 35285.

Siegele, D.A., Imlay, K.R.C., and Imlay, J.A. (1996) The stationary-phase-exit defect of cydC (surB) mutants is due to the lack of a functional terminal cytochrome oxidase. J Bacteriol **178**: 6091–6096.

Snyder, S.H., and Bredt, D.S. (1992) Biological roles of nitric oxide. Sci Am **266**: 68–77.

Sorge, N.M. Van, Beasley, F.C., Gusarov, I., Gonzalez, D.J., Köckritz-Blickwede, M. Von, Anik, S., et al. (2013) Methicillin-resistant Staphylococcus aureus bacterial nitric-oxide synthase affects antibiotic sensitivity and skin abscess development. J Biol Chem **288**: 6417–6426.

Spiro, S. (2006) Nitric oxide-sensing mechanisms in Escherichia coli. Biochem Soc Trans **34**: 200–202.

Spiro, S. (2007) Regulators of bacterial responses to nitric oxide. FEMS Microbiol Rev **31**: 193–211.

Stenberg, F., Heijne, G. von, and Daley, D.O. (2007) Assembly of the cytochrome bo_3 complex. J Mol Biol **371**: 765–773.

Stevanin, T.M., Ioannidis, N., Mills, C.E., Kim, S.O., Hughes, M.N., and Poole, R.K. (2000) Flavohemoglobin Hmp Affords Inducible Protection for Escherichia coli Respiration, Catalyzed by Cytochromes *bo′* or bd, from Nitric Oxide. J Biol Chem **275**: 35868–35875.

Stewart, P.S., and William Costerton, J. (2001) Antibiotic resistance of bacteria in biofilms. Lancet **358**: 135–138.

Sudhamsu, J., and Crane, B.R. (2009) Bacterial nitric oxide synthases: what are they good for? Trends Microbiol **17**: 212–218.

Thomas-White, K., Brady, M., Wolfe, A.J., and Mueller, E.R. (2016) The bladder is not sterile: History and current discoveries on the urinary microbiome. Curr Bl Dysfunct Rep **11**: 18–24 https://www.ncbi.nlm.nih.gov/pmc/articles/PMC4864995/pdf/nihms756605.pdf.

Tommaso, P. Di, Moretti, S., Xenarios, I., Orobitg, M., Montanyola, A., Chang, J.M., et al. (2011) T-Coffee: a web server for the multiple sequence alignment of protein and RNA sequences using structural information and homology extension. Nucleic Acids Res **39**: W13–W17.

Totsika, M., Beatson, S.A., Sarkar, S., Phan, M.D., Petty, N.K., Bachmann, N., et al. (2011) Insights into a multidrug resistant Escherichia coli pathogen of the globally disseminated ST131 lineage: genome analysis and virulence mechanisms. PLoS One **6**: e26578.

Totsika, M., Moriel, D.G., Idris, A., Rogers, B.A., Wurpel, D.J., Phan, M.D., et al. (2012) Uropathogenic Escherichia coli mediated urinary tract infection. Curr Drug Targets **13**: 1386–1399.

Tseng, C.P., Albrecht, J., and Gunsalus, R.P. (1996) Effect of microaerophilic cell growth conditions on expression of the aerobic (cyoABCDE and cydAB) and anaerobic (narGHJI, frdABCD, and dmsABC) respiratory pathway genes in Escherichia coli. J Bacteriol **178**: 1094–1098.

Tucker, N.P., Hicks, M.G., Clarke, T.A., Crack, J.C., Chandra, G., Brun, N.E. Le, et al. (2008) The transcriptional repressor protein NsrR senses nitric oxide directly via a [2Fe-2S] cluster. PLoS **3**: e3623.

Vallance, P. (2003) Nitric oxide: therapeutic opportunities. Fundam Clin Pharmacol **17**: 1–10.

Vasil'eva, S. V., Stupakova, M. V., Lobysheva, I.I., Mikoyan, V.D., and Vanin, A.F. (2001) Activation of the Escherichia coli SoxRS-regulon by nitric oxide and its physiological donors. Biochem **66**: 984–988.

Vicente, J.B., Scandurra, F.M., Rodrigues, J. V., Brunori, M., Sarti, P., Teixeira, M., and Giuffrè, A. (2007) Kinetics of electron transfer from NADH to the Escherichia coli nitric oxide reductase flavorubredoxin. FEBS J **274**: 677–686.

Villanueva, C., and Giulivi, C. (2011) Subcellular and cellular locations of nitric oxide synthase isoforms as determinants of health and disease. Free Radic Biol Med **49**: 307–316.

Walsh, T.R., Weeks, J., Livermore, D.M., and Toleman, M.A. (2011) Dissemination of NDM-1 positive bacteria in the New Delhi environment and its implications for human health: an environmental point prevalence study. Lancet Infect Dis **11**: 355–362.

Wang, H., and Gunsalus, R.P. (2000) The nrfA and nirB nitrite reductase operons in Escherichia coli are expressed differently in response to nitrate than to nitrite. J Bacteriol **182**: 5813–5822.

Wang, J., Vine, C.E., Balasiny, B.K., Rizk, J., Bradley, C.L., Tinajero-Trejo, M., et al. (2016) The roles of the hybrid cluster protein, Hcp, and its reductase, Hcr, in high affinity nitric oxide reduction that protects anaerobic cultures of Escherichia coli against nitrosative stress. Mol Microbiol **100**: 877–892.

Wang, X., and Zhao, X. (2009) Contribution of oxidative damage to antimicrobial lethality. Antimicrob Agents Chemother **53**: 1395–1402.

Wang, Z.-Q., Lawson, R.J., Buddha, M.R., Wei, C.-C., Crane, B.R., Munro, A.W., and Stuehr, D.J. (2007) Bacterial flavodoxins support nitric oxide production by Bacillus subtilis nitric-oxide synthase. J Biol Chem **282**: 2196–2202.

Weigel, L.M., Steward, C.D., and Tenover, F.C. (1998) gyrA mutations associated with fluoroquinolone resistance in eight species of Enterobacteriaceae. Antimicrob Agents Chemother **42**: 2661–2667.

Welch, R.A., Burland, V., Plunkett, G., Redford, P., Roesch, P., Rasko, D., et al. (2002) Extensive mosaic structure revealed by the complete genome sequence of uropathogenic Escherichia coli. Proc Natl Acad Sci **99**: 17020–17024.

Wessel, D.L., Adatia, I., Marter, L.J. Van, Thompson, J.E., Kane, J.W., Stark, A.R., and Kourembanas, S. (1997) Improved oxygenation in a randomized trial of inhaled nitric oxide for persistent pulmonary hypertension of the newborn. Pediatrics **100**: 1–7.

Wiles, T.J., Kulesus, R.R., and Mulvey, M.A. (2008) Origins and virulence mechanisms of uropathogenic Escherichia coli. Exp Mol Pathol **85**: 11–19.

Wink, D.A., Hines, H.B., Cheng, R.Y.S., Switzer, C.H., Flores-Santana, W., Vitek, M.P., et al. (2011) Nitric oxide and redox mechanisms in the immune response. J Leukoc Biol **89**: 873–891.

Wirth, T., Falush, D., Lan, R., Colles, F., Mensa, P., Wieler, L.H., et al. (2006) Sex and virulence in Escherichia coli: an evolutionary perspective. Mol Microbiol **60**: 1136–1151.

Wonderen, J.H. van, Burlat, B., Richardson, D.J., Cheesman, M.R., and Butt, J.N. (2008) The nitric oxide reductase activity of cytochrome c nitrite reductase from Escherichia

coli. J Biol Chem **283**: 9587–9594.

World Health Organization (WHO) (2014) Antimicrobial resistance; global report on surveillance. Antimicrob Resist Glob Rep Surveill .

Wu, G., Corker, H., Orii, Y., and Poole, R.K. (2004) Escherichia coli Hmp, an "oxygen-binding flavohaemoprotein", produces superoxide anion and self-destructs. Arch Microbiol **182**: 193–203.

Wullt, B., Bergsten, G., Connell, H., Röllano, P., Gebretsadik, N., Hull, R., and Svanborg, C. (2000) P fimbriae enhance the early establishment of Escherichia coli in the human urinary tract. Mol Microbiol **38**: 456–464.

Yang, J.H., Bening, S.C., and Collins, J.J. (2017) Antibiotic efficacy — context matters. Curr Opin Microbiol **39**: 73–80.

Yang, J.H., Bhargava, P., McCloskey, D., Mao, N., Palsson, B.O., and Collins, J.J. (2017) Antibiotic-induced changes to the host metabolic environment inhibit drug efficacy and alter immune function. Cell Host Microbe **22**: 757–765.

Yong, D., Toleman, M.A., Giske, C.G., Cho, H.S., Sundman, K., Lee, K., and Walsh, T.R. (2009) Characterization of a new metallo-β-lactamase gene, bla_{NDM-1} , and a novel erythromycin esterase gene carried on a unique genetic structure in Klebsiella pneumoniae sequence type 14 from India. Antimicrob Agents Chemother **53**: 5046–5054.

Yu, H., Sato, E.F., Nagata, K., Nishikawa, M., Kashiba, M., Arakawa, T., et al. (1997) Oxygen-dependent regulation of the respiration and growth of Escherichia coli by nitric oxide. FEBS Lett **409**: 161–165.

Zankari, E., Hasman, H., Cosentino, S., Vestergaard, M., Rasmussen, S., Lund, O., et al. (2012) Identification of acquired antimicrobial resistance genes. J Antimicrob Chemother **67**: 2640–2644.

Appendix

Appendix A-1. MLST details of all isolates of the Kent collection.

Multilocus sequence typing (MLST) was performed in all isolates of the collection using the Achtman typing scheme (Maiden et al., 1998).

Strain Number	KC Number	ST	ST Complex	Adk	fumC	gyrB	icd	mdh	purA	recA
188	KC1	ST69	ST69cplx	21	35	27	6	5	5	4
189	KC2	ST404	ST14cplx	14	14	10	14	17	7	74
190	KC3	ST162	ST469	9	65	5	1	9	13	6
191	KC4	ST1406	None	46	156	2	25	5	16	19
192	KC5	ST69	ST69cplx	21	35	27	6	5	5	4
193	KC6	ST58	ST155cplx	6	4	4	16	24	8	14
194	KC7	ST131	None	53	40	47	13	36	28	29
195	KC8	ST73	ST73cplx	36	24	9	13	17	11	25
196	KC9	ST69	ST69cplx	21	35	27	6	5	5	4
197	KC10	ST131	None	53	40	47	13	36	28	29
198	KC11	ST59	ST59cplx	27	32	24	29	26	19	22
199	KC12	ST1148	None	6	95	3	18	11	7	14
200	KC13	ST95	ST95cplx	37	38	19	37	17	11	26
201	KC14	ST10	ST10cplx	10	11	4	8	8	8	2
202	KC15	ST73	ST73cplx	36	24	9	13	17	11	25
203	KC16	ST73	ST73cplx	36	24	9	13	17	11	25
204	KC17	unknown	None	9	260	15	26	11	26	6
205	KC18	ST131	None	53	40	47	13	36	28	29
206	KC19	ST131	None	53	40	47	13	36	28	29
207	KC20	ST685	None	8	11	4	8	8	8	2
208	KC21	ST95	ST95cplx	37	38	19	37	17	11	26
209	KC22	ST357	None	13	40	13	13	23	25	66

210	KC23	ST1618	None	36	24	9	13	17	11	159
211	KC24	ST73	ST73cplx	36	24	9	13	17	11	25
212	KC25	ST131	None	53	40	47	13	36	28	29
213	KC26	ST421	ST95cplx	37	38	19	37	17	8	26
214	KC27	ST404	ST14cplx	14	14	10	14	17	7	74
215	KC28	ST69	ST69cplx	21	35	27	6	5	5	4
216	KC29	ST73	ST73cplx	36	24	9	13	17	11	25
217	KC30	ST73	ST73cplx	36	24	9	13	17	11	25
218	KC31	ST404	ST14cplx	14	14	10	14	17	7	74
219	KC32	ST640	None	13	147	93	13	17	28	30
220	KC33	unknown	None	53	40	47	13	36	28	25
221	KC51	unknown	None	36	24	9	13	17	11	30
222	KC35	ST640	None	13	147	93	13	17	28	30
223	KC36	ST10	ST10cplx	10	11	4	8	8	8	2
224	KC37	ST141	None	13	52	10	14	17	25	17
225	KC38	unknown	None	13	167	19	13	36	28	30
226	KC39	ST73	ST73cplx	36	24	9	13	17	11	25
227	KC40	ST69	ST69cplx	21	35	27	6	5	5	4
228	KC41	ST95	ST95cplx	37	38	19	37	17	11	26
229	KC42	ST404	ST14cplx	14	14	10	14	17	7	74
230	KC43	ST95	ST95cplx	37	38	19	37	17	11	26
231	KC44	ST73	ST73cplx	36	24	9	13	17	11	25
232	KC45	ST405	ST405cplx	35	37	29	25	4	5	73
233	KC46	ST127	None	13	14	19	36	23	11	10
234	KC47	ST69	ST69cplx	21	35	27	6	5	5	4
235	KC48	ST73	ST73cplx	36	24	9	13	17	11	25

236	KC49	ST131	None	53	40	47	13	36	28	29
237	KC50	ST69	ST69cplx	21	35	27	6	5	5	4

Appendix B-1. Characterisation of the isolates of the Kent collection.

Each isolate was characterized for sequence-type (ST), phylogenetic group, and antibiotic resistance profile based on the phenotype observed during the disc diffusion assay.

				Antibiotics[1]								
Strain	KC number	ST	Phylogenetic group	AMX	CTX	CAP	CIP	GEN	MEM	NIT	TMP	PME
MS188	KC1	ST69	D	S	S	S	S	S	S	S	S	S
MS189	KC2	ST404	B2	S	S	S	S	S	S	S	S	S
MS190	KC3	ST162	B1	R	S	R	R	S	S	R	R	S
MS191	KC4	ST1406	D	R	S	S	S	S	S	S	S	S
MS192	KC5	ST69	D	S	S	S	S	S	S	S	S	S
MS193	KC6	ST58	B1	R	S	S	S	S	S	S	R	S
MS194	KC7	ST131	B2	R	S	S	I	S	S	S	S	S
MS195	KC8	ST73	B2	R	S	S	S	S	S	S	R	S
MS196	KC9	ST69	D	R	S	S	S	S	S	S	R	S
MS197	KC10	ST131	Unknown	R	S	S	R	S	S	S	S	S
MS198	KC11	ST59	F	S	S	S	S	S	S	S	S	S
MS199	KC12	ST1148	B1	S	S	S	S	S	S	S	S	S
MS200	KC13	ST95	B2	S	S	S	S	S	S	S	R	S
MS201	KC14	ST10	A	S	S	S	S	S	S	S	S	S
MS202	KC15	ST73	B2	R	S	S	S	S	S	S	S	S
MS203	KC16	ST73	B2	S	S	S	S	S	S	S	S	S
MS204	KC17	Unknown	B1	S	S	S	S	S	S	S	S	S
MS205	KC18	ST131	B2	R	R	S	R	R	S	S	R	S
MS206	KC19	ST131	B2	R	S	S	R	R	S	S	R	S
MS207	KC20	ST685	B2	S	S	S	S	S	S	S	S	S

MS208	KC21	ST95	B2	S	S	S	S	S	S	S	S	S
MS209	KC22	ST357	B2	S	S	S	S	S	S	S	S	S
MS210	KC23	ST1618	B2	S	S	S	S	S	S	S	S	S
MS211	KC24	ST73	B2	S	S	S	S	S	S	S	S	S
MS212	KC25	ST131	B2	S	S	S	S	S	S	S	S	S
MS213	KC26	ST421	B2	S	S	S	S	S	S	S	S	S
MS214	KC27	ST404	B2	S	S	S	S	S	S	S	S	S
MS215	KC28	ST69	A	R	S	S	S	S	S	S	S	S
MS216	KC29	ST73	B2	R	S	S	S	S	S	S	S	S
MS217	KC30	ST73	B2	R	S	S	S	S	S	S	R	S
MS218	KC31	ST404	B2	S	S	S	S	S	S	S	S	S
MS219	KC32	ST640	B2	S	S	S	S	S	S	S	S	S
MS220	KC33	Unknown	B2	R	R	S	R	R	S	S	R	S
MS221	KC51	Unknown	B2	S	S	S	S	S	S	S	S	S
MS222	KC35	ST640	B2	S	S	S	S	S	S	S	S	S
MS223	KC36	ST10	A	S	S	S	S	S	S	S	S	S
MS224	KC37	ST141	B2	S	S	S	S	S	S	S	S	S
MS225	KC38	Unknown	B2	S	S	S	S	S	S	S	S	S
MS226	KC39	ST73	B2	R	S	S	S	S	S	S	S	S
MS227	KC40	ST69	D	S	S	S	S	S	S	S	S	S
MS228	KC41	ST95	B2	S	S	S	S	S	S	S	S	S
MS229	KC42	ST404	B2	S	S	S	S	S	S	S	S	S
MS230	KC43	ST95	B2	S	S	S	S	S	S	S	S	S
MS231	KC44	ST73	B2	S	S	S	S	S	S	S	S	S
MS232	KC45	ST405	F	R	R	S	R	R	S	S	R	S
MS233	KC46	ST127	B2	R	S	S	S	S	S	S	S	S

MS234	KC47	ST69	D	R	S	S	R	S	S	S	R	S
MS235	KC48	ST73	B2	R	S	S	S	S	S	S	R	S
MS236	KC49	ST131	B2	R	S	S	R	R	S	S	R	S
MS237	KC50	ST69	D	R	S	S	S	S	S	S	R	S

[1)] AMX – amoxicillin; CTX – cefotaxime; CAP – chloramphenicol; CIP – ciprofloxacin; GEN – Gentamicin; MEM – meropenem; NIT – nitrofurantoin; TMP – Trimethoprim; PME – colistin; S – sensitive; R – resistant; I - intermediate

Appendix C-1. Acquired resistance genes.

Acquired resistance genes identified for each isolate, using the ResFinder database.

MS number	KC number	Antibiotic classes							
		Aminoglycoside	**Beta-Lactam**	**Fluoroquinolone[1]**	**MLS**	**Phenicol**	**Sulfanilamide**	**Tetracycline**	**Trimethoprim**
MS188	KC1								
MS189	KC2								
MS190	KC3	aadA5; strA; strB	blaTEM-1B			catA1	sul2	tet(B)	dfrA17
MS191	KC4								
MS192	KC5								
MS193	KC6	strA; strB	blaTEM-1B				sul2		dfrA5
MS194	KC7		blaTEM-1B				sul2		
MS195	KC8	strB; aadA1	blaTEM-1B; blaSHV-1				sul2; sul1	tet(D)	dfrA14
MS196	KC9	strB; strA; aadA5	blaTEM-1B		mph(A)		sul1; sul2	tet(B)	dfrA17
MS197	KC10		blaTEM-1B						
MS198	KC11								
MS199	KC12								
MS200	KC13								dfrA5
MS201	KC14								
MS202	KC15	aadA1	blaTEM-1B				sul1		
MS203	KC16	aadA1					sul1		
MS204	KC17								
MS205	KC18	aac(3)-IIa; aac(6')lb-cr; aadA5	blaOXA-1; blaCTX_M-15	aac(6')Ib-cr	mph(A)		sul1		dfrA17

MS206	KC19	aac(3)-IId; aadA5	blaTEM-1B			sul1		dfrA17
MS207	KC20							
MS208	KC21							
MS209	KC22							
MS210	KC23					sul2	tet(A)	
MS211	KC24							
MS212	KC25							
MS213	KC26							
MS214	KC27							
MS215	KC28							
MS216	KC29		blaSHV-1					
MS217	KC30	strB; strA	blaTEM-1B			sul1; sul2	tet(B)	dfrA1
MS218	KC31							
MS219	KC32							
MS220	KC33	aac(3)-IIa; aac(6')Ib-cr; aadA5	blaCTX-M-15; blaOXA-1	aac(6')Ib-cr	mph(A)	sul1	tet(A)	dfrA17
MS221	KC51							
MS222	KC35							
MS223	KC36							
MS224	KC37							
MS225	KC38							
MS226	KC39	aadA1	blaSHV-1			sul1		
MS227	KC40							
MS228	KC41							
MS229	KC42							

MS230	KC43								
MS231	KC44								
MS232	KC45	aadA5; aac(3)-IIa; aac(6')lp-cr	blaCTX-M-15; blaOXA-1	aac(6')Ib-cr	mph(A)		sul1	tet(B)	dfrA17
MS233	KC46		blaTEM-1B						
MS234	KC47	aadA5	blaTEM-1B			catA1	sul1; sul2	tet(B)	dfrA17
MS235	KC48	strB	blaTEM-1B				sul2		dfrA14
MS236	KC49	strB; strA; aadA5; aac(3)-Iid	blaTEM-1B		mph(A)		sul2; sul1	tet(A)	dfrA17
MS237	KC50	strA; strB	blaTEM-1B				sul1; sul2		dfrA7

1) *aac(6')Ib*-cr confers resistance to both aminoglycosides and low levels of ciprofloxacin (a fuoroquinolone)

Appendix D-1. Linear regression and correlation between antibiotic resistance and virulence.

Correlation between the virulence potential and the degree of antibiotic resistance (reflected by the number of different antibiotics to which each isolate was experimentally resistant to) was analysed with the Pearson Correlation Coefficient (Pearson r = -0.0097; p-value = 0.95). Virulence potential was calculated as the percentage of the 151 virulence genes identified that are carried in a given isolate. The linear relation between the two variables was also assessed using linear regression ($r^2 = 9.4x10^{-5}$).

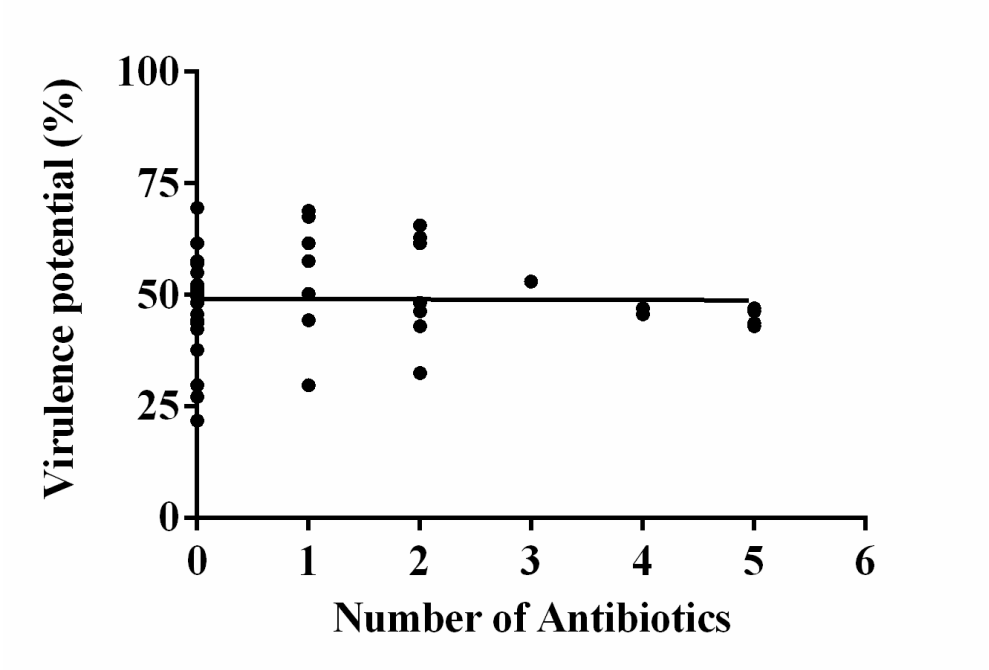

Appendix E-1. Alignment of Gyrase subunit A.

Alignment of the protein sequences of gyrase subunit A of all isolates of the Kent collection identifies isolates KC3, KC7, KC10, KC18, KC19, KC33, KC45, KC47, and KC49 as being ciprofloxacin resistant due to mutations at amino acid position 83 (Serine to Leucine) and/or amino acid position 87 (Aspartate to Asparagine) (Weigel et al., 1998).

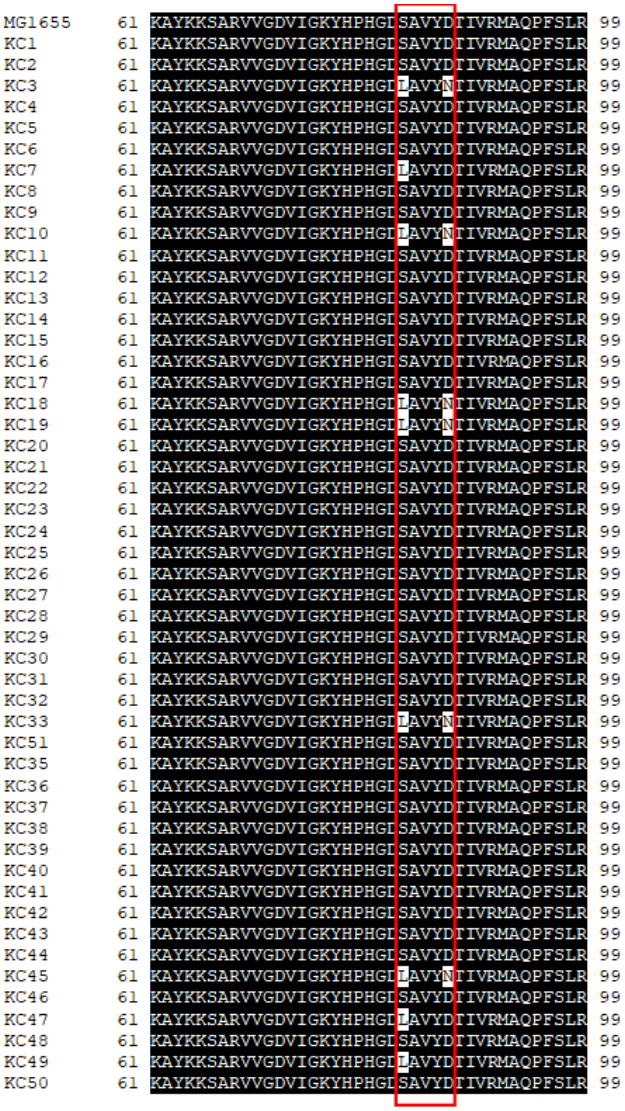

Appendix F-1. Susceptibility of KC45 to NO-donor NOC-12.

Susceptibility of bacterial strains to NO was tested by growth in M9 minimal medium in the presence of different concentrations of the NO-donor NOC-12. Growth of MG1655 (A), EC958 (B), and KC45 (C) was followed for 8 h. Error bars represent standard deviation. Each data point is the mean of three biological repeats, each one comprising three technical repeats. The doubling time (D) was calculated based on the readings that were taken during 1.5h of growth following the addition of NOC-12. Error bars represent standard deviation. (*: Student's unpaired t-test; p-value < 0.05).

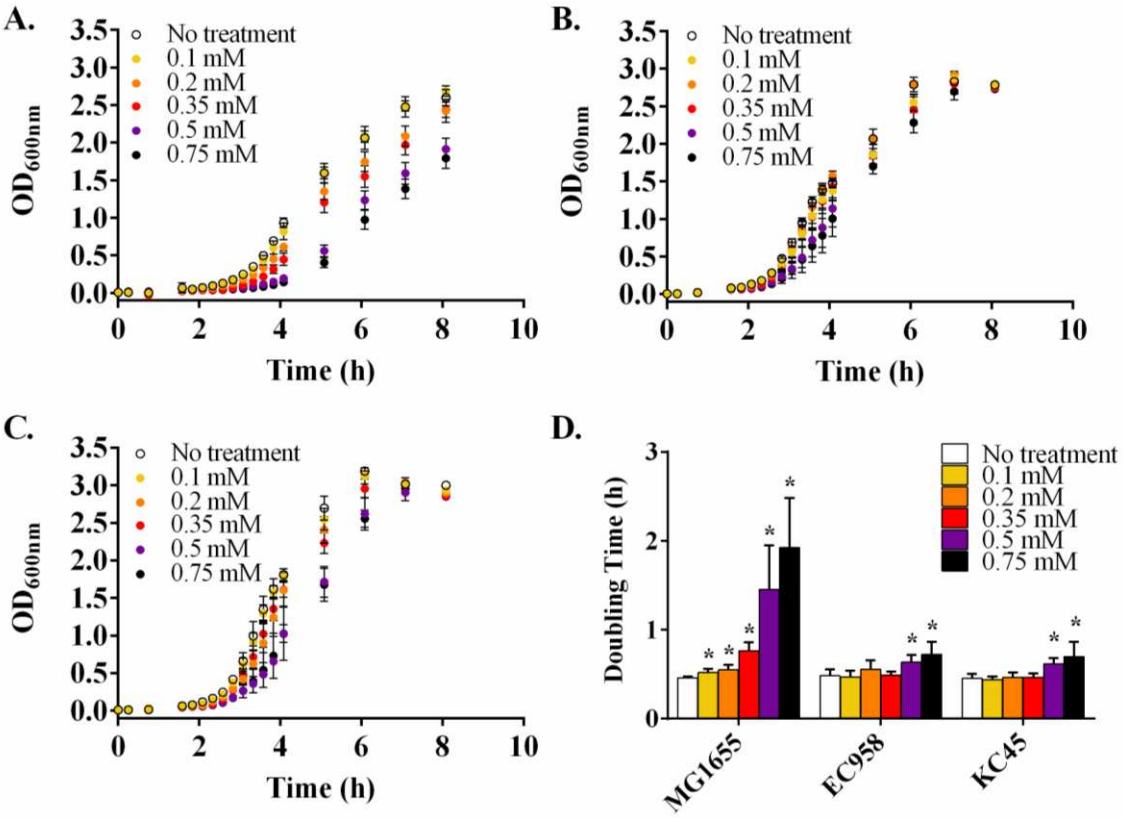

Appendix G.1 – Engineering of cyoA E. coli EC958 knockout mutant using λ-red mutagenesis.

A) cyoA gene of E. coli EC958. The chloramphenicol resistance cassette from plasmid pKD3, amplified by PCR using the primers cyoA_Cm_fw and cyoA_Cm_rev2, was electroporated onto E. coli EC958 harbouring pKOBEG. B) Recombinant colonies (colonies 1-5) were screened by colony PCR with primers cyoA_Sc_fw and cyoA_Sc_rev2 (Expected molecular size: 1390 bp). A positive control ('Positive') containing E. coli EC958 wild-type harbouring pKOBEG was also prepared (Expected molecular size: 1300 bp). Recombinant colonies were then grown in LB at 43°C for curing of the pKOBEG plasmid. Only colonies with a chloramphenicol resistant and gentamicin sensitive phenotype were stocked and used for the survival assays.